Biochemical and cellular characterization of the interplay between glutamine metabolism, mTOR and Notch1 signaling in cancer therapy

Tra Ly Nguyen

université de BORDEAUX

THÈSE PRÉSENTÉE

POUR OBTENIR LE GRADE DE

DOCTEUR DE

L'UNIVERSITÉ DE BORDEAUX

École Doctorale Sciences de la Vie et de la Santé

Spécialité Biochimie

Par Tra Ly NGUYEN

Biochemical and cellular characterization of the interplay between glutamine metabolism, mTOR and Notch1 signaling in cancer therapy

Caractérisation biochimique et cellulaire de l'interaction entre le métabolisme de la glutamine et la signalisation de mTOR et Notch1 comme thérapie contre le cancer

Sous la direction de : Dr. Raúl V. DURÁN-DÍAZ

Soutenue le 24 avril 2018

Membres du jury :

M. MERLIO Jean-Philippe	PU à l'Université de Bordeaux	Président
M. SEILIEZ Iban	DR à l'INRA à St Pée sur Nivelle	Rapporteur
Mme VASSEUR Sophie	DR INSERM, CRCM Marseille	Rapporteur
M. VELASCO Guillermo	PU à l'Université de Madrid	Examinateur
Mme MOREAU Violaine	DR INSERM, Université de Bordeaux	Examinateur
M. MARAVER Antonio	CR INSERM, IRCM Montpellier	Examinateur
M. DURÁN-DÍAZ Raúl	CR INSERM, IECB Bordeaux	Directeur de thèse

To the jury members, Pr. Jean-Philippe Merlio, Pr. Guillermo Velasco, Dr. Iban Seiliez, Dr. Sophie Vasseur, Dr. Violaine Moreau and Dr. Antonio Maraver.
Your participation in this jury is a great honor for me. I sincerely thank you for agreeing to judge my thesis work, despite the time and effort it requires. Your critical analysis will no doubt help me to improve the scientific quality of my work.

To my thesis supervisor, Dr. Raúl V. Durán
I would like to express my sincere gratitude to my supervisor. I would not have succeeded in completing my PhD without your continued guidance, your advice and your continuous support during these three and a half years. I have learned so much from you, particularly from all of our Friday meetings. Thank you for always listening to me and giving me the freedom to follow my own scientific curiosity. Your guidance was very important during the research and the preparation of this thesis. I could not imagine having a better supervisor and mentor for my PhD study.

To the members of the lab,
Thank you Clément Bodineau, my favorite labmate, for all of your help, support and positive thoughts. I really enjoy working with you, discussing science and sharing life stories. You always encourage me and correct my “perfect” French level. I will be there when your turn comes around!
Thank you Dr. Silvia Terés and Dr. Victor Villar, for the warm welcome when I first came to the lab. I took my first steps in a research lab with both of you. Thank you for all the advice during some difficult moments.
Thank you Dr. Sarah Courtois, for sharing these 3 years of PhD together and for your advice during the thesis preparation.
Thank you Dr. Marie-Julie Nokin for taking care of my projects. It was a great honor to have your solid support at the end of the thesis.
Thank you Oriane Galmar, my intern student and now PhD student. You helped me greatly during your internship and thanks for your encouragement during the thesis preparation.
Thank you Malaurie Eugénie for your kindness and your care.

To the members of Royou’s team,
I would like to express my great appreciation for all the members of Royou’s team, especially Dr. Damien Goutte-Gattat, Lou Bouit, Priscillia Pierre-Elies, Dr. Cedric Landmann and Dr. James Jenkins Wallace. I had a beautiful PhD thanks to all of you. You welcomed me into your lab as if I was a member of it. You always said yes when I needed you without hesitation. Special thanks to Dr. Damien Goutte-Gattat for your advice and your technical help and to Lou Bouit for your kindness and your care.

To other colleagues, **I would extend my thanks:**
To Mariline Yot for your support and your ability to listen to me. You are always kind with me, trying to make me feel better when difficult moments arose.
To Dr. Benjamin Drogat for your advice in critical moments and for your help during the thesis preparation. Especially for the jokes, that I don’t really understand most of the time!
To Dr. David Santamaría and Sonia San José for your scientific advice and your encouragement all the time.
To Catherine Duprat and Myriam Mederic for always being available and helping me to have a good lab life.

Thanks to all the collaborators who have contributed to these works. Dr. Mercedes Tomé, Dr. Benoît Rousseau, Julien Izotte, Dr. Jean-Max Pasquet, Dr. Marion Bouchecareilht, Dr. Muriel Priault, Dr. Elodie Richard and Vincent Pitard.
To Stéphanie Durrieu for sharing your knowledge and supporting me.
To Isabelle Frémaux and Dr. Florian Alonso for your support, being there when I most needed.
Thank to Dr. Nassima Meriem Gueddouda, Dr. Camila Parrot, Dr. Amy Diallo, Dr. Clémence Rabin, Dr. Vanessa Delcroix for sharing your own PhD experiences, helping me with my transition into a better PhD life!

To my friends and my family,
Thank you to, my parents, my parents-in-law and my host family for your care and your encouragement. I know it was hard for you to understand what I was doing but you still keep supporting me during this very long process.
Thank you, chị Mai for sharing these three years of PhD. We have been together through the most difficult times.
Thank you Hằng, anh Nam, chị Hương, chị Hà, anh Giang, chị Hải Anh, anh Vinh for your constant support.
Special thanks to my husband. You asked to be thanked at the beginning of the acknowledgements, but we always save the best till last (but not least!). A simple thank you is not enough. You have been here next to me for more than three years, days and nights, weeks and week-ends. Thank you for supporting me through ups and downs, for listening to all the crazy stories about my lab life. I always say, I could not have made this thesis happens without you. I cannot wait to enjoy the next step with you!

I had a beautiful PhD thank to all of you!
You are all my best company for this beautiful life experience.

<u>Titre</u> : Caractérisation biochimique et cellulaire de l'interaction entre le métabolisme de la glutamine et la signalisation de mTOR et Notch1 comme thérapie contre le cancer

Résumé :

La tumorigenèse est un processus multi-étapes, constituée d'altérations génétiques qui conduisent à la transformation maligne des cellules humaines normales. Au cours de cette transformation maligne, l'activité de différentes voies oncogéniques est augmentée. Les voies de signalisation mTORC1 et Notch1 sont des voies oncogéniques bien connues qui jouent un rôle central dans la régulation de la croissance et du métabolisme cellulaires. Les traitements anti-mTORC1 et Notch1 sont approuvées en tant que thérapies anticancéreuses pour plusieurs types de tumeurs. Néanmoins, les cellules cancéreuses développent des résistances à ces inhibiteurs induisant un nombre important de rechute et donc d'échec de ces traitements. Ainsi, le but principal de ce travail est d'étudier l'inhibition des voies de signalisation mTORC1 et Notch1 dans les cellules cancéreuses afin de concevoir de nouvelles stratégies thérapeutiques anticancéreuses. En premier lieu, nous avons décrit une nouvelle classe d'inhibiteurs de mTORC1 qui présente une cytotoxicité spécifique vis-à-vis des cellules cancéreuses. Nous avons démontré que l'ICSN3250, un analogue de l'halituline marine cytotoxique, inhibe mTORC1 et induit la mort cellulaire. Le mécanisme moléculaire de cette inhibition est basé sur le déplacement de l'acide phosphatidique, un lipide activateur du complexe mTORC1, du domaine FRB de la protéine mTOR. Dans un deuxième temps, nous avons étudié le lien entre le métabolisme de la glutamine et la signalisation de Notch1 dans la leucémie lymphoblastique aiguë à lymphocytes T (T-ALL). Les changements métaboliques dans les cellules cancéreuses sont nécessaires à une prolifération cellulaire rapide et la croissance tumorale. Nous avons généré une lignée de cellule T-ALL dont la voie de signalisation Notch1 est constitutivement active et analysé les conséquences de cette activation sur le métabolisme de la glutamine. En effet, en absence de glutamine, l'activation de Notch1 induit la mort cellulaire par apoptose en perturbant l'accumulation de la glutamine synthétase, une enzyme qui permet la production de glutamine. Ce travail de thèse a donc permis de décrire de nouvelles stratégies pour cibler les voies mTORC1 et Notch1 dans le cancer. De futures investigations seront nécessaires pour étudier leur efficacité dans les thérapies anti-cancéreuses.

Mots clés : mTOR, Notch1, glutamine, métabolisme, cancer, thérapie.

Title: Biochemical and cellular characterization of the interplay between glutamine metabolism, mTOR and Notch1 signaling in cancer therapy

Abstract:

Tumorigenesis is a multistep process, consisting of genetic alterations that drive the malignant transformation of normal human cells. During this transformation, different oncogenic pathways are upregulated. mTORC1 and Notch1 signaling are well-known oncogenic pathways which play a central role in the regulation of cell growth and metabolism. Anti-mTORC1 and Notch1 therapies are approved as cancer treatments for several types of tumor but there are still developed resistances and relapse diseases. Thus, the main aim of this work is to study the inhibition of mTORC1 and Notch1 signaling pathway in cancer cells in order to design new therapeutic anti-cancer strategies. In the first place, we reported new class of mTORC1 inhibitors which has cytotoxicity specifically towards cancer cells. We demonstrated that ICSN3250, an analogue of the cytotoxic marine alkaloid halitulin, inhibited mTORC1 and induced cell death. The molecular mechanism of this inhibition is based on the displacement of the lipid phosphatidic acid, an activator of mTORC1 complex, from the FRB domain of mTOR protein. At the second stage, we have studied the connection between glutamine metabolism and Notch1 signaling in T-cell acute lymphoblastic leukemia (T-ALL). Metabolic changes in cancer cells are advantageous for rapid cell proliferation and tumor growth. We have generated Notch1-driven T-ALL cells and analyzed the consequences of Notch1 activation on glutamine metabolism. Indeed, under glutamine withdrawal, Notch1 upregulation induced apoptotic cell death by disrupting the accumulation of glutamine synthetase, a glutamine producing-enzyme. Overall, this thesis work allowed to describe new strategies to target mTORC1 and Notch1 pathways in cancer, which need future investigations to study their efficacy in therapies.

Keywords: mTOR, Notch1, glutamine, metabolism, cancer, therapy.

Unité de recherche

INSERM U1218 ACTION – Institut Bergonié, 229 cours de l'Argonne, 33000 BORDEAUX

Résumé en français

mTOR est une sérine/thréonine kinase très conservée qui intègre plusieurs stimuli pour réguler la croissance et le métabolisme cellulaire. mTOR forme deux complexes fonctionnellement et structurellement distincts, appelés mTORC1 et mTORC2. mTORC1 est principalement activé par la présence d'acides aminés, par des facteurs de croissance, par l'état bioénergétique de la cellule, et par la disponibilité de l'oxygène. Au niveau de ses fonctions, mTORC1 régule la synthèse des protéines, la biogenèse des ribosomes, l'absorption de nutriments et l'autophagie en réponse à des facteurs de croissance, des acides aminés, et de l'énergie cellulaire (Duran & Hall, 2012). Dans le contrôle de mTORC1 par des facteurs de croissance, le complexe de la sclérose tubéreuse (TSC) et le co-activateur de mTORC1, Rheb jouent un rôle crucial. L'un des mécanismes par lesquels la voie TSC / Rheb contrôle mTORC1 implique la production d'acide phosphatidique (PA), qui se lie directement à mTOR dans le domaine FRB et active mTORC1 en aval de TSC / Rheb. En effet, la régulation négative de la production de PA est suffisante pour diminuer l'activité de mTORC1. En raison de son rôle central dans le contrôle de la croissance cellulaire et le métabolisme, mTORC1 est activé dans de nombreux types de tumeurs pour soutenir la croissance de la tumeur. Cette régulation positive de mTORC1 constitue une étape cruciale pendant la dérégulation de la signalisation cellulaire lors de la transformation maligne.

L'objectif principal de la première partie de cette thèse est l'étude de l'effet de l'inhibition de mTORC1 par une nouvelle classe d'inhibiteurs qui cible spécifiquement les cellules cancéreuses. En raison des résultats modestes de inhibiteurs de mTORC1 pour la stratégie anti-cancer, le développement de nouveaux traitements est sous

enquêtes. Dans ce projet, nous avons étudié l'inhibition de mTORC1 par un composé synthétisé, ICSN3250, un analogue de l'alcaloïde marin cytotoxique l'halituline. Particulièrement, seules les cellules cancéreuses sont sensibles à ce composé, tandis que les cellules non cancéreuses ont montré jusqu'à 100 fois moins de sensibilité à ICSN3250, contrairement à d'autres inhibiteurs qui n'ont pas montré de sélectivité. Le mécanisme moléculaire de cette inhibition est basé sur le déplacement de PA, l'activateur de mTORC1, du domaine FRB de mTOR. En outre, ICSN3250 est capable d'affecter la capacité de PA à surmonter la régulation négative TSC2 sur mTORC1, qui est la nouveauté de notre travail dans la conception de ce nouvel inhibiteur mTOR. Ce travail a été soumis à Cancer Research en Janvier 2018 et il est en deuxième révision.

L'objectif principal de la deuxième partie de cette thèse est de fournir une compréhension fondamentale de l'interaction mécanistique entre la transformation métabolique et la dérégulation de la signalisation cellulaire pendant l'origine et la progression de la leucémie. Nous avons étudié les changements métaboliques dans des modèles cellulaires de leucémie lymphoblastique aigüe à cellules T (T-ALL) générés par l'activation de la voie Notch1 (modèles cellulaires NDALL), et la contribution de ces changements métaboliques dans la progression du cancer. Une attention particulière sera prêtée au rôle potentiel du métabolisme de la glutamine dans NDALL, et à l'interaction entre le métabolisme de la glutamine et la voie de signalisation mTORC1. La voie oncogénique la plus importante pour la transformation des cellules T est l'activation de la signalisation par la voie Notch1. Il a été constaté que des mutations conduisant à l'activation de la voie Notch1 sont présentes dans plus de 50% des patients atteints de T-ALL, ce qui souligne l'implication directe de Notch1

dans la prolifération et la survie des cellules de leucémie. Malgré le rôle oncogénique principal de la signalisation Notch dans T-ALL, l'inhibition de la signalisation Notch en utilisant des inhibiteurs de γ-sécrétase (GSI) a montré une activité anti-leucémique très modeste contre des lignées cellulaires humaines de T-ALL, exerçant principalement un effet cytostatique avec peu ou pas d'apoptose. Aussi, les premiers essais cliniques ont été limités par des effets de toxicité excessive sur l'épithélium intestinal des patients. La résistance au traitement avec les GSI peut être provoquée par la perte mutationnelle de PTEN, conduisant à l'activation constitutive de la voie PI3K/AKT/mTOR (Tzoneva & Ferrando, 2012). En fait, plusieurs indices connectent la signalisation Notch avec l'activation de la voie mTOR dans T-ALL. Curieusement, le traitement avec GSI supprime la phosphorylation de multiples protéines impliquées dans la signalisation de la voie de mTORC1, ce qui suggère un rôle mécanistique de la signalisation Notch dans l'activation de mTORC1. Notamment, le blocage simultané de la voie Notch et de la voie mTORC1 a un effet synergique dans la suppression de la croissance de NDALL. (Chan et al., 2007). Ainsi, cette inhibition simultanée a attiré notre attention comme une stratégie de co-traitement potentiel contre NDALL. Cependant, la connexion mécanistique entre les deux voies n'est pas claire.

Aujourd'hui, notre compréhension de la reprogrammation métabolique dans les leucémies de type T-ALL est très limitée, mais des études récentes ont montré des changements dans le métabolisme des acides aminés, notamment la glutamine, dans les lignées cellulaires NDALL (Basak et al., 2014). Il faut noter que parmi les changements métaboliques qui se produisent au cours de l'origine et la progression du cancer, la dépendance des cellules cancéreuses à la glutamine constitue une adaptation importante pour maintenir la demande d'énergie qui soutient la croissance et la prolifération rapide (Souba 1993). La glutamine est métabolisée par un processus

dénomé glutaminolyse, c'est-à-dire, la déamination de la glutamine pour synthétiser de l'alpha-cétoglutarate, un processus catalysé par la glutaminase et par la glutamate déshydrogénase. La glutaminase est régulée au niveau de l'expression par l'oncogène c-MYC (Gao et al., 2009), et son activité est en corrélation avec la croissance de nombreuses tumeurs (Perez-Gomez et al., 2005). Récemment nous avons démontré que l'augmentation de la glutaminolyse dans les cellules tumorales provoque également la dérégulation de la signalisation cellulaire par l'activation de la voie mTORC1 (Duran et al., 2012; Duran et al., 2013). Ainsi, la glutamine en combinaison avec la leucine active mTORC1 en augmentant la glutaminolyse et la production d'alpha-cétoglutarate. L'augmentation de la glutaminolyse stimule mTORC1, la croissance cellulaire et l'autophagie, deux processus contrôlés par mTORC1. Par contre, l'inhibition de la glutaminolyse prévient l'accumulation d'alpha-cétoglutarate et l'activation subséquente de mTORC1. Le rôle du métabolisme de la glutamine dans la dérégulation de mTORC1 dans NDALL n'est pas connu. Comme indiqué plus haut, l'implication de c-MYC (un activateur connu de la glutaminolyse) dans l'interaction entre les voies mTORC1 et Notch1 ouvre la possibilité que la glutaminolyse pourrait servir de médiateur pour l'activation de mTORC1 dans NDALL. Par conséquent, l'objectif de cette proposition est de déterminer les changements dans le métabolisme de la glutamine dans des modèles cellulaires de NDALL, établissant un rôle mécanistique potentiel de c-MYC et de l'activation de la glutaminolyse dans l'activation de mTORC1 sur ces modèles de leucémie médiés par Notch1. En outre, en suivant une approche métabolomique, nous allons étudier d'autres changements métaboliques qui se produisent lors de l'activation de Notch dans les cellules T-ALL qui pourraient être pertinents pour la progression de la tumeur. Enfin, nous allons estimer la dépendance des modèles cellulaires de NDALL sur le métabolisme de la

glutamine et sur l'activation de mTORC1, pour proposer et valider des co-traitements potentiels ciblant ces deux éléments comme une stratégie thérapeutique contre la leucémie médiée par Notch1. Pour tester si le métabolisme de la glutamine joue un rôle mécanistique dans la dérégulation de la signalisation cellulaire grâce à l'activation de mTORC1 dans NDALL, nous allons développer des modèles cellulaires de T-ALL dans lesquelles la signalisation Notch1 est suractivée. En suivant une approche multidisciplinaire impliquant la biochimie, la biologie cellulaire, la métabolomique, la bioénergétique, l'enzymologie, et la biologie translationnelle, nous allons tester si l'activation de Notch1 dans ces modèles augmente le métabolisme de la glutamine et, par conséquence, la signalisation mTORC1. Un lien mécanistique entre Notch, glutaminolyse et mTORC1 suggère que les traitements ciblant à la fois la glutaminolyse et l'activation de mTORC1 pourraient avoir un effet synergique contre les leucémies lymphoblastiques dans lesquelles la voie Notch1 est activée.

Durant cette thèse, en utilisant des approches *in vitro* et *in vivo*, nous avons montré que les cellules leucémiques médiées par Notch1 sont dépendantes au niveau de glutamine extracellulaire et ils subissent une mort cellulaire par apoptose lors du sevrage de la glutamine, qui est appelée une "dépendance à la glutamine". De plus, la surexpression de Notch1 dans les cellules leucémiques Notch1-négatives est suffisante pour induire une dépendance à la glutamine. Mécaniquement, Notch1 est capable de réguler les enzymes métaboliques du métabolisme de la glutamine, entraînant une augmentation du catabolisme de la glutamine et une diminution de l'anabolisme de la glutamine. En conséquence, cibler le métabolisme de la glutamine pourrait être considéré comme une stratégie thérapeutique contre la leucémie avec Notch1 élevée.

Dans l'ensemble, cette étude a montré deux exemples clairs ciblant le lien entre le métabolisme de la cellule et la signalisation cellulaire pour éliminer spécifiquement les cellules cancéreuses. La transduction du signal reprogramme le métabolisme cellulaire afin de remplir les besoins anaboliques et énergétiques des tumeurs, favorisant la croissance et la prolifération cellulaire. Cependant, la relation entre la signalisation cellulaire et le métabolisme n'est pas unidirectionnelle. En détectant les niveaux de métabolites intracellulaires qui affectent l'état des principales voies métaboliques, les cellules peuvent exercer un contrôle par rétroaction sur leurs réseaux de signalisation. Ces mécanismes permettent aux cellules de croître et de proliférer en accord avec leurs états métaboliques et en fonction de la disponibilité de l'environnement extracellulaire. Comprendre le mécanisme moléculaire de cette connexion aidera à comprendre comment la viabilité des cellules cancéreuses sont déterminées en réponse aux variations du niveau de nutriments environnementaux. Le traitement à base de la restriction nutritionnelle, comme ICSN3250, déplétion en glutamine ou L-asparaginase, sera développé pour cibler la connexion entre l’état métabolique et la signalisation cellulaire dans le cancer.

Table of contents

Table index

Figure Index

Abbreviations

4EBP1: eIF4E binding protein 1
ACC: acetyl-CoA carboxylase
ACLY: ATP-citrate lyase
AML: acute myeloid leukemia
AMPK: AMP-activated protein kinase
ANK: ankyrin
APC/C: anaphase-promoting complex
ARF: ADP-ribosylation factor
ATF4: activating transcription factor 4
ATG: autophagy-related protein
B-ALL: B-cell acute lymphoblastic leukemia
BM: bone marrow
CAD: carbamoyl-phosphate synthetase 2, aspartate transcarbamylase, dihydroorotase
CDK: cyclin-dependent kinase
CLP: common lymphoid progenitor
CMP: common myeloid progenitor
CREB2: cAMP-responsive element-binding 2
CRTC2: CREB regulated transcription coactivator 2
DAP1: death-associated protein 1
DEPDC5: DEP domain-containing protein 5
DEPTOR: domain-containing mTOR-interacting protein
DG kinase: diacylglycerol kinase
DLL: delta-like ligand
DNA: deoxyribonucleic acid
DSL: Delta-Serrate-Lag2
EGF: epidermal growth factor
eIF: eukaryotic translation initiation factor
ERK: extracellular signal-regulated kinase
ETP: early T-cell progenitor
EV: empty vector
^{18}F-FDG: ^{18}F-fluorodeoxyglucose
FASN: fatty acid synthase
FBXW7: F-box and WD repeat domain containing 7
FKBP12: FK506-binding protein of 12 kDa
FLCN: folliculin
FNIP1/2: folliculin-interacting proteins 1 and 2
FOXO: Forkhead-box Class O
FRB: FKBP12-rapamycin-binding
GAP: GTPase-activating protein
GATOR: GAP activity toward RAGs
GLUD/GDH: glutamate dehydrogenase
GEF: guanine exchange factor
GFP: green fluorescent protein
GLS: glutaminase
GLUL/GS: glutamine synthetase
GMP: granulocyte-monocyte progenitor
GSI: γ-secretase inhibitor
GSSG: oxidized glutathione
HAT: histone acetyltransferase
HCC: hepatocellular carcinoma
HD: heterodimerization
HES: hairy and enhancer of split
HEY/HESR: hairy and enhancer of split-related
HIF: hypoxia inducible factor
HK: hexokinase
HSC: hematopoietic stem cell
IDH: isocitrate dehydrogenase
IGF-1: insulin-like growth factor 1
IGF1R: insulin-like growth factor 1 receptor
IL-7: interleukin-7
IRS1: insulin receptor substrate 1
JAG: jagged
JAK: janus tyrosine kinase
JMJ: jumonji
KRAS: v-Ki-ras2 kirsten rat sarcoma viral oncogene homolog
LKB1: liver kinase B1
LNR: lin12-Notch repeat
LPAAT: lysophosphatidic acyltransferase
LRS: leucyl-tRNA synthetases
MAML: mastermind-like
MAPK: mitogen-activated protein kinase
MEP: megakaryocytic-erythroid progenitor
MIOS: WD repeat-containg protein MIO
mLST8: mammalian lethal with SEC13 protein 8
MPP: multipotent progenitor

mRNA: messenger ribonucleic acid
MSO: methionine sulfoximine
MTHFD2: methylene-tetrahydrofolate dehydrogenase 2
mTORC1/2: mammalian target of rapamycin complex 1/2
NADPH: nicotinamide adenine dinucleotide phosphate
NECD: Notch extracellular domain
NICD: Notch intracellular domain
NK: natural killer
NPRL2: nitrogen permease regulator 2-like protein
NRR: negative regulatory region
PA: phosphatidic acid
PARP: poly(ADP-ribose) polymerase
PDCD4: programmed cell death 4
PDK1: phosphoinositide-dependent kinase 1
PEST: proline/glutamic acid/serine/threonine
PET: positron emission tomography
PFK: phosphofructokinase
PGC-1α: peroxisome-proliferator-activated receptor coactivator-1α
PHD: prolyl hydroxylase
PHGDH: phosphoglycerate dehydrogenase
PI: propidium idodide
PI3K: phosphoinositide 3-kinase
PIKK: phosphoinositide kinase-related protein kinase
PK: pyruvate kinase
PLD: phospholipase D
POFUT1: protein O-fucosyltransferase1
POGLUT: protein O-glucosyltransferase
PPAR: peroxisome proliferator-activated receptor
PPP: pentose phosphate pathway
PRAS40: proline-rich Akt substrate of 40 kDa
PRPP: phosphoribosyl pyrophosphate
PTEN: phosphatase and tensin homolog
Q: glutamine
RalA: ras-related protein A
RAM: RBPjκ association module
RAP: rapamycin
Raptor: regulatory-associated protein of mTOR
REDD1: regulated in DNA damage and development 1
Rheb: RAS homolog enriched in brain
RNA: ribonucleic acid
ROS: reactive oxygen species
RSK: 90 kDa ribosomal S6 kinase
SDH: succinate dehydrogenase
SKP2: S phase kinase-associated protein 2
SLC: solute carrier family
SQSTM1: sequestosome-1
SREBP: sterol responsive element binding protein
T-ALL: T-cell acute lymphoblastic leukemia
TAD: transactivation domain
TCA: tricarboxylic acid
TFEB: transcription factor EB
THF: tetrahydrofolate
TMD: transmembrane domain
TSC: tuberous sclerosis complex
ULK1: unc-51 like autophagy activating kinase
UPS: ubiquitine-proteasome system
v-ATPase: vacuolar H(+)- adenosine triphosphatase
WDR: WD repeat-containing protein
YY1: yin-yang 1

INTRODUCTION

1. mTORC1 signaling

1.1 mTOR discovery

Living organisms need to coordinate the availability of nutrients with the growth of cells, tissues and organs in response to a changing environment. The *mammalian target of rapamycin* (mTOR) is a key player in this coordination in eukaryotic organisms. Firstly discovered in yeast as the direct target of the macrolide *rapamycin*[1], mTOR is a serine/threonine kinase highly conserved from unicellular eukaryotes to humans, belonging to the PIKK (*phosphoinositide kinase-related protein kinase*) family. mTOR forms two functionally and structurally distinct complexes, *mTOR complex 1* (mTORC1, sensitive to rapamycin) and *mTOR complex 2* (mTORC2, insensitive a rapamycin)[2]. Probably due to its sensitivity to rapamycin, mTORC1 is the most studied among the two complexes. mTORC1 is regulated by diverse signals, including growth factors, amino acids availability, metabolic stress, oxygen availability, and by the bioenergetics status of the cell. In response to these inputs, mTORC1 regulates a broad range of major processes in the cell, stimulating anabolism (including protein and lipid synthesis) and repressing catabolic processes (such as autophagy)[3]. Due to its major contribution to cell growth, mTORC1 is deregulated in several disorders, including cancer, diabetes and neurodegeneration, becoming an interesting target for therapeutic approaches to improve health and lifespan[3].

The discovery of mTOR had begun after the discovery of the macrolide antibiotic rapamycin in 1964. It was first discovered in the budding yeast *Saccharomyces cerevisiae* following a screening for rapamycin resistance[1,4,5]. In yeast, TORC1 is composed of Tor, Lst8, Kog1 and Tco89 proteins. In mammals, mTORC1 contains mTOR, mLST8 (*mammalian lethal with SEC13 protein 8*), Raptor (*regulatory-*

associated protein of mTOR), PRAS40 (*proline-rich Akt substrate of 40 kDa*) and DEPTOR (*domain-containing mTOR-interacting protein*) (**Figure 1**).

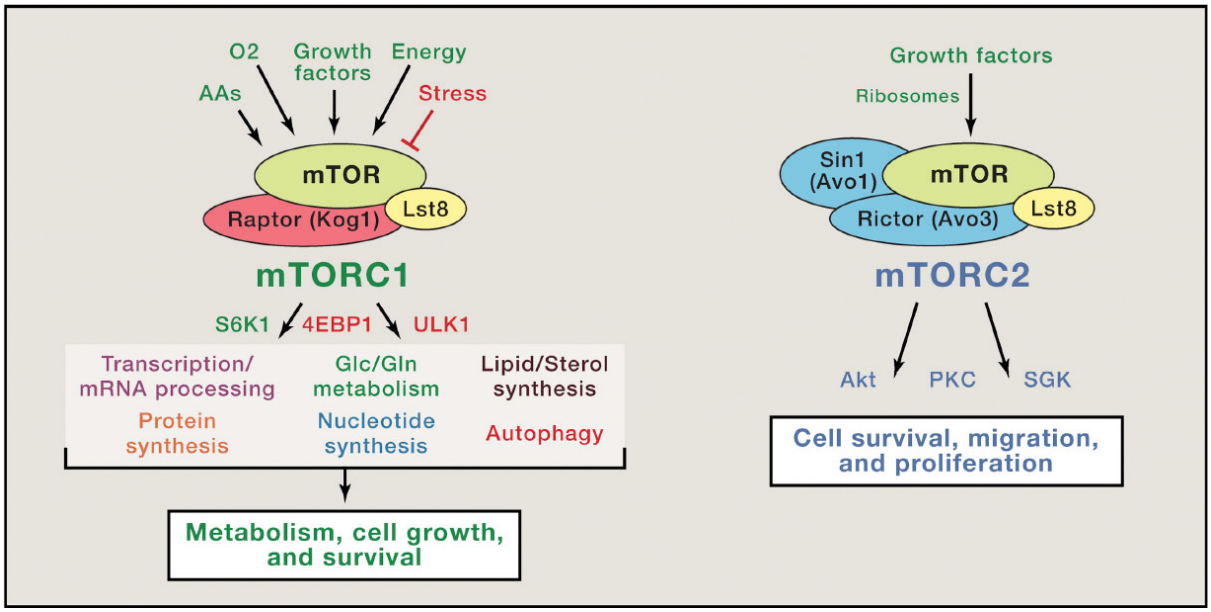

Figure 1. The core component of mTORC1 and mTORC2

Upstream and downstream signals of each complex are depicted.
(Modified from *Blenis 2017 Cell 171(1):10-13*).

Raptor serves as a complex scaffold, recruiting substrates to the kinase active site through their TOS (*TOR signaling*) motifs[6,7]. PRAS40 and DEPTOR are both mTORC1 suppressors, likely acting as competitive substrates to bind to Raptor[8,9]. mLST8 does not play a necessary role in mTORC1 (but specifically in mTORC2)[10]. In addition, structural studies showed that mTORC1 forms an obligate dimer[11–13]. The mechanism of action of rapamycin inhibition includes the formation of the complex rapamycin-FKBP12 (*FK506-binding protein of 12 kDa*). Then, the rapamycin-FKBP12 complex binds to the specific FRB (*FKBP-rapamycin-binding*) domain of mTOR and partially obstruct the active site, preventing the entry of substrates[14].

1.2 Functions of mTORC1

1.2.1 Building blocks for cell growth

1.2.1.1 Protein synthesis and ribosome biogenesis

mTORC1 regulates protein synthesis and ribosome biogenesis through the phosphorylation of S6K1 (*p70S6 Kinase 1*) and 4EBP1 (*eIF4E binding protein 1*). S6K1 and 4EBP1 were the first identified mTOR substrates in metazoans and they remain as the best characterized[15–18]. Upon mTORC1 inhibition, S6K1 remains unphosphorylated and binds to the multi-subunit scaffold eIF3 (*eukaryotic translation initiation factor 3*)[19] in an inhibitory conformation. In response to growth-induced stimuli, mTORC1 gets activated and phosphorylates S6K1 on its hydrophobic motif site (Thr389). This phosphorylation liberates S6K1 from eIF3, and facilitates the subsequent activating phosphorylation of S6K1 by PDK1 (*3-phosphoinositide-dependent kinase 1*) on Thr229[20,21]. Once activated, S6K1 phosphorylates and activates numerous substrates promoting mRNA translation initiation. Among these substrates, the best characterized is the rpS6 (*ribosomal protein S6*), a component of 40S ribosome subunit. However, the significance of S6 phosphorylation by S6K1 in S6 functionality remains unclear[22,23]. S6K1 also phosphorylates and activates eIF4B, a positive regulator of the 5' cap binding eIF4F complex[24,25]. In parallel, S6K1 phosphorylates PDCD4 (*programmed cell death 4*), an inhibitor of eIF4A, to promote the degradation of PDCD4[26], leading to the activation of eIF4A.

Likewise, 4EBP1 is not phosphorylated in conditions of mTORC1 inhibition, leading to its interaction with eIF4E, thus preventing eIF4E-eIF4G interaction[27]. The activation of mTORC1 induces the phosphorylation of 4EBP1 by mTORC1 at multiples sites (Thr37, Thr46, Thr70, Ser65), triggering the dissociation of 4EBP1 from eIF4E, allowing the binding of eIF4G to eIF4E and the recruitment of eIF4A. All these steps lead to

formation of the eIF4F complex (consisting of eIF4E, eIF4G and eIF4A) on the 5'-cap. In addition, the freshly formed complex recruits the 40S ribosome and the ternary complex to form the 48S translation pre-initiation complex (**Figure 2**).

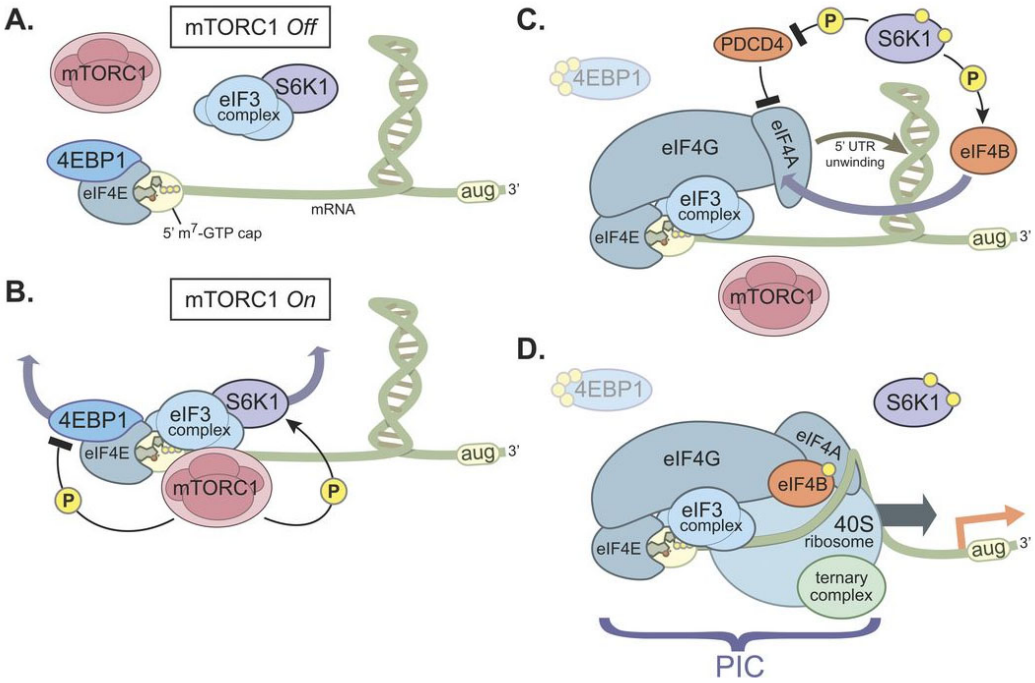

Figure 2. Model of cap-dependent translation by mTORC1/4EBP1 and mTORC1/S6K1 axis.

(**A**) When mTORC1 is inactive, 4EBP1 binds to eIF4E on the mRNA 5'-cap to suppress assembly of the pre-initiation complex. (**B**) In response to mTORC1-activating stimuli, mTORC1 phosphorylates 4EBP1 and S6K1, inducing 4EBP1 release from eIF4E and S6K1 release from eIF3. (**C**) Upon the release of 4EBP1 and S6K1, the eIF4F complex, consisting of eIF4G, eIF4E and eIF4A, is assembled at the 5'-cap. In parallel, S6K also phosphorylates eIF4B, an eIF4A enhancer, and PDCD4, an eIF4A inhibitor. (**D**) Binding of the 40S ribosome and the ternary complex (eIF2, Met-tRNA and GTP) at the 5'-cap with these factors to form the pre-initiation complex and to initiate cap-dependent translation. (Modified from *Magnuson et al., 2012 Biochem J. 441(1):1-21*).

1.2.1.2 Lipid synthesis

mTORC1 controls lipid signaling through *de novo* lipid synthesis activation and lipid catabolism inhibition, in order to promote membrane synthesis for cell proliferation and long-term storage. During *de novo* lipid synthesis, the transcription factors SREBPs (*sterol responsive element binding protein*) plays an importing role in the control

lipogenic gene expression, necessary for lipid homeostasis, such as ACC (*acetyl-CoA carboxylase*), FASN (*fatty acid synthase*), and SCD-1 (*stearoyl-CoA desaturase 1*). mTORC1 promotes the trafficking, processing, and transcription of SREBPs[28–31] (**Figure 3**). SREBP and its downstream biosynthetic machinery for the synthesis of fatty acids and sterols can be activated in a S6K1-dependent manner, but its molecular mechanism remains unclear[28,32]. Furthermore, S6K1-independent activation of SREBP involves the activity of CRTC2 (*CREB regulated transcription coactivator 2*), Lipin1, and p300. CRTC2, a master regulator of gluconeogenesis, inhibits the translocation of SREBP from the endoplasmic reticulum to the Golgi. Inhibition of CRTC2 upon mTORC1-mediated phosphorylation attenuates its inhibitory effect on SREBP1 maturation[33]. Lipin1, a phosphatidic phosphatase, acts as an inhibitor of nuclear SREBP activity. mTORC1-mediated phosphorylation of Lipin1 blocks its nuclear entry and allows SREBP-dependent gene transcription[34]. SREBP-1c is also acetylated by the HAT (*histone acetyltransferase*) p300[35], and mTORC1-dependent phosphorylation of p300 is necessary for lipid synthesis through the activation of SREBP-1c[36]. Taken together, and through all these different pathways, SREBP mediates mTORC1-dependent lipogenesis.

The role of mTORC1 in lipid synthesis is particularly marked during adipogenesis, the biological process of mature adipocytes formation from adipose cell precursors though the enhanced synthesis and accumulation of triglycerides. This process is mediated by PPARγ (*peroxisome proliferator-activated receptor γ*), a nuclear receptor that controls fatty acid uptake, synthesis, esterification and storage in adipose cells[37]. PPARγ expression and activity are controlled by mTORC1. The molecular mechanism is mediated by 4EBP1[38], and through SREBP1-dependent PPARγ ligand production[39].

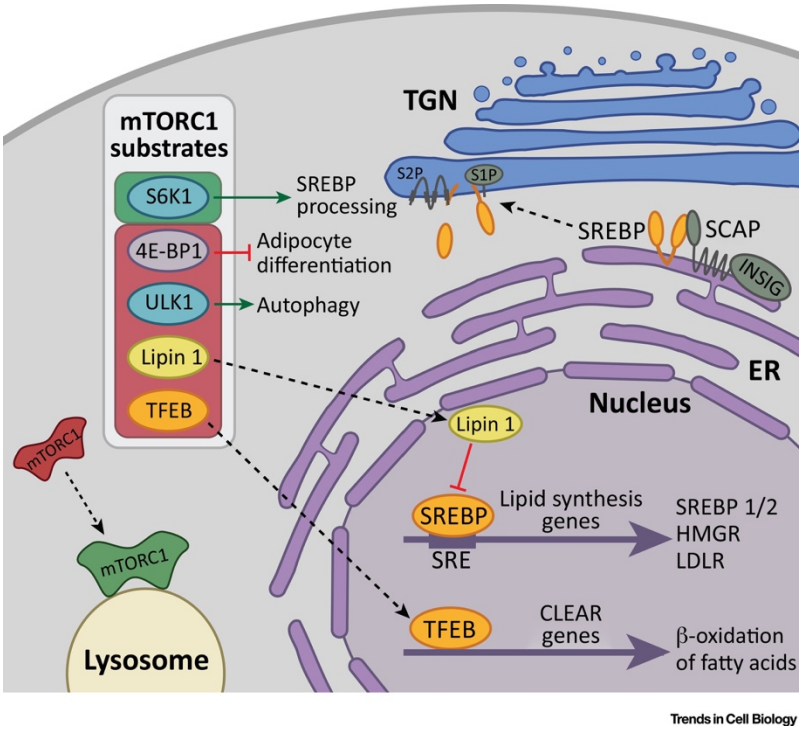

Figure 3. Lipid biogenesis and lipid catabolism regulation by mTORC1.

(From *Thelen & Zoncu 2017 Trends in Cell Biology 27(11):833-850*).

The transcription factor TFEB (*bHLH leucine zipper transcription factor EB*) regulates lysosome biogenesis, autophagosome formation and their fusion with the lysosome[40]. In addition, TFEB promotes beta-oxidation of fatty acids by upregulating the expression of PPARα and PGC1α (*PPARγ coactivator 1 α* or *peroxisome-proliferator-activated receptor coactivator-1α*)[41]. mTORC1-mediated phosphorylation of TFEB induces its interaction with the cytosolic protein 14-3-3 and blocks its translocation to the nucleus, repressing its transcriptional activity[42–44]. Thus, in parallel to the activation of lipid synthesis, mTORC1 inhibits lipid catabolism through TFEB inhibition.

1.2.1.3 Nucleotide synthesis

Nucleotides are building blocks for DNA and RNA, which are necessary for cell proliferation. Emerging evidences show that mTORC1 upregulates the synthesis of nucleotides. Through several approaches, in addition to enhancing the *de novo*

synthesis of lipids, mTORC1/S6K1-dependent SREBP activity induces the oxidative PPP (*pentose phosphate pathway*)[28]. Moreover, mTORC1 promotes the expression of PPP genes which contribute in the production of ribose moieties for the synthesis of both purine and pyrimidine nucleotides.

Pyrimidine nucleotide (CMP, UMP) is a nitrogen-containing base that is synthetized from glutamine, bicarbonate ($HCO3^-$), and aspartate with ribose-5-phosphate, derived from the PPP. Phosphoproteomic and metabolomic analyses revealed that mTORC1 promotes pyrimidine synthesis through S6K1-mediated CAD (*carbamoyl-phosphate synthetase 2, aspartate transcarbamylase, dihydroorotase*) phosphorylation and activation[45,46] (**Figure 4**). CAD catalyses the first three steps in *de novo* pyrimidine synthesis. The S6K1-mediated phosphorylation of CAD on S1859 induces its oligomerization, leading to an increased pyrimidine synthesis, and stimulating S phase progression. This regulation of CAD by mTORC1/S6K1 increase the pool of nucleotides available for the DNA replication and RNA synthesis that are necessary for cell growth.

Purine synthesis is a pathway that assembles carbon and nitrogen from glutamine, aspartate, glycine, bicarbonate ($HCO3^-$) and formyl unit from the THF (*tetrahydrofolate*) cycle on a PRPP (*5-phosphoribosyl-1-pyrophosphate*) molecule to form purine nucleotide (AMP, GMP). mTORC1 promotes purine synthesis through the ATF4-dependent upregulation of MTHFD2 (*methylene-tetrahydrofolate dehydrogenase 2*), an important enzyme of the mitochondrial THF cycle. In response to growth-induced stimuli, ATF4 induces also the expression of other enzymes of the serine synthesis (PSAT1 and PSPH) and the mitochondrial THF cycle (SHMT2), in order to increase the production of formyl units required for *de novo* purine synthesis[47].

In summary, in response to growth-induced stimuli, mTORC1 upregulates anabolic processes such as protein synthesis, lipid synthesis, and nucleotide synthesis. These mTORC1 functions are mediated by S6K1, 4EBP1 and SREBP1 which are all phosphorylated by mTORC1, inducing a signaling cascade pathway to control cell growth and proliferation.

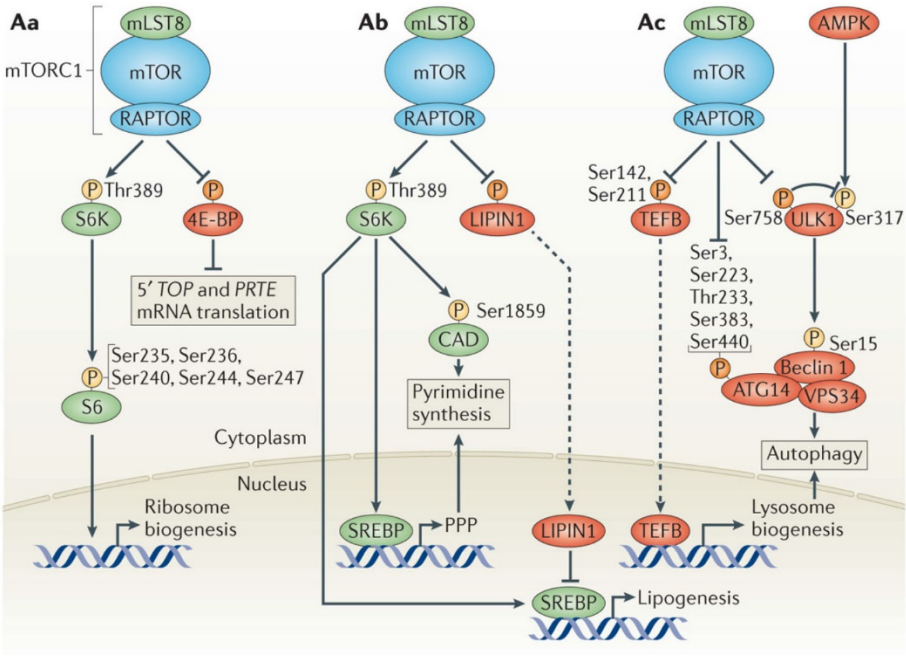

Figure 4. Anabolic processes controlled by mTORC1.

(**A**) mTORC1 promotes ribosome biogenesis. (**B**) mTORC1 activated nucleotide and lipid synthesis. (**C**) mTORC1 inhibited autophagy.
(Modified from *Shimobayashi & Hall 2014 Nat Rev Mol Cell Biol. 15(3):155-62*).

1.2.2 Control of anabolic metabolism

Cellular metabolism is also controlled by mTORC1 in order to have enough metabolites and energy for cell proliferation. mTORC1 exerts this regulation in many different ways.

1.2.2.1 Glucose metabolism

Through oxidative glycolysis, cells use glucose for energy production and building block assembly, necessary for cell growth[48,49]. As a central controller of cell growth, mTORC1 promotes the shift in glucose usage from oxidative phosphorylation to

aerobic glycolysis, facilitating metabolic intermediates production for the biosynthesis of macromolecules. Indeed, mTORC1 increases glycolytic flux by activating both the transcription and the translation of HIF1α (*hypoxia inducible factor 1* α), which induces the expression of glucose transporters GLUT1, GLUT3 and several glycolytic enzymes such as PKM2 (*pyruvate kinase M2 subtype*) or HK (*hexokinase*)[50–54]. Moreover, mTORC1/SREBP pathway increases the carbon flux from glucose through the oxidative PPP to generate NADPH and other intermediary metabolites needed for proliferation and growth[28]. Interestingly, mTORC1-dependent glucose metabolism activation leads, in certain circumstances, to glucose addiction in cancer cells[55–57].

1.2.2.2 Glutamine metabolism

In addition to glucose, the amino acid glutamine (the most abundant amino acid in the blood of mammals) is a major nutrient that fuels cellular energetic to allow cell growth. The relationship between glutamine and mTORC1 is very tight, as glutamine metabolism activates mTORC1[58,59], and in turns glutamine metabolism is controlled by mTORC1activity[60–62]. The connexion between glutamine and mTORC1 will be detailed in further section of the second chapter.

1.2.2.3 Mitochondrial metabolism

Growing cells need not only glucose and glutamine, but also a number of mitochondrial intermediates to generate building blocks. Thus, it is not surprising that mTORC1 controls and stimulates mitochondrial oxidative activities through different mechanisms. In skeletal muscle tissues and cells, mTORC1 regulates the interaction of YY1 (*yin-yang 1*) with PGC1α, affecting the transcriptional function of this complex, which regulates the expression of mitochondrial genes involved in oxidative functions[63]. In addition to that, mTORC1 controls mitochondrial biogenesis and

function by promoting translation of nucleus-encoded mitochondria-related mRNAs through 4EBP1 inhibition[64].

1.2.2.4 Other metabolic pathways

Amino acids contributing to the so-called *one carbon metabolism* (e.g. serine and glycine) integrate different stimuli through folate and methionine cycles, to induce cell proliferation[65]. This type of metabolism has been revealed to play an important role in diseases in which mTORC1 is involved, such as cancer. Indeed, mTORC1 has been reported to control serine/glycine *de novo* synthesis in osteosarcoma cells through the regulation of the expression of genes involved glycolysis and serine/glycine synthesis[66].

Recently, mTORC1 has been shown to regulate polyamine metabolism in addition to other anabolic processes in prostate cancer[67]. Polyamines are small polycations, containing two, three, or four amine groups which have diverse functions such as maintaining chromatin conformation and membrane stability. The control of polyamine concentration is very tight because polyamine excess leads to hydrogen peroxide release[68]. mTORC1 regulates polyamines flux through phosphorylation-dependent stability of pro-AMD1 (*s-adenosyl-L-methionine decarboxylase 1*)[67]. This mTORC1-mediated induction in polyamine synthesis explains the high levels of polyamines observed in highly proliferating cells.

1.2.3 Regulation of protein turnover

In addition to inducing cell anabolism, mTORC1 controls cell growth by suppressing cell catabolism. Two major catabolic processes are known to operate downstream of mTORC1 signaling: autophagy and protein degradation through the ubiquitin-proteasome system.

1.2.3.1 Autophagy

Autophagy is a multistep degradation process that is necessary for macromolecules recycling and maintenance of cellular homeostasis. During autophagy, cellular components are sequestered into autophagosomes (double membrane bound vesicles) that will fuse with lysosomes to form the autolysosomes in which the proteolytic degradation happens[69]. Autophagy is activated by AMPK (*AMP-activated protein kinase*) signaling and inhibited by mTORC1[70]. Indeed, mTORC1 regulates different steps of autophagy. The protein kinase ULK1 (*Unc-51 like autophagy activating kinase*), belonging to the ULK complex, is the key downstream target of mTORC1 in the control of autophagy[71–73] (**Figure 3-4**). Under nutrient-rich conditions, mTORC1 phosphorylates and inhibits ULK1 at Ser757, preventing its interaction with AMPK, and thus inactivating autophagy[70]. Upon mTORC1 inhibition, AMPK interacts with and activates ULK1 by phosphorylating several residues (Ser555, Ser317 and Ser777). Then ULK1 will induce autophagy by activating the lipid kinase VPS34, necessary for autophagosome formation[74].

In addition to ULK1 phosphorylation, mTORC1 directly phosphorylates two other autophagy-activating proteins: ATG13, a positive regulator of ULK1[71–73], and ATG14, a VPS34-associated component[75]. Therefore, mTORC1 directly phosphorylates and inhibits different mediators that positively control autophagy.

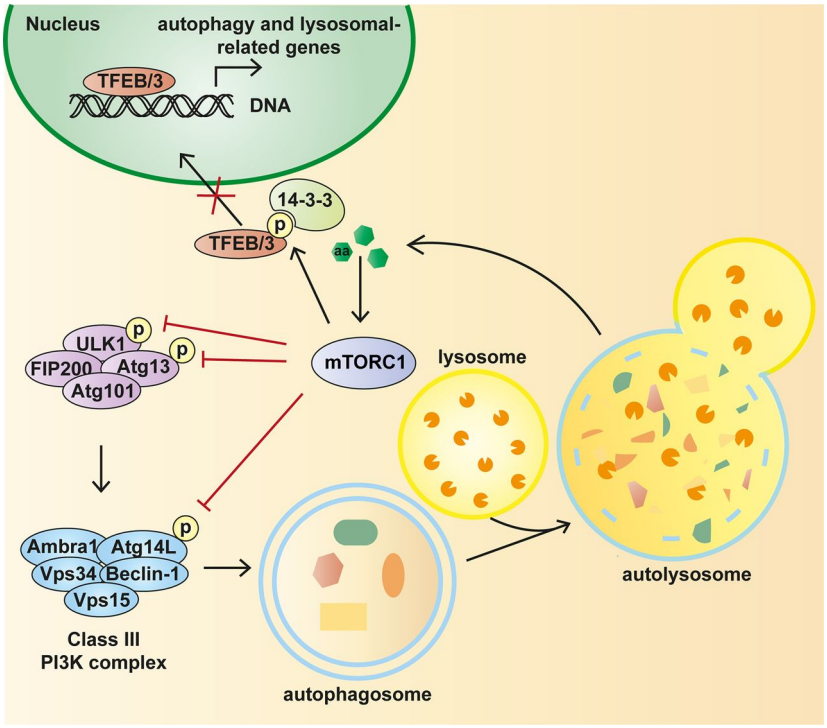

Figure 5. Regulation of autophagy by mTORC1.

To control autophagy in response to amino acid stimuli, mTORC1 phosphorylates ULK, ATG13, ATG14-containing Vps34 complex and TFEB. When mTORC1 is inhibited, the activation of autophagy allows the cell to maintain necessary energy and metabolites for surviving the starvation condition.
(From *Rabanal-Ruiz et al., 2017 Essays Biochem 61(6):565-584*).

Indirectly, mTORC1 controls autophagy through the transcription factor TFEB, which controls lysosome biogenesis and autophagy[40,42–44]. mTORC1-mediated TFEB phosphorylation prevents its nuclear translocation and represses the transcription of lysosomal and autophagy-related genes. In addition, mTORC1 controls autophagy in a fine-tuning manner through the HAT p300[36] and NRBF2/Atg38[76]. Finally, DAP1 (*death-associated protein 1*) negatively controls autophagy when its mTORC1-mediated phosphorylation is removed upon mTORC1 inactivation. The control of autophagy by DAP1 aims at limiting the over-activation of autophagy, maintaining the homeostasis balance. The molecular mechanism of DAP1-mediated autophagy limitation is still unknown[77].

In the context of cancer, autophagy has a dual role, preventing tumor initiation[78], but in the other side supporting cell survival under metabolic stress[59]. Thus, the close connection between mTORC1 and autophagy allows an efficient response in function of nutrient availability, depending on the stage and context of the cancer.

1.2.3.2 Ubiquitin-proteasome system

UPS (*ubiquitin-proteasome system*) is a main mechanism for protein catabolism, through which proteins targeted for degradation are tagged by ubiquitine multimers and degraded by the 26S proteasome[79]. UPS-mediated protein degradation is tightly controlled, and its perturbation leads to diverse disease such as cancer and neurodegeneration[80–83]. As a major regulator of protein catabolism, mTORC1 also controls protein homeostasis through UPS inhibition. Indeed, mTORC1 inhibition increases proteasome-dependent proteolysis through an increase in protein ubiquitination without affecting the proteasome activity[84]. In addition to this, mTORC1 inhibition also induces proteasome abundance via ERK5 (*extracellular signal-regulated kinase 5*) activation[85]. Paradoxically, the team of Prof Brendan Manning reported that mTORC1 activation induces an increase in cellular proteasome content through the expression of NRF1 (*nuclear factor erythroid-derived 2-related factor 1*). This opposite effect of mTORC1 positively regulating proteasome content was explained by the authors as a necessary mechanism for the removal of misfolded protein upon mTORC1-induced protein synthesis[86]. Further investigations are needed to better understand how mTORC1 coordinates these opposite effects to control proteasomal degradation of targeted proteins.

1.3 Upstream regulation of mTORC1

Four main upstream mechanisms of mTORC1 regulation will be described below: amino acid availability, growth factor signaling, hypoxic and bioenergetics stress, and lipid sensing (**Figure 6**).

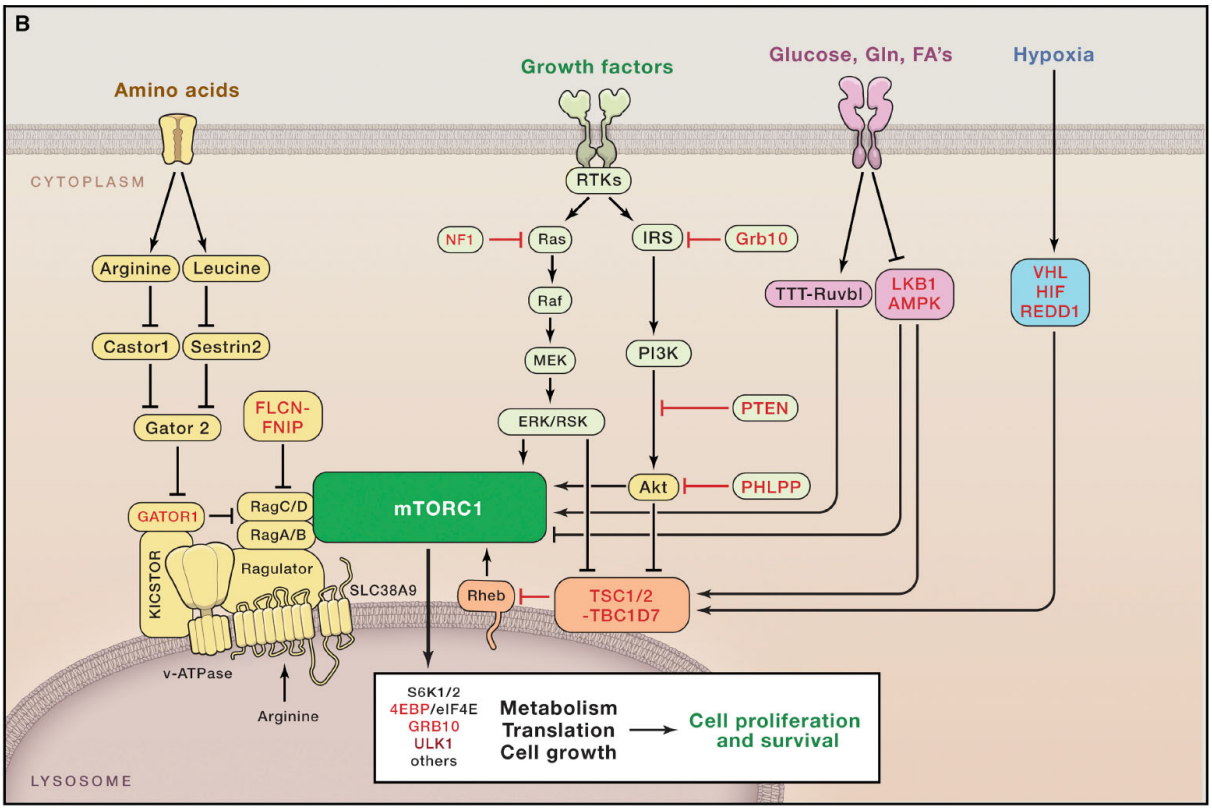

Figure 6. Summary of main upstream regulators of mTORC1 in response to activating stimuli.

Tumor suppressors are in red, whose loss of expression/function occurs in cancer. Positive regulators of mTORC1 are in green, which are often activated by mutation or overexpression in cancer.
(From *Blenis 2017 Cell 171(1):10-13*).

1.3.1 Amino acids

mTORC1 activation by amino acid involves predominantly the conserved Rag family of small GTPases on the surface of the lysosome. Four mammalian Rags (RagA, RagB, RagC, RagD) are localized at the surface of the lysosome independently of amino acid availability using the pentameric Ragulator complex as a scaffold[87–91]. In yeast, Rag orthologues are the Gtr1/2 GTPases[92–94], which localize to the surface of

the vacuole and bind to the ternary complex Ego[95,96] (analogue to the Ragulator complex) (**Figure 7**).

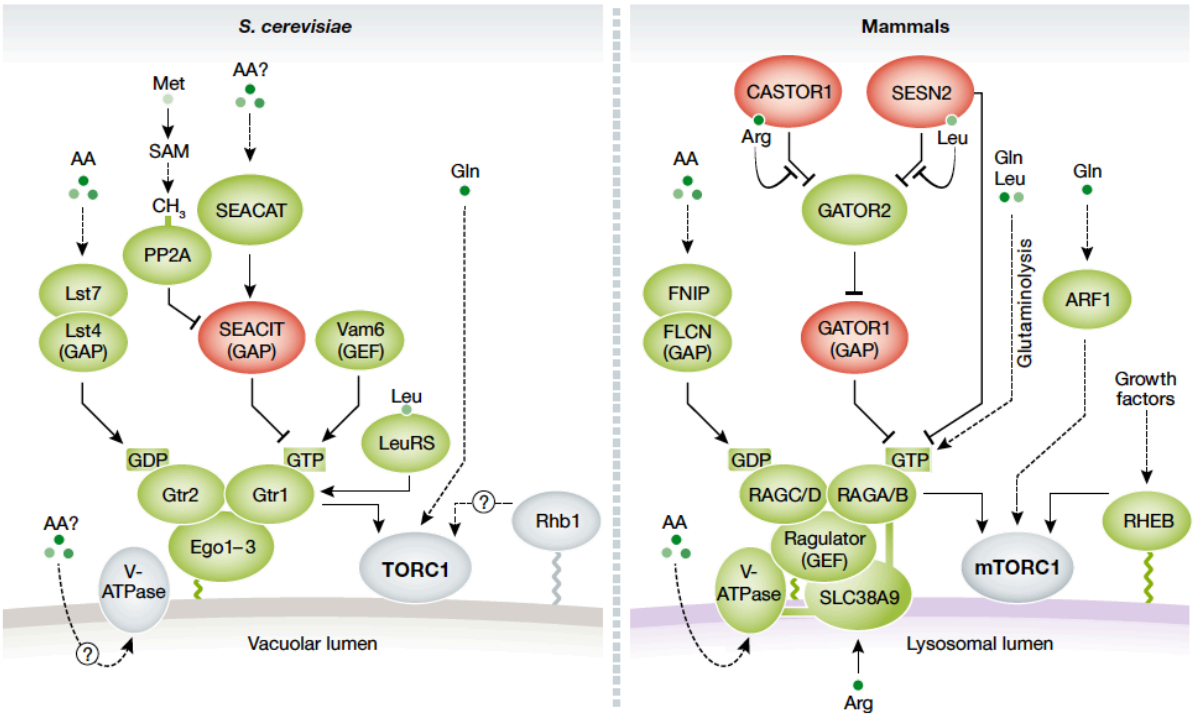

Figure 7. Regulation of TORC1 by amino acids in yeast (left) and mammals (right).

Proteins shown in green promote TORC1 activation. Proteins in red inhibit TORC1. Dashed lines indicate indirect interactions.
(From *González & Hall 2017 The EMBO Journal 36:397-408*).

The Rag GTPases function in a heterodimeric form in which RagA or RagB interact with RagC or RagD. In conditions of amino acid availability, the subunit RagA/B is loaded with GTP, while the subunit RagC/D is GDP loaded, rendering an active conformation of the heterodimer[97,98]. Under this active conformation, mTORC1 binds to the Rag heterodimer through Rag-Raptor interaction, which leads to the translocation of mTORC1 to the lysosomal surface[99]. Once at the lysosomal surface, mTORC1 is fully activated through its direct interaction with the co-activator Rheb (*RAS homolog enriched in brain*). Rheb is a growth factor-stimulated small GTPase which, upon growth factor stimulus, is GTP-loaded to allow the full activation of

mTORC1[100,101]. Thus, both amino acids and growth factors are necessary to completely activate mTORC1 (see below for a full description of mTORC1 activation by growth factors).

Since the finding of the Rag GTPases as nutrient sensors for mTORC1 activation, different proteins have been identified as regulators of the nucleotide binding status of the Rags, operating either as GAP (*GTPase-activating proteins*) or GEF (*guanine exchange factors*) of these small GTPases. GEFs regulate the replacement of GDP by GTP, while GAPs stimulate the intrinsic GTPase activity of a related GTPase to convert GTP into GDP. In the context of the Rag GTPases, Ragulator and Gator1 have respectively GEF and GAP activity toward RagA/B. Ragulator consists of p18/Lamtor1, p14/Lamtor2, MP1/Lamtor3, HBXIP/Lamtor4 and C7orf59/Lamtor5, among which p18/Lamtor1 is a critical scaffold element for the Ragulator-Rag GTPase complex described by different structural studies[88,90,91,102]. Although all 5 subunits are needed for the GEF activity, the exact mechanism of Ragulator's GEF activity is still unknown. In yeast, Ego complex (ortholog to the Ragulator) does not play the same role, as the vacuolar protein Vam6 has been proposed to be the GEF for Gtr1[97].

The mammalian heterotrimeric protein complex Gator1 (*GAP activity toward RAGs 1*) is composed of DEPDC5 (*DEP domain-containing protein 5*), NPRL2 (*nitrogen permease regulator 2-like protein*), and NPRL3[103,104]. Gator1 is tethered to the lysosomal surface through the Kicstor complex (consisting of KPTN, ITFG2, C12orf66, and SZT2)[105,106] and negatively regulated by Gator2 complex, consisting of SEC13 (*protein SEC13 homolog*), SEH1L (*nucleoporin SEH1*), WDR24 (*WD repeat-containing protein 24*), WDR59, and MIOS (*WD repeat-containg protein MIO*)[103,107]. In the case of the RagC/D subunit, FLCN (*Folliculin*) and its binding partners FNIP1/2

(*folliculin-interacting proteins 1 and 2*) have been described to operate as GAPs in mammals[108,109], while no GEFs have been described so far.

The question about how cells integrate the information about each amino acid availability to coordinate the response regarding the nucleotide loading state of the Rag GTPases is far to be well understood. Similarly, it is not well known how the concerted regulation of all the members of the amino acids-mediated mTORC1 activation pathway takes place. Even how amino acid availability is sensed and signalled to the Rags are still elusive, although different sensors have been described in the literature. Two main mechanisms by which mammalian cells sense amino acids have been describe, the *lysosomal pathway* and the *cytosolic pathway*. In the lysosome surface, v-ATPase (*vacuolar H(+)- adenosine triphosphatase*) plays an intermediate role of an "inside-out" mechanism, in which amino acids must accumulate in the lysosomal lumen to initiate signaling[110]. Then, amino acids inside the lumen can affect the Rag nucleotide state through the ATP hydrolysis capacity and the associated rotation of the v-ATPase. Cytosolic amino acids, such as leucine, arginine and glutamine, signal to mTORC1 mostly through the Gator1/Gator2 complexes[3].

For leucine sensing, Sestrin and leucyl-tRNA synthetase are two sensors that mediate leucine signaling in mTORC1 pathway. Sestrins negatively regulate mTORC1 through Gator2 inhibition[111–114] and leucine stimulation dissociates Sestrin2 from Gator2 to activate mTORC1. Furthermore, decreased leucine import due to the loss of glutamine (SLC1A5) or leucine (SLC7A5-SLC3A2) transporters impairs mTORC1 activity[115].

By following a mechanism similar to the one described for Sestrins, Castor1/2 were discovered as cytosolic arginine sensors[116,117]. Under arginine deprivation, Castor1/2 binds to Gator2 preventing Gator2-mediated mTORC1 activation. Moreover, the

transporter SLC38A9 have been proposed to be a lysosomal arginine sensor that also controls mTORC1 activation[118–120].

In addition to the role as efflux solute for leucine import, glutamine can activate mTORC1 both in Rag-dependent and Rag-independent manners. In cooperation with leucine, glutamine is able to induce the GTP loading of Rag, thus activation mTORC1, by following a mechanism in which PHDs (*Prolyl Hydroxylases Domain*) have been involved[58,121]. In addition to that, glutamine also stimulates lysosomal translocation and activation of mTORC1 via the small GTPase ARF1 (*ADP-ribosylation factor 1*) and v-ATPase in a Rag-independent manner[122]. The metabolism of glutamine and its connection to mTORC1 will be discussed below in a specific section.

1.3.2 Growth factors

mTORC1 regulation by growth factors imply the role of the tumor suppressor TSC1/TSC2 complex (*tuberous sclerosis complex*), a key negative regulator of mTORC1. TSC is a heterotrimeric complex comprising TSC1, TSC2 and TBC1D7[123], and its lost-of-function mutations lead to the development of tuberous sclerosis complex, or Bourneville's disease, due to the hyperactivation of mTORC1. TSC2 has a GAP function toward the small GTPase Rheb[124,125], while TSC1 acts as a scaffold to stabilize TSC2 and TBC1D7. The role of TBC1D7 is not fully understood, but its loss causes the dissociation of the complex[123].

Growth factors, particularly insulin and IGF1 (*insulin-like growth factor 1*) inhibit TSC complex in a PI3K (*phosphoinositide 3-kinase*)-dependent manner. Upon TSC inhibition, the GAP activity of TSC is reduced, leading to the GTP loading of lysosomal Rheb. Then Rheb will interact with lysosomal translocated mTORC1 (induced by amino acid availability, as explained above). The mechanism of how Rheb activates mTORC1 is still elusive[126,127]. A structural study by cryo-electron microscopy reported

that Rheb binds to mTOR distally from the kinase active site and causes a global conformational change that allosterically realigns active-site residues, accelerating catalysis[128].

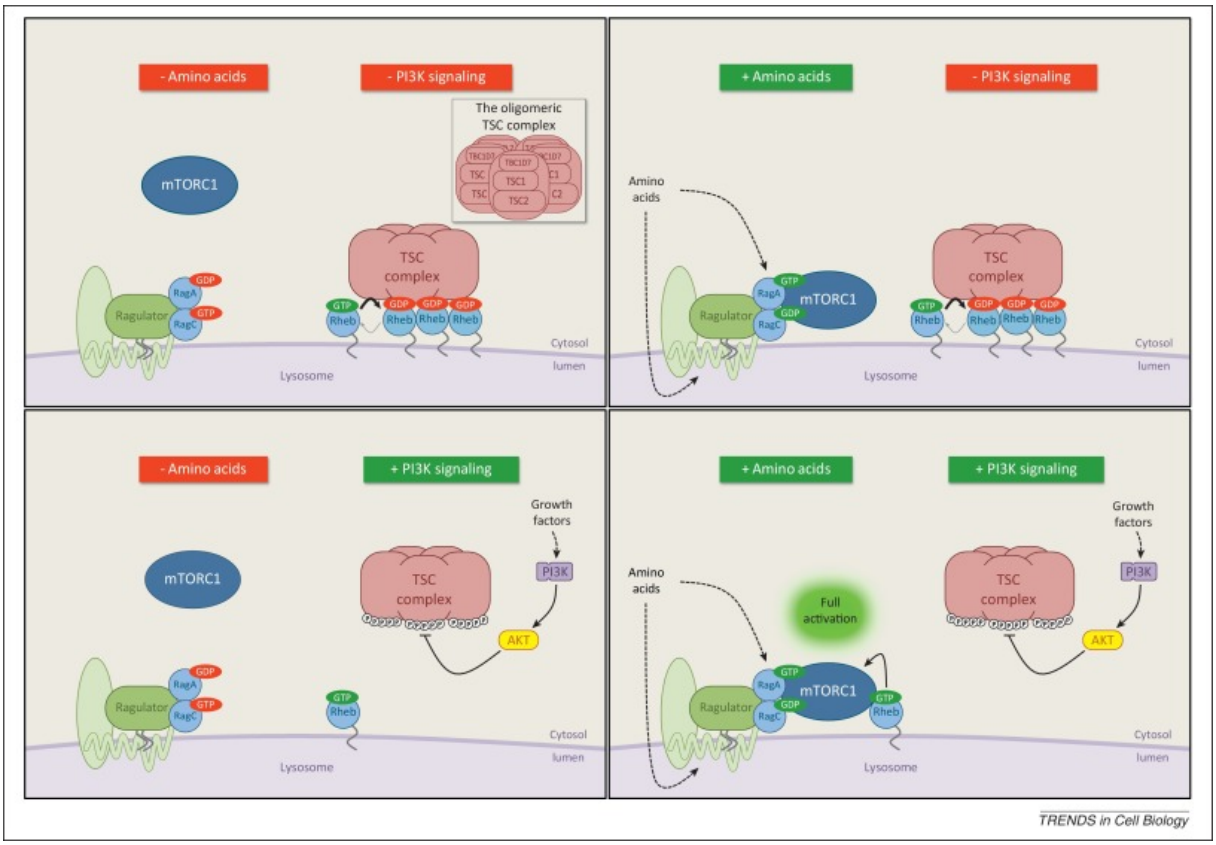

Figure 8. Rheb mediates mTORC1 activation in response to PI3K/AKT-dependent growth factor signals.

Amino acid signaling and growth factor-PI3K signaling promote mTORC1 in parallel to fully activating mTORC1 pathway. The molecular mechanism is detailed in the text. (Modified from *Dibble and Cantley 2015 Trends in Cell Biology 25(9):545-555*).

Growth factors and mitogen-dependent signaling pathways control mTORC1 activity via two mains mechanisms. On the one hand, through the insulin/IGF-1 pathway mediated by PI3K and PDK1, the AKT-dependent phosphorylation of TSC2 inhibits and dissociates TSC complex from the lysosomal membrane, where Rheb localizes[129,130] (**Figure 8**). In addition to TSC2 phosphorylation, AKT phosphorylates also PRAS40 in mTORC1 to disrupt the inhibitory interaction Raptor-PRAS40, allowing

mTORC1 to be fully activated[127,131]. On the other hand, the MAPK (*mitogen-activated protein kinase*) ERK and its effector RSK (*90 kDa ribosomal S6 kinase*), via Ras signaling pathway, phosphorylate and inhibit TSC2[132,133]. Also, ERK and RSK phosphorylate Raptor to promote mTORC1 activity[134,135]. Besides, Wnt pathway and the inflammatory cytokine TNFα phosphorylate and inhibit TSC2 and TSC1 respectively to activate mTORC1[136,137]. Taking together, through Rheb and Rag GTPase family, mTORC1 signaling pathway integrates amino acid and growth factor inputs to be fully activated.

1.3.3 Energy, oxygen, stress and DNA damage

For cell growth and proliferation, in addition to positive growing signals and building blocks, cells also need energy. Energy sensing in growing cells is greatly related to glucose availability and metabolism. The sensing of the energetic status of the cell acts through the conserved AMPK pathway. In conditions of glucose deprivation, or after the inhibition of glycolysis/mitochondrial respiration, AMP/ATP ratio and ADP/ATP ratio are increased, due to a decrease in ATP synthesis. This increase in AMP/ATP ratio leads to the activation of AMPK, which promotes catabolic processes like autophagy, and inhibits anabolic processes such as protein synthesis, through mTORC1 inhibition. AMPK inhibits mTORC1 via TSC activation or Raptor inhibition[138,139]. Interestingly, v-ATPase-Ragulator have been shown to activate AMPK through AXIN-LKB1 on lysosome surface and therefore to inhibit mTORC1 under energy stress[140]. Besides, mTORC1 can sense glucose availability independently of AMPK, through the inhibition of the Rag GTPases[141,142].

Growing cells also need to detect other intracellular/environmental stresses that are incompatible with growth, hypoxia or DNA damage. These stresses control mTORC1 following opposite mechanisms. In one side, redox stress upregulates mTORC1

through TSC1/2-Rheb pathway, by increasing the GTP-bound state of Rheb[143]. However, energy stress downregulates mTORC1 via p38β-PRAK-mediated Rheb inhibition[144]. Controversially, p38β enhances mTORC1 activity under arsenite treatment via Raptor phosphorylation[145]. Thus, p38 enhances or reduces mTORC1 activity in function of different environmental stresses by regulating different components of mTORC1 pathway.

In the case of oxygen availability, it is well stablished the capacity of hypoxia to inhibit mTORC1. The hypoxia-dependent inhibition of mTORC1 follows two mechanisms: an AMPK-mediated mechanisms[146], and a HIF1-dependent mechanism. The second one involves the upregulation of REDD1 (*Regulated in DNA damage and development 1*), a HIF1 target gene which activates TSC complex[147,148]. Indeed, REDD1 binds to 14-3-3 protein and disrupts the interaction of TSC2/14-3-3, leading to TSC1/2 activation and mTORC1 inhibition[149]. In addition, it has been speculated that hypoxia could inhibit mTORC1 also through direct inhibition of PHD activity, which has been demonstrated to mediate glutaminolysis-induced mTORC1 activation[121]. Interestingly, and in contrast to what has been described for HIF1, HIF2 acts as an mTORC1 activator via the amino acid transporter SLC7A5, a HIF2-dependent target, in lung and liver tissues[150].

1.3.4 Lipid sensing

PLD (*Phospholipase D*) is an enzyme involved in cell growth, and as a consequence it is upregulated in a large number of different types of tumors. In mammals, there are two isoforms of PLD: PLD1 and PLD2, both of them shown to activate mTORC1 through phosphatidic acid (PA) production and through their own expression[151,152]. PA is a phospholipid, known as an indicator of lipid sufficiency in dividing cells. PA can be generated by the hydrolysis of phosphatidylcholine by PLD, by LPAAT (*lysophosphatidic acid acyltransferase*) or DG (*diacylglycerol*) kinases. This is a central

metabolite for membrane phospholipid biosynthesis. PA-mediated mTORC1 activation connects mTORC1 to both lipids and glucose metabolism. Originally, PA and its analogues were shown to activate mTORC1 from exogenous supply[153,154]. The effect of PA towards mTORC1 depends on amino acids availability, and is suppressed by rapamycin treatment or by over-activation of TSC1/2. Suppression of PLD-generated PA with primary alcohols inhibit mTORC1 activity[155], while PA production by other enzymes, such as LPAAT[156] or DG kinase[157], increases mTORC1 activity, showing that PA is physiologically necessary for mTORC1 activation. Finally, lipid sensing by mTORC1 was confirmed via *de novo* synthesis of PA which inhibition resulted in G1 cell cycle arrest[158]. PA production is also induced by Rheb, as PLD is a downstream target of Rheb (**Figure 9**). Rheb binds to and activates PLD in a GTP-dependent manner, then PLD-generated PA interacts and upregulates mTORC1[159]. Additionally, RalA (*Ras-related protein A*) and the GTPase ARF6 (*ADP-ribosylation factor 6*) are acting downstream of Rheb to induce this production induced by growth factor[160–162]. Furthermore, amino acids can induce PLD translocation to the lysosome and increase its activity through the class III PI3K hVps34[163]. Thus, PLD-derived PA contributed to nutrient mediated mTORC1 activation, and PA is necessary but not sufficient to activate mTORC1. There are different hypotheses about the mechanism of PA-mediated mTORC1 activation. These hypotheses mostly suggest two potential mechanisms: either PA interaction with the FRB domain in mTOR[153] enhances mTORC1 activity, or it increases the stability of the mTORC1 complex[164]. Controversially, in a study that showed for the first time the anti-oncogenic role of PA-mediated PLD function, production of PA was recently shown to activate LKB1, which would result in an AMPK-mediated inhibition of mTORC1[165]. The balance between PA-

mediated mTORC1 activation and PA-mediated LKB1 upregulation is cell type specific and dependent of the pathway activation.

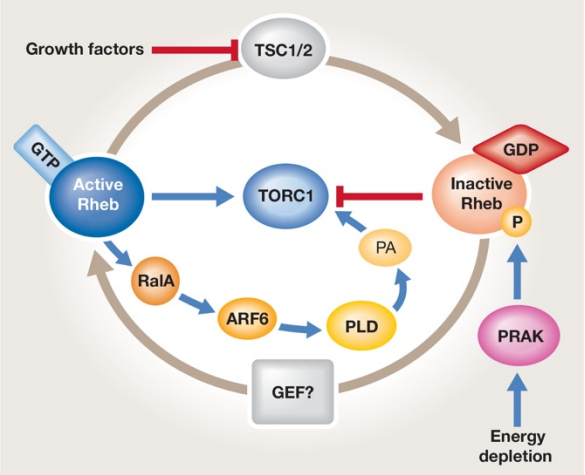

Figure 9. Phosphatidic acid-mediated mTORC1 activation.

(From *Durán & Hall 2012 EMBO reports 13(2):121-128*).

1.4 mTORC1 inhibitors in anti-cancer therapies

Playing an important role in cell growth regulation, mTORC1 is frequently dysregulated in cancer. Loss or inactivation of tumor suppressors such as TSC1/2 or PTEN (*Phosphatase and TENsin homolog*), leads to an increased mTORC1 signaling pathway and promote tumorigenesis[138]. Moreover, downstream targets of mTORC1 such as S6K1 or 4EBP1 are aberrantly activated in several human cancers with very poor prognosis. Overall, due to its key role in tumor growth and survival, mTORC1 has emerged as an important target for anti-cancer therapies (**Figure 10**). Thus, the development of new generation mTOR inhibitors in anti-cancer therapies is a very attracting and challenging research field.

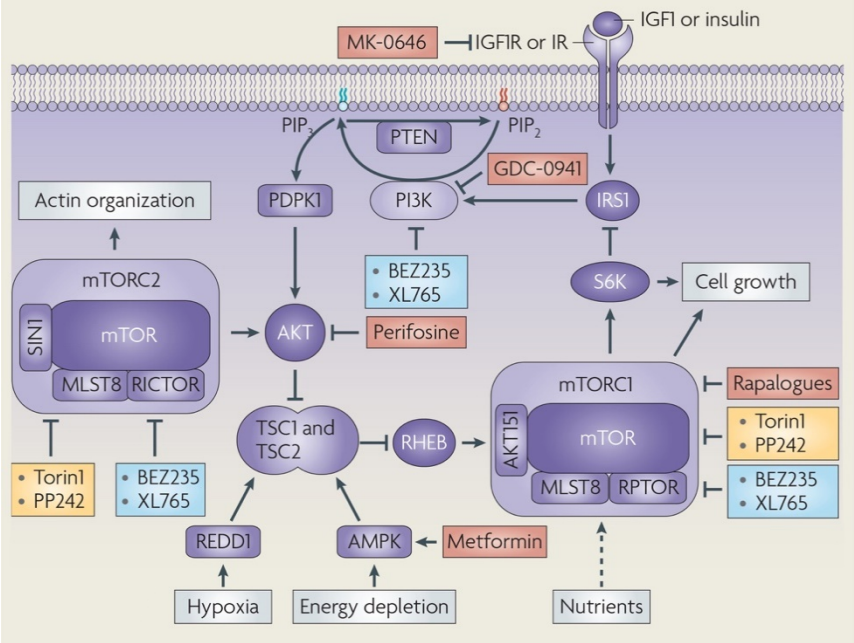

Figure 10. Different classes of mTOR inhibitors.

First class of inhibitors and activators shown in red. Inhibitors for both mTORC1 and mTORC2 shown in yellow. Dual inhibitors for PI3K and mTORC1 and mTORC2 shown in blue. (From *Tennant et al., 2010 Nat Rev Cancer 10:267-277*).

1.4.1 Mechanism of rapamycin-mediated mTORC1 inhibition

Originally extracted from *Streptomyces hygroscopicus,* rapamycin was the first discovered mTORC1 inhibitor. It was originally used as an antibiotic due to its antifungal properties. Rapamycin was discovered in 1964 on Easter Island (Rapa Nui), a South Pacific Polynesian island by Seghgal and collegues[166]. After its discovery, rapamycin became well known thanks to its remarkable antifungal, immunosuppressive, and anticancer effects. Then, TOR/mTOR was found to be the target of rapamycin in yeast and mammals[1,167–170].

The molecular mechanism of rapamycin-mediated mTORC1 inhibition is still elusive. What we know is that rapamycin forms a complex with FKBP12 which then by to the FRB domain of mTOR[168]. The binding of rapamycin/FKBP12 to the FRB domain of mTOR somehow impairs the interaction between mTOR and Raptor, blocking the entry

of mTORC1 substrates to the active site[171,172]. However, at high concentrations, rapamycin can bind directly to the FRB domain without forming the complex with FKBP12[173]. In contrast to mTORC1, mTORC2 is insensitive to the effect of rapamycin, but some studies revealed that prolonged rapamycin treatment leads to mTORC2 inhibition only in some cell types[174,175]. Rapamycin has a very poor water solubility, limiting its bioavailability. That's why rapamycin analogues have been developed.

1.4.2 Different classes of mTOR inhibitors

1.4.2.1 First generation of mTOR inhibitors

The first class of mTORC1 inhibitors are called *rapalogs*, such as temsirolimus (CCI-779), everolimus (RAD001) or ridaforolimus (AP23573), which are rapamycin analogues, conceived to improve its pharmacokinetics properties. The chemical modifications introduced in these analogues do not modify their interaction with FKBP12 neither with mTOR, following the same mechanism as explained above. Among all, temsirolimus and everolimus were approved for the treatment of advanced stage renal cell carcinoma and sarcoma, respectively[176,177]. In contrast to the results obtained in cells, rapalogs do not efficiently inhibit cancer proliferation *in vivo*, showing mostly disease stabilization due to their cytostatic effects and lack of cytotoxicity[178,179]. Different reasons have been invoked to explain this inefficacy. Firstly, rapalogs only act towards mTORC1, and do not inhibit mTORC2. Secondly, rapalogs cannot inhibit totally the phosphorylation of 4E-BP1[180]. And third, rapalogs induce PI3K/AKT phosphorylation and upregulation by blocking the negative-feedback loop from S6K1 to IRS1 (*insulin receptor substrate-1*). Indeed, mTORC1-mediated S6K1 phosphorylation leads to the inhibition of IRS1, further inhibiting the PI3K/AKT pathway[181,182]. As a consequence of the release of this negative feedback, AKT

pathway gets activated upon rapamycin/rapalogs treatment, leading to drug resistance and tumor survival.

Despite their limited efficiency, this type of inhibitors is still tested in combination with standard chemotherapies or additional targeted therapies. The properties of the rapalogs (high specificity, minimal side effects, and clinical approval) are beneficial for combinations with other therapies to increase cytotoxicity and to induce tumor regression. Indeed, combination of rapalogs with chemotherapeutics such as paclitaxel and cisplatin induces a stronger anti-tumor effectiveness than single-agent therapy[183]. Similarly, their combination with IGF1R (*insulin-like growth factor-1 receptor*) antagonists (a strategy currently under clinical evaluation) enhances the anti-proliferative effect of rapalogs in breast cancer, prostate cancer, and in myelomas[184].

1.4.2.2 Second generation of mTOR inhibitors

ATP-competitive inhibitors or active site mTOR inhibitors have been developed to inhibit both mTORC1 and mTORC2, such as Torin1, PP242, WYE-354 and Ku-0063794[185–188]. As expected, these inhibitors block not only the phosphorylation of S6K1 but also the phosphorylation of 4EBP1 and AKT, having in consequence stronger effects than rapamycin on cell growth inhibition. Despite their potential toxicity, some of these inhibitors have been already tested in clinical trials and showed potential anti-cancer efficacy. However, they have only shown limited success in KRAS driven tumors[189], for which combinational therapy may be needed.

Because of the similarity between the kinase domains of mTOR and of PI3K, the development of dual mTOR/PI3K inhibitors has been an active field of research during last years[190]. The dual inhibition of mTOR and PI3K pathways would eliminate the negative consequences derived from the rapamycin-induced negative feedback loop inhibition, as explained above. Nevertheless, despite good promising original results,

some types of cancer showed insensitivity to this dual inhibition, together with additional problems derived of an increased cytotoxicity[191,192].

1.4.2.3 Alternative routes of mTOR inhibition

As phosphatidic acid is an activator of mTOR complex stability, development of PA-competitive inhibitors becomes an alternative strategy to develop mTOR inhibitors. PA-competitive inhibitors have been reported to reduce phosphorylation of S6K1[193]. Alternatively, as PA is generated by PLD1, strategies directed to inhibit of PLD1 could also be envisioned for the inhibition of mTOR. Farnesylthiosalicylic acid and farnesyltransferase inhibitors inhibit mTOR activity by disrupting the localization of Rheb and promoting dissociation of Raptor from mTOR *in vitro*[194]. Finally, as mTORC1 is an amino acid sensor, amino acid starvation could be an attracting option of indirectly inhibit mTORC1. For example, asparaginase treatment (already approved for acute lymphoblastic leukaemia therapy) reduces asparagine and glutamine levels in the circulation, with the corresponding downregulation in mTORC1 activity[195].

2. Glutamine metabolism

2.1 Metabolic transformation in cancer cells

Among the different hallmarks of cancer[196], metabolic transformation plays a key role in the adaptation of cancer cells to a changing environment. Cancer cells harbor oncogenic mutations, leading to an increase in nutrient uptake, and altering their metabolism to support anabolic processes for cell growth and proliferation.

2.1.1 Uptake

In order to guarantee a rapid cell proliferation, cancer cells firstly need to increase the uptake of nutrients from the extracellular environment. Glucose and glutamine are two main nutrients that cancer cells uptake from extracellular environment. Cancer cells become easily "addicted" to glucose and glutamine, as their withdrawal can induce cell death. Through the catabolism of glucose and glutamine, the cells produce both carbon intermediates as building blocks and reducing power for macromolecules production and ATP generation. The increase in glucose consumption by cancer cells was first described by Otto Warburg[48]. He saw that cancer cells consume 10-times more glucose than non-proliferating normal cells, and they converted glucose to lactate instead of using that glucose for respiration using oxygen. The so-called "Warburg effect" (or aerobic glycolysis) has become a well-known and common metabolic phenotype allowing tumor to fulfil the energetic requirement for cell growth[49]. PET (*positron emission tomography*)-based imaging of the high uptake of a radioactive fluorine-labeled glucose analogue ^{18}F-FDG (*^{18}F-fluorodeoxyglucose*) by cancer cells is used as an imaging tool for the detection of several cancers and for the treatment response[197]. Cancer cells acquired oncogenic alterations to increase glucose uptake, independently of external stimuli. For instance, PI3K/AKT pathway promotes both the expression of glucose transporter GLUT1 mRNA and the translocation of GLUT1

protein from endomembranes to the cell surface[198,199]. Furthermore, AKT potentiates the activity of HK and PFK (*phosphofructokinase*) enzymes, which catalyse rate-limiting steps of glycolysis, in order to induce glucose consumption to branching pathways[200–202]. Additionally, GLUT1 mRNA expression is upregulated by Src or Ras protein, mostly in the presence of two enhancer elements in the gene[203]. Thus, oncogenic signaling pathways, which are often upregulated in cancer, share also another common point to induce glucose import.

High glutamine demand was first described by Harry Eagle, when he saw that cultured HeLa cells required 10 to 100 times more of glutamine than any other amino acid[204]. Not only as carbon source, glutamine is also a nitrogen source for *de novo* biosynthesis of different nitrogen-containing building blocks, such as purine and pyrimidine nucleotides, glucosamine-6-phosphate, and nonessential amino acids. Moreover, glutamine participates in the uptake of essential amino acids from extracellular environment. For example, leucine is imported through the plasma membrane by the amino acid antiporter LAT1/SLC7A5 in coupling with an efflux of glutamine[205]. Indeed, LAT1/SLC7A5 expression has been reported to be increased in several cancer types[206,207]. Due to the high demand of glutamine, this amino acid is also used for imaging based on ^{18}F-labeled glutamine tracers in preclinical and clinical studies, especially when the use of ^{18}F-FDG is not feasible, like in the brain[208,209]. The mechanisms of glutamine uptake regulation are still being identified. The principal regulator of glutamine utilization is the transcription factor c-myc, which is often upregulated in proliferating cells[210,211]. Indeed, c-myc induces the transcription of glutamine transporters, such as SLC1A5/ASCT2, and also promotes the expression of glutamine-catabolized enzymes such as GLS1 (*glutaminase 1*) and CAD, in order to encourage glutamine uptake by converting glutamine to glutamate[212–214]. In addition,

glutamine uptake can be negatively regulated by Rb tumor suppressor family, whose deletion increase glutamine uptake via the E2F-dependent upregulation of ASCT2 and GLS1[215]. Thus, glutamine consumption is supported by the activity of c-myc and E2F transcription factors which regulate cell cycle, to ensure the cellular access to glutamine for DNA replication.

2.1.2 Metabolic intermediates for biosynthesis

Despite the original idea of Otto Warburg that aerobic glycolysis was originated as a consequence of mitochondrial dysfunction, subsequent studies showed that mitochondria of cancer cells are still functional and able to conduct oxidative phosphorylation. To adapt to a rapid proliferation, cancer cells need building blocks, intermediary metabolites and reducing power as NADPH. Glycolysis can robustly provide these demands, providing glycolytic intermediates which are diverted into branching pathways (**Figure 11**). A prominent case of a pathway which use glycolytic intermediates is the PPP. Glucose-6-phosphate from glucose can be oxidized by G6PD (*glucose-6-phosphate dehydrogenase*) to generate NADPH and ribose-5-phosphate, necessary for nucleotide synthesis. PPP is often upregulated in tumors and their enzymes are frequently overexpressed in cancer[216,217]. Another important case is the use of glycolytic 3-phosphoglycerate as a precursor for the serine and glycine metabolism through the *one-carbon cycle*. Several studies have revealed that the gene encoding PHGDH (*3-phosphoglycerate dehydrogenase*), the rate-limiting serine biosynthesis enzyme, is amplified in breast cancers and melanomas[218,219]. Serine and glycine metabolism, derived from glycolytic 3-phosphoglycerate, provide advantages for cell growth, such as nucleotide synthesis, DNA methylation, glutathione production and NADPH generation. Interestingly, in both examples of branching

pathways, there are enzymes controlled and regulated by mTORC1, proving a tight link between mTORC1 and metabolic transformation.

After feeding all branching pathways, the excess of glycolytic flux is converted to lactate to preserve a sufficient pool of NAD^+ for glycolysis and also to avoid the TCA (*tricarboxylic acid*) cycle inhibition due to excess NADH. Still, a percentage of pyruvate enters the mitochondria, and a great portion of citrate generated at the TCA cycle from this pyruvate will be secreted to the cytosol through the mitochondrial tricarboxylate carrier. Once at the cytosol, citrate is transformed to acetyl-CoA and oxaloacetate, which is converted to malate for mitochondrial anaplerosis[220,221]. Citrate-derived acetyl-CoA is used as a precursor for lipid biosynthesis and protein acetylation.

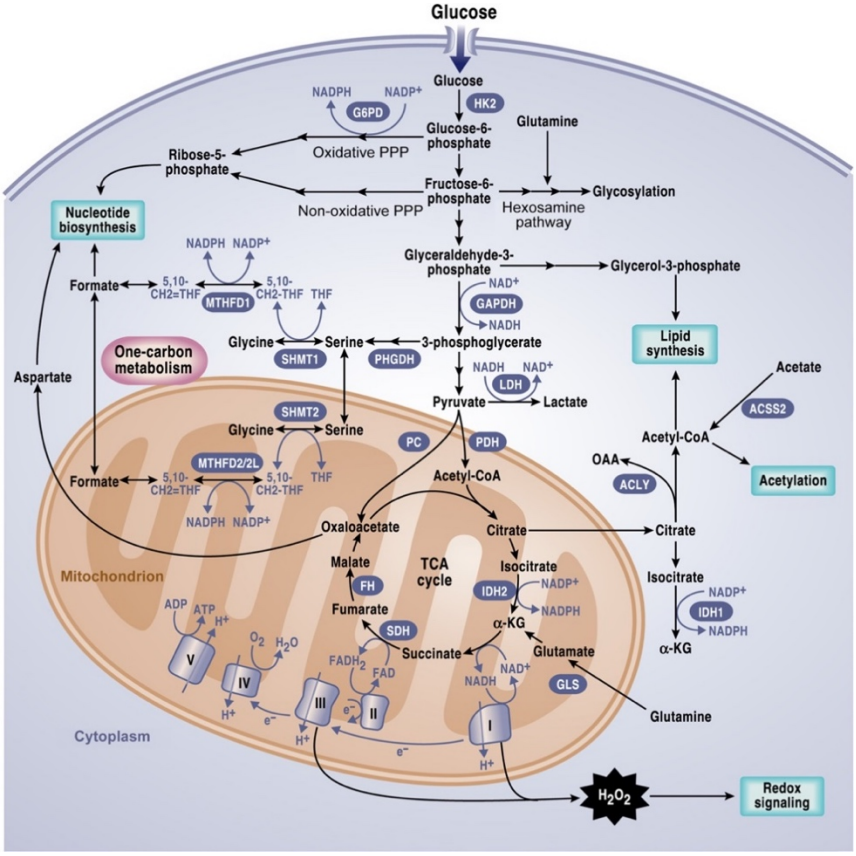

Figure 11. Metabolic transformation of cancer cells.

Glycolysis, mitochondrial TCA cycle and other affected metabolic pathways are represented in this figure. Metabolic enzymes, which are mutated in cancer, are highlighted in blue. (From *DeBerardinis & Chandel 2016 Sci Adv 2(5):e1600200*).

In addition to glycolytic intermediates, TCA cycle intermediates are also used for biosynthetic precursors accumulation. The first example is citrate-derived acetyl-CoA, whose production is increased by PI3K/AKT-mediated ACLY (*ATP-citrate lyase*) enzyme[222]. Secondly, the TCA cycle also provides metabolic precursors for the synthesis of nonessential amino acids, such as aspartate and asparagine from oxaloacetate, or proline and arginine from α-ketoglutarate. Then, aspartate will be used for nucleotide biosynthesis. Indeed, enabling aspartate synthesis is an essential role of the oxidative phosphorylation in cell proliferation[223,224].

Due to the release of citrate to the cytosol, the maintenance of the pool of TCA cycle intermediates need additional influx, also called *anaplerosis*. The main anaplerotic source in growing cells is glutamine[225]. In c-myc-transformed cells, glutamine deprivation could disrupt the TCA cycle and induce cell death, which can be rescued by the addition of oxaloacetate or α-ketoglutarate[226]. Glutamine-derived α-ketoglutarate is oxidized into oxaloacetate to maintain the production of citrate. During hypoxia or under certain oncogenic conditions, α-ketoglutarate could be converted directly to citrate (following a reversed TCA cycle), in order to generate the cytosolic acetyl-CoA when glucose-derived acetyl-CoA is insufficient[227].

2.2 Glutamine utilization in cancer cells

Glutamine is the most abundant free amino acid in the blood, whose circulating concentration is around 0.5 mM. Despite being a nonessential amino acid, glutamine is physiologically an essential source of carbon and nitrogen for cancer cell proliferation. As discussed above, glutamine uptake is increased specifically in cancer cells that have dysregulated oncogenes and tumor suppressors, such as c-myc. Glutamine is catabolized by different enzymes, including GLS, CAD or GFAT (*glutamine fructose-6-phosphate amidotransferase*). As an anaplerotic source,

glutamine is converted to α-ketoglutarate through mitochondrial glutaminolysis. Glutamine is first deamidated to glutamate, in an irreversible reaction catalysed by the enzyme GLS. Then, glutamate is deaminated to α-ketoglutarate by the enzyme GLUD1/GDH (*glutamate dehydrogenase*) or by several aminotransferases to produce other non-essential amino acids. Subsequently, α-ketoglutarate enters the TCA cycle to replenish the mitochondrial citrate pool. GLS is the rate-limiting enzyme of glutaminolysis, whose regulation is controlled tightly. There are 2 isoforms of GLS which are encoded by two genes in mammals, the *kidney-type glutaminase* (GLS1) and the *liver-type glutaminase* (GLS2). GLS1 is the main isoform expressed in cancer cells and has been shown to be upregulated in a wide variety of cancers, including breast, lung, cervix and brain[228]. GLS1 is inhibited by its product, glutamate[229]. GDH activity is also increased in tumor cells and leucine, a key amino acid from a signaling point of view, is an allosteric activator of GDH to induce the production of α-ketoglutarate and prevent GLS inhibition by glutamate accumulation[230]. As discussed above, glutamine is imported by the transporter SLC1A5, while leucine is taken up through the bidirectional antiporter SLC7A5 which exports glutamine out of the cell. Thus, glutamine modulates glutaminolysis in combination with leucine.

Glutamine can be synthetized by the cells through GLUL/GS (*glutamine synthetase*) which catalyses the condensation reaction between glutamate and ammonia in an ATP-dependent manner and generates glutamine. In mammals, GS is mostly expressed in the liver, brain, and muscle. GS has been found to be a marker of HCC (*hepatocellular carcinoma*) and its elevated expression may enhance the metastatic potential in HCC patients[231]. Moreover, GS expression is accompanied with a poor survival in glioblastoma patients[232].

In this section, different uses of glutamine metabolism in proliferating cells will be discussed, including its role as carbon and nitrogen source for nucleotides and amino acids synthesis, as well as its role in the regulation of redox homeostasis and gene expression.

2.2.1 Carbon donor

Glutamine-derived carbon incorporation into the TCA cycle is necessary for the bioenergetic needs and biosynthetic precursors of the cells. Glutamine-derived α-ketoglutarate can fuel fatty acids synthesis through the reductive carboxylation mediated by IDH (*isocitrate dehydrogenase*) (**Figure 12**). Emerging evidences have reported the role of glutamine mediating reductive carboxylation for lipid biosynthesis and also for redox homeostasis in cancer with dysfunctional mitochondria or under hypoxia[227,233–235].

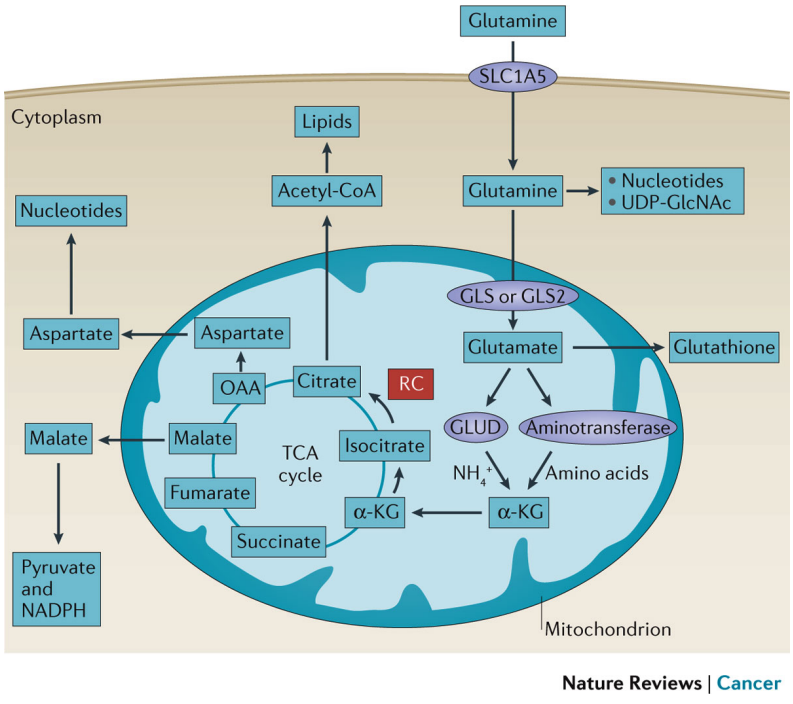

Figure 12. Different uses of glutamine in cancer cells.

Glutamine is imported into the cell through transporters such as SLC1A5 and then contribute to nucleotide biosynthesis, amino acid synthesis and other metabolic pathways, supporting cell growth and proliferation.
(From *Altman et al., 2016 Nature Review 16:619-634*).

2.2.2 Nitrogen donor

Glutamine has two atoms of reduced nitrogen, called α-nitrogen and γ-nitrogen. At the level of nucleotide synthesis, glutamine is the nitrogen donor for enzymes in the purine synthesis, including PRPP amidotranferase, FGAMS/PFAS (*phosphoribosyl formylglycinamidine synthetase*), and GMP synthetase. But glutamine also acts as nitrogen donor form enzymes involved the pyrimidine synthesis, including CAD and CTP synthetase (**Figure 13**). Thus, one glutamine molecule is used in the production of uracil and thymine, two for cytosine and adenine, and three for a guanine base. Besides that, purine and pyrimidine synthesis use also glutamine-derived aspartate, whose supplementation can rescue cell cycle arrest caused by glutamine deprivation[236]. Interestingly, only the γ-nitrogen of glutamine is used for nucleotide synthesis. This nitrogen is also required for the synthesis of NAD, glucosamine-6-phosphate (a precursor for protein glycosylation), and asparagine, a non-essential amino acid that compensates for glutamine deprivation[237].

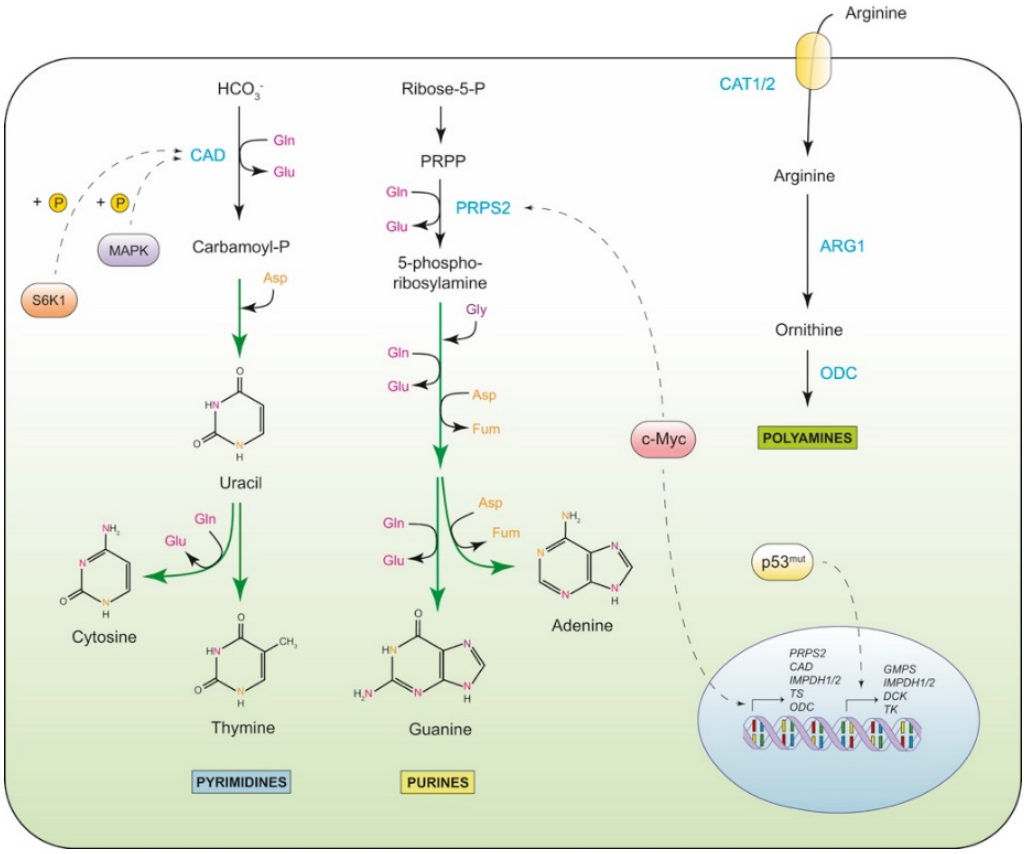

Figure 13. Glutamine as nitrogen donor for nucleotide synthesis.

Glutamine is used by different enzymes as nitrogen source for purine and pyrimidine synthesis. (From *Pavlova & Thompson 2016 Cell Metab. 23(1):27-47*).

The α-nitrogen of glutamine is used to produce other non-essential amino acids or polyamines via transamination (**Figure 14**). This reaction is catalysed by a family of aminotransferases to produce alanine[238], aspartate[239], serine[240], proline[241] and ornithine[242]. Glutamine is the source of at least 50% of non-essential amino acids used in protein synthesis by cancer cells[243]. It is estimated that glutamine represents in average to 4.7% of all amino acid residues in human proteome, but obviously the percentage can differ from protein to protein[244]. Hence, glutamine is a key structural building block in the biosynthesis of proteins, nucleotides, non-essential amino acids and polyamines to support biomass accumulation and rapid rates of proliferation.

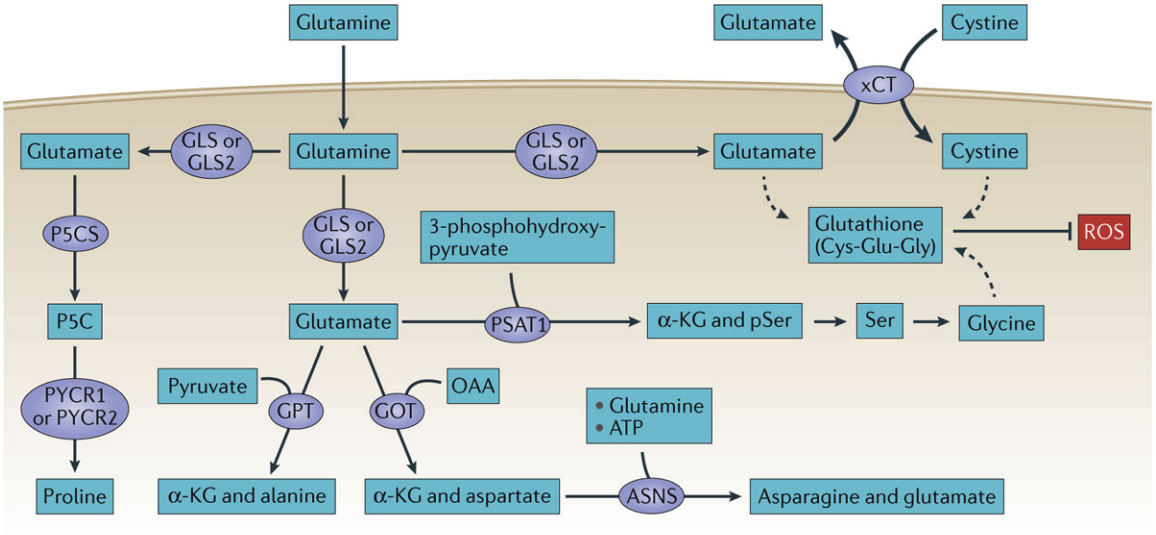

Figure 14. The role of glutamine in non-essential amino acids synthesis.

Glutamine-derived glutamate is a nitrogen donor for the transamination involved in amino acid synthesis, including alanine, aspartate and serine. Glutamine is a nitrogen donor for asparagine production.
(From *Altman et al., 2016 Nature Review 16:619-634*).

2.2.3 Redox homeostasis control

During tumorigenesis, cancer cells encounter oxidative stress continuously. In order to maintain oxidative homeostasis, the cells need to increase their antioxidant capacity. Glutamine metabolism plays a major role in the cellular anti-oxidative mechanisms. Glutamine-derived glutamate is used in the synthesis of glutathione, through the condensation with cysteine and glycine by glutamate-cysteine ligase and glutathione synthetase (**Figure 15**). Tracer experiment with labelled ^{13}C-glutamine showed an enrichment of ^{13}C carbons in glutathione. Accordingly, glutamine starvation reduces the glutathione pool of transformed cells[226,245]. Moreover, as cystine is an extracellular source of cysteine, cystine uptake is facilitated by the efflux of glutamate via the xCT antiporter. Once inside the cell, cystine is converted to cysteine, which is then incorporated into glutathione. Indeed, pharmacological inhibition of xCT increases ROS (*reactive oxygen species*) level and suppresses tumor growth[246,247]. Lastly,

glutamine oxidation supports redox homeostasis by supplying carbon to malic enzymes, which produce NADPH. Indeed, in proliferating cells, NADPH is used not only for the lipid synthesis, but also for the reduction of oxidized glutathione (GSSG)[248].

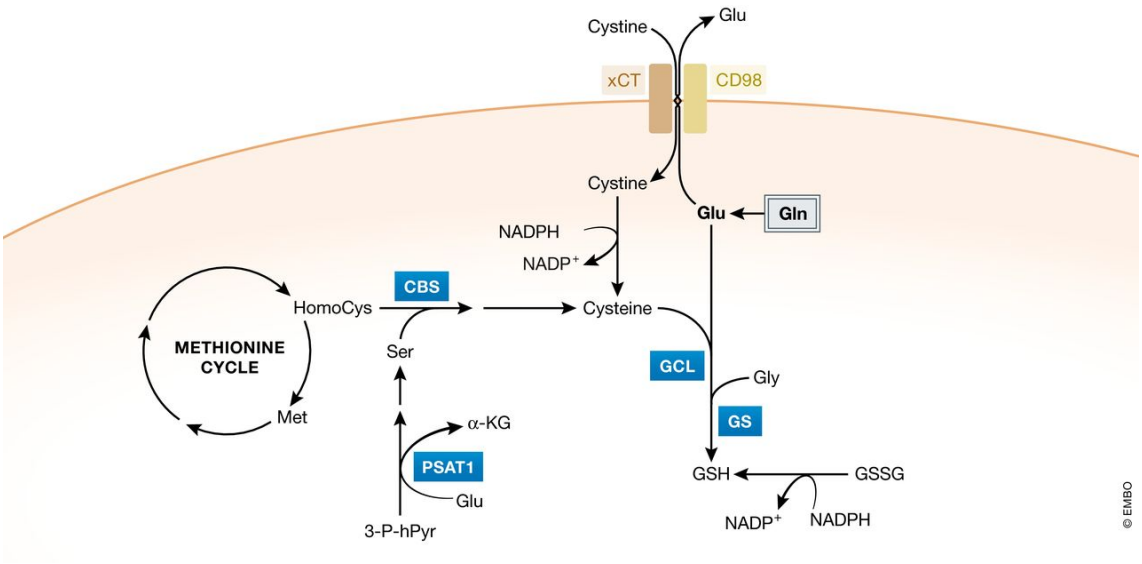

Figure 15. The key role of glutamine in glutathione biosynthesis.

Glutamine contributes to the synthesis of the tripeptide glutathione (composed of glutamate, cysteine and glycine), which neutralizes the reactive oxygen species (ROS) and protects the cells from oxidative stress.
(From *Zhang and Thompson 2017 EMBO 36(10):1302-1315*).

2.2.4 Chromatin organization

Glutamine metabolism does not only generate building blocks and energy for cell growth, but also produces co-substrates for cellular regulatory cascades, including those that regulate chromatin organization. Actually, glutamine-derived α-ketoglutarate is a co-substrate of dioxygenase enzymes, including the TET family and the JMJ (*jumonji*) family (**Figure 16**). Enzymes from the TET and JMJ family catalyse histone and DNA demethylation and they are inhibited by the accumulation succinate, the by-product of these enzymes.

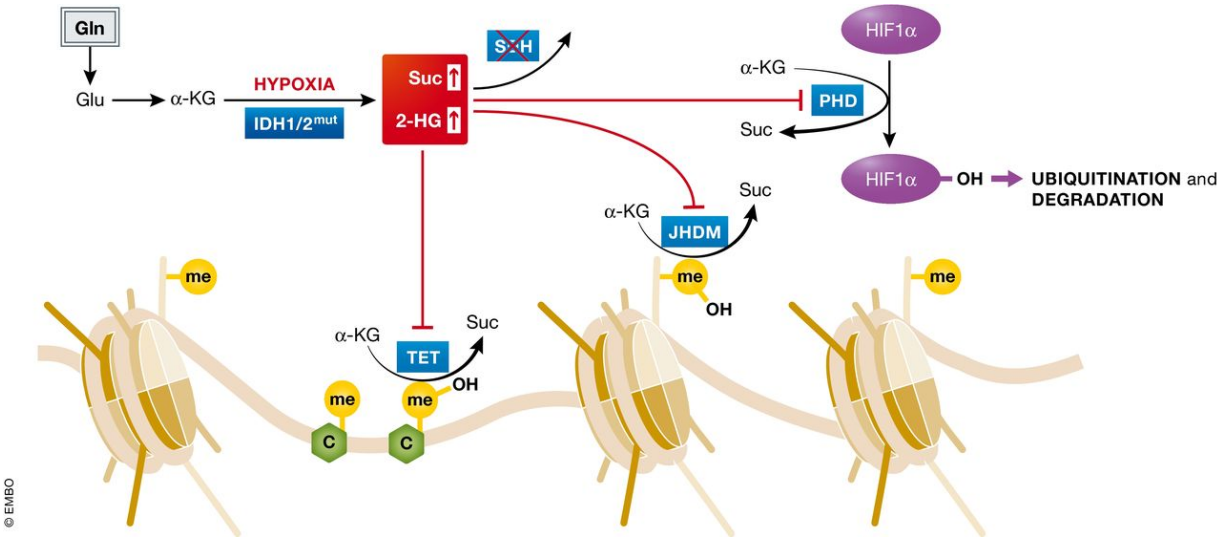

Figure 16. The role of glutamine-derived α-ketoglutarate in the regulation of chromatin organization.

(From *Zhang and Thompson 2017 EMBO 36(10):1302-1315*).

One example of the role of glutamine-derived α-ketoglutarate in the regulation of histone and DNA methylation is the neomorphic mutations in IDH1/2[249,250]. Moreover, loss-of-function mutations of SDH (*succinate dehydrogenase*) increase cellular succinate level, which inhibits DNA demethylation and contribute to tumorigenesis[251,252]. Finally, low glutamine in the core region of solid tumors led to histone hypermethylation due to decreased α-ketoglutarate level, resulting in cell dedifferentiation and therapeutic resistance in melanoma cells[253]. Accordingly, glutamine metabolism plays a role in gene expression through the contribution of α-ketoglutarate and succinate to chromatin structure modification.

2.3 Glutamine addiction in cancer

Due to the high demand of cancer cells for glutamine, glutamine metabolism is highly regulated in order to maintain cellular biosynthesis and cell growth. Thus, the machinery which regulates glutamine metabolism, needs to be very efficient to increase the cellular access to glutamine. The first mechanism to enhance glutamine

acquisition is to induce glutamine uptake. Different glutamine transporters are known, especially SLC1A5/ASCT2 which is controlled by c-myc or E2F. SLC1A5 is highly expressed in triple-negative breast cancer patients, correlating with poor survival in tumor-bearing mice[254]. Besides, other transporters such as SLC38A1/SNAT1 and SLC38A2/SNAT2 can compensate for the depletion of SLC1A5/ASCT2 to contribute to glutamine uptake[255].

The expression and activity of glutaminolytic enzymes, GLS and GDH, are also tightly regulated. GLS is inhibited by its product glutamate or by inorganic phosphate. SIRT5, which is overexpressed in lung cancer, decrease the succinylation of GLS to regulate ammonia production and ammonia-induced autophagy[256]. The transcription factor c-myc induces the expression of GLS through the repression of miR-23a and miR-23b[62]. Furthermore, additional mechanisms are reported to regulate GLS, such as RNA-binding protein regulation of alternative splicing[257,258] or protein degradation through the ubiquitin ligase complex APC/C^{Cdh1} during cell cycle progression[259].

Similar to GLS, GDH expression and activity are controlled by different effectors. GDH is allosterically regulated by activators like ADP and leucine, or by inhibitors like ATP, GTP and palmitoyl-CoA[260–262]. At the level of post-translational modification, the sirtuin SIRT4 ADP-ribosylates and downregulates GDH in beta-pancreatic cells, thereby decreasing insulin secretion in response to amino acids during calorie-sufficient conditions[263]. When the extracellular glutamine level is limited, some cancer cell lines are able to induce GS expression in order to escape from glutamine deficient-induced cell death. GS has been found to be overexpressed in some cancers, such as breast cancer or glioblastoma, promoting cell proliferation [232,264]. GS transcription is activated by different oncogenic pathways, such as PI3K-PKB-FOXO pathway[265], c-myc[266], and Yap1/Hippo pathway[267]. Moreover, GS is inactivated by extracellular glutamine

because the presence of glutamine induces GS acetylation by p300/CBP protein, facilitating its ubiquitination and proteasomal degradation[268–270].

Glutamine addiction appears when cancer cells undergo cell death in conditions of glutamine limitation or when glutamine metabolism is inhibited. Many cancer cells which rely on glutamine catabolism for building blocks and energy have been reported to be addicted to glutamine[226,271–273] (**Figure 17A**). Glutamine-addicted cells exhibit a decreased survival, or even undergo apoptotic cell death, associated with an increased in DNA damage, an overproduction of ROS or a decreased GSH/GSSG ratio. In this context, the oncogenic transcription factor c-myc plays a key role in the induction of glutamine addiction[211,226]. Together, these results suggested that this phenotype could be exploited as cancer therapy through the use of inhibitors of glutaminolytic enzymes or treatment which induce glutamine depletion like L-asparaginase.

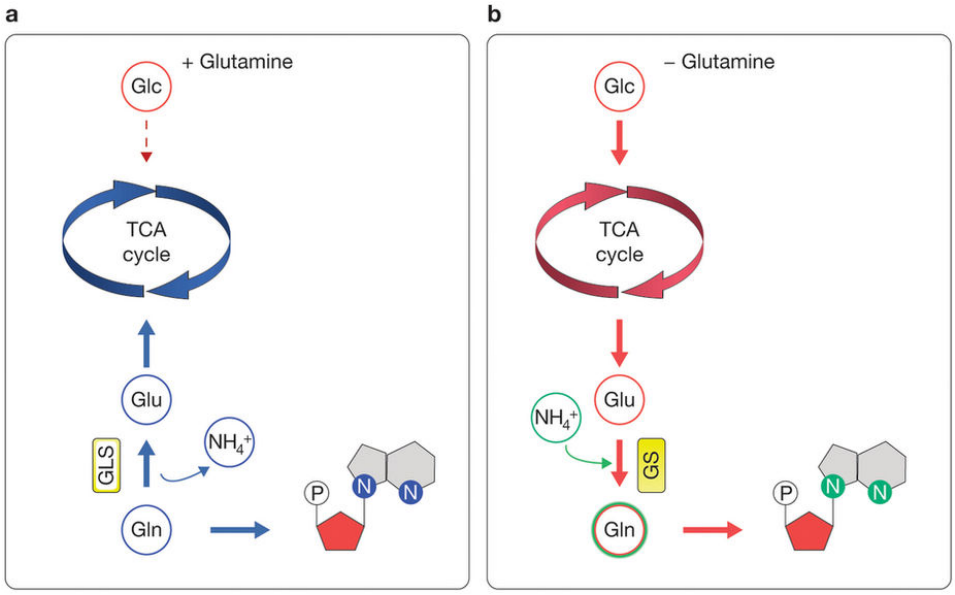

Figure 17. Glutamine addiction in cancer cells.

(**A**) Under glutamine-abundant conditions, cancer cells use glutamine as carbon and nitrogen donor for cell growth. (**B**) Upon glutamine deprivation, some cell types can induce glutamine synthetase (GS) for de novo glutamine synthesis, thus the cells are independent of extracellular glutamine.
(From *Krall & Christofk 2015 Nat Cell Biology 17(12):1515-1517*).

On the contrary, some cell types show glutamine independence due to the expression of GS. Indeed, glioma cells can synthetize glutamine from glutamate through the activity of GS, maintaining the cell proliferation during glutamine deprivation[274] (**Figure 17B**). Also, those cells use glucose as a source for TCA cycle anaplerosis, which can sufficiently provide α-ketoglutarate for glutamate and glutamine synthesis. However, the source of the free ammonia necessary for glutamine synthesis is not clear. Alternatively, some cell types can adapt to glutamine withdrawal using asparagine[237,275]. Asparagine is indeed playing a role in the exchange of extracellular amino acids, especially serine, arginine and histidine[276]. Despite that asparagine is synthetized from glutamine through asparagine synthetase, how cancer cells adapt their metabolic needs during glutamine deprivation remains to be elucidated.

2.4 Therapeutic applications

Given the dependence of cancer cells on glutamine metabolism, targeted therapies have been developed against glutamine metabolism, from glutamine uptake to glutamine-catalysed enzymes (**Table 1**). The inhibition of GLS got the attention due to the dysregulation of GLS in a variety of cancers. Indeed, GLS inhibitors have shown promising tumor-suppressive activities in preclinical models for 968 and BPTES, or even in clinical models for CB-839[277,278]. CB-839 has shown efficacy in triple-negative breast cancer and haematological malignancies therapies[278,279]. In addition to GLS inhibitors, strategies targeting the conversion of glutamate into α-ketoglutarate, such as GDH inhibitors and aminotransferase inhibitors, have also been evaluated in preclinical models of breast cancer and neuroblastoma[280–282].

Table 1. Different strategies to target glutamine metabolism in cancer.

(From *Altman et al., 2016 Nature Review 16:619-634*).

Class	Drug	Status
Glutamine mimic	• DON[16] • Azaserine[16] • Acivicin[16]	• Off-target effect on nucleotide biosynthesis[16,226] • Limited by toxicity[16,227]
Glutamine depletion	L-Asparaginase[100,101,228–230]	• Off-target toxic conversion of glutamine to glutamate[231,232] • Limited by toxicity[100,101] • FDA-approved to treat ALL[102]
GLS inhibitors	968 (REF. 233)	Preclinical tool[237]
	BPTES[172,234–236]	Preclinical tool[151,173]
	CB-839 (REFS 53,54)	Phase I clinical trial
SLC1A5 inhibitors	• Benzylserine[238,239] • γ-FBP[240] • GPNA[241]	Preclinical tools[238–241]
GLUD inhibitors	EGCG[242,243]	Tool compound[65,67]
	R162 (REF. 148)	Preclinical tool compound[148]
Aminotransferase inhibitors	AOA[65,143]	• Clinically used to treat tinnitus[244] • Toxic at higher doses[143]
SLC7A11 or xCT system inhibitors	Sulfasalazine[18]	FDA approved for arthritis[18]
	Erastin[245]	Tool compound, induces iron-dependent ferroptosis[246]

ALL, acute lymphoblastic leukaemia; AOA, aminooxyacetate; DON, 6-diazo-5-oxo-l-norleucine; FDA, US Food and Drug Administration; γ-FBP, γ-folate binding protein; GLS, kidney-type glutaminase; GLUD, glutamate dehydrogenase; GPNA, L-γ-glutamyl-*p*-nitroanilide.

Nevertheless, most of the compounds are still in the preclinical evaluation stage, or have been directly discarded due to high cytotoxicity. Furthermore, some limitations derived of treatment resistance to targeted therapies against glutamine metabolism have been reported. Induction of pyruvate carboxylase can allow tumor cells to use glucose-derived pyruvate instead of glutamine for anaplerosis, inducing a glutamine-independent growth[283–285]. Also, glutamate-derived glutamine production through GS activity could be another mechanism to overcome glutamine addiction and to promote resistance to glutaminolysis inhibitors[274]. However, combination therapy between glutamine metabolism inhibitors and other pathways inhibitors induced a stronger apoptotic response and enhanced anti-tumor efficacy (**Table 2**). For instance, mTOR inhibition in glioblastoma multiforme cell lines led to a compensatory upregulation of glutamine metabolism, promoting mTOR inhibitor resistance. Thus, combined

inhibition of mTOR and GLS resulted in synergistic tumor cell death and growth inhibition in xenograft mouse models[286].

Table 2. Synergistic effect of the combination between glutamine metabolism inhibition with different pharmacological treatments.

(From *Altman et al., 2016 Nature Review 16:619-634*).

Co-treatment	Rationale	Refs
Metformin	Metformin decreases glucose oxidation to increase cellular dependence on glutamine	247
GLUT1 inhibition	Combined downregulation of glucose transport (apigenin) and glutaminase causes severe metabolic stress	248
Glycolysis inhibition (2-DG)	Blockade of compensatory glutamine contribution to TCA cycle, nucleotides and mTOR signalling blocks growth in 2-DG-resistant cells	249
Mitochondrial pyruvate carrier inhibition	Specific chemical inhibition of pyruvate transport into the mitochondrion synergizes with inhibition of glutaminolysis to cause increased death	250
Transglutaminase inhibition	Combined inhibition of glutaminase and transglutaminase causes potentially lethal acidification	251
mTOR inhibition	Consistent with the role of glutamine in mTOR activation and mTOR control of metabolism, GLS and mTOR inhibition are synthetically lethal	219,252
ATF4 activation	Glutamine withdrawal activates the ISR, and further activating this pathway with the retinoid derivative fenretinide causes increased cancer cell death	65
BCL-2 inhibition	Inhibiting GLS causes apoptosis through altered metabolism, with the effect exacerbated by inhibition of the anti-apoptotic protein BCL-2	53
HSP90 inhibition	Consistent with a role of GLS in controlling ROS and ER stress, HSP90 and GLS inhibition cause ER stress-induced cell death via ROS	253
BRAF inhibition	BRAF inhibition resistance causes a shift to glutamine dependence; thus, combination therapy may be used to combat this resistance	254
NOTCH inhibition	NOTCH1 promotes glutaminolysis in T-ALL, sensitizing NOTCH-inhibited T-ALL cells to genetic and pharmacological GLS inhibition	255
EGFR inhibition	GLS inhibition restores sensitivity to the EGFR inhibitor erlotinib in cells that have developed resistance	256

ATF4, activating transcription factor 4; 2-DG, 2-deoxyglucose; EGFR, epidermal growth factor receptor; ER, endoplasmic reticulum; GLS, kidney-type glutaminase; GLUT1, glucose transporter 1; HSP90, heat shock protein 90; ISR, integrated stress response; ROS, reactive oxygen species; T-ALL, T cell acute lymphoblastic leukaemia; TCA, tricarboxylic acid.

2.5 Glutamine metabolism and mTORC1 pathway

Glutamine metabolism and mTORC1 pathway have a tight connection through different mechanisms. As explained above in detail, the activation of mTORC1 by glutamine and other amino acids is mediated by the Rag GTPase pathway. In addition, glutamine plays a role as the efflux solute for the import of leucine which supports glutamine to activate mTORC1 through glutaminolysis. Moreover, glutamine and leucine cooperate to produce α-ketoglutarate through glutaminolysis, which ultimately

activates mTORC1. Indeed, short-term glutaminolysis induces mTORC1 lysosomal translocation and activation via the Rag GTPase, then inhibiting autophagy and promoting cell growth[58]. Moreover glutaminolysis-mediated mTORC1 activation required PHD enzymatic activity in a HIF-independent manner[121]. Those evidences highlight the role of glutaminolysis-PHD-mTORC1 axis in cancer growth. Besides, glutamine stimulates lysosomal translocation and activation of mTORC1 via the small GTPase ARF1 and v-ATPase in RagA and RagB knockout cells without Ragulator contribution[122].

In agreement with this positive connection between glutaminolysis and mTORC1, FOXO-mediated expression of GS inhibits mTOR signaling by blocking its lysosomal translocation[265]. This mechanism is important for maintaining autophagy during nutrient deprivation. Hence, mTORC1 sense glutamine availability in both directions: when glutamine is available, mTORC1 is activated via α-ketoglutarate production; but mTORC1 is inactivated when glutamine production is triggered.

The connection between glutamine metabolism and mTORC1 present additional connection branches, as glutamine also plays a role in autophagy-induced mTORC1 restoration during amino acid starvation[287]. Thus, glutamine recycling, supported by autophagy, is sufficient to reactivate mTORC1 under restrictive conditions.

However, and paradoxically, long-term glutaminolysis activation during nutritional restriction induces an unbalanced activation of mTORC1 during nutrient deprivation and promotes apoptosis[59]. This type of metabolic-induced cell death is called “glutamoptosis”, which supports a tumor suppressor role of glutamine metabolism and mTORC1 (normally known as pro-proliferative inducers) during nutritional imbalance (**Figure 18**). During glutamoptosis, mTORC1-mediated inhibition of autophagy leads to the accumulation of the autophagic cargo protein SQSTM1/p62. Then SQSTM1/p62

interacts with Caspase 8 and activates it to trigger apoptosis. Strikingly, the inhibition of mTORC1 by rapamycin promoted cell survival upon amino acid starvation, which could partially explain the resistance to rapamycin treatment observed in some tumor cells.

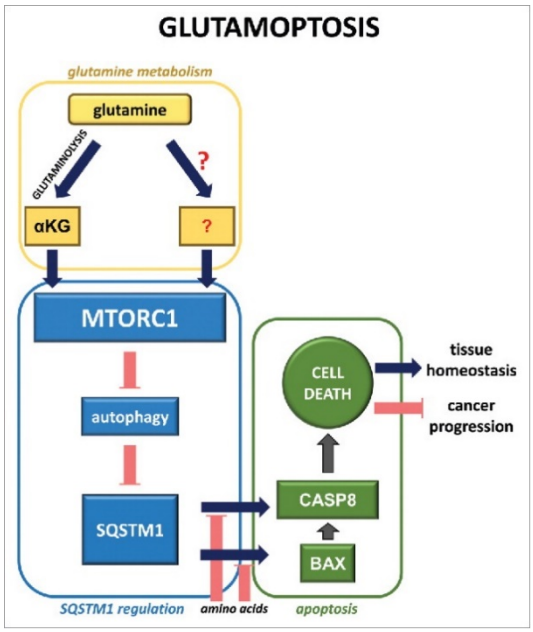

Figure 18. Molecular mechanism of glutamoptosis.

The aberrant activation of mTORC1 during amino acid withdrawal induces an accumulation of SQSTM1/p62, which interacts with Caspase 8 and induces apoptotic cell death. (From *Villar & Durán 2017 Autophagy 13(6):1078-1079*).

Conversely, mTORC1 can regulate glutamine metabolism via different mechanisms. GLS and GDH are both regulated by mTORC1 pathway. Mechanistically, mTORC1 inhibits the transcription of SIRT4 by degrading its activator CREB2 (*cAMP-responsive element-binding 2*), thereby activating GDH[60,263,288]. Also, mTORC1 activate GLS through S6K1/eIF4B-dependent mRNA translation of c-myc, leading to GLS expression by repressing miR-23a/b[61,62]. Intriguingly, in an organotypic 3D tissue culture model, mTORC1 supports the expression of aminotransferases and the suppression of GDH in proliferating cells[289]. Thus, the regulation of glutamine metabolism by mTORC1 is cell type-dependent and needs to be elucidate further.

Moreover, mTORC1 controls glutamine transporters SLC1A4 and SLC1A5 expression, thereby promoting glutamine uptake upon androgen receptor signaling in prostate cancer[290]. Interestingly, different evidences have shown that glutamine flux through glutamine transporters activates mTOR signaling[291].

In summary, glutamine uptake and metabolism have a tight connection with mTOR signaling. As both pathways are upregulated in many cancers, strategies which target both glutamine metabolism and mTORC1 signaling have shown synergistic effects against cell growth and proliferation[286].

3. Notch1 signaling

3.1 T-cell acute lymphoblastic leukaemia

3.1.1 Hematopoiesis and T-cell development

3.1.1.1 Hematopoiesis

Among stem cells, HSCs (*hematopoietic stem cells*) are one of the best characterized, presenting self-renewal capacities, quiescence state and the ability of differentiation. All mature blood cells are derived from HSCs, located in the BM (*bone marrow*), through a developmental process called *hematopoiesis*[292]. Throughout this process, HSCs differentiate to become MPPs (*multipotent progenitors*), which by turn originate either CMPs (*common myeloid progenitors*) or CLPs (*common lymphoid progenitors*)[293]. CMPs will differentiate into GMPs (*granulocyte-monocyte progenitors*) and MEPs (*megakaryocytic-erythroid progenitors*), while CLPs are restricted to differentiate into T lymphocytes, B lymphocytes and NK (*natural killer*) cells (**Figure 19**). Differently to other hematopoietic lineages, T-cell development occurs in the thymus. The ETPs (*early T-cell progenitors*) from the CLPs migrate to the thymus at the cortico-medullary junction[294] and commit to the mature and functional T-cell lineage through a differentiation process supported by the thymus[295,296] (**Figure 20**).

3.1.1.2 T-cell acute lymphoblastic leukemia

Haematological malignancies or blood cancer are tumors that affect the blood, BM, lymph and lymphatic system. There are two different types of leukemias: *acute leukemias* which is fast-growing leukemias and *chronic leukemias* which develop more showly. *Acute leukemias* result from the transformation of a hematopoietic progenitor which does not differentiate, undergoing uncontrolled proliferation. This proliferation leads to the accumulation of blast cells in the BM, in blood, and in other organs.

According to the expression of the specific antigens, acute leukemias are classified as AML (*acute myeloid leukemia*), T-ALL (*T-cell acute lymphoblastic leukemia*) or B-ALL (*B-cell acute lymphoblastic leukemia*).

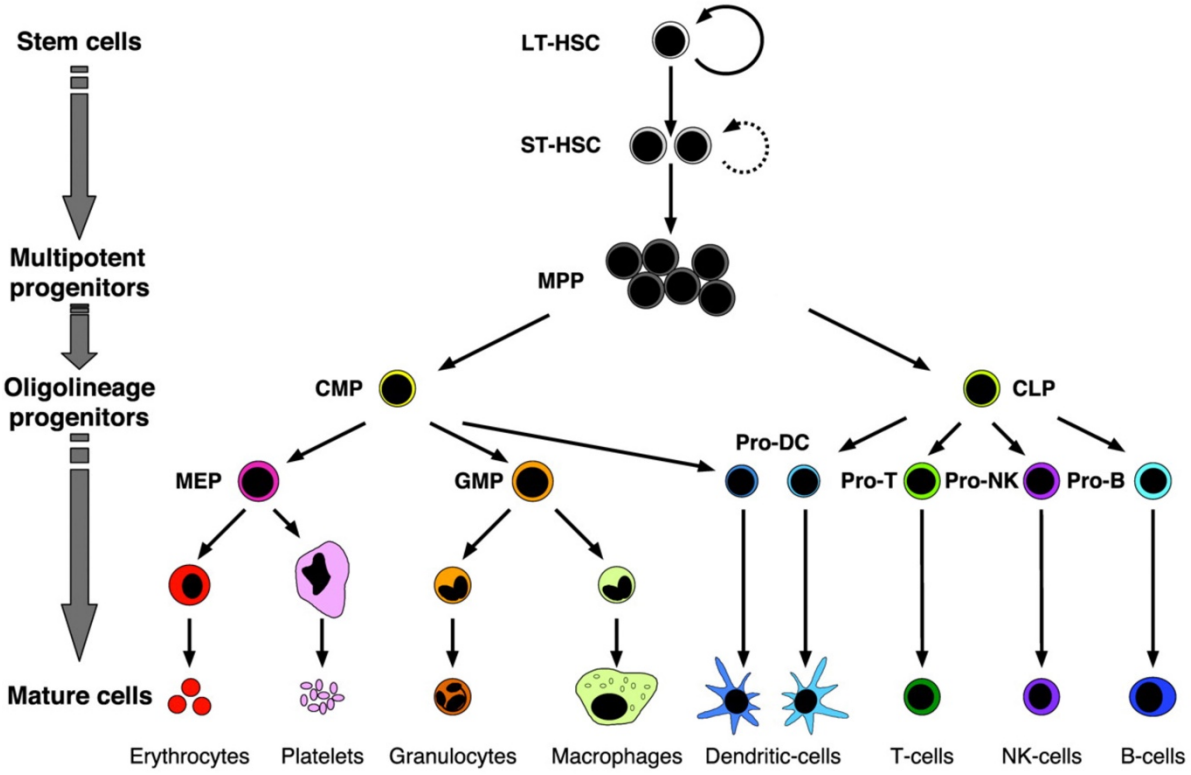

Figure 19. Different progenitor cell lineages from hematopoietic stem cells during hematopoiesis.

(Modified from *Passegué et al. PNAS 2003; 100:suppl 1:11842-11849*).

T-ALL is an aggressive form of hematologic tumor which appears from the uncontrolled clonal proliferation of T-cell progenitor cells. This hematologic malignancy is found in 15% of paediatric and 25% of adult cases of ALL and is characteristically more frequent in males than females[297]. Clinically, T-ALL patients show aggressive features, such as high level of circulating white blood cells, mediastinal thymic masses with pleural effusions, and increased risk meningeal infiltration of the central nervous system[298]. Based on the expression of specific immunophenotypic markers related to T-cell development, three T-ALL subgroups are defined: immature T-ALL, T-ALL with an

early cortical immunophenotype, and T-ALL with a mature late cortical thymocyte immunophenotype[299,300].

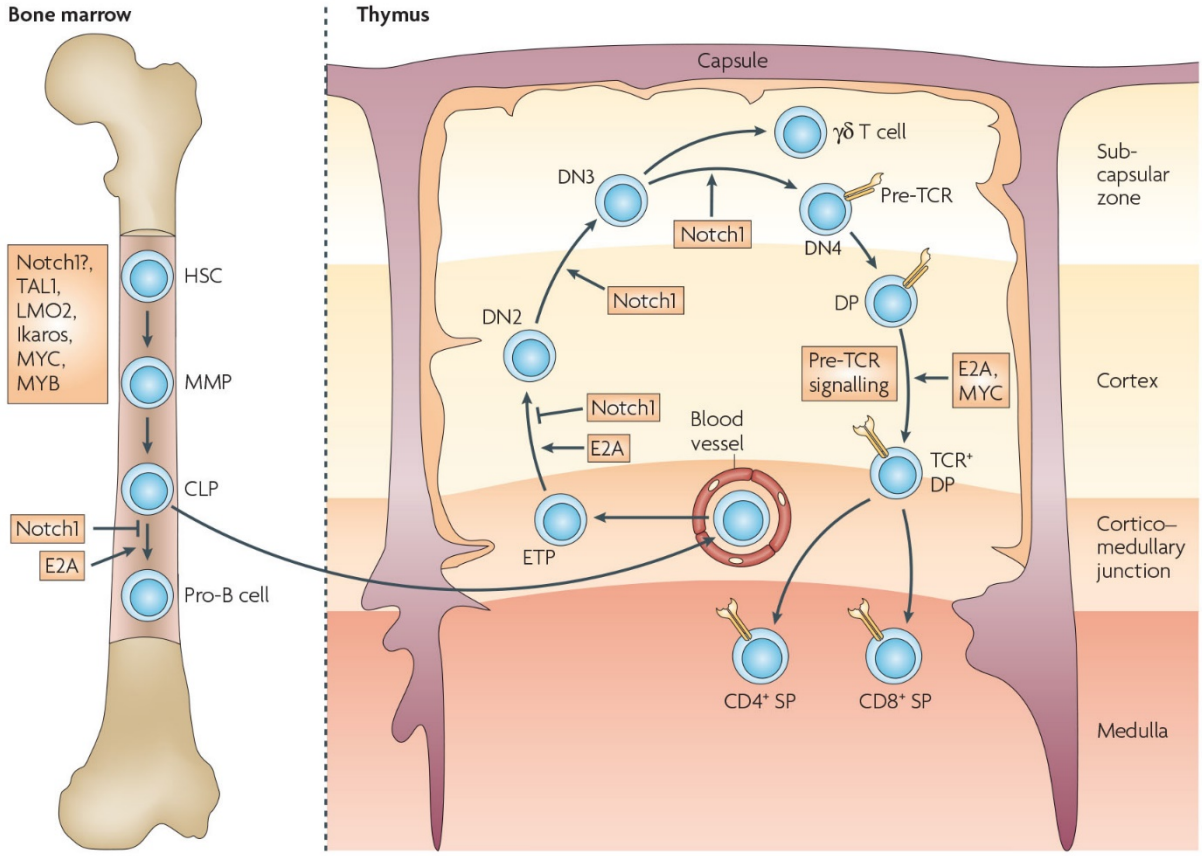

Figure 20. Stages of T-cell development and T-cell-leukaemia-related oncogenes.

Derived from the common lymphoid progenitors (CLPs) of the bone marrow, the T-cell-lineage progenitors (ETPs) migrate to the thymus and commit to the T-cell lineage, progressing through different stages of differentiation, at which oncogenes that are known to be associated with T-cell acute lymphoblastic leukaemia and required in the bone marrow and thymus are also depicted.
(From *Aifantis et al., 2008 Nat Rev Immunol. 8(5):380-90*).

3.1.2 Chemotherapy resistance and relapse

T-ALL patients have cure rates of ca. 10%, substantially lower than the 40% obtained in B-ALL patients[301]. The introduction of intensified chemotherapy protocols had improved therapy outcomes, reaching up to 80% of survival rates in children[302] and 60% in adults[298]. Despite this significant improvement of the outcome of patients, still a significant percentage of both childhood and adult patients do not survive due to

therapy resistance or relapsed disease after a transient initial response[303]. Moreover, the current treatments are associated with severe toxicity and adverse side effects. Thus, a better understanding of the molecular basis of T-ALL origin and progression is essential for the proposal, design and validation of more specific, highly effective and less toxic treatment against this type of leukemia.

3.1.3 Genetic alteration mechanisms

The malignant transformation process of T-cells is very complex. It is sustained by the activation of oncogenic drivers promoting cell anabolism, cell cycle progression and cell growth of the T-cell progenitors. T-ALLs frequently show chromosomal translocations of T-cell receptor gene, resulting in ectopic expression of oncogenic transcription factors (such as TAL1, LMO1, LMO2, TLX1 and TLX3)[304–306]. Activating mutations of different oncogenic signaling pathways are also reported, including RAS and JAK pathways for example[307,308]. Furthermore, they have a deregulation of CDKN2A and CDKN2B cell cycle regulators, and the loss of transcription factors that act as tumor suppressor (such as GATA3, RUNX1, ETV6 and BCL11B)[309,310]. In addition, a recent genome-wide sequencing study reported a correlation between age and the number of somatic mutations in T-ALL, showing that particular genes are preferentially affected in adults versus children[311]. The list of the main mutations observed in T-ALL, including the frequencies in pediatric and adult cases is detailed in **Table 3**. Among all mutations found in T-ALL, more than 50% of patients have highly activated Notch1 signaling pathway, uniformly identified in both pediatric and adult cases[312]. Notch1 plays a main role during T-cell development in the thymus, by interacting with the ligand present in the thymic epithelial stromal cells[313–315]. Due to the high frequency of its upregulation, Notch1 signaling pathway has become one of the most oncogenic drivers of T-ALL transformation. Thus, understandings the role of

Notch1 in T-ALL transformation would be helpful to design new target for anti-leukemic therapy.

Table 3. Mutation frequencies in adult and pediatric T-ALLs.

(Table from *Girardi et al., 2017 Blood 129(9):1113-1123*).

Gene	Type of genetic aberration	Frequency	
		Pediatric	Adult
Notch signaling pathway			
FBXW7	Inactivating mutations	14	14
NOTCH1	Chromosomal rearrangements/activating mutations	50	57
Cell cycle			
CDKN2A	9p21 deletion	61	55
CDKN2B	9p21 deletion	58	46
RB1	deletions	12	
Transcription factors			
BCL11B	Inactivating mutations/deletions	10	9
ETV6	Inactivating mutations/deletions	8	14
GATA3	Inactivating mutations/deletions	5	3
HOXA	Chromosomal rearrangements/inversions/expression	5	8
LEF1	Inactivating mutations/deletions	10	2
LMO2	Chromosomal rearrangements/inversions/expression	13	21
MYB	Chromosomal rearrangements/duplications	7	17
NKX2.1/NKX2.2	Chromosomal rearrangements/expression	8	
RUNX1	Inactivating mutations/deletions	8	10
TAL1	Chromosomal rearrangements/5' super-enhancer mutations/deletions/expression	30	34
TLX1	Chromosomal rearrangements/deletions/expression	8	20
TLX3	Chromosomal rearrangements/expression	19	9
WT1	Inactivating mutation/deletion	19	11
Signaling			
AKT	Activating mutations	2	2
DNM2	Inactivating mutations	13	13
FLT3	Activating mutations	6	4
JAK1	Activating mutations	5	7
JAK3	Activating mutations	8	12
IL7R	Activating mutations	10	12
NF1	Deletions	4	4
KRAS	Activating mutations	6	0
NRAS	Activating mutations	14	9
NUP214-ABL1/ ABL1 gain	Chromosomal rearrangement/duplication	8	
PI3KCA	Activating mutations	1	5
PTEN	Inactivating mutations/deletion	19	11
PTPN2	Inactivating mutations/deletion	3	7
STAT5B	Activating mutations	6	6
Epigenetic factors			
DNMT3A	Inactivating mutations	1	14
EED	Inactivating mutations/deletions	5	5
EZH2	Inactivating mutations/deletions	12	12
KDM6A/UTX	Inactivating mutations/deletions	6	7
PHF6	Inactivating mutations/deletions	19	30
SUZ12	Inactivating mutations/deletions	11	5
Translation and RNA stability			
CNOT3	Missense mutations	3	8
mTOR	Activating mutations	5	
RPL5	Inactivating mutations	2	2
RPL10	Missense mutations	8	1
RPL22	Inactivating mutations/deletion	4	0

3.2 Notch1 signaling in T-ALL

Mammalian Notch family is constituted by four members, named Notch1-4. In contrast, 2 members have been described in *Caenorhabditis elegans* (cLIN-12 and cGLP-1), and only one in *Drosophila* (Notch). Notch proteins which are transmembrane receptors, participating in the embryonic development, cellular transformation, cell fate decisions, and cell-cycle progression[316]. These receptors are heterodimeric proteins, generated upon metalloprotease-mediated cleavage of a single peptide which are composed of an extracellular ligand-binding subunit (known as *Notch extracellular domain* or NECD), a single-pass transmembrane domain, and an intracellular subunit with a transcriptional activity (known as *Notch intracellular domain* or NICD).

Placed at the C terminus, NECD consists of 29-36 tandem EGF (*epidermal growth factor*)-like repeats that mediate interactions with Notch ligands or sense extracellular calcium ion, affecting the signaling efficiency[317,318] (**Figure 21**). Following the EGF repeats, the NRR (*negative regulatory region*) is composed by three cysteine-rich LNR (*Lin12-Notch repeats*) and a HD (*heterodimerization domain*), which physically connects NECD and NICD. NRR blocks the ligand-independent activation of Notch receptor[319,320]. The transmembrane-intracellular domain of Notch is constituted of several domains, which have functions in protein-protein interaction and Notch signaling activation: a TMD (*transmembrane domain*), a RAM (*RBPjκ association module*) domain, NLSs (*nuclear localization sequences*), seven ANK (*ankyrin*) repeats domain, and a TAD (*transactivation domain*) containing the PEST (*proline/glutamic acid/serine/threonine-rich motifs*) domain. RAM and ANK domains mediate the interaction of Notch with the DNA-binding protein CSL[321,322], while PEST domain plays a critical role in the turnover of Notch protein[323,324].

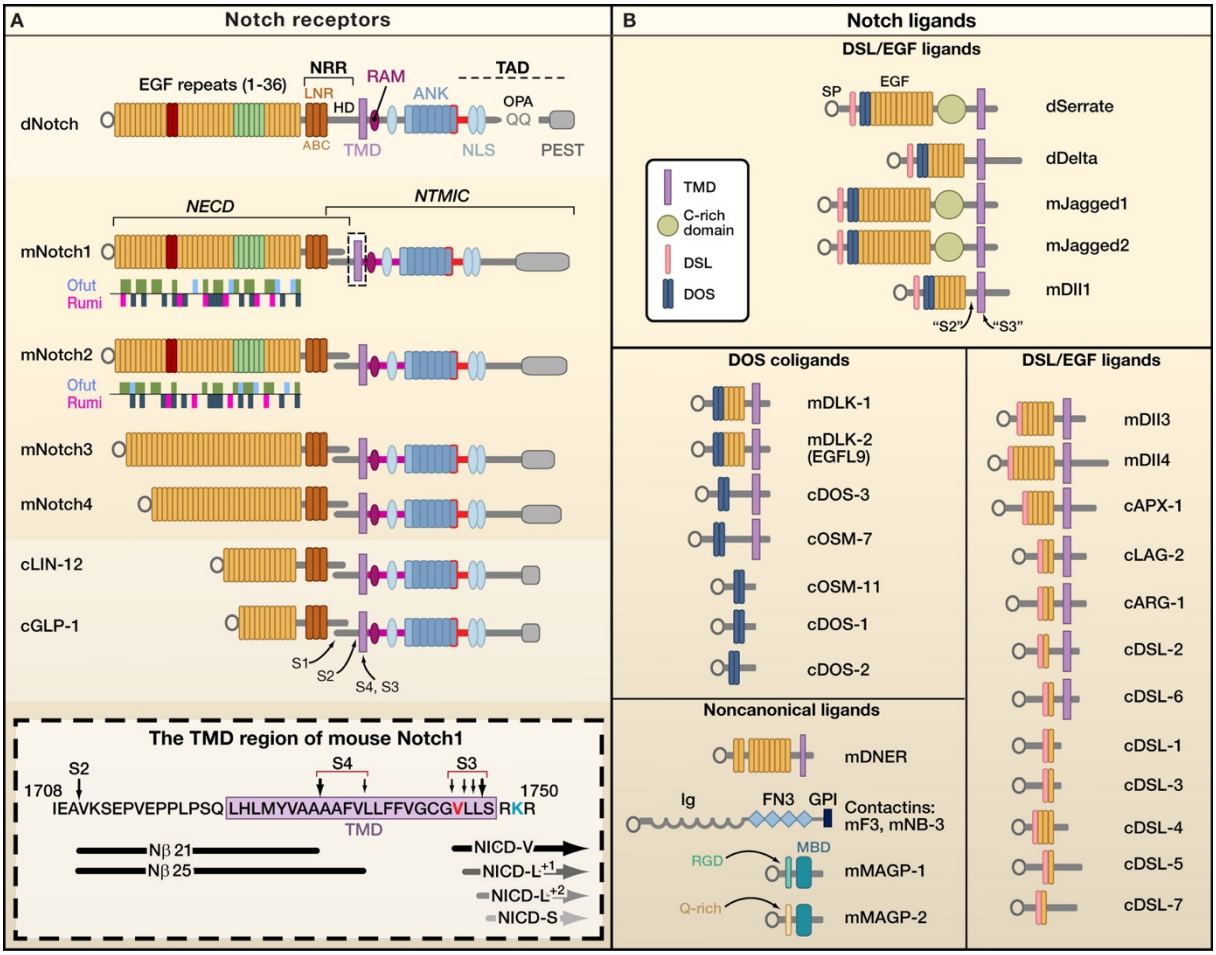

Figure 21. Structure of Notch receptor (A), ligands and coligands (B)

(From *Kopan & Ilagan, 2009 Cell 137(2):216-33*).

First discovered in *Drosophila*, Notch1 was identified in humans through a t(7;9)(q34;q34.3) chromosomal translocation observed in some patients with T-ALL[325,326]. Since only 1% to 3% of patients of T-ALL were found to carry this translocation, the mechanistic role of Notch1 at the origin and development of this malignancy was not clear initially. Later, it was found that additional activating mutations leading to the upregulation of Notch1 pathway are present in more than 50% of the patients with T-ALL, highlighting the direct implication of Notch1 in the proliferation and survival of leukemic cells[312]. In addition, Notch signaling plays also an important role in the tumorigenesis of other types of cancer, notably glioblastoma and colorectal carcinoma[327,328]. Moreover, Notch has been reported to present tumor

suppressing functions in mouse skin, as well as a growth inhibitor effect in keratinocytes, hepatocellular carcinoma, small-cell lung cancer, and bladder cancer[329–332]. Thus, cellular context seems to be key in determining Notch function.

3.2.1 Basic mechanisms of Notch signaling activation

The interaction of the extracellular domain of Notch with ligands of the DSL (*Delta-Serrate-Lag2*) family on the surface of the neighbouring cell leads to two consecutive proteolysis cleavages of Notch receptor. Cleavages by α- secretase/metalloprotease family (ADAM10/Kuzmanian, ADAM17/ TACE) and by γ-secretases release the NICD domain into the cytoplasm[333–336] (**Figure 22**). Once NICD is released from the membrane, it translocates to the nucleus to bind to the DNA-binding transcription factor RBPSUH (*Recombining Binding Protein, Suppressor of Hairless*, also known as RBP-J or CSL). This interaction leads to the release of the co-repressor complex and recruits the transcriptional complex, consisting of MAML (*Mastermind-like*) proteins and the HAT p300[321,337,338]. After recruitment, this complex will interact with RNA polymerase 1 and activate the Notch target gene transcription. The best-characterized Notch downstream target genes are members of the HES (*Hairy and enhancer-of-split*) family, the HEY/HESR (*Hairy and enhancer-of-split-related*) family[339,340], and the transcription factor c-myc[341].

Besides the canonical Notch pathway described above, a non-canonical pathway is also reported upon Notch activation. This pathway is implicated in the regulation of cell differentiation, cell metabolism and tumorigenesis[342–344]. The main characteristic of the non-canonical pathway is CSL-independent activation of Notch1 signaling, participating in the crosstalk of Notch signaling with different pathways, such as the Wnt pathway, PI3K/AKT, mTOR, and JNK. The Notch target gene c-myc is reported to be upregulated also by non-canonical Notch signaling pathway[345].

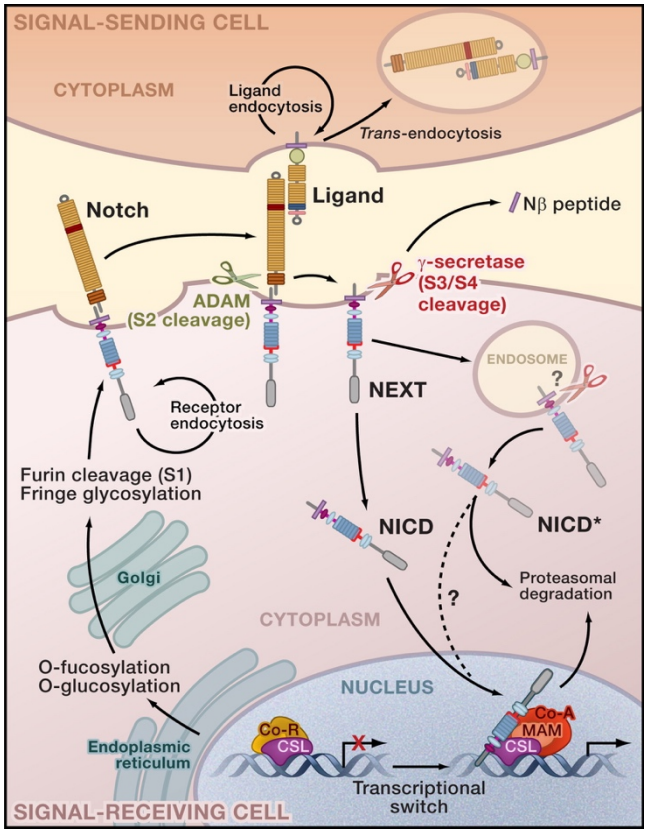

Figure 22. Activation of the Notch Signaling Pathway mediated by posttranscriptional modifications and regulated proteolysis.

(From *Kopan & Ilagan, 2009 Cell 137(2):216-33*).

3.2.2 Modulation of Notch1 signal transduction

Since the discovery of the important role played by Notch1 in T-ALL, a number of modulators of Notch1 signaling have been identified. **Table 4** summarizes these modulators.

3.2.2.1 Expression and endocytic trafficking of DSL ligands and Notch receptors

In mammalian cells, the DSL ligand family consists of five transmembrane ligands: the Jagged (JAG) ligands JAG1 and JAG2, and Delta-like (DLL) ligands DLL1, DLL3 and DLL4. They all have an extracellular domain containing EGF-like repeats, a cysteine-rich DSL domain which is required for their interaction with Notch receptors, a single transmembrane domain, and an intracellular domain[346–348] (**Figure 21**). The activation of Notch signaling by ligand interaction from neighbour cells is a trans-activation

process which positively regulates the transcriptional activity of Notch. But cis-ligands (expressed from the same cells) inhibit Notch signaling through Notch degradation[349–351] and prevent ligand-independent Notch activation[352]. Moreover, each ligand has a specificity for a particular member of the Notch family, and also a subsequent specificity for downstream target activation in a tissue-dependent manner.

Table 4. Core Components and Modifiers of the Notch Pathway.

(From *Kopan & Ilagan, 2009 Cell 137(2):216-33*).

Component Function	Type	*Drosophila*	*Caenorhabditis elegans*	Mammals
Receptor		Notch	LIN-12, GLP-1	Notch 1–4
Ligand	DSL/DOS	Delta, Serrate		Dll1, Jagged1 and 2
	DSL only		APX-1, LAG-2, ARG-2, DSL1–7	Dll3 and 4
	DOS Coligands		DOS1–3, OSM7 and 11	DLK-1, DLK-2/EGFL9
	Noncanonical			DNER, MAGP-1 and -2, F3/ Contactin1, NB-3/Contactin6
Nuclear Effectors	CSL DNA-binding transcription factor	Su(H)	LAG-1	RBPjκ/CBF-1
	Transcriptional Coactivator	Mastermind	LAG-3	MAML1-3
	Transcriptional Corepressors	Hairless, SMRTR		Mint/Sharp/SPEN, NCoR/ SMRT, KyoT2
Receptor Proteolysis	Furin convertase (site 1 cleavage)	?	?	PC5/6, Furin
	Metalloprotease (site 2 cleavage)	Kuzbanian, Kuzbanian-like, TACE	SUP-17/Kuzbanian, ADM-4/TACE	ADAM10/Kuzbanian, ADAM17/TACE
	γ-secretase (site 3/site 4 cleavage)	Presenilin, Nicastrin, APH-1, PEN-2	SEL-12, APH-1, APH-2, PEN-2	Presenilin 1 and 2, Nicastrin, APH-1a-c, PEN-2
Glycosyltransferase modifiers	O-fucosyl-transferase	OFUT-1	OFUT-1	POFUT-1
	O-glucosyl-transferase	RUMI		
	β1,3-GlcNAc-transferase	Fringe		Lunatic, Manic, and Radical Fringe
Endosomal Sorting/ Membrane Trafficking Regulators	Ring Finger E3 Ubiquitin ligase (ligand endocytosis)	Mindbomb 1–2, Neuralized		Mindbomb, Skeletrophin, Neuralized 1–2
	Ring Finger E3 Ubiquitin ligase (receptor endocytosis)	Deltex		Deltex 1–4
	HECT Domain E3 Ubiquitin ligase (receptor endocytosis)	Nedd4, Su(Dx)	WWP-1	Nedd4, Itch/AIP4
	Negative regulator	Numb		Numb, Numb-like, ACBD3
	Neuralized Inhibitors	Bearded, Tom, M4		
	Other endocytic modifiers	sanpodo		
NICD Degradation	F-Box Ubiquitin ligase	Archipelago	SEL-10	Fbw-7/SEL-10
Canonical Target bHLH Repressor Genes		*E(spl)*	*REF-1*	*HES/ESR/HEY*

DSL ligand endocytosis and trafficking are necessary for canonical Notch signaling activation and two not mutually exclusive models have been proposed to explain how DSL endocytosis leads to effective signal activation: the “ligand activation” model, and the “pulling force” model, as explained in **Figure 23**.

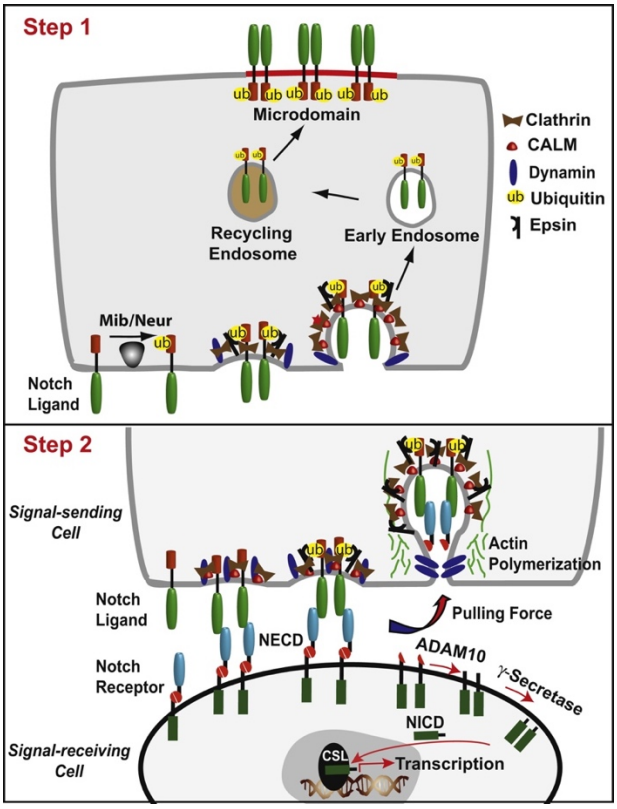

Figure 23. Models of ligand endocytosis in Notch signaling activation.

(**Step 1**) "Ligand activation" model. DSL ligands are ubiquitinated by Mib/Neur and undergo recycling endocytosis in order to return to the plasma membrane under active state (**Step 2**). "Pulling force" model. Ligand endocytosis exerts a pulling force to dissociate Notch extracellular domain (NECD) from the intact Notch heterodimer, allowing activating proteolysis of Notch receptor by ADAM10 and γ-secretase. (From *Weinmaster & Fischer 2011 Dev Cell 21(1):134-44*).

As with the DSL ligands, endocytosis and endosomal trafficking of Notch receptor are playing crucial roles in the availability of Notch receptor for ligand binding. Notch endocytosis is necessary for ligand-dependent Notch activation in both signal-sending and signal-receiving cells[353]. Moreover, disruption of endocytic trafficking leads to proteolytic cleavage in a ligand-independent manner, which induces ectopic activation of Notch signaling[354,355]. Several proteins have been involved in the control of the availability of Notch receptors for ligand binding, as summarized in **Figure 24**.

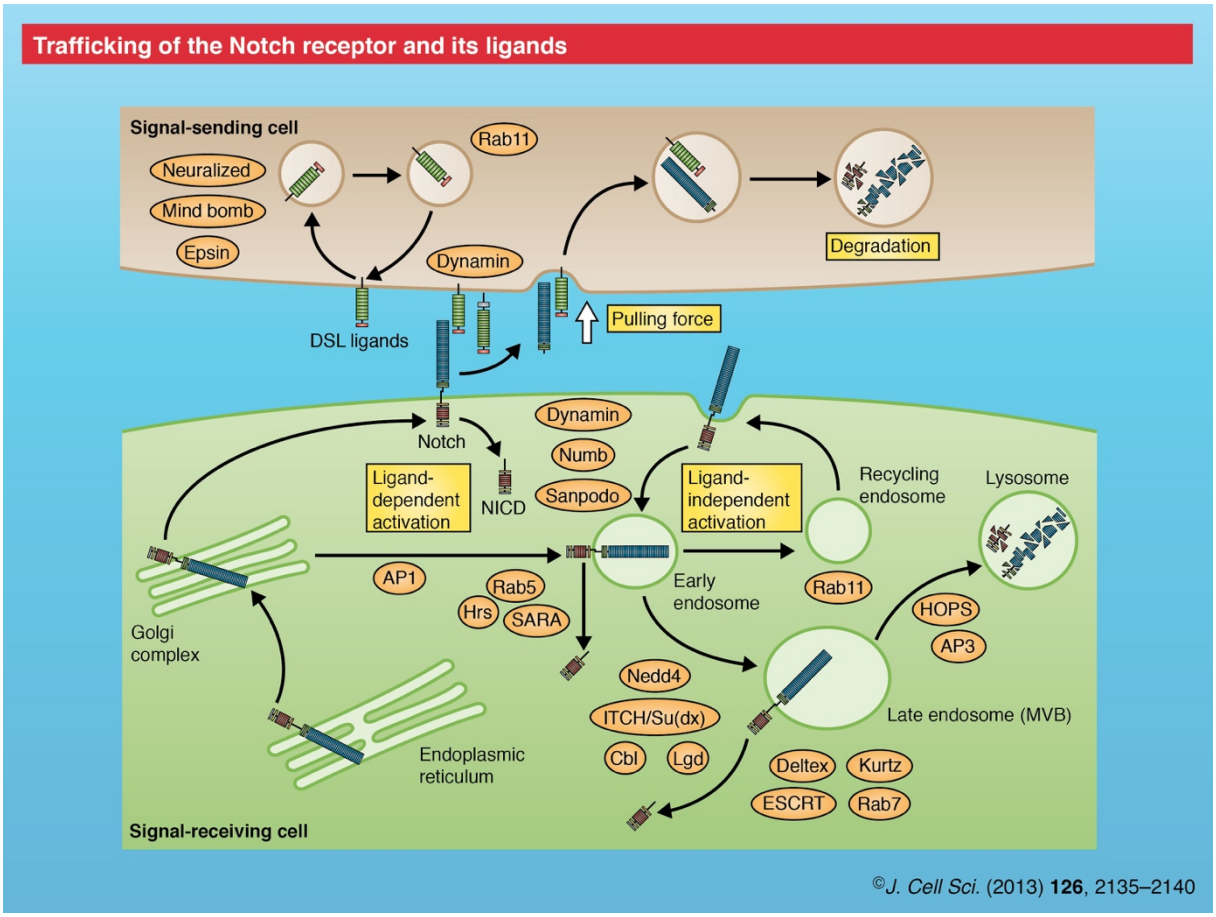

Figure 24. Overview of the endocytosis and trafficking of Notch receptor.

Notch endocytosis is triggered by Dynamin, Numb or Sanpodo and ubiquitinated by different E3 ubiquitin ligases toward recycling or lysosomal degradation.
(From *Hori et al., 2013 J Cell Sci. 126:2135-40*).

3.2.2.2 Post-translational modifications of Notch receptors

Notch1 receptors are firstly synthetized as a single protein (pre-Notch1) before undergoing posttranslational modifications at the endoplasmic reticulum and the Golgi due to the activity of POFUT1 (*protein O-fucosyltransferase1*), POGLUT (*protein O-glucosyltransferase*), Furin et Fringe. Fucosylation and glycolysation by POFUT1 and POGLUT, respectively, are necessary for the processing of Notch1 from the endoplasmic reticulum to the Golgi and also for Notch functioning[356,357] (**Figure 25**).

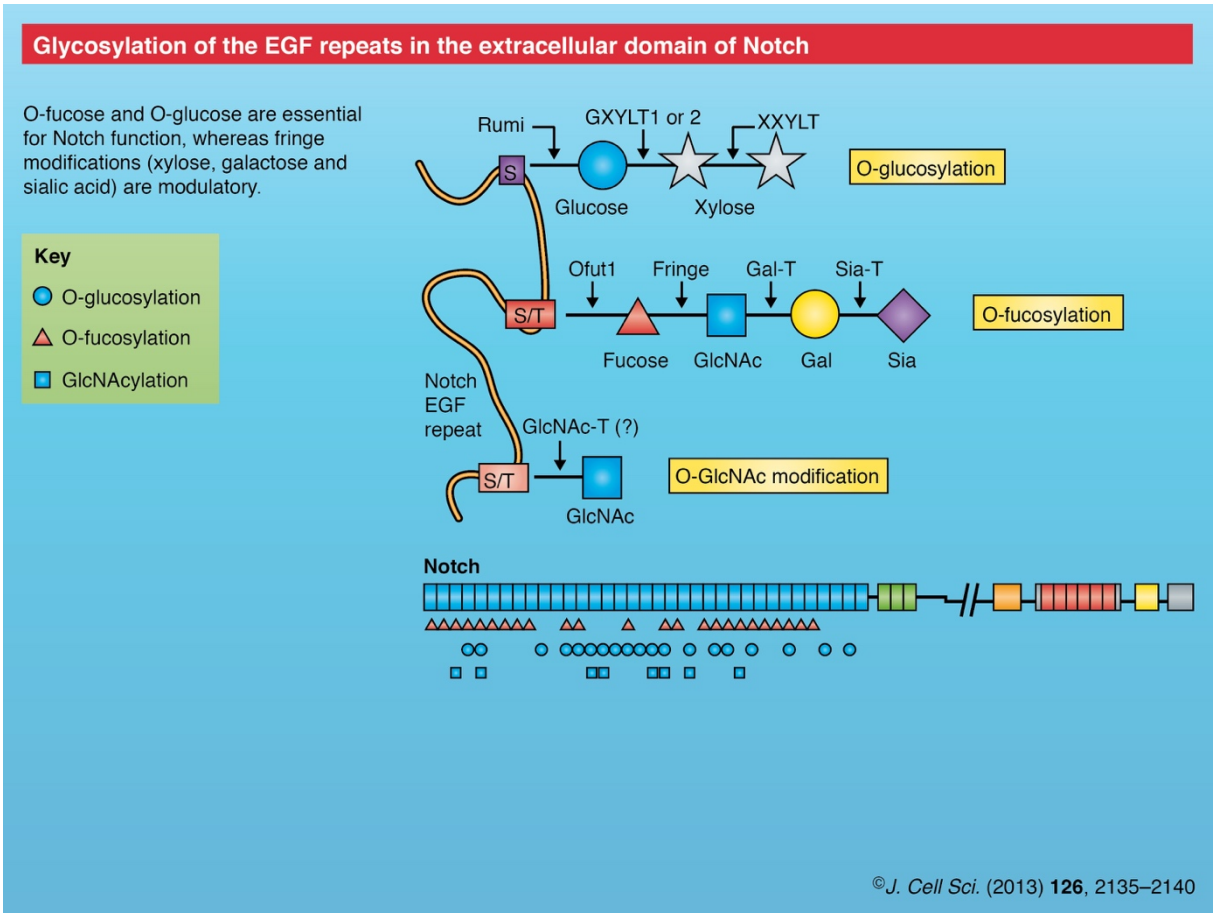

Figure 25. Glycosylation of the extracellular domain of Notch.

O-fucose modifications by Ofut1/POFUT1 enhance Notch affinity for DSL ligands, while O-glucose modifications by Rumi/POGLUT increase receptor proteolysis after ligand interaction. Additionally, modifications by Fringe are necessary for ligand-receptor interaction modulation.
(From *Hori et al., 2013 J Cell Sci. 126:2135-40*).

O-glucosylation and O-fucosylation are both required for Notch activation but they play different roles. O-fucose modifications directly enhance Notch affinity for DSL ligands, while O-glucose modifications increase receptor proteolysis after ligand interaction[358]. Furin convertase catalyses the S1 cleavage to convert the Notch precursor peptide into a final heterodimer, composed of the NECD non-covalently attached to the NICD through the HD domain[359]. Both the O-glucosylation and O-fucosylation on Notch proteins can be elongated to a trisaccharide or tetrasaccharide by different enzymes. Among that, the Fringe family (or N-Acetylglucosaminyl transferase) is participating in

the addition of acetylglucosamine which is indispensable for ligand-receptor interaction and for Notch signaling[360]. Fucose analogs have been developed to block the binding between Notch and its ligands, to repress the activation of Notch signaling[361]. Once processed, the receptor is then endosome-transported to the plasma membrane to enable ligand binding in a manner regulated by Deltex and inhibited by NUMB.

In addition to glycosylation, Notch receptors can be modified by ubiquitination, phosphorylation, acetylation and hydroxylation. Particularly, NICD is subject to a variety of post-translational modifications that tightly regulate Notch activity. Thus, phosphorylation of NICD by GSK3β protects it from proteasomal degradation and enhances ligand-activated signaling[362], while phosphorylation by CDK8 kinase within the PEST domain induce the degradation of NICD (as described below). Mono-ubiquitination can activate Notch[363], while poly-ubiquitination leads to downregulation of Notch signaling.

3.2.2.3 Notch degradation

Notch signaling is modulated by NICD degradation after the activation of several signal from its transcriptional activity. Sustained NICD accumulation by the mutations of PEST domain or mutations that stabilize NICD can lead to T-ALL. Thus, NICD degradation is also a well-regulated process to ensure the turnover of the receptor. For this purpose, NICD is phosphorylated within the PEST domain by the CDK8 kinase and targeted for proteasomal degradation by E3 ubiquitin ligases, including Sel10/FBXW7. Through this mechanism, the transcription activation complex is disassembled and Notch signaling is turned off[364,365]. FBXW7 (*F-box and WD repeat domain containing 7*; also known as AGO and SEL10), is a component of a SCF-E3 ubiquitin ligase complex that is able to bind, ubiquitinate and induce the proteasome-mediated degradation of Notch1 and c-myc[323,366]. FBXW7 recognizes and binds to the

phosphorylated residues in the PEST domain. FBXW7 mutations, present in around 20% of T-ALL patients, have been reported within the WD40 substrate-binding domain, inhibiting its interaction with NICD and inducing the constitutive active Notch1 signaling[367,368]. There is a negative correlation between FBXW7 and PEST domain mutations in T-ALL. Thus, samples with mutations of FBXW7 do not present PEST mutations, and *vice versa*. These data imply that inactivating FBXW7 mutations and Notch1 PEST domain mutations have similar effects on the Notch stabilization by inhibiting proteasomal degradation. Moreover, mutations of FBXW7 lead to the stabilization of other oncogenes, including c-myc and presenilin-1, a component of γ-secretase protease complex, which play also an important role in leukemic growth[369,370]. Interestingly, Notch1 can indirectly down-modulate the transcription of FBXW7 through miR-223 activity, allowing an aberrant activation of Notch1 to overcome the effect of FBXW7 activity during leukemogenesis[371].

3.2.2.4 Intrinsic Notch mutations

Aberrant activation of Notch1 signaling in T-ALL could be due to mutations in Notch1 receptor itself, or in components that negatively regulate the pathway. The chromosomal translocation t(7;9)(q34;q34.3) results in high expression of a truncated Notch1 receptor either as NICD or as a membrane-bound protein which lacks the extracellular domain and is constitutively processed into NICD by the γ-secretase complex[326,341]. However, sequencing of T-ALL cells and patient samples showed that the majority of mutations found in the Notch1 locus are located in two regions, the HD and PEST domain (**Figure 26**). PEST domain mutations were identified in T-ALL patients, resulting from the insertion of translational termination codons, or from the mutation of the FBWX7 degron region[372]. These mutations increase the half-life of the intracellular domain by preventing FBXW7 interaction and Notch1 degradation.

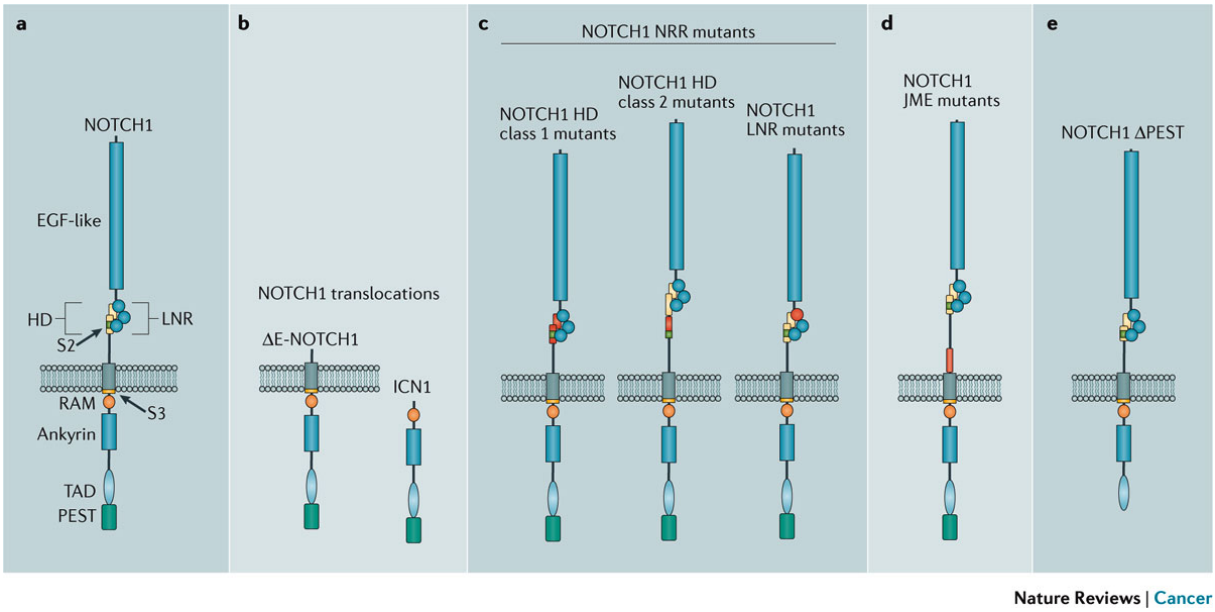

Figure 26. Different intrinsic mutations of Notch proteins.

(**a**) Full length wild-type Notch receptor with its functional domains. (**b**) Truncated form ΔE-Notch1 due to chromosomal translocations. (**c**) Notch1 receptor with mutated HD and LNR domains. (**d**) Notch1 juxtamembrane expansion (JME) mutants. (**e**) Notch1 receptor with mutated PEST domain. Sequences altered by the various Notch1 mutations are highlighted in red. (From *Belver & Ferrando 2016 Nat Rev Cancer 16(8):494-507*).

HD domain is located in the transmembrane domain of Notch, where the extracellular domain interacts with the intracellular domain to form a heterodimer. Mutations found in the HD domain result in ligand-independent proteolytic cleavage of Notch, leading to constitutive activation of the Notch signaling pathway[312,319]. Particularly, about 20% of patients with T-ALL harbor co-occurrence of HD and PEST domain mutations, leading to highly activated Notch1 signaling. Therefore, two convergent activation mechanisms which contribute to aberrant Notch1 activation in T-ALL: the ligand-independent receptor activation (via HD domain mutations), and the impaired signaling termination through NICD stabilization (via PEST domain mutations or FBXW7 mutations).

3.2.3 Genes and pathways controlled by Notch1

During last years, the intense work of a great number of research teams identified a still expanding network of signaling pathways operating downstream of Notch1. A representation of the most prominent among them is represented in **Figure 27**. Although the bHLH transcriptional factors Hes1 and Hey1 and the transcription factor c-myc are the best-characterized targets of Notch1, Notch1 also activates major cellular pathways such as PI3K/AKT/mTOR pathway, and interleukin 7.

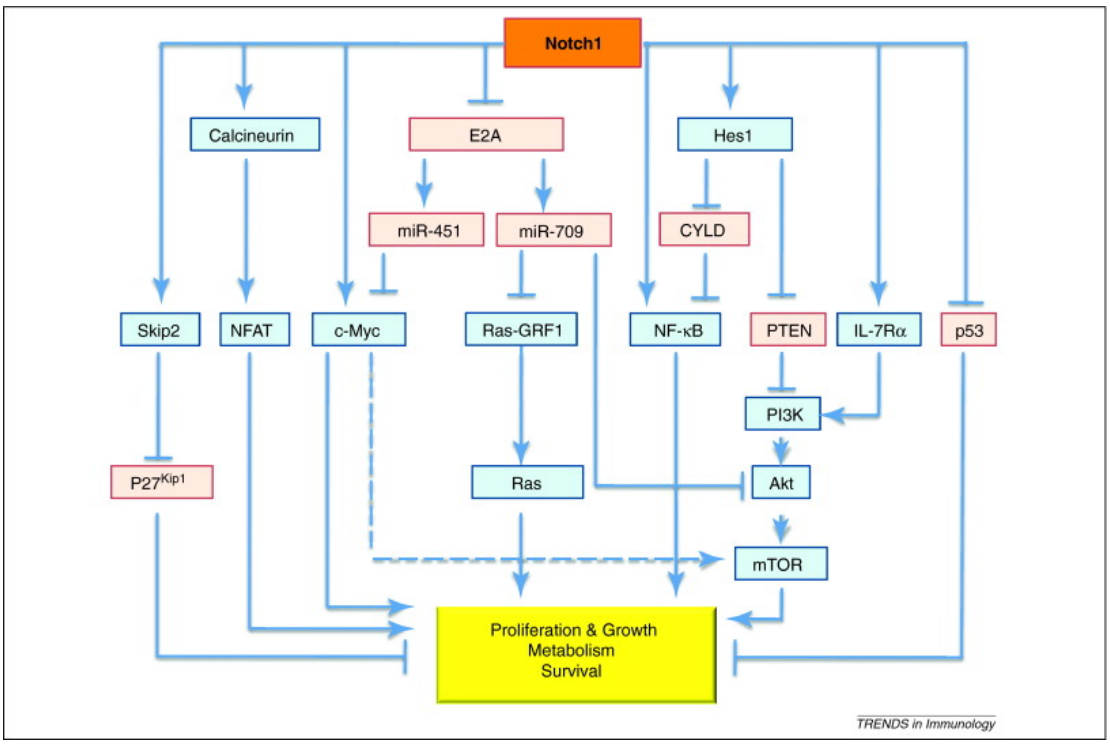

Figure 27. Downstream signaling pathways of Notch1 in T-ALL.

Different direct and indirect regulatory proteins, which are downstream of Notch1, contribute to the development of T-ALL. Growth promoting signaling pathways and proteins are highlighted in blue, whereas growth inhibitory proteins are shown in red. (From *Koch & Radtke 2011 Trends Immunol. 32(9):434-42*).

3.2.3.1 c-myc

As a direct target of Notch1, c-myc plays a central role in promoting cell growth and metabolism of T-ALL. The inhibition of Notch1 signaling downregulates rapidly c-myc, and loss of Notch1 signaling in some T-ALL cells can be partially rescued by

overexpression of c-myc[341,373], underscoring the prominent participation of c-myc in Notch1-dependent signaling. c-myc plays different functions, including the regulation of anabolic genes expression, metabolism, cell growth, stem cell-renewal and differentiation[341]. Its alterations are rarely found in T-ALL (less than 5%), but c-myc is one of the most frequently activated oncogenes in T-ALL through different deregulated pathways. As a result, more than 50% of T-ALL cases have an increased c-myc transcription due to Notch1 upregulation[373]. Besides, c-myc is also activated post-translationally as a consequence of mutations in FBXW7 or PTEN/PI3K/AKT/mTORC1 pathway, which impair its ubiquitination or phosphorylation-mediated degradation[369,374]. This relationship is indeed bidirectional, as c-myc, via microRNA-30a, modulates Notch1: microRNA-30a, a member of a family of miRNAs that are transcriptionally suppressed by c-myc, directly binds to and inhibits Notch1 and Notch2 expression[375]. However, although c-myc and Notch1 regulated genes have a broadly overlapping profile, Notch1 is still oncogenically dominant over c-myc, because c-myc is incapable of maintaining T-ALL tumors in the absence of NICD[376].

3.2.3.2 Hes-1

Hes-1 is a bHLH transcriptional repressor which plays a key role in the induction and maintenance of T-ALL, modulating cell cycle, cell growth signaling and quiescence[377,378]. Loss-of-function mutations or knockdown of Hes1 induce a severe block in proliferation and an increase in cell death in Notch1-driven T-ALL cells, indicating that Notch1-induced T-ALL is Hes1-dependent[379,380]. Hes1 exerts its functions in T-ALL through the inhibition of PTEN[381] and CYLD[382,383]. PTEN is a negative regulator of the PI3K/mTORC1 pathway. Hence, the transcriptional repression of PTEN by Hes1 points to the link between Notch1 signaling and mTORC1

pathway. Through the repression of the deubiquitinase CYLD, a negative regulator of IKK activity, Hes1 mediates the indirect activation of the NF-κB pathway[384].

3.2.3.3 Interleukin-7

IL-7 (*interleulin-7*) and its receptor IL-7R, are essential for normal T-cell development and homeostasis. IL7 signaling plays also a role in T-ALL progression, and appears mutated in T-ALL with somatic gain-of-function mutations in 10% of patients with T-ALL[237,385]. Moreover, 18% of adult and 2% of pediatric T-ALL cases have activating mutations in *JAK1*, which encodes a tyrosine kinase that directly binds to IL-7Rα[386]. Active Notch1 binds to a conserved CSL-binding site in the human IL7R gene promoter and regulates IL7R transcription and IL-7Rα expression via the CSL-MAML complex[387]. In turn, IL-7Rα activation leads to PI3K signaling upregulation to promote T-ALL proliferation[388].

3.2.3.4 Cell cycle

Cell cycle progression is a tightly controlled cellular process that is regulated by several checkpoints. Notch1 promotes proliferation via increased G1/S cell cycle progression in T-ALL. γ-secretase inhibitor (GSI) treatment (which leads to Notch1 signaling inhibition) of these cells results in a G0/G1 arrest. Cyclin D3, a direct target of Notch1 necessary for Notch1-driven T-ALL[389], in conjunction with their catalytic partners CDK4 (*cyclin-dependent kinase 4*) and CDK6 (also upregulated by Notch1[389]), facilitate the progression through the G1 phase. The expression of cyclin D3 rescues T-ALL cell lines from GSI-induced G1 arrest. Furthermore, Notch1 can promote premature entry into S phase in hematopoietic progenitors by inducing the transcription of the E3 ubiquitin ligase SKP2 (*S phase kinase-associated protein 2*) and the subsequent proteasome-mediated degradation of the CDK inhibitors CDKN1B (p27/Kip1) and

CDKN1A (p21/Cip1)[390]. Finally, Notch induces cell-cycle progression through direct activation of myc-dependent cell cycle regulatory mechanisms[391].

3.2.3.5 Metabolism

Notch1 signaling is recognized as a key player on metabolism regulation in several organs and tissues, including liver, brain, adipose tissue, and the immune system, making Notch1 pathway a potential target to treat metabolic disease[392]. The role of Notch1 in T-ALL metabolism regulation is not well known. Glutaminolysis has been reported to be a critical pathway for leukemia cell growth downstream of Notch1 and also a key determinant of the response of anti-Notch1 therapies *in vivo*[393]. However, the precise mechanism connection Notch1 and glutaminolysis regulation is not known. In addition, Notch1 can also promote glycolytic metabolism through PI3K/AKT pathway[393,394], driving mitochondrial oxidative metabolism through c-myc activity[341]. In chronic lymphocytic leukemia, Notch1 and c-myc signaling mediates the glycolytic switch induced by stromal cells of the BM[395]. This glycolytic switch increases the glycolytic capacity accompanied by an increased glucose uptake, expression of glucose transporter, and glycolytic enzymes. Likewise, Notch1 activation in chronic myelogenous leukemia alters mitochondrial metabolic pathways, such as oxidative phosphorylation, glutamine metabolism, TCA cycle, and fatty acid oxidation[396].

3.2.4 The interplay between glutamine metabolism, Notch1 and mTORC1

3.2.4.1 Crosstalk between Notch1 and mTORC1 signaling

The role of Notch1 as regulator of cell growth is supported partially by the activation of the PI3K/AKT/mTORC1 pathway in T-cell progenitors and in T-ALL cells. Constitutive activation of mTOR signaling has been reported in some T-ALL cases to regulate cell viability, cell size and cell proliferation[397]. In particular, alterations in PTEN, PI3K, or AKT leading to mTORC1 activation frequently occur in T-ALL patients[398]. Furthermore,

mTORC1 mediates the control of IL-4-dependent proliferation of T-ALL through cell cycle regulation[399] or IL-7-mediated T-ALL viability[400]. Interestingly, loss of mTORC1 blocks the development of early T-cell progenitors and leukemia[401], and Raptor deficiency in T-ALL models results in cell cycle arrest and the efficient eradication of leukemia both *in vitro* and *in vivo*. Likewise, targeted inhibition of mTORC1 has been reported as an efficient strategy against T-ALL in different studies[402–404], highlighting the potential importance of mTOR signaling as a therapeutic targets in T-ALL.

The connection between Notch1 and mTORC1 is complex (**Figure 28**). In one side, Notch1 activation is mTOR-dependent. In TSC1/2-deficient cells, hyperactive mTORC1 positively regulates Notch1 signaling through the induction of STAT3/p63/Jagged signaling cascade[405]. Furthermore, Notch and c-myc upregulation upon PI3K/mTOR inhibition or mTORC1/2 dual inhibition provides with a potential mechanism of resistance in different tumors, including breast cancer or brain tumors[406–408]. However, the molecular mechanism by which PI3K/AKT/mTORC1 regulates Notch1 are not clear, and sometimes follow opposite directions. For instance, it has been reported that active forms of AKT inhibit the nuclear localization of NICD [409], while PI3K-regulated SGK kinase enhances FBXW7-mediated degradation of NICD[410]. Also, GSKα and GSKβ, both of them AKT substrates, have an ambiguous role in the regulation of Notch1 signaling[362,411,412].

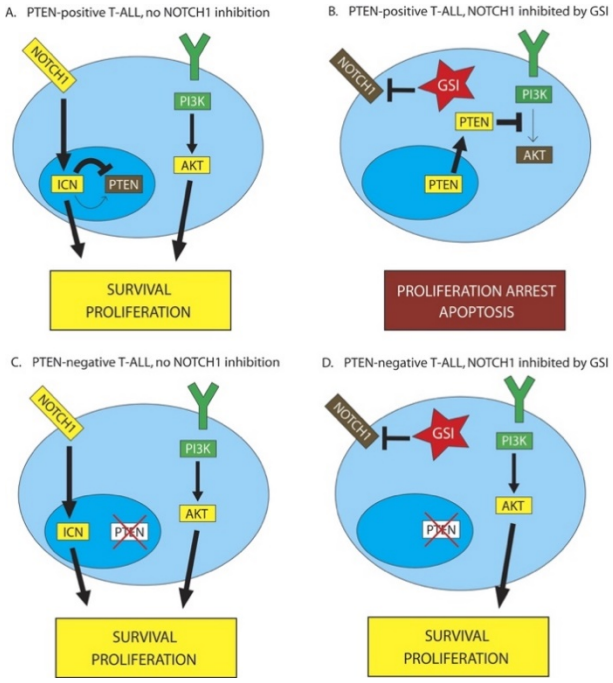

Figure 28. The crosstalk between Notch1 and PI3K/AKT signaling pathways.

(**A and B**). In PTEN-positive T-ALL, Notch1 inhibition leads to proliferation arrest and induces apoptosis. Thus, those cells are dependent of Notch1 signaling for survival and proliferation. (**C and D**). In the absence of PTEN, Notch1 inhibition cannot inhibit cell proliferation due to the constitutive activation of PI3K/AKT pathway. PTEN-negative T-ALL are independent of Notch1 and are resistant to Notch1 inhibition. (From *Gutierrez & Look 2007 Cancer Cells 12(5):411-3*).

In other hand, Notch1 is not only a downstream effector of PI3K/mTORC1 pathway, but it is also an upstream effector of mTORC1 signaling. Stem cell expansion *in vitro* and *in vivo* is regulated by Notch signaling, which induces the expression of Hes3 and Shh (*Sonic hedgehoc* (Shh) through the activation of AKT/STAT3/mTORC1 axis[413]. mTORC1 also mediates Notch1-dependent cell survival of p53 wild type cancer cells during chemotherapy response, and mTORC1 inhibition using rapamycin efficiently blocks Notch1-induced chemoresistance[414]. In addition, downregulation of Notch1 pathway using GSI is accompanied by the inhibition of mTORC1 signaling[415,416,417,418]. Moreover, the combination of GSI and rapamycin treatments shows a synergistic effect in the suppression of tumor growth of T-ALL. But again, the molecular mechanism of Notch-mTORC1 connection is also elusive in T-ALL. Some results suggest a

PTEN/PI3K/AKT-dependent, as Notch1 inhibition using GSI in T-ALL fails to block the growth of T-ALL cell lines carrying PTEN mutation or deletion[381]. Indeed, under Notch1 inhibition, PTEN is reactivated and inhibits PI3K/AKT/mTORC1 pathway. But in parallel, Notch1 can upregulate mTORC1 in a PI3K/AKT-independent manner, following a c-myc-dependent mechanism[417]. However, the precise mechanism by which c-myc activates mTORC1 is unknown. As c-myc is a well-known regulator of the enzyme GLS of glutaminolysis[213], which in turn activates mTORC1 signaling[58], an attractive possibility is that glutamine metabolism might play an intermediary role in Notch1-dependent mTORC1 activation in T-ALL.

3.2.4.2 Crosstalk between glutamine metabolism and Notch1 signaling

While the connection between mTORC1 and glutamine is well studied, the link between Notch1 and glutamine metabolism is far less understood. In a publication of the team of Prof Adolfo Ferrando, glutaminolysis was reported to play a critical role in leukemia progression downstream of Notch1, being a key determinant of the response to anti-Notch1 therapies *in vivo*[393]. Mechanistically, inhibition of Notch1 induces glutaminolysis inhibition and triggers autophagy supporting leukemic survival and cell growth by recycling essential metabolites required for leukemic cell metabolism. The combination between Notch1 and GLS inhibition has a synergistic effect and induced marked therapeutic responses *in vivo*. However, loss of PTEN can abrogate the therapeutic response to this combination. Confirming the control of GLS by Notch1, an independent study in glioblastoma cells reached similar conclusions, showing a decrease of intracellular glutamate after Notch1 blockade[419]. In addition, the increase of Notch1 signaling induces glucose and glutamine transport, and supports protein O-GlcNAcylation in T-cells through O-GlcNAc transferase activity. The enzyme O-GlcNAc transferase is necessary for Notch-mediated self-renewal and malignant

transformation of β-selected T cell progenitors during thymus development[420]. Ambiguously, a comparative metabolomics study showed that upregulation of Notch1 signaling decreases expression of GLS, GDH, OAT (*ornithine aminotransferase*) and glutamine consumption[396]. These authors also showed that an increases glutamine utilization disrupts Notch signaling pathway with a decrease in cleaved Notch1, RBP-J, Hey1 expression and in Notch activity, adding more confusion rather than explanations to the relationship between glutamine and Notch1. In conclusion, our understanding about this connection between Notch1 and glutamine metabolism is very modest. And although Notch1 signaling has been reported to regulate cell metabolism, this connection needs more investigations for the design of better therapeutic strategies in the cancer field, especially in T-ALL.

3.3 Notch1-driven T-ALL therapies

Given the important role of Notch1 signaling in cell proliferation and cell growth in T-ALL, the possibility of developing anti-Notch1 targeted therapies in this disease was conceived years ago. A summary of these strategies is represented in **Figure 29**.

3.3.1 Inhibition of Notch1 using γ-secretase inhibitors

As explained above, the γ-secretase complex contributes to the cleavage of Notch receptor, leading to the activation of Notch signaling. GSI block the activity of all four Notch receptors and showed good efficiency in T-ALL treatment in early studies. Indeed, Notch inhibition by GSI results in rapid clearance of activated Notch1, downregulation of Notch1 target genes, reduction of cell growth and cell proliferation by inducing G1 cell cycle arrest[421]. However, GSI treatment has shown drug-related toxicity or relapsed resistance[422]. The most common toxicity of GSI comes from inhibition of gastrointestinal Notch1 signaling, inducing severe intestinal crypt goblet cell metaplasia, which is a significant obstacle for the clinical development of these

drugs[423]. These adverse side effects result from the important role played by Notch1 and Notch2 in the intestinal epithelium to control cell proliferation and cell differentiation[424]. However, this unfavorable toxicity could be limited using intermittent dosing strategies[425].

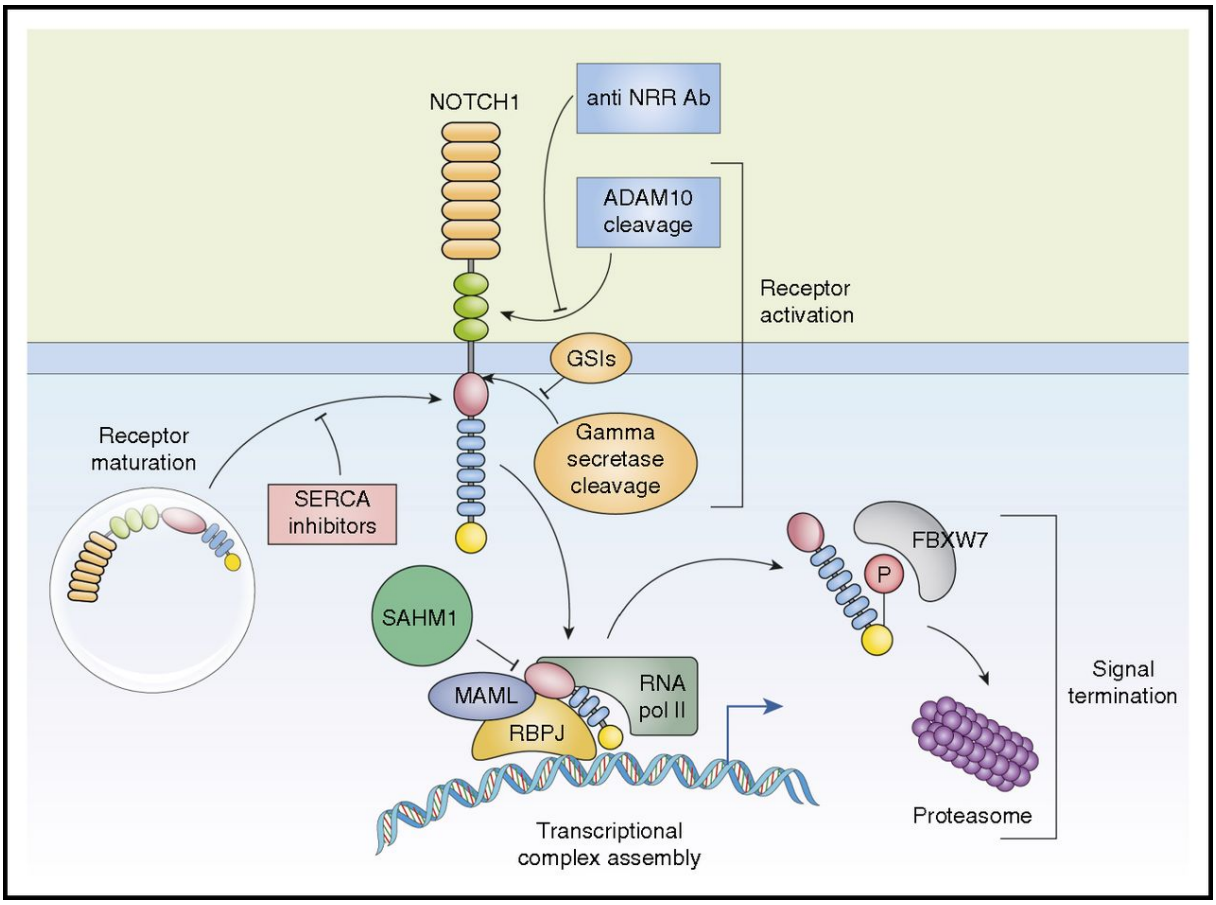

Figure 29. Different strategies to target Notch signaling pathway.

γ-secretase inhibitors, anti-NRR antibody and staple peptide SAHM1 are developed respectively to inhibit the cleavage and the transcription activity of Notch receptor. (From *Sanchez-Martin & Ferrando 2017 Blood 129:1124-1133*).

In addition to the drug-related toxicity, anti-Notch1 therapies design has to confront treatment resistance in T-ALL cells. Upon GSI treatment, T-ALL cells may have accumulated additional mutations, including PI3K/AKT/mTORC1 reactivation or PTEN mutational loss, to bypass the effects of Notch1 inhibition[381]. Thus, a combination of GSI with other targeted therapies appears as an alternative approach to overcome GSI

resistance in T-ALL and to improve the efficacy of anti-Notch1 therapies. For instance, combinational therapies of GSI together with PI3K/AKT/mTORC1 inhibitors[417,418], CDK inhibitors[426], or NF-κB inhibitors[427] have been shown to increase its antileukemic effects.

3.3.2 Inhibition of Notch1 by therapeutic antibodies

Alternative strategies to target the Notch1 pathway include specific Notch1-inhibitory antibodies, which interfere with the processing of Notch1-mutant proteins. Different classes of blocking anti-Notch antibodies had been developed. The first type is an anti-Notch1 antibodies binding to the extracellular NRR region of the receptor, which protects the Notch1 protein from metalloprotease cleavage[428–430]. The second class are ligand competitors which bind to the EGF-repeat region of Notch receptors and block the ligand binding domain[431]. Globally, anti-Notch antibodies significantly induce cell cycle arrest and reduce cell proliferation with an increase of apoptosis *in vitro* and *in vivo* against T-ALL cell lines. These antibodies that selectively inhibit either Notch1 or Notch2 receptor exert anticancer activity in animal models without reduced toxicity, whereas combination of both type of antibodies have similar levels of toxicity than GSI treatment[430]. Lastly, antibodies against Notch ligands have shown anticancer effects by preventing the activation of Notch receptors by endogenous ligand in solid tumors[432–434]. Overall, inhibition of Notch1 by therapeutic antibodies has the advantage of better specificity but reduced bio-distribution and half-life.

3.3.3 Blocking Peptides

The development of blocking peptides which target the Notch transcriptional factor complex is the next therapeutic tool to inhibit the growth of transformed T-ALL cells. For example, the synthetic, cell-permeable peptide SAHM1, derived from MAML1, directly binds to the pre-assembled Notch-CSL complex and compete with MAML1, its

co-activator[435]. The binding of SAHM1 to Notch-CSL blocks the transcription of Notch-downstream target genes and thus inhibits leukemic progression through the inhibition of Notch signaling. However, this strategy inhibiting the Notch transcriptional complex will still block the signaling of all four Notch receptors with potential side effects resulting from the simultaneous inhibition of Notch1 and 2 in the intestine. In addition to that, Zimz1 has been recently showed as a direct and selective cofactor of Notch1 to control the expression of certain Notch target genes such as c-myc[436]. Thus, the development of staple peptides could be used to target the interaction between Zmiz1 and NICD. The use of small peptides has some advantages of good permeability, small size, high specificity and ability to disrupt protein-protein interactions, thus a strong anti-tumor effects[437].

3.3.4 Therapeutic targeting of downstream signaling components of the Notch pathway

Targeting the downstream signaling components of Notch pathway is also another therapeutic strategy. Several downstream targets of Notch are known, including c-myc, Hes1, and Hey1. Direct suppression of c-myc by JQ1, a BRD4 inhibitor, or SAHA, a HDAC inhibitor, have been shown to decrease c-myc expression levels and to inhibit leukemic progression in mouse models of Notch1-induced T-ALL and human T-ALL xenografts[438,439]. Silvestrol, an inhibitor of eIF4A (i.e., an indirect inhibitor of protein translation) can obliterate oncoproteins including c-myc, Notch, Cdk6, and Bcl2, showing strong antileukemic effects against T-ALL cells and in leukemic xenografts models[440]. Inhibition of Hes1 using perhexiline, a small molecule inhibitor of mitochondrial carnitine palmitoyltransferase-1, induces robust antileukemic activity against Notch1-induced leukemias *in vitro* and *in vivo*[379]. Finally, pharmacologic or genetic inhibition of IGF1R, a direct Notch1 target, also inhibits growth and viability of T-ALL cells and influence the leukemia-initiating cell activity of Notch1-induced

tumors[441]. Increased p53 activity using low-molecular-mass compounds that stabilize p53, such as Nutlin-3, or that induce refolding of p53 mutants into a form with wild-type activity, such as PRIMA-1 and RITA, provides also an attractive avenue for therapeutic intervention in Notch-driven T-ALL.

Objectives of the thesis

In this thesis, we have evaluated the connection of cell signaling deregulation and metabolism transformation in cancer, particularly mTORC1 signaling, Notch1 signaling, and glutamine metabolism. As deeply explained in the Introduction section, both mTORC1 and Notch1 signaling pathways are deregulated in cancer, promoting tumor growth and disease progression. Although some treatments targeting these two signaling pathways are currently available in the clinics, these treatments present problems of therapy resistance and relapsed disease. Thus, the objectives of this thesis focused on studying new strategies to target mTORC1 and Notch1 signaling to treat cancer. In the first chapter, I aimed at finding new mTOR inhibitors that, contrary to previously reported inhibitors, could efficiently eliminate cancer cells. Particularly, I concentrated in the molecular action mechanisms of a new class of mTORC1 inhibitor, termed ICSN3250. Our hypothesis proposed that ICSN3250 could act by displacing PA from the active site of mTOR, which might result in cancer cytotoxicity. In the second chapter, I aimed at investigating the metabolic changes resulting from Notch1 signaling upregulation in T-ALL cells. In this case, our hypothesis proposed that Notch1 signaling could induce changes in the metabolism of glutamine, leading to the deregulation of mTORC1. Through both chapters, we proposed a molecular link between mTORC1 pathway, glutamine metabolism, and Notch1 signaling which would constitute a new strategy for the design of targeted therapies against cancer.

RESULTS

Chapter one: A novel mechanism of mTOR inhibition displacing phosphatidic acid induces enhanced cytotoxicity specifically in cancer cells.

Aims of the project

The main aim of this project is about the study of the effect of mTORC1 inhibition by a new class of inhibitors which targets specifically cancer cells. Due to modest results of mTORC1 inhibitors for anti-cancer strategy, the development of new treatment is under investigations. In this project, we have studied the mTORC1 inhibition by a newly synthetized compound, ICSN3250, an analogue of the cytotoxic marine alkaloid halitulin. Interestingly, only cancer cells are sensitive to this compound, while non-cancer cells showed up to 100-fold less sensitivity to ICSN3250, in contrast to other inhibitors which did not show selectivity. The molecular mechanism of this inhibition is based on the displacement of PA (phosphatidic acid), an activator of mTORC1 complex, from the FRB domain of mTOR. Furthermore, ICSN3250 is able to affect PA ability to overcome the TSC2 negative regulation on mTORC1, which is the novelty of our work in the design of this new mTOR inhibitor.

This work has been submitted to Cancer Research in January 2018 and it is under correction after the first revision.

A novel mechanism of mTOR inhibition displacing phosphatidic acid induces enhanced cytotoxicity specifically in cancer cells

Tra-Ly Nguyen[1], Maxim Egorov[2], Clément Bodineau[1], Joanna Wdzieczak-Bakala[3], Maria Concepcion Garcia-Alvarez[3], Jérôme Bignon[3], Odile Thoison[3], Bernard Delpech[3], Georgiana Surpateanu[3], Yves-Michel Frapart[4], Fabienne Peyrot[4,5], Kahina Abbas[4], Silvia Terés[1], Pierre Soubeyran[6], Bogdan I. Iorga[3,8], Raúl V. Durán[1,8], and Pascal Collin[3,4,7,8]

[1] Institut Européen de Chimie et Biologie, INSERM U1218, Université de Bordeaux, 2 Rue Robert Escarpit, 33607 Pessac, France

[2] ATLANTHERA, 3 Rue Aronnax, 44821 Saint-Herblain Cedex, France

[3] Institut de Chimie des Substances Naturelles, CNRS UPR 2301,1 Avenue de la Terrasse, 91198 Gif-sur-Yvette, France

[4] Laboratoire de Chimie et Biochimie Pharmacologiques et Toxicologiques, CNRS UMR8601, Université Paris Descartes, Sorbonne Paris Cité, 45 Rue des Saints Pères, 75006 Paris, France

[5] Ecole Supérieure du Professorat et de l'Education de l'Académie de Paris, Sorbonne Université, 10 rue Molitor, 75016 Paris, France

[6] Institut Bergonié, INSERM U1218, Université de Bordeaux, 229 Cours de l'Argonne, 33076 Bordeaux, France

[7] Université Paris Diderot, UFR Odontologie, 5 Rue Garancière, 75006, Paris, France

Running title: Targeting cancer cells with a new class mTORC1 inhibitor

Key words: cancer, cytotoxicity, ICSN3250, mTOR, phosphatidic acid

Financial support: This work was supported by funds from the following institutions: Centre National de la Recherche Scientifique-CNRS, Institut National de la Santé et de la Recherche Médicale - INSERM, Fondation pour la Recherche Médicale, the Conseil Régional d'Aquitaine, Fondation ARC pour la Recherche sur le Cancer, Ligue Contre le Cancer - Gironde, SIRIC-BRIO, Institut de Chimie des Substances Naturelles -ICSN, Institut Européen de Chimie et Biologie, Université Paris-Descartes, Société d'Accélération de Transfert de Technologie d'Ile de France-SATT IDF-innov.

[8] To whom correspondence should be addressed:

Raúl V. Durán. Institut Européen de Chimie et Biologie, 2 Rue Robert Escarpit, 33607 Pessac, France. Tlf: +33 (0) 54 000 2259. FAX: +33 (0) 54 000 2215. E-mail: raul.duran@inserm.fr.

Pascal Collin. University Paris Diderot, Dental University, 5 rue Garancière, 75006 Paris, France. E-mail: pascal.collin@cnrs.fr

Bogdan I. Iorga. Institut de Chimie des Substances Naturelles, 1 Avenue de la Terrasse, 91198 Gif-sur-Yvette, France. E-mail: bogdan.iorga@cnrs.fr

Conflict of interests: PC, ME, JWB, BD, JB, and OT are authors of a patent of ICSN3250 for the treatment of cancer (patent application WO2014/060366).

Word count: 5312

Total number of Figures: 6

Total number of Supplementary Figures: 5

Total number of tables: 0

Total number of Supplementary Tables: 1

Abstract

The mammalian target of rapamycin (mTOR) is a central cell growth regulator highly activated in cancer cells to allow rapid tumor growth. The use of mTOR inhibitors for anti-cancer strategy has been approved for some types of tumors, with only modest results. We recently reported the synthesis of ICSN3250, a halitulin-analogue with enhanced cytotoxicity. Now we found that ICSN3250 is a specific mTOR inhibitor that operates through a mechanism distinct from those described for previous mTOR inhibitors. Indeed, ICSN3250 competes with and displaces phosphatidic acid from the FRB domain in mTOR, thus preventing mTOR activation and leading to cytotoxicity. Docking and molecular dynamics simulations evidenced not only the high conformational plasticity of the FRB domain, but also the specific interactions of both ICSN3250 and phosphatidic acid with the FRB domain in mTOR. Furthermore, ICSN3250 toxicity was shown to act specifically in cancer cells, as non-cancer cells showed up to 100-fold less sensitivity to ICSN3250, in contrast to other mTOR inhibitors which did not show selectivity. Thus, our results defined ICSN3250 as a new-class of mTOR inhibitors that specifically targets cancer cells.

Introduction

The serine/threonine kinase mTOR (mammalian target of rapamycin) is a master regulator of cell growth, highly conserved among eukaryotes (1,2). mTOR is organised in two structurally and functionally different complexes: the rapamycin-sensitive mTORC1 (mTOR complex 1), and the rapamycin-insensitive mTORC2 (mTOR complex 2) (3–6). mTORC1 is mostly activated by the presence of amino acids, by growth factors, by the bioenergetics status of the cell, and by oxygen availability. In the control of mTORC1 by growth factors, the tuberous sclerosis complex (TSC) and the mTORC1 co-activator Rheb play a crucial role (7,8). One of the mechanisms by which the TSC/Rheb pathway controls mTORC1 involves the production of phosphatidic acid (PA), which binds directly to mTOR at the FRB domain and activates mTORC1 downstream of TSC/Rheb. Indeed, the downregulation of PA production is sufficient to decrease mTORC1 activity (9,10).

As a major cell growth regulator, mTORC1 is recurrently upregulated in cancer cells to allow rapid growth of tumors (11). Indeed, the use of rapamycin analogues has been approved as anti-cancer therapy for certain types of cancer. However, the results of these treatment are very modest with respect to patient survival and quality of life (12). Several reasons have been invoked for these modest results in the clinics, including the reactivation of a negative feedback loop downstream of mTORC1 that activates PI3K pathway (13), the absence of mTORC2 inactivation upon rapamycin treatment (5), and recently, the potential features of mTORC1 as a tumor suppressor (14,15). Still, inhibition of mTOR and the design of new compounds that increase cancer cytotoxicity upon mTOR inhibition is an active field of research, with recent reports proposing new-generation mTOR inhibitors that overcome resistance to mTOR inhibition in tumors and effectively induce tumor regression (16). However, to date, most of these mTOR inhibitors tested either showed a limited cytotoxicity towards cancer cells (having mostly a cytostatic effect), or showed an excessive cytotoxicity towards non-cancer cells, thus increasing adverse side effects.

Recently, we reported the synthesis and cytotoxicity of ICSN3250, an analogue of the cytotoxic marine alkaloid halitulin (see Figure1a for the chemical structure of this compound) (17). Halitulin was firstly reported in 1998 as a bisquinolinylpyrrole isolated from the sponge *Haliclona tulearensis*, showing cytotoxicity against several tumor cell lines (18). Our previous work concluded with the synthesis of a panel of halitulin analogues through the formation of N-substituted 3,4-diarylpyrroles. Among them, ICSN3250 (also called compound 25) was selected as a very potent derivative, presenting a high cytotoxicity at a nanomolar concentration in a caspase-independent cell death mechanism (17). Our preliminary results indicated an increased autophagy in cancer cells treated with ICSN3250. However, the exact mechanism of action of ICSN3250 underlying its toxicity, and the specificity of this cytotoxicity towards highly proliferative (cancer) cells, were not examined previously.

In this report we investigated the molecular mechanism by which ICSN3250 induces toxicity in cancer cells. Starting from a targeted screening analysing several signaling pathways, we identified the mTORC1 pathway as a main target inhibited by ICSN3250 in the nanomolar range. Our results indicated that ICSN3250 inhibited mTORC1 by following an unprecedented mechanism that involved its competition with PA at the FRB domain of mTOR. This particular mechanism of mTOR inhibition conducted to a potent and selective cytotoxicity observed in cancer cells upon ICSN3250 treatment, which was not observed in non-cancer cells. Our results thus defined ICSN3250 as a new-class mTORC1 inhibitor and validated ICSN3250 as a potential anti-cancer drug for future clinical assays.

Materials and Methods

ICSN3250 synthesis

ICSN3250 (5,5'(1-(3-(azacyclotridecan-1-yl)propyl)-1*H*-pyrrole-3,4-diyl)bis(3-nitrobenzene-1,2-diol)) was synthesized as described previously(17) and in a published patent application WO2014/060366(28). Briefly, a new efficient "one-pot" method of unsymmetrically substituted pyrroles synthesis was applied. It includes the condensation of an α-haloketone, first with a primary amine, and then with an aldehyde. Subsequent intramolecular cyclization of this *in situ* generated β-ketoenamine (enamine onto a ketone) results in formation of pyrrole based ICSN3250 molecule.

Reagents and antibodies

Antibodies against mTOR (#2983, dilution 1:150), S6 (#2217, dilution 1:1000), phospho-S6 (Ser235/236) (#4856, dilution 1:1000), S6K (#2708, dilution 1:1000), phospho-S6K(T389) (#9205, dilution 1:1000), 4EBP1 (#9452, dilution 1:1000), phospho-4EBP1(T37/46) (#2855, dilution 1:1000), AKT (#4691, dilution 1:1000), phospho-AKT(Ser473) (#4060, dilution 1:1000), phospho-AKT(Thr308) (#13038, dilution 1:1000), AMPKα (#5832, dilution 1:1000), phospho-AMPKα(Thr172) (#2535, dilution 1:1000), p53 (#2524, dilution 1:1000), phospho-p53(Ser15) (#9284, dilution 1:1000), p44/42 MAPK (#4695, dilution 1:1000), phospho-p44/42 MAPK(Thr202/Tyr204) (#9106, dilution 1:1000), phospho-p65(Ser536) (#3033, dilution 1:1000), p62 (#5114, dilution 1:1000), LC3 AB (#12741, dilution 1:1000), b-actin (#4967, dilution 1:1000), RAPTOR (#2280, dilution 1:1000), TSC2 (#4308, dilution 1:1000) and Flag (#14793, dilution 1:1000) were obtained from Cell Signaling Technology. Antibodies against p65 (#sc-8008, dilution 1:1000) were obtained from Santa Cruz Biotechnology Inc. Antibody against CD63 (SAB4700215, dilution 1:400) was obtained from Sigma. The secondary antibodies anti-mouse (#7076, dilution 1:1000) and anti-rabbit (#7074, dilution 1:1000) were obtained from Cell Signaling Technology. Phosphatidic acid (PA), Rapamycin (RAP) and paraformaldehyde were obtained from Sigma. pcDNA3-FLAG-Rheb plasmid (Addgene #19996) was a gift from Fuyuhiko Tamanoi.

144

145 ***Cell lines and culture conditions***

146 HCT116, U2OS, U87, and K562 cells were obtained from ATCC. GFP-LC3 expressing U2OS
147 cells were kindly provided by Eyal Gottlieb (Cancer research UK, Glasgow, UK). WT and
148 TSC2-/- MEFs were kindly provided by David J. Kwiatkowski (Harvard Medical School, USA).
149 HCT116, U2OS and U87 cells were grown in DMEM high glucose (4.5 g/L) (GIBCO), and
150 K562 cells in RPMI (GIBCO), both supplemented with 10% of fetal bovine serum (Dominique
151 Dutscher), glutamine (2 mM), penicillin (Sigma, 100U/mL) and streptomycin (Sigma, 100
152 mg/mL), at 37° C, 5% CO2 in humidified atmosphere. Human umbilical vein endothelial cells
153 (HUVECs) were obtained from Promocell (Germany) and cultured according to the supplier's
154 instructions in endothelial cell growth medium 2 containing growth factors and 2% fetal calf
155 serum. Primary normal human dermal fibroblasts (NHDF) derived from adult skin tissue were
156 purchased from Lonza and cultured according to the supplier's instructions in fibroblast growth
157 medium containing human basic fibroblast growth factor (bFGF), insulin and 2% fetal calf
158 serum. Human follicle dermal papilla cells (HFDPC) isolated from human dermis originating
159 from lateral scalp were purchased fromTebu-Bio (Le Perray en Yvelines, France) and grown
160 in Follicle Dermal Papilla Cells Medium containing 4% FCS, 0.4% bovine pituitary extract, 1
161 ng/mL bFGF and 5 µg/mL of insulin (Tebu-Bio). The cells were maintained at 37°C in a
162 humidified atmosphere containing 5% CO2. Mycoplasma contamination check was carried
163 out using the VenorGeM Kit (Minerva Biolabs GmbH, Germany). When indicated, ICSN3250
164 (dissolved in DMSO before further dilution in assay mixture) was added at the indicated
165 concentration. PA was added to a final concentration of 1, 10 or 100 µM.

166

167 ***Plasmids and transfections***

168 Plasmid transfections were carried out using Jetpei (Polyplus Transfection) according to the
169 manufacturer's instructions. Briefly, 70% confluent cells were transfected with 5 µg of plasmid.
170 24 hours later cells were treated with ICSN3250 for 24 more hours.

171

Western Blot

HCT116 cells, U2OS cells, $TSC2^{+/+}$ MEFs, and $TSC2^{-/-}$ MEFs were seeded in 10cm plates. After the treatment, cells were washed with phosphate-buffered saline (PBS 1X) and lysed on ice using home-made RIPA buffer (Tris-HCl 50 mM pH 7.5, NaCl 150mM, NP-40 1%, sodium deoxycholate 0.5%, EDTA 2mM, NaF 10mM) supplemented with protease inhibitors (Sigma), phosphatase inhibitors (Sigma) and PMSF 1mM (AppliChem). Protein quantification was performed with BCA assay kit (Thermo Fisher). After electrophoresis, the proteins were transferred to a nitrocellulose membrane (BioRad) with Trans-Blot Turbo Transfer System (Bio-Rad). The membranes were incubated for 30 minutes in PBS 1X with 0.01% Tween-20 and 5% bovine serum albumin (BSA). Primary antibodies were incubated overnight at 4° C and secondary antibodies were incubated for 2 hours at room temperature. Finally, membranes were imaged using the Chemi Doc MP Imager (Bio-Rad).

In vitro kinase assays

In vitro kinase assays of mTOR, AKT1, EGFR, PDK1, SRC, PKCα, and PKCε were performed at CEREP Company (France). *In vitro* kinase assays of PI3Kα, PI3Kβ, PI3Kγ, and PI3Kδ were performed using the PI3 Kinase Activity/Inhibitor ELISA assay from Merck-Millipore (USA). Detailed procedures of these in vitro kinase assays are described in Supplementary Material and Methods.

Immunoprecipitation

After treatment, cells were washed twice with cold PBS, then they were lysed with IP lysis buffer (40mM Hepes pH 7.5, 120mM NaCl, 1mM EDTA, 0.3% CHAPS), supplemented with protease inhibitor cocktail and phosphatase inhibitor cocktail (Sigma). Protein extracts were incubated overnight at 4° C with anti-mTOR antibodies and then 4 hours at 4° C with magnetic beads (Pierce Protein A/G Magnetic Beads, Thermo Fisher). Subsequently, beads were washed twice with cold PBS and eluted with Laemmli buffer for Western Blot analysis.

Cell viability

To assess cell viability, 10 000 cells per well were seeded in triplicate in 96-well plates. The number of cells were determined using the TC20 Automated Cell Counter (Bio-Rad) according to the manufacturer's protocol. Briefly, after the respective treatments cells were detached with trypsin/EDTA and 10 µl of the cells suspension were mixed with 10 µl trypan blue 5% solution (Bio-Rad) and analysed with the cell counter. Alternatively, cell viability was assessed using the CellTiter-Blue Cell Viability Assay (Promega). After the treatment, 20 µl of the reagent was added to each well and the plate was incubated for 1 - 4 hours at 37° C, 5% CO2 in humidified atmosphere. The fluorescence was recorded at 560/590nm in a Tristar2 LB942 (Berthold) device to determine the cell viability.

Cell cycle analysis: Exponentially growing cancer cells (HCT116) were incubated with ICSN3250 or DMSO for 24 h. Cell-cycle profiles were determined by flow cytometry on a FC500 flow cytometer (Beckman–Coulter, France).

Confocal microscopy

Cells were grown on coverslips in 12 wells plates. Subsequently, after the treatments, cells were rinsed with ice-cold PBS and fixed with 4% paraformaldehyde in PBS for 30 minutes at room temperature. After the fixation, cells were permeabilized using PBS with Triton-X 0.05% during 10 minutes, and then blocked with BSA 5% in PBS for 30 minutes. When required, cells were incubated with primary antibody for 1 hour at 37° C. After three washes with PBS, the coverslip was incubated for 1 hour at 37° C with the appropriate secondary antibody (anti-rabbit Alexa488, dilution 1:400 or anti-mouse Alexa555, dilution 1:400, obtained from Invitrogen). Finally, coverslips were mounted with Prolong containing DAPI (Invitrogen). Fluorescence was detected using a Leica confocal microscopy. Images were analysed using Image J software.

Molecular modeling

Three-dimensional structures of ligands were generated using CORINA version 3.44 (http://www.molecular-networks.com). Molecular docking calculations were carried out using GOLD software(29) and GoldScore scoring function, with the protein 2NPU(25) (representative conformer 1) as receptor. The binding site was defined as a sphere with 15 Å radius around a point with coordinates -6.449,6.669,-5.742. In agreement with our previous studies(30–34) showing that an enhanced conformational search is beneficial, especially for large molecules, a search efficiency of 200 % was used to better explore the ligand conformational space. All other parameters were used with the default values. Molecular dynamics simulations were carried out with GROMACS version 4.6.5(35) using the OPLS-AA(36) force field. Each system was energy-minimized until convergence using a steepest descents algorithm. Molecular dynamics with position restraints for 200 ps was then performed, followed by the production run of 100 ns. During the position restraints and production runs, the Berendsen method(37) was used for pressure and temperature coupling. Electrostatics were calculated with the particle mesh Ewald method(38). The P-LINCS algorithm(39) was used to constrain bond lengths, and a time step of 2 fs was used throughout. Ligand topologies for the OPLS-AA force field were generated using MOL2FF, an in-house developed script, and were deposited into the Ligandbook repository(40) with IDs 2929 (https://ligandbook.org/package/2929) and 2930 (https://ligandbook.org/package/2930). DFT calculations were carried out using Gaussian09, version D01(41). Experimental pKa values were taken from Jencks & Regenstein (1968)(42). All calculations were performed using the High-Performance Computing (HPC) facilities available at the ICSN (Gif-sur-Yvette, France). Images were generated with Pymol, version 1.8.6 (http://pymol.org).

Statistics

The results are expressed as a mean ± SEM of at least three independent experiments. *t* test comparison was used to evaluate the statistical difference between two groups. One-way ANOVA followed by Bonferroni's comparison as a post hoc test was used to evaluate the

255 statistical difference between more than two groups. Statistical significance was estimated
256 when $p<0.05$.
257
258 ***Data availability***
259 The authors declare that all the data supporting the findings of this study are available within
260 the article and its supplementary information files and from the corresponding author upon
261 reasonable request.

Results

ICSN3250 specifically inhibits mTORC1 pathway

To better understand the consequences at cell signaling level of ICSN3250 in human cells, we treated two human cancer cell lines, the colorectal carcinoma cell line HCT116 and the osteosarcoma cell line U2OS, with increasing concentrations of ICSN3250, and we performed a targeted screening of different signaling pathways. These included AMPK pathway (determined by the phosphorylation of AMPK at residue Thr172), p53 pathway (determined by the phosphorylation of p53 at residue Ser15), PI3K pathway (determined by the phosphorylation of AKT at residue Thr308), ERK pathway (determined by the phosphorylation of p44/42 MAPK at residue Thr202/Tyr204), NF-κB pathway (determined by the phosphorylation of p65 at residue Ser536), mTORC1 pathway (determined by the phosphorylation of S6K at residue Thr389) and mTORC2 (determined by the phosphorylation of AKT at residue Ser473). As shown in Figure 1b-h, the only pathway that showed a clear inhibition upon ICSN3250 treatment in HCT116 cells was mTORC1 pathway. Indeed, some other pathways, such as PI3K and mTORC2 showed an increase in the phosphorylation of their respective downstream targets. This increase would be in agreement with a specific inhibition of mTORC1 pathway, and the subsequent release of the negative feedback loop that leads to PI3K re-activation (13). Similar results were obtained in U2OS cells (Supplementary Figure S1a-g).

To further confirm the inhibition of mTORC1 pathway by ICSN3250, we performed a dose dependent and time course analysis of ICSN3250 treatment by looking at 3 well-known targets of mTORC1 pathway, S6K, S6 and 4EBP1. Dose dependent analysis showed a complete inhibition of mTORC1 at concentrations equal or higher than 50nM of ICSN3250 (Figure 1i and Supplementary Figure S1h). Time course analysis showed a slow yet efficient inhibition of mTORC1 that reached a maximal inhibition upon 8 - 15 hours of treatment (Figure 1j and Supplementary Figure S1i). This is considerably slower than previously reported mTORC1 inhibitors, such as rapamycin or PP242. Further confirming the capacity

of ICSN3250 to inhibit mTORC1, we also observed that ICSN3250 treatment induced an increase in autophagy, negatively regulated by mTORC1 (19), as determined by increasing levels of LC3-II, by decreasing levels of the adaptor protein p62, and by the accumulation of GFP-LC3 puncta, all of them standard markers of autophagy (Figure 1k-n and Supplementary Figure S1j-k). Finally, ICSN3250 treatment caused cell cycle arrest at G0/G1 phase in HCT116 cells, as expected upon mTORC1 inhibition (Figure 1o). Altogether, our results indicated that ICSN3250 is a specific inhibitor of mTORC1 that efficiently inhibits downstream targets of mTORC1 at concentrations higher than 50nM, by following a time course kinetic slower than previously reported mTORC1 inhibitors.

ICSN3250 is not a kinase inhibitor of mTOR

As the time course analysis of mTORC1 inhibition showed that ICSN3250 is a particularly slow inhibitor of mTORC1, we wondered if the mechanism of action of ICSN3250 towards mTORC1 inhibition differs from previously reported mTORC1 inhibitors. Rapamycin and its analogues, as well as dual mTORC1/mTORC2 inhibitors, act as kinase inhibitors of mTOR, with a fast time-course kinetics. Thus, we analysed if ICSN3250 is a kinase inhibitor of mTOR *in vitro*. The results shown in Figure 2a indicated that, although ICSN3250 had a capacity to inhibit the kinase activity of mTOR, this effect occurred at concentrations much higher (10 μM) than the observed inhibition of mTORC1 in cells (50 nM). This result confirmed that ICSN3250 is not a kinase inhibitor of mTOR, thus suggesting that its action mechanism is different that the mechanism of other mTORC1 inhibitors. Indeed, at 100 nM, ICSN3250 did not show any inhibitory capacity towards PI3Kα, β, γ, or δ (Supplementary Figure S2a). Similarly, ICSN3250 even at 500 nM did not show any inhibitory activity towards other kinases analysed, such as PKCα, PKCε, SRC, AKT1, EGFR and PDK1 (Supplementary Figure S2b).

ICSN3250 does not prevent lysosomal translocation of mTORC1

Next, we investigated if ICSN3250 prevents the translocation of mTORC1 to the surface of the lysosome, a well-known mechanism involved in the activation of mTORC1 by nutritional inputs(20). As previously observed, the presence of amino acids was sufficient to induce the characteristic co-localization of mTOR with lysosomal markers, such as CD63 (Figure 2b). As shown in Figure 2b, and quantified in Figure 2c, the addition of 100 nM of ICSN3250 (a concentration at which mTORC1 was completely inhibited, see Figure 1h) to HCT116 cells did not prevent the co-localization of mTOR with CD63, clearly indicating that lysosomal localization of mTORC1 was not impaired by ICSN3250. Again, similar results were obtained in U2OS cells (Supplementary Figure 2c-d). Further, even when ICSN3250 was not able to prevent the amino acid-induced lysosomal translocation of mTORC1, still ICSN3250 was able to prevent the activation of mTORC1 mediated by amino acid in both cell lines (Figure 2d and Supplementary Figure S2e), again suggesting that the inhibition of mTORC1 occurred once mTORC1 is at the lysosomal surface. Finally, to further discard that lysosomal translocation is involved in the mechanism of action of ICSN3250, we over-expressed a de-localized Flag-Rheb (the mTORC1 co-activator physiologically localized at the lysosome), that renders mTORC1 activation outside the lysosome. As expected, Flag-Rheb overexpression induced mTORC1 activation in the absence of amino acids (Supplementary Figure S2f-g). However, delocalized Flag-Rheb did not prevent the inhibitory effect of ICSN3250 towards mTORC1 activity (Figure 2e and Supplementary Figure S2h), finally confirming that ICSN3250 operates after the translocation of mTORC1 to the lysosome.

ICSN3250 does not destabilize mTORC1

mTORC1 destabilization has been proposed as a mechanism of mTORC1 inhibition upon certain metabolic stresses (21). Thus, we investigated if ICSN3250 destabilizes mTORC1 as

an inhibitory mechanism. For this purpose, we immunoprecipitated mTOR and analysed the presence of the specific mTORC1 component Raptor in the immunoprecipitates. As expected, in the absence of the compound, Raptor was observed upon mTOR immunoprecipitation (Figure 2f). Our results showed that, upon 24 hours of treatment, ICSN3250 was not able to prevent the interaction of mTOR with Raptor (Figure 2f). Hence, we concluded that the mechanism of action of ICSN3250 does not affect the integrity of the mTORC1, localized at the lysosome.

ICSN3250 antagonizes with phosphatidic acid to inhibit mTORC1

As our results so far indicated that ICSN3250 inhibits mTORC1 after its translocation to the lysosomal surface, we investigated the mechanism that allow mTORC1 activation at the lysosome. These mechanisms are controlled by the Tuberous Sclerosis Protein 1/2 complex (TSC complex), that exerts a negative regulation towards mTORC1 (7). To investigate if TSC complex plays a role in the mechanism of action of ICSN3250, we treated $TSC^{+/+}$ MEFs and $TSC2^{-/-}$ MEFs with increasing concentrations of ICSN3250. Similarly, to what we observed in cancer cell lines, ICSN3250 induced a complete inhibition of mTORC1 at concentrations higher than 50nM in $TSC^{+/+}$ MEFs, as determined by the dephosphorylation of the kinase S6K and the ribosomal protein S6 (Figure 3a). Concomitantly, we observed an activation of autophagy (as determined by increasing LC3II levels), as expected upon mTORC1 inhibition. However, the inactivation of TSC complex in $TSC2^{-/-}$ MEFs induced a complete recovery of mTORC1 activity even in the presence of ICSN3250 at 100nM (Figure 3a). The absence of inhibition of mTORC1 in $TSC2^{-/-}$ MEFs was followed by a lack of activation of autophagy, as determined by LC3II levels. We concluded that the activation of mTORC1 mediated by TSC complex might be involved in the mechanism of action of ICSN3250.

366 The production of phosphatidic acid (PA) by Phospholipase D1 (PLD1) has been
367 previously invoked as a mechanism of the regulation of mTORC1 by TSC complex (22), and
368 it is largely known that PA binds to and activates mTORC1 (9). Thus, we hypothesised that
369 ICSN3250 could compete with PA in mTORC1 binding, thus displacing PA from its binding
370 site, leading to mTORC1 inhibition downstream of TSC complex. To test this hypothesis, we
371 first performed a competitive analysis of mTORC1 activation between PA and ICSN3250.
372 For this purpose, we treated HCT116 cells with ICSN3250 (100nM) in the presence of
373 increasing concentrations of PA (0 to 100 μM). As we observed previously, ICSN3250 alone
374 induced the inhibition of mTORC1 as determined by the dephosphorylation of its
375 downstream targets S6 and 4EBP1. However, co-incubation of cells with PA induced a
376 dose-dependent reactivation of mTORC1 even in the presence of ICSN3250 (Figure 3b and
377 Supplementary Figure S3a). Concomitantly, the PA-mediated reactivation of mTORC1 even
378 in the presence of ICSN3250 was followed by the inhibition of autophagy, as determined by
379 LC3-II and p62 levels and GFP-LC3 aggregation (Figure 3c-e and Supplementary Figure
380 S3b). Conversely, increasing concentrations of ICSN3250 limited the activation of mTORC1
381 and the inhibition of autophagy induced by PA (Figure 3f-g and Supplementary Figure S3c-
382 d). These results strongly suggest that ICSN3250 antagonizes with PA to inhibit mTORC1.

383

384 ***ICSN3250 binds to the FRB domain of mTOR and displaces phosphatidic acid***

385 To further confirm the previous conclusion that ICSN3250 antagonizes with PA, we
386 performed molecular docking calculations to identify the binding modes of ICSN3250 and PA
387 within the FRB domain of mTOR. Three different protonation states of the catechol group in
388 ICSN3250 were considered during the docking process (i.e. neutral and deprotonated on
389 either OH group) and the strongest interactions and the best protein-ligand shape
390 complementarity were obtained with the form deprotonated on the OH situated *ortho* from
391 the NO_2 substituent. We computed the pKa of this OH group using the protocol described by
392 Muckerman *et al.*(23) (DFT calculations on a simplified analogue of ICSN3250 with implicit

393 solvent and removal of the systematic error, see the Methods section and Supplementary
394 Table 1 for more details) and we found a value of 5.93±0.55, meaning that this group is
395 negatively charged at physiological pH. This is in strong agreement with the docking results,
396 showing interactions between this group and the positively charged side chains of Lys2095
397 on one side and of Arg2042 on the other (Figure 4).

398 The FRB domain of mTOR (apo form) and the docking complexes with ICSN3250
399 and PA were further used for molecular dynamics (MD) simulations (100 ns each), to take
400 into account two factors that were missing in the docking process: protein flexibility and the
401 presence of explicit aqueous solvent. As expected, the apo simulation reached very quickly
402 an equilibrium conformation that is conserved until the end. In contrast, the two complexes
403 evolved slowly towards an equilibrium structure which is attained only after 75-80 ns
404 (Supplementary Figure S4), highlighting the need for relatively long MD simulations in the
405 study of flexible proteins. The representative equilibrium structures from these simulations
406 (Figures 4 and 5) showed a number of interesting elements. The protein surface is very
407 flexible, changing the shape according to the interaction partner. Consequently, a very good
408 protein-ligand surface complementarity was observed for the two complexes, bringing an
409 important contribution to the ligand affinity, which is complemented by strong ionic
410 interactions between nitrocatechol groups and Lys2095 and Arg2042 in the case of
411 ICSN3250 and between the phosphate group and Arg2109 in the case of PA (Figure 4). The
412 interaction between ICSN3250 and its binding site showed three distinct regions: i) the ionic
413 interaction between the nitrocatechol groups and Lys2095 and Arg2042 that was already
414 mentioned; ii) a π-stacking interaction between the pyrrole ring and Phe2039 and iii) the
415 interaction between the macrocycle and a hydrophobic subpocket composed of residues
416 Trp2101, Tyr2105, Phe2108, Leu2031 and Tyr2104. Ser2035, which was shown to be
417 important for the interaction of mTOR with rapamycin(24), is also part of the binding site
418 (Figure 5a-b). ICSN3250 is relatively flat on the protein surface, whereas PA is deeply buried
419 with its two hydrophobic tails that interact with a subpocket containing Trp2101, Tyr2105,

Phe2108, Leu2031, Leu2054, Tyr2104, Ser2035, Phe2039, Leu2051, Tyr2038, Val2044 and Met2047. Only the phosphate head is solvent-exposed and interacts with Arg2109 (Figure 5c-d). This orientation is similar to the one previously observed by NMR(25), with the exception of the tail chains that are more deeply buried in our case.

Overall, the residues involved in the interaction between mTOR and the two ligands studied in this work clearly show a significant overlapping of the two binding sites. Our results supported that ICSN3250 binds to the FRB domain of mTOR and displaces PA, leading to mTORC1 inhibition. This mechanism defines ICSN3250 as a new-class mTORC1 inhibitor.

Inhibition of mTORC1 by ICSN3250 is responsible for its cytotoxicity in cancer cells

Previously, we reported that ICSN3250 showed an increased cytotoxicity in human cells (17). Our results demonstrating that ICSN3250 acts as a new-class mTOR inhibitor led us to investigate if the inhibition of mTORC1 was the primary reason for the cytotoxicity induced by ICSN3250. For this purpose, we investigated if the re-activation of mTORC1 mediated by TSC ablation in $TSC2^{-/-}$ MEFs protected from the cytotoxic effect of ICSN3250. As shown in Figure 6a and Supplementary Figure S5a, $TSC2^{-/-}$ MEFs showed an increased protection against cytotoxicity induced by ICSN3250 with respect to $TSC^{+/+}$ MEFs (as control, $TSC^{-/-}$ MEFs did not show an increased viability with respect to $TSC^{+/+}$ in the absence of the compound, Supplementary Figure S5a-b). Similarly, treatment of HCT116 cells with PA (100 μM), which we previously showed to be sufficient to re-activate mTORC1 (see Figure 3b), also prevented the cytotoxic effect of ICSN3250 in a dose-dependent manner (Figure 6b-d). Thus, the reactivation of mTORC1 (induced either by TSC ablation or by PA treatment) was sufficient to block ICSN3250-induced cytotoxicity. This result clearly suggested that the inhibition of mTORC1 by ICSN3250 is responsible for its cytotoxicity. Furthermore, the particular mechanism of mTORC1 inhibition induced by ICSN3250 (displacing PA), is likely the reason of the increased cytotoxicity showed by this compound with respect to other

mTORC1 inhibitors, such as rapamycin. Indeed, while rapamycin induced a stronger inhibition of mTORC1 than ICSN3250 (Figure 6e), it did not cause the cytotoxic effect that we observed upon ICSN3250 treatment (Figure 6f). Compared with a panel of mTOR inhibitors, ICSN3250 was not the most potent mTORC1 inhibitor among them as determined by the dephosphorylation of mTORC1-downstream targets (Supplementary Figure S5c-d), but yet it ranked among the most cytotoxic compounds for cancer cells, showing the lowest IC50 values (Figure 6g and Supplementary Figure S5e). Hence, we concluded that the qualitative (and not quantitative) differences between the inhibition exerted by ICSN3250 with respect to other mTOR inhibitors are key for the marked cytotoxicity induced by ICSN3250.

Finally, to validate the potential applicability of ICSN3250 for pre-clinical tests as an anticancer drug, we confirmed the selective cytotoxicity of the compound towards cancer cells. With this purpose, we compared the cytotoxicity of ICSN3250 in a panel of cells including both cancer cells and non-cancer cells. As shown in Figure 6h, ICSN3250 showed a cytotoxicity in cancer cells that was 10-100 times more potent than its cytotoxicity in human non-cancer cells. Furthermore, compared with other mTOR inhibitors that showed cytotoxicity in cancer cells (such as INK 128, gedatolisib or VS-5584), ICSN3250 is substantially less toxic in human primary normal cells (Figure 6i), further validating its action mechanism as particularly interesting to develop anti-cancer strategies.

Discussion

The results shown herein presented ICSN3250 as a new-class mTORC1 inhibitor that act through a mechanism that differs from those described by other mTOR inhibitors. ICSN3250 is an analogue of the cytotoxic marine alkaloid halitulin, previously reported to present an increased cytotoxicity (17). However, the mechanism of action underlying this cytotoxicity was not known. Our results showed a specificity of ICSN3250 targeting mTORC1, without inhibiting other signaling pathways, such as AMPK, p53, PI3K, ERK, NF-κB, or even mTORC2. Surprisingly, ICSN3250 did not affect the kinase activity of mTOR, neither the stability of mTOR complex. Instead, our results showed that ICSN3250 binds to the FRB domain of mTOR, displacing PA as a mechanism for mTORC1 inhibition. Indeed, increasing amounts of exogenously added PA or TSC ablation restored mTORC1 activity. This competition with PA seems to be key for the cytotoxicity of ICSN3250, as exogenously added PA not only restored mTORC1, but also restored cell viability. Of note, our inhibitor did not show an increased capacity to inhibit mTORC1 with respect to previously reported mTOR inhibitors, but yet it showed a particularly high cytotoxic effect in cancer cells, showing a lower IC50 than typical inhibitors such as temsirolimus, accepted by FDA as a treatment against renal cell carcinoma. Importantly, the cytotoxicity of ICSN3250 towards non-cancer cells is substantially lower than the most potent of the other inhibitors of mTOR, placing ICSN3250 as a good candidate for future clinical assays.

mTOR inhibition has been approved as a cancer therapy for several types of tumor (26). Yet, the efficiency of those treatments is very modest. Rapamycin and analogues showed mostly cytostatic effect, which in the patient results in a mild delay of tumor growth, with little effect (although statistically significant) in patient survival. These modest results have been explained by the re-activation of PI3K pathway as a consequence of the release of negative feedback loop downstream of mTORC1 (13). This is why a new generation of dual mTORC1/mTORC2 inhibitors and PI3K/mTOR inhibitors are being proposed and tested. However, these inhibitors still show increased cytotoxicity in non-cancer cells. Besides, the

use of monotherapies targeting single signaling pathways to treat cancer is under reconsideration. Due to the intrinsic genetic heterogeneity of tumors and the rapid evolution and adaptation of tumor cells during the progression of the disease, developing drug resistance is a recurrent problem during treatment, particularly when monotherapies have been used. Rapid and selective cytotoxicity towards cancer cells, as showed by ICSN3250, avoiding cytostatic effect, seems to be necessary to reduce drug resistance in tumor cells. Still, the efficacy of ICSN3250 to selectively target tumor cells *in vivo* remains to be elucidated.

As mTORC1 is not the only protein activated by PA, it could be envisioned that other mechanisms or pathways could be involved in ICSN3250-induced cytotoxicity. However, our results showing that mTORC1 re-activation in $TSC2^{-/-}$ cells restored cell viability indicated that mTORC1 inhibition is at the basis of ICSN3250-induced cytotoxicity. The unprecedented mechanism of action of ICSN3250, displacing PA to induce mTORC1 inhibition, seems to be key to explain the specific cytotoxicity for cancer cells showed by this type of mTORC1 inhibitor. Why this action mechanism of action would be more cytotoxic than mTOR kinase inhibition mediated by ATP-competitive inhibitors would require further investigations. As ICSN3250-induced PA displacement from the FRB domain of mTOR would likely occur at the surface of the lysosome (where mTORC1 is located upon activation), it could be hypothesized that this displacement causes a collapse in the lysosomal surface, perturbing lysosomal function and leading to cell death, as proposed for other types of stress (27). Alternatively, the slower inactivation of mTORC1 mediated by ICSN3250 as compared with other mTOR inhibitors that we observed could be playing in favour of its cytotoxicity, as our recent results showed that a fast and complete inhibition of mTORC1 upon rapamycin treatment prevents apoptotic cell death during nutritional imbalance (14).

Finally, our results make particular emphasis in the control of mTORC1 activity by PA, a regulation that has not received as much attention as the regulation exerted by amino acids or by PI3K signaling. However, our results clearly indicated that interfering with PA binding in

519 the FRB domain of mTOR is indeed an effective approach to inhibit mTORC1 even in the
520 presence of amino acids and growth factors, underscoring the importance of PA for
521 mTORC1 activity. Besides, as mentioned above, the regulation of mTORC1 by PA seems to
522 be particularly important at the cell physiology level, as the interference with the mTOR-PA
523 interaction resulted in cell death.

524 In conclusion, ICSN3250 defines a new-class of mTORC1 inhibitors that, due to its particular
525 mechanism of action, induces cell death specifically in tumor cells but not in non-cancer
526 cells. Further research will determine the applicability of this type of compound for anti-
527 cancer therapy.

Acknowledgements

This work was supported by funds from the following institutions: Centre National de la Recherche Scientifique-CNRS, Institut National de la Santé et de la Recherche Médicale - INSERM, Fondation pour la Recherche Médicale, the Conseil Régional d'Aquitaine, Fondation ARC pour la Recherche sur le Cancer, Ligue Contre le Cancer - Gironde, SIRIC-BRIO, Institut de Chimie des Substances Naturelles -ICSN, Institut Européen de Chimie et Biologie, Université Paris-Descartes, Société d'Accélération de Transfert de Technologie d'Ile de France-SATT IDF-innov. pcDNA3-FLAG-Rheb plasmid (Addgene #19996) was a gift from Fuyuhiko Tamanoi. GFP-LC3 expressing U2OS cells were kindly provided by Eyal Gottlieb (Cancer research UK, Glasgow, UK). We thank Professor J.Y. Lallemand, director of the ICSN (2000-2009). We extend our thanks to A. Pinault for skillful technical assistance. We would like to remember Dr. C. Marazano (†11/12/2008), who initiated and supervised the initial biomimetic synthesis of ICSN3250, one of the halituline's analogues.

Author contribution

PC conceived the project. PC, RVD, and BII designed experiments. TLN, CB, MCGA, JB, FP, KA, GS, ST, and BII performed experiments. ME, OT, and BD synthesized the ICSN3250 compound. TLN, PC, RVD, and BII analysed data. PC, RVD, BII, JWB, YMF, and PS secured funding. RVD wrote the manuscript. All the authors read and approved the manuscript.

References

1. Saxton RA, Sabatini DM. mTOR Signaling in Growth, Metabolism, and Disease. *Cell*. **2017**;168:960–76.

2. González A, Hall MN. Nutrient sensing and TOR signaling in yeast and mammals. *EMBO J*. **2017**;36:397–408.

3. Loewith R, Jacinto E, Wullschleger S, Lorberg A, Crespo JL, Bonenfant D, et al. Two TOR complexes, only one of which is rapamycin sensitive, have distinct roles in cell growth control. *Mol Cell*. **2002**;10:457–68.

4. Kim DH, Sarbassov DD, Ali SM, King JE, Latek RR, Erdjument-Bromage H, et al. mTOR interacts with raptor to form a nutrient-sensitive complex that signals to the cell growth machinery. *Cell*. **2002**;110:163–75.

5. Sarbassov DD, Ali SM, Kim D-H, Guertin DA, Latek RR, Erdjument-Bromage H, et al. Rictor, a Novel Binding Partner of mTOR, Defines a Rapamycin-Insensitive and Raptor-Independent Pathway that Regulates the Cytoskeleton. *Curr Biol*. **2004**;14:1296–302.

6. Jacinto E, Loewith R, Schmidt A, Lin S, Rüegg MA, Hall A, et al. Mammalian TOR complex 2 controls the actin cytoskeleton and is rapamycin insensitive. *Nat Cell Biol*. **2004**;6:1122–8.

7. Inoki K, Li Y, Zhu T, Wu J, Guan KL. TSC2 is phosphorylated and inhibited by Akt and suppresses mTOR signalling. *Nat Cell Biol*. **2002**;4:648–57.

8. Durán R V., Hall MN. Regulation of TOR by small GTPases. *EMBO Rep*. **2012**;13:121–8.

9. Fang Y, Vilella-Bach M, Bachmann R, Flanigan A, Chen J. Phosphatidic Acid-Mediated Mitogenic Activation of mTOR Signaling. *Science (80-)*. **2001**;294:1942–5.

10. Fang Y, Park IH, Wu AL, Du G, Huang P, Frohman MA, et al. PLD1 Regulates mTOR Signaling and Mediates Cdc42 Activation of S6K1. *Curr Biol*. **2003**;13:2037–44.

11. Menon S, Manning BD. Common corruption of the mTOR signaling network in human tumors. *Oncogene*. **2009**;27:S43–51.

12. Hudes G, Carducci M, Tomczak P, Dutcher J, Figlin R, Kapoor A, et al. Temsirolimus, interferon alfa, or both for advanced renal -cell carcinoma. *N Engl J Med*. **2007**;356:2271–81.

13. Um SH, Frigerio F, Watanabe M, Picard F, Joaquin M, Sticker M, et al. Absence of S6K1 protects against age- and diet-induced obesity while enhancing insulin sensitivity. *Nature*. **2004**;431:200–5.

14. Villar VH, Nguyen TL, Delcroix V, Terés S, Bouchecareilh M, Salin B, et al. mTORC1 inhibition in cancer cells protects from glutaminolysis-mediated apoptosis during nutrient limitation. *Nat Commun*. **2017**;8:1–12.

15. Villar VH, Nguyen TL, Terés S, Bodineau C, Durán R V. Escaping mTOR inhibition for cancer therapy: Tumor suppressor functions of mTOR. *Mol Cell Oncol*. **2017**;4:e1297284.

16. Rodrik-Outmezguine VS, Okaniwa M, Yao Z, Novotny CJ, McWhirter C, Banaji A, et al. Overcoming mTOR resistance mutations with a new-generation mTOR inhibitor. *Nature*. **2016**;534:272–6.

17. Egorov M, Delpech B, Aubert G, Cresteil T, Garcia-Alvarez MC, Collin P, et al. A concise formation of N-substituted 3,4-diarylpyrroles-synthesis and cytotoxic activity. *Org Biomol Chem*. **2014**;12:1518–24.

18. Kashman Y, Koren-Goldshlager G, Gravalos G, Schleyer M. Halitulin, a new cytotoxic alkaloid from the marine sponge Haliclona tulearensis. *Tetrahedron Lett*. **1999**;40:997–1000.

19. Villar VH, Merhi F, Djavaheri-Mergny M, Durán R V. Glutaminolysis and autophagy in cancer. *Autophagy*. **2015**;11:1198–208.

20. Sancak Y, Bar-Peled L, Zoncu R, Markhard AL, Nada S, Sabatini DM. Ragulator-Rag complex targets mTORC1 to the lysosomal surface and is necessary for its activation by amino acids. *Cell*. **2010**;141:290–303.

21. Kim SG, Hoffman GR, Poulogiannis G, Buel GR, Jang YJ, Lee KW, et al. Metabolic stress controls mTORC1 lysosomal localization and dimerization by regulating the TTT-RUVBL1/2 complex. *Mol Cell*. **2013**;49:172–85.

22. Sun Y, Fang Y, Yoon M-S, Zhang C, Roccio M, Zwartkruis FJ, et al. Phospholipase D1 is an effector of Rheb in the mTOR pathway. *Proc Natl Acad Sci U S A*. **2008**;105:8286–91.

23. Muckerman JT, Skone JH, Ning M, Wasada-Tsutsui Y. Toward the accurate calculation of pKa values in water and acetonitrile. *Biochim Biophys Acta - Bioenerg*. **2013**;1827:882–91.

24. Yang H, Rudge DG, Koos JD, Vaidialingam B, Yang HJ, Pavletich NP. mTOR kinase structure, mechanism and regulation by the rapamycin-binding domain. *Nature*. **2013**;497:217–23.

25. Veverka V, Crabbe T, Bird I, Lennie G, Muskett FW, Taylor RJ, et al. Structural characterization of the interaction of mTOR with phosphatidic acid and a novel class of inhibitor: compelling evidence for a central role of the FRB domain in small molecule-mediated regulation of mTOR. *Oncogene*. **2008**;27:585–95.

26. FDA Approval for Everolimus [Internet]. Natl. Cancer Inst. 2013. Available from: https://www.cancer.gov/about-cancer/treatment/drugs/fda-everolimus

27. Aits S, Jaattela M. Lysosomal cell death at a glance. *J Cell Sci*. **2013**;126:1905–12.

28. Collin P, Egorov M, Delpech B, Bakala J, Achab M, Bignon J, et al. N-substituted 3,4-bis(catechol)pyrrole compounds, and the preparation and use thereof in the treatment of cancer. Patent number: WO2014/060366. France; 2014.

29. Verdonk ML, Mortenson PN, Hall RJ, Hartshorn MJ, Murray CW. Protein−Ligand Docking against Non-Native Protein Conformers. *J Chem Inf Model*. **2008**;48:2214–25.

30. Surpateanu G, Iorga BI. Evaluation of docking performance in a blinded virtual screening of fragment-like trypsin inhibitors. *J Comput Aided Mol Des*. **2012**;26:595–601.

31. Colas C, Iorga BI. Virtual screening of the SAMPL4 blinded HIV integrase inhibitors dataset. *J Comput Aided Mol Des*. **2014**;28:455–62.

32. Martiny VY, Martz F, Selwa E, Iorga BI. Blind Pose Prediction, Scoring, and Affinity Ranking of the CSAR 2014 Dataset. *J Chem Inf Model*. **2016**;56:996–1003.

33. Selwa E, Martiny VY, Iorga BI. Molecular docking performance evaluated on the D3R Grand Challenge 2015 drug-like ligand datasets. *J Comput Aided Mol Des*.

2016;30:829–39.

34. Selwa E, Elisée E, Zavala A, Iorga BI. Blinded evaluation of farnesoid X receptor (FXR) ligands binding using molecular docking and free energy calculations. *J Comput Aided Mol Des*. **2017**;in press.

35. Pronk S, Páll S, Schulz R, Larsson P, Bjelkmar P, Apostolov R, et al. GROMACS 4.5: a high-throughput and highly parallel open source molecular simulation toolkit. *Bioinformatics*. **2013**;29:845–54.

36. Jorgensen WL, Schyman P. Treatment of Halogen Bonding in the OPLS-AA Force Field: Application to Potent Anti-HIV Agents. *J Chem Theory Comput*. **2012**;8:3895–901.

37. Berendsen HJC, Postma JPM, van Gunsteren WF, DiNola A, Haak JR. Molecular dynamics with coupling to an external bath. *J Chem Phys*. **1984**;81:3684–90.

38. Essmann U, Perera L, Berkowitz ML, Darden T, Hsing L, Pedersen LG. A smooth particle mesh Ewald method. *J Chem Phys*. **1995**;103:8577–93.

39. Hess B. P-LINCS: A Parallel Linear Constraint Solver for Molecular Simulation. *J Chem Theory Comput*. **2008**;4:116–22.

40. Domański J, Beckstein O, Iorga BI. Ligandbook: An online repository for small and drug-like molecule force field parameters. *Bioinformatics*. **2017**;33:1747–9.

41. Frisch MJ, Trucks GW, Schlegel HB, Scuseria GE, Robb MA, Cheeseman JR, et al. Gaussian 09, Rev: D01. Pittsburgh, Pa, USA: Gaussian, Inc.,; 2009.

42. Jencks WP, Regenstein J. Handbook of Biochemistry-Selected Data for Molecular Biology. 1st ed. Sober HA, editor. The Chemical Rubber Co., Cleveland; 1968.

Figure Legends

Figure 1. ICSN3250 specifically inhibited mTORC1 pathway. (**A**) Chemical structure of ICSN3250. (**B-H**) HCT116 cells were treated with the indicated concentration of ICSN3250 during 24 h. Cell extracts were analysed by western blot to determine the activation of the following pathways: (B) AMPK pathway (determined by the phosphorylation of AMPK at residue Thr172); (C) p53 pathway (determined by the phosphorylation of p53 at residue Ser15); (D) PI3K pathway (determined by the phosphorylation of AKT at residue Thr308); (E) ERK pathway (determined by the phosphorylation of p44/42 MAPK at residue Thr202/Tyr204); (F) NF-κB pathway (determined by the phosphorylation of p65 at residue Ser536); (G) mTORC1 pathway (determined by the phosphorylation of S6K at residue Thr389); (H) mTORC2 (determined by the phosphorylation of AKT at residue Ser473). (**I**) HCT116 cells were treated with the indicated concentration of ICSN3250 during 24 h. Cell extracts were analysed by western blot to determine the activation of the mTORC1 pathway through the phosphorylation of its downstream targets S6K, S6, and 4EBP1. (**J**) HCT116 cells were treated with 100 nM of ICSN3250 during the indicated time. Cell extracts were analysed as in I. (**K**) HCT116 cells were treated with the indicated concentration of ICSN3250 during 24 h. Cell extracts were analysed by western blot to determine the activation of autophagy through the levels of LC3-II and p62. (**L**) HCT116 cells were treated with 100 nM of ICSN3250 during the indicated time. Cell extracts were analysed as in K. (**M-N**) GFP-LC3 expressing U2OS cells were treated as indicated for 24 h. Autophagosome formation upon GFP-LC3 aggregation was determined (M) and quantified (N) using confocal microscopy. The scale bar represents 20 μm. (**O**) HCT116 cells were treated with the indicated concentration of ICSN3250 during 24 h. Cell cycle distribution was analysed by flow cytometry. Graphs show mean values ± s.e.m. (n=3). *P<0.05 (Anova post hoc Bonferroni).

Figure 2. ICSN3250 did not act through mechanisms previously described for other mTOR inhibitors. (**A**) *In vitro* kinase assay of mTOR in the presence of the indicated concentrations of ICSN3250. Human recombinant mTOR kinase was incubated for 30 min with increasing concentration of ICSN3250 (10^{-10} to 10^{-5}M) as indicated, and the relative mTOR kinase activity was determined in percentage with respect to untreated control. (**B-C**) mTOR localization in HCT116 cells treated with or without 100 nM of ICSN3250 during 24h, as indicated. mTOR localization was determined (B) and quantified (C) by immunodetection using confocal microscopy. CD63 was used as a lysosomal marker. (**D**) HCT116 cells were treated with 100 nM of ICSN3250 either in the presence or the absence of amino acids (AA) during 24 h. Cell extracts were analysed by western blot to determine the activation of the mTORC1 pathway through the phosphorylation of its downstream targets S6K, S6, and 4EBP1. (**E**) HCT116 cells were transfected with either an empty vector or with a vector expressing Flag-Rheb as indicated. 24 hours later, cells were treated with or without 100 nM of ICSN3250. Cell extracts were analysed by western blot to determine the activation of the mTORC1 pathway through the phosphorylation of its downstream targets S6K, S6, and 4EBP1. (**F**) Immunoprecipitation of mTOR in HCT116 cells treated with or without 100 nM of ICSN3250. Co-precipitation of Raptor was detected by western blot. Presence of both mTOR and Raptor in whole cell extracts (WCE) was included as controls. Graphs show mean values ± s.e.m. (n=3).

Figure 3. ICSN3250 antagonized with phosphatidic acid to inhibit mTORC1. (**A**) $TSC2^{+/+}$ and $TSC2^{-/-}$ MEFs were treated with increasing concentrations of ICSN3250 as indicated for 24 hours. Cell extracts were analysed by western blot to determine the activation of the mTORC1 pathway and autophagy through the phosphorylation of its downstream targets S6K and S6, and through LC3-II levels, respectively. (**B-C**) HCT116 cells were treated with increasing concentrations of PA in the presence of 100 nM ICSN3250. Cell extracts were analysed by western blot to determine the activation of the mTORC1 pathway through the

phosphorylation of its downstream targets S6K, S6, and 4EBP1 (B), and to analyse the inhibition of autophagy by determining the levels of LC3-II and p62 (C). (**D-E**) GFP-LC3 expressing U2OS cells were treated with increasing concentrations of ICSN3250 in the presence of 100 μM of PA. Autophagosome formation upon GFP-LC3 aggregation was determined (D) and quantified (E) using confocal microscopy. (**F-G**) HCT116 cells were treated with increasing concentrations of ICSN3250 in the presence of 100 μM PA. Cell extracts were analysed by western blot to determine the activation of the mTORC1 pathway through the phosphorylation of its downstream targets S6K, S6, and 4EBP1 (F), and to analyse the inhibition of autophagy by determining the levels of LC3-II and p62 (G). Graphs show mean values ± s.e.m. (n=3). *P<0.05 (Anova post hoc Bonferroni).

Figure 4. FRB domain of mTOR adopts different conformations in the apo form and in complex with ICSN3250 and PA. (A-B) Representative conformation for FRB domain of mTOR (apo form) extracted from a 100 ns molecular dynamics simulation. **(C-F)** Representative conformations for complexes between FRB domain of mTOR and ICSN3250 (C-D) or PA (E-F) extracted from 100 ns molecular dynamics simulations. The protein and the ligands (ICSN3250 and PA) are shown as surface representations colored in grey, magenta and orange, respectively. Ligands and key protein residues feature partial transparency of surface that unveils a stick representation of the atoms.

Figure 5. ICSN3250 and PA have partially overlapping binding sites. (A-D) Residues involved in the interactions with ICSN3250 (A-B) and PA (C-D). The protein is colored in grey and represented in cartoon mode. Protein residues involved in interactions and the ligands ICSN3250 and PA are represented in stick mode and colored in green, magenta and orange, respectively. Ionic interactions and hydrogen bonds are represented as dashed lines.

Figure 6. Inhibition of mTORC1 by ICSN3250 is responsible for its cytotoxicity in cancer cells. (**A**) Cell viability of $TSC^{+/+}$ and $TSC^{-/-}$ MEFs treated with ICSN3250 100 nM for 72 hours. (**B**) Cell viability of HCT116 cells treated with increasing concentrations of PA in the presence of 100nM ICSN3250. (**C-D**) Cell viability (C) and representative microscopy images (D) of HCT116 cells treated with increasing concentrations of ICSN3250 in the presence of 100 μM PA. (**E-F**) mTORC1 activation, determined by the phosphorylation of downstream target S6 (E) and cell viability (F) of HCT116 cells treated either with 100 nM rapamycin or with 100 nM ICSN3250. (**G**) IC50 values of different mTOR inhibitors in HCT116 cells. (**H**) Cell viability of both cancer (in red) and non-cancer (in blue) cell lines treated with different concentrations of ICSN3250 as indicated. (**I**) IC50 values of different mTOR inhibitors in the non-cancer cells NHDF. Graphs show mean values ± s.e.m. (n=3). *P<0.05 (*t* test).

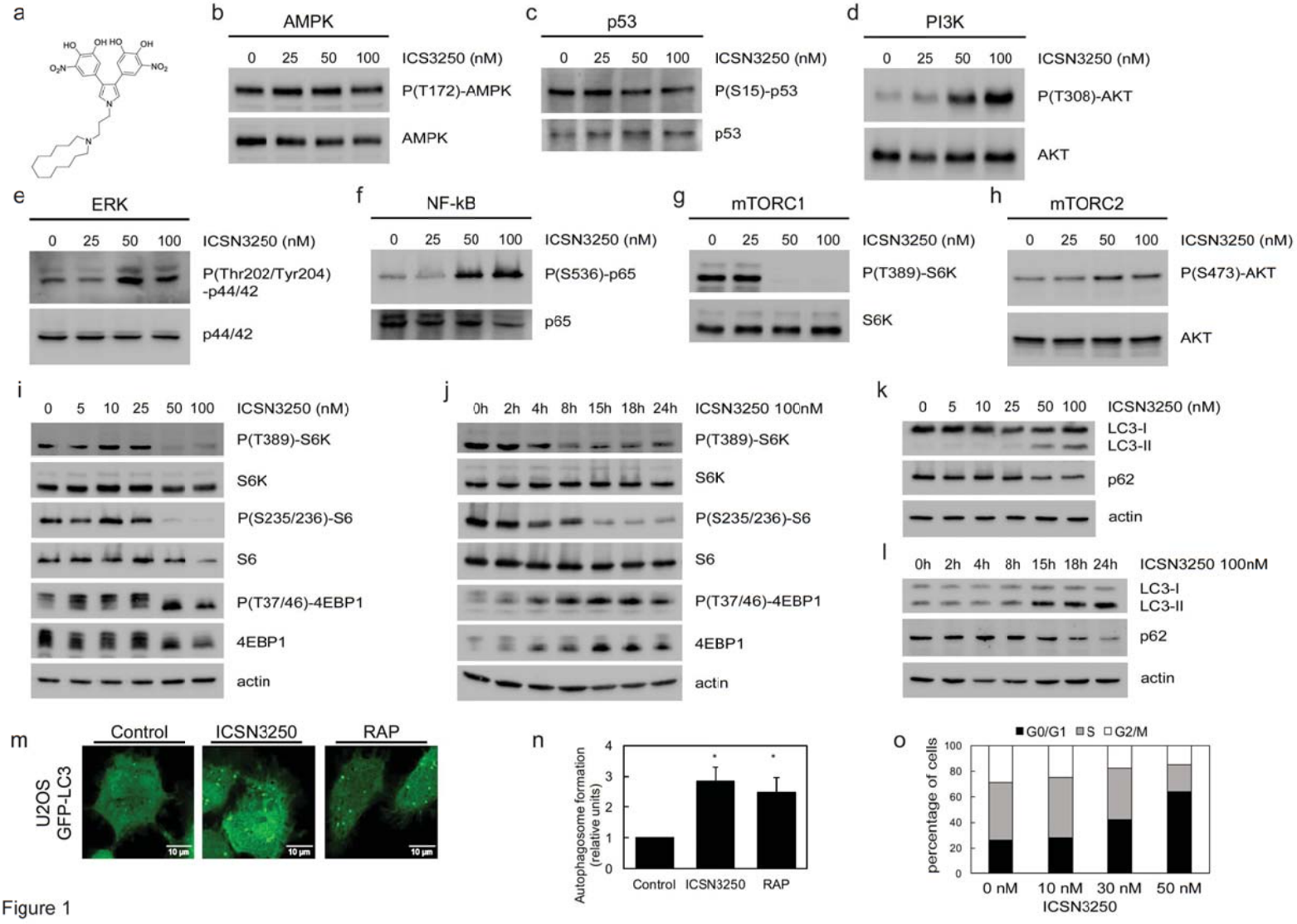
a
b
AMPK
0 25 50 100 ICS3250 (nM)
P(T172)-AMPK
AMPK
c
p53
0 25 50 100 ICSN3250 (nM)
P(S15)-p53
p53
d
PI3K
0 25 50 100 ICSN3250 (nM)
P(T308)-AKT
AKT
e
ERK
0 25 50 100 ICSN3250 (nM)
P(Thr202/Tyr204) -p44/42
p44/42
f
NF-kB
0 25 50 100 ICSN3250 (nM)
P(S536)-p65
p65
g
mTORC1
0 25 50 100 ICSN3250 (nM)
P(T389)-S6K
S6K
h
mTORC2
0 25 50 100 ICSN3250 (nM)
P(S473)-AKT
AKT
i
0 5 10 25 50 100 ICSN3250 (nM)
P(T389)-S6K
S6K
P(S235/236)-S6
S6
P(T37/46)-4EBP1
4EBP1
actin
j
0h 2h 4h 8h 15h 18h 24h ICSN3250 100nM
P(T389)-S6K
S6K
P(S235/236)-S6
S6
P(T37/46)-4EBP1
4EBP1
actin
k
0 5 10 25 50 100 ICSN3250 (nM)
LC3-I
LC3-II
p62
actin
l
0h 2h 4h 8h 15h 18h 24h ICSN3250 100nM
LC3-I
LC3-II
p62
actin
m
Control
ICSN3250
RAP
U2OS GFP-LC3
10 μm
n
Autophagosome formation (relative units)
Control ICSN3250 RAP
o
G0/G1 S G2/M
percentage of cells
0 nM 10 nM 30 nM 50 nM
ICSN3250

Figure 1

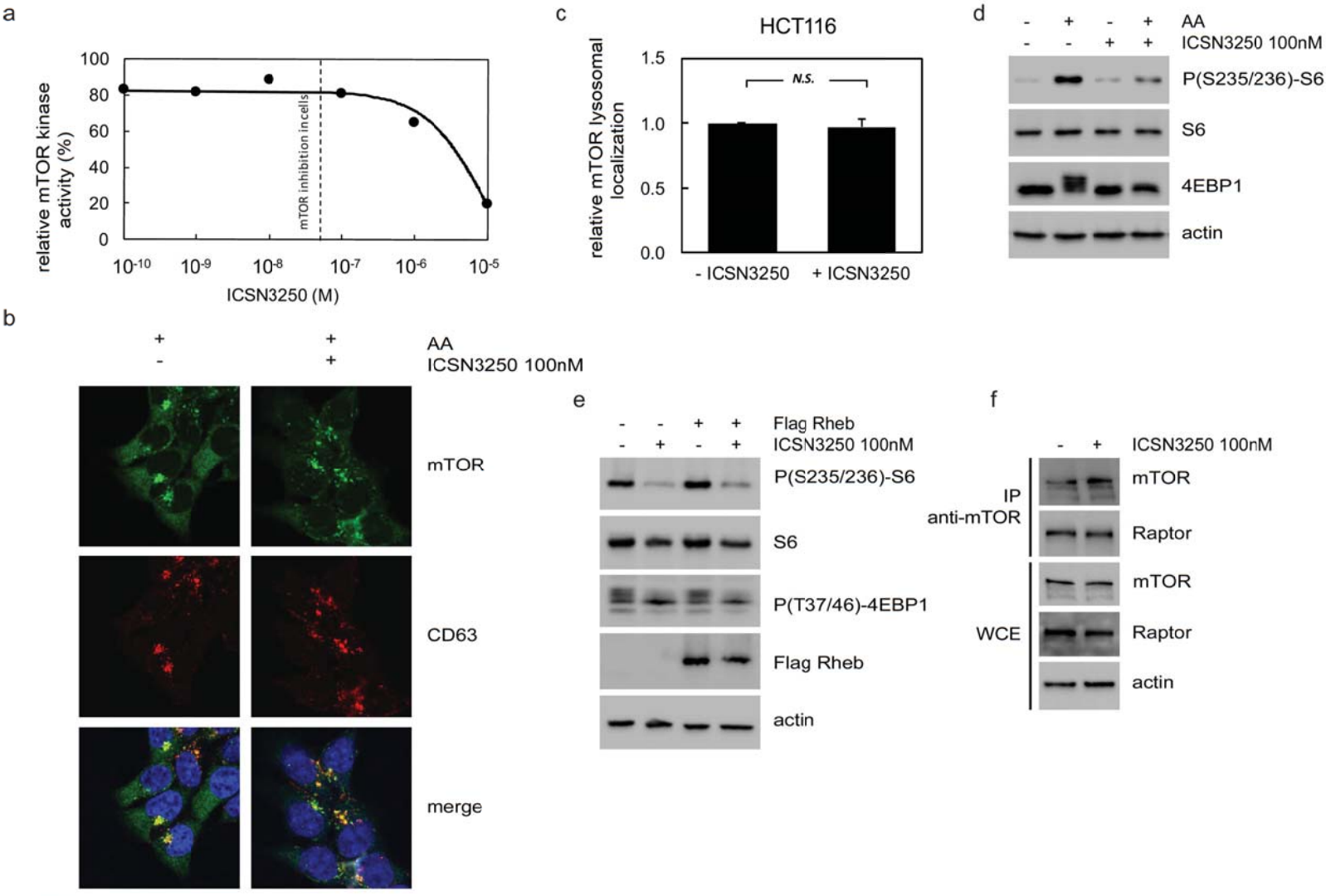
a
relative mTOR kinase activity (%)
100
80
60
40
20
0
mTOR inhibition in cells
10-10
10-9
10-8
10-7
10-6
10-5
ICSN3250 (M)
c
HCT116
relative mTOR lysosomal localization
1.5
1.0
0.5
0.0
N.S.
- ICSN3250
+ ICSN3250
d
AA
ICSN3250 100nM
P(S235/236)-S6
S6
4EBP1
actin
b
AA
ICSN3250 100nM
mTOR
CD63
merge
e
Flag Rheb
ICSN3250 100nM
P(S235/236)-S6
S6
P(T37/46)-4EBP1
Flag Rheb
actin
f
ICSN3250 100nM
IP
anti-mTOR
mTOR
Raptor
WCE
mTOR
Raptor
actin

Figure 2

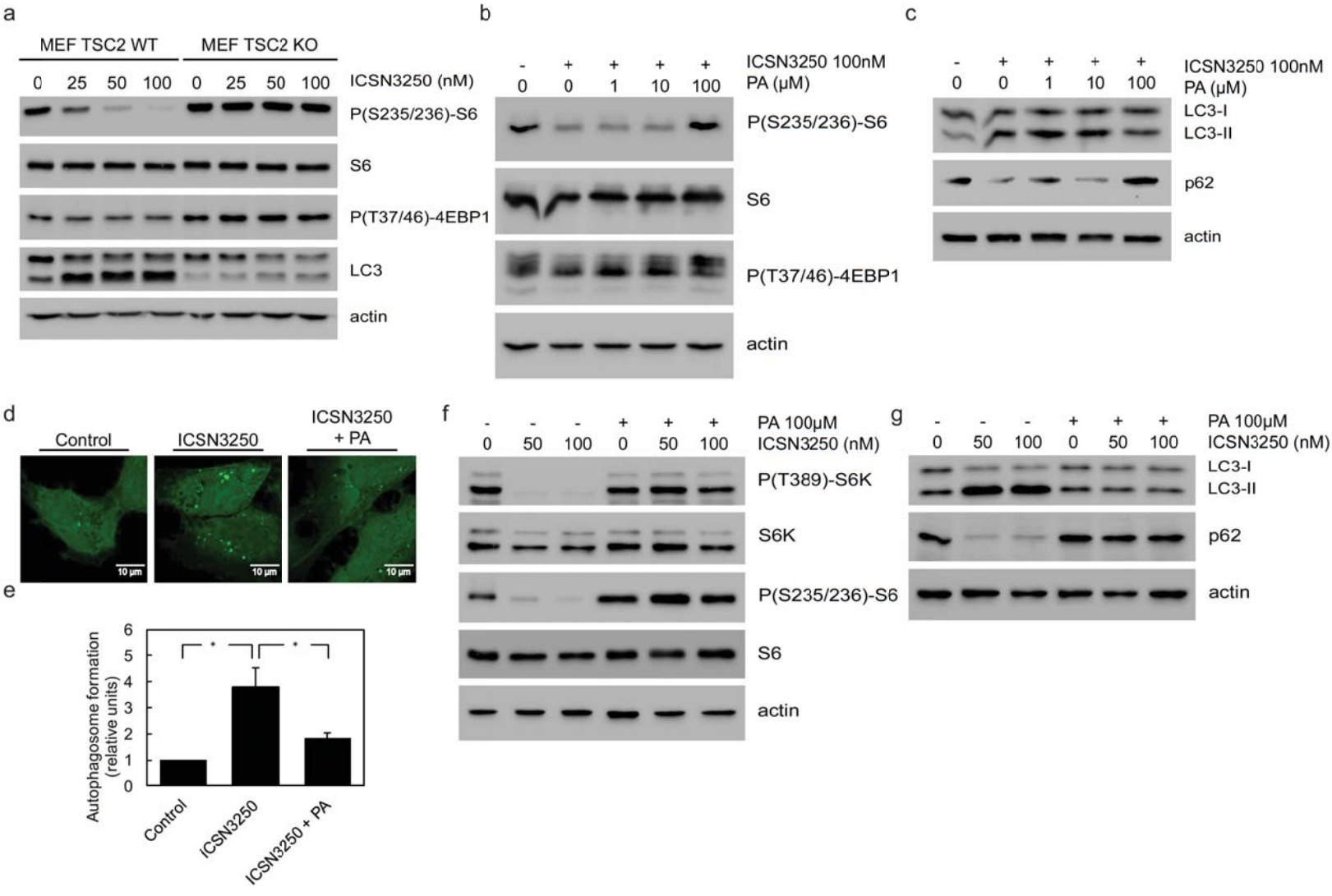
a
MEF TSC2 WT
MEF TSC2 KO
0 25 50 100 0 25 50 100
ICSN3250 (nM)
P(S235/236)-S6
S6
P(T37/46)-4EBP1
LC3
actin
b
- + + + +
0 0 1 10 100
ICSN3250 100nM
PA (μM)
P(S235/236)-S6
S6
P(T37/46)-4EBP1
actin
c
- + + + +
0 0 1 10 100
ICSN3250 100nM
PA (μM)
LC3-I
LC3-II
p62
actin
d
Control
ICSN3250
ICSN3250 + PA
10 μm
e
Autophagosome formation (relative units)
0 1 2 3 4 5 6
Control
ICSN3250
ICSN3250 + PA
f
- - - + + +
0 50 100 0 50 100
PA 100μM
ICSN3250 (nM)
P(T389)-S6K
S6K
P(S235/236)-S6
S6
actin
g
- - - + + +
0 50 100 0 50 100
PA 100μM
ICSN3250 (nM)
LC3-I
LC3-II
p62
actin

Figure 3

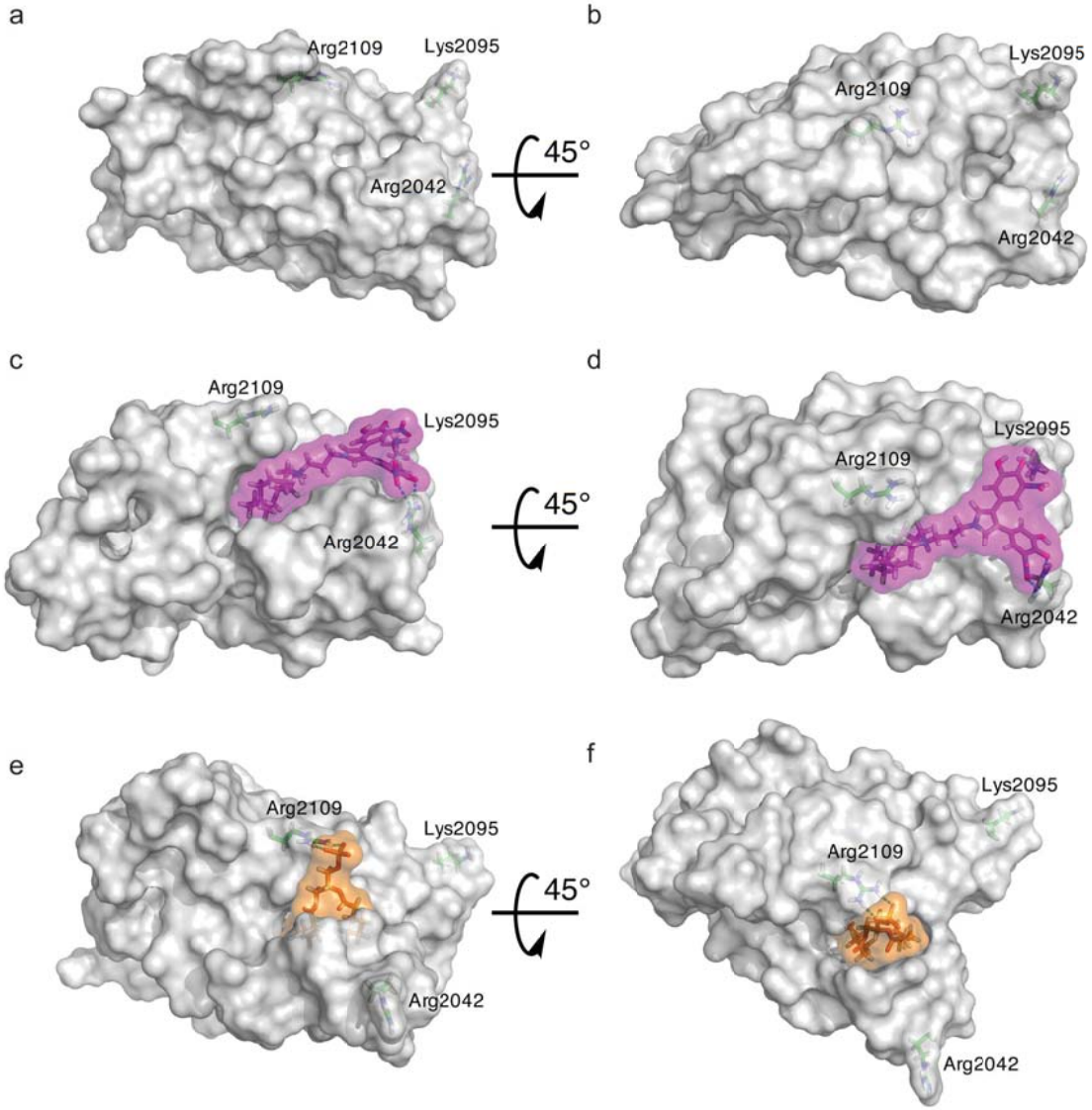
a
Arg2109
Lys2095
Arg2042
45°
b
Lys2095
Arg2109
Arg2042
c
Arg2109
Lys2095
Arg2042
45°
d
Lys2095
Arg2109
Arg2042
e
Arg2109
Lys2095
Arg2042
45°
f
Lys2095
Arg2109
Arg2042

Figure 4

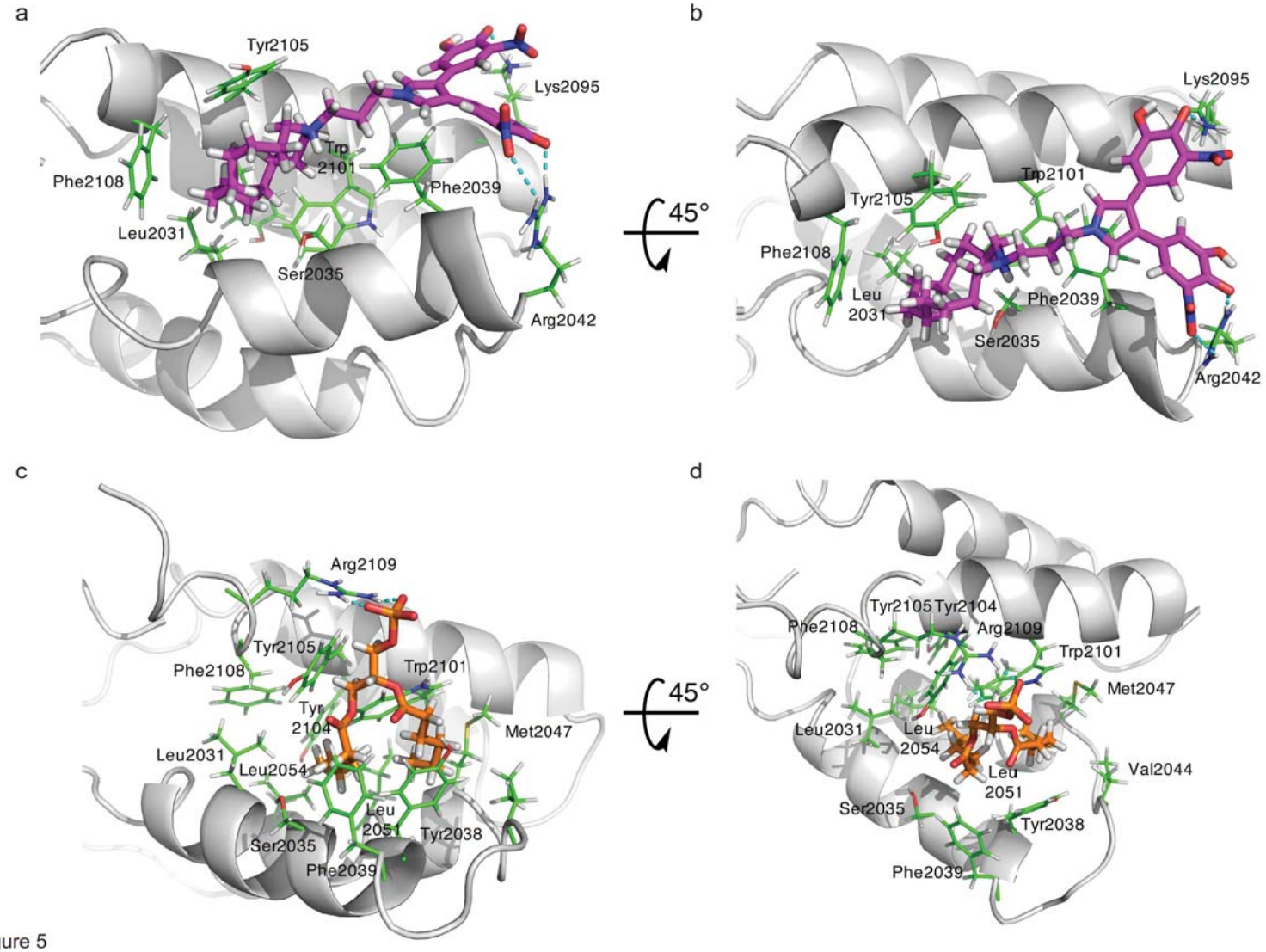
a
Tyr2105
Lys2095
Trp
2101
Phe2108
Phe2039
Leu2031
Ser2035
Arg2042
45°
b
Lys2095
Trp2101
Tyr2105
Phe2108
Leu
2031
Phe2039
Ser2035
Arg2042
c
Arg2109
Tyr2105
Phe2108
Trp2101
Tyr
2104
Met2047
Leu2031
Leu2054
Leu
2051
Tyr2038
Ser2035
Phe2039
45°
d
Tyr2105
Tyr2104
Phe2108
Arg2109
Trp2101
Met2047
Leu2031
Leu
2054
Leu
2051
Val2044
Ser2035
Tyr2038
Phe2039

Figure 5

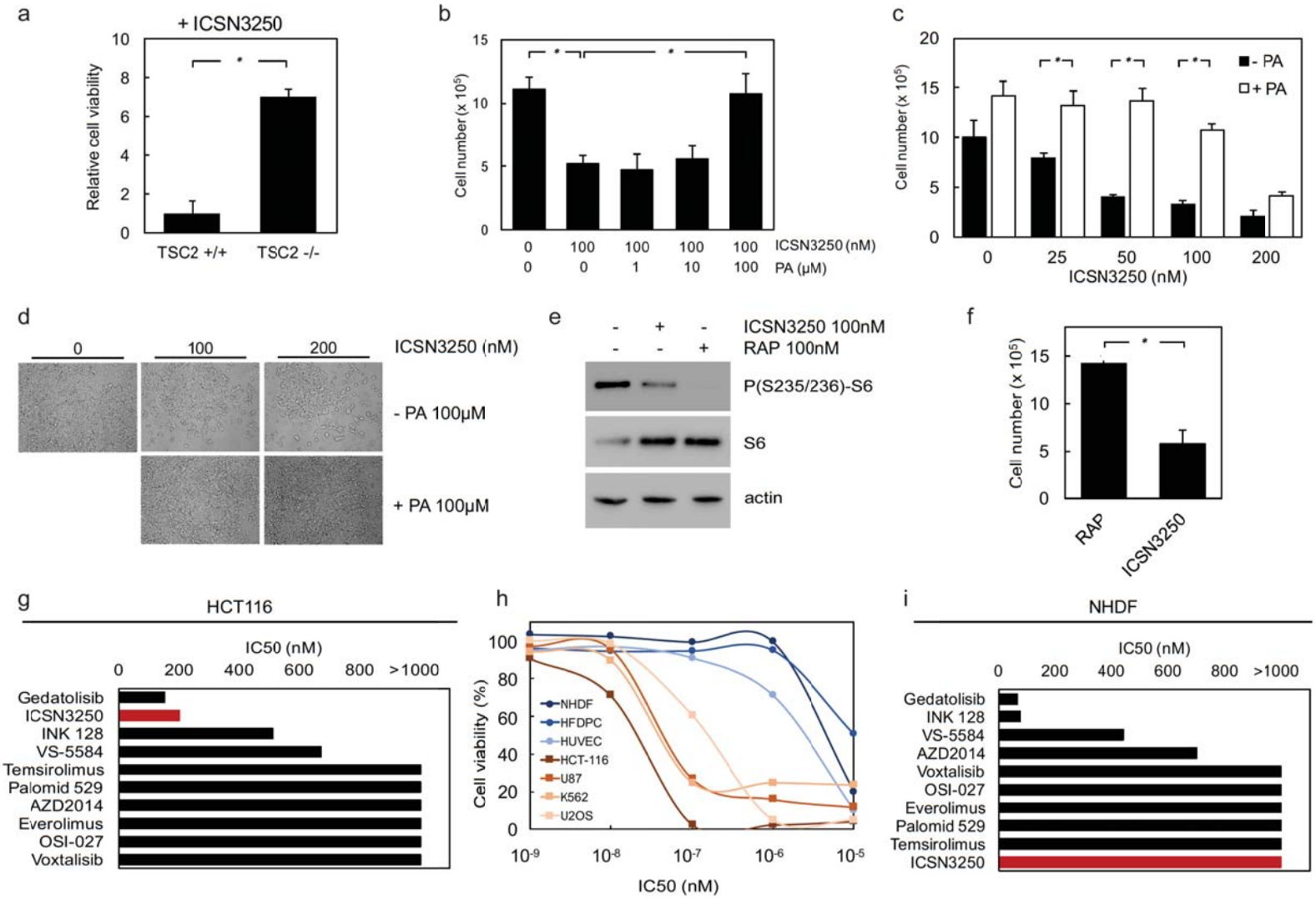
a
+ ICSN3250
Relative cell viability
TSC2 +/+
TSC2 -/-
b
Cell number (x 10^5)
ICSN3250 (nM)
PA (μM)
c
Cell number (x 10^5)
- PA
+ PA
ICSN3250 (nM)
d
ICSN3250 (nM)
- PA 100μM
+ PA 100μM
e
ICSN3250 100nM
RAP 100nM
P(S235/236)-S6
S6
actin
f
Cell number (x 10^5)
RAP
ICSN3250
g
HCT116
IC50 (nM)
Gedatolisib
ICSN3250
INK 128
VS-5584
Temsirolimus
Palomid 529
AZD2014
Everolimus
OSI-027
Voxtalisib
h
Cell viability (%)
NHDF
HFDPC
HUVEC
HCT-116
U87
K562
U2OS
IC50 (nM)
i
NHDF
IC50 (nM)
Gedatolisib
INK 128
VS-5584
AZD2014
Voxtalisib
OSI-027
Everolimus
Palomid 529
Temsirolimus
ICSN3250

Figure 6

Supplementary information

A novel mechanism of mTOR inhibition displacing phosphatidic acid induces enhanced cytotoxicity specifically in cancer cells

Tra-Ly Nguyen, Maxim Egorov, Clément Bodineau, Joanna Wdzieczak-Bakala, Maria Concepcion Garcia-Alvarez, Jérôme Bignon, Odile Thoison, Bernard Delpech, Georgiana Surpateanu, Yves-Michel Frapart, Fabienne Peyrot, Kahina Abbas, Silvia Terés, Pierre Soubeyran, Bogdan I. Iorga, Raúl V. Durán, and Pascal Collin

Supplementary Material and Methods

In vitro kinase assays

mTOR assay

This assay is based on TR-FRET (time-resolved fluorescence resonance energy transfer). The LANCE® Ultrakinase assay uses ULight-FLGFTYVAP peptide, ATP and a human recombinant mTOR kinase. After 30 min of incubation at room temperature, phospho-FLGTYVAP was measured. PI-103 was used as internal control with an IC50 of 71 nM. ICSN3250 test concentration ranged from 10^{-10} M to 10^{-5} M.

Akt1 assay

This assay is based on TR-FRET (time-resolved fluorescence resonance energy transfer). The LANCE® Ultrakinase assay uses CREBtide-CKRREILSRRPSYRK peptide, ATP and a human recombinant Akt1 kinase. After 60 min of incubation at room temperature, phospho-CREBtide CKRREILSRRPSYRK was measured. Staurosporine was used as internal control with an IC50 of 35 nM. ICSN3250 test concentration was at 500 nM.

EGFR assay

This assay is based on TR-FRET (time-resolved fluorescence resonance energy transfer). The LANCE® Ultrakinase assay uses ULight-CAGAGAIETDKEYYTVKD peptide, ATP and a human recombinant EGFR kinase. After 15 min of incubation at room temperature, phospho-

ULight -CAGAGAIETDKEYYTVKD was measured. PD153035 was used as internal control with an IC50 of 0.13nM. ICSN3250 test concentration was at 500 nM.

PDK1 assay

This assay is based on TR-FRET (time-resolved fluorescence resonance energy transfer). The LANCE® Ultrakinase assay uses ULight-FLGFTYVAP peptide, ATP and a human recombinant FDK1 kinase. After 90 min of incubation at room temperature, phospho-ULight -FLGFTYVAP was measured. Staurosporine was used as internal control with an IC50 of 200 nM. ICSN3250 test concentration was 500 nM.

PKCα and PKCε assay

This assay is based on HTRF (Homogeneous time-resolved fluorescence). For PKCα, the assay uses biotinyl-βAβAβAKIQASFRGHMARKK peptide (60 nM), ATP and a human recombinant PKCα kinase. After 15 min of incubation at room temperature, phosphor-biotinyl-βAβAβAKIQASFRGHMARKK was measured. Bis10 was used as internal control with an IC50 of 3.4 nM. ICSN3250 test concentration ranged from 10^{-9} M to 10^{-6} M.

For PKCβ, the assay uses biotinyl-βAβAβAKIQASFRGHMARKK peptide (400nM), ATP and a human recombinant PKCβ kinase. After 60 min of incubation at room temperature, phospho biotinyl-βAβAβAKIQASFRGHMARKK was measured. Bis10 was used as internal standard with an IC50 of 10 nM. ICSN3250 test concentration ranged from 10^{-9} M to 10^{-6} M.

SRC assay

This assay is based on TR-FRET (time-resolved fluorescence resonance energy transfer). The LANCE® detection method use the substrate Ulight-Poly GAT[EAY(1:1:1)]n, ATP, and a human recombinant SRC kinase expressed in insect cells. After 60 min of incubation the fluorescence transfer was measured at λ_{ex}=337 nm, λ_{em}=620 nm and λ_{em}=665 nm using a microplate reader (Envision, Perkin Elmer). Staurosporine was used as internal standard with an IC50 of 7.6 nM. ICSN3250 test concentration ranged from 10^{-9} M to 10^{-6} M

PI3K assay

The inhibition of PI3Ks (PI3Kα, PI3Kβ, PI3Kγ, PI3Kδ) activity was determined using the PI3 Kinase Activity/Inhibitor ELISA assay from Merck-Millipore (USA). The recombinant GRP-1 protein capture PIP3 generated as part of the kinase reaction or the biotinylated PIP3 tracer. The captured PIP3 tracer was detected using streptavidin-HRP conjugates and a colorimetric read out at 450 nm, following a kinase reaction (for 30 minutes). This colorimetric signal negatively correlates with PI3 kinase activity. Assay were carried out in 96 well assay plates in the presence or absence of the ICSN3250 compound. Wortmannin (100nM) was used as internal standard with an IC50 of 10 nM. Absorbance was recorded at 450 nm with a spectrophotometric plate reader PolarStar Omega (BMG Labtech, Germany).

Supplementary Tables

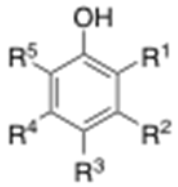

Supplementary Table 1. DFT-based prediction of aqueous pK_a value for **P1**, a simplified analogue of **ICSN3250**, using the protocol described in Muckerman *et al*.[1] The linear fit (lfit) coefficients obtained from our dataset were a_0=10.512 and a_1=2.596, with R^2=0.93705.

	R^1	R^2	R^3	R^4	R^5	$pK_{a,exp}$	$pK_{a,calc}$	$pK_{a,lfit}$	$\Delta pK_{a,exp-lfit}$
T1	H	H	H	H	H	9.95	3.58	9.94	0.01
T2	H	H	NO_2	H	H	7.14	1.97	7.00	0.14
T3	H	NO_2	H	H	H	8.35	2.81	8.53	-0.18
T4	NO_2	H	H	H	H	7.23	1.86	6.79	0.44
T5	H	H	OH	H	H	9.96	4.23	11.14	-1.18
T6	H	OH	H	H	H	9.44	3.54	9.88	-0.44
T7	OH	H	H	H	H	9.48	3.35	9.51	-0.03
T8	H	H	Me	H	H	10.19	3.72	10.19	0.00
T9	H	Me	H	H	H	10.08	3.66	10.10	-0.02
T10	Me	H	H	H	H	10.28	3.38	9.58	0.70
T11	H	H	Ph	H	H	9.51	3.53	9.85	-0.34
T12	H	Ph	H	H	H	9.59	3.57	9.92	-0.33

[1] Muckerman JT, Skone JH, Ning M, Wasada-Tsutsui Y. Toward the accurate calculation of pKa values in water and acetonitrile. *Biochim Biophys Acta*. **2013**, *1827*, 882-891.

T13	Ph	H	H	H	H	9.93	3.49	9.78	0.15
T14	NO_2	H	H	H	OH	6.66	1.39	5.93	0.73
T15	NO_2	NO_2	H	H	OH	4.39	0.23	3.80	0.59
T16	H	NO_2	H	H	OH	6.89	1.71	6.52	0.37
T17	NO_2	H	NO_2	H	H	4.11	0.65	4.58	-0.47
T18	NO_2	H	H	NO_2	H	5.22	1.13	5.44	-0.22
T19	NO_2	H	H	H	NO_2	5.23	0.33	3.99	1.24
T20	H	NO_2	NO_2	H	H	5.42	1.22	5.61	-0.19
T21	NO_2	H	NO_2	H	NO_2	0.96	-0.79	1.92	-0.96
Standard deviation									**0.56**
Root mean square error									**0.55**
P1	NO_2	H	Pyrr	H	OH		1.39	**5.93**	

Pyrr = *N*-methyl-3-pyrrolyl

Supplementary figure legends

Supplementary Figure 1. ICSN3250 specifically inhibited mTORC1 pathway. (**A-G**) U2OS cells were treated with the indicated concentration of ICSN3250 during 24 h. Cell extracts were analysed by western blot to determine the activation of the following pathways: (A) AMPK pathway (determined by the phosphorylation of AMPK at residue Thr172); (B) p53 pathway (determined by the phosphorylation of p53 at residue Ser15); (C) PI3K pathway (determined by the phosphorylation of AKT at residue Thr308); (D) ERK pathway (determined by the phosphorylation of p44/42 MAPK at residue Thr202/Tyr204); (E) NF-κB pathway (determined by the phosphorylation of p65 at residue Ser536); (F) mTORC1 pathway (determined by the phosphorylation of S6K at residue Thr389); (G) mTORC2 (determined by the phosphorylation of AKT at residue Ser473). (**H**) U2OS cells were treated with the indicated concentration of ICSN3250 during 24 h. Cell extracts were analysed by western blot to determine the activation of the mTORC1 pathway through the phosphorylation of its downstream targets S6K, S6, and 4EBP1. (**I**) U2OS cells were treated

with 100 nM of ICSN3250 during the indicated time. Cell extracts were analysed as in H. (**J**) U2OS cells were treated with the indicated concentration of ICSN3250 during 24 h. Cell extracts were analysed by western blot to determine the activation of autophagy through the levels of LC3-II and p62. (**K**) U2OS cells were treated with 100 nM of ICSN3250 during the indicated time. Cell extracts were analysed as in J.

Supplementary Figure 2. ICSN3250 did not act through mechanisms previously described for other mTOR inhibitors. (**A-B**) Relative *in vitro* kinase activity of different protein kinases as indicated in the presence of 100nM ICSN3250 (100% of activity was estimated as the activity of each protein kinase in the absence of ICSN3250). (**C-D**) mTOR localization in U2OS cells treated with or without 100 nM of ICSN3250 during 24h, as indicated. mTOR localization was determined (C) and quantified (D) by immunodetection using confocal microscopy. CD63 was used as a lysosomal marker. (**E**) U2OS cells were treated with 100 nM of ICSN3250 either in the presence or the absence of amino acids (AA) during 24 h. Cell extracts were analysed by western blot to determine the activation of the mTORC1 pathway through the phosphorylation of its downstream targets S6K, S6, and 4EBP1. (**F-G**) HCT-116 (F) or U2OS (G) cells were transfected with either an empty vector or with a vector expressing Flag-Rheb as indicated. 24 hours later, cells were incubated either in the presence or the absence of amino acids (AA). Cell extracts were analysed by western blot to determine the activation of the mTORC1 pathway through the phosphorylation of its downstream target S6. (**H**) U2OS cells were transfected with either an empty vector or with a vector expressing Flag-Rheb as indicated. 24 hours later, cells were treated with or without 100 nM of ICSN3250. Cell extracts were analysed by western blot to determine the activation of the mTORC1 pathway through the phosphorylation of its downstream target S6. Graphs show mean values ± s.e.m. (n=3).

Supplementary Figure 3. ICSN3250 antagonized with phosphatidic acid to inhibit mTORC1. (**A-B**) U2OS cells were treated with increasing concentrations of PA in the presence of 100 nM ICSN3250. Cell extracts were analysed by western blot to determine the activation of the mTORC1 pathway through the phosphorylation of its downstream targets S6K, S6, and 4EBP1 (A), and to analyse the inhibition of autophagy by determining the levels of LC3-II and p62 (B). (**C-D**) U2OS cells were treated with increasing concentrations of ICSN3250 in the presence or absence of 100 μM PA, as indicated. Cell extracts were analysed by western blot to determine the activation of the mTORC1 pathway through the phosphorylation of its downstream targets S6K, S6, and 4EBP1 (C), and to analyse the inhibition of autophagy by determining the levels of LC3-II and p62 (D).

Supplementary Figure 4. Root-mean-square deviation (RMSD) of mTOR protein during molecular dynamics simulations: apo form (top), complex with ICSN3250 (middle) and complex with phosphatidic acid (bottom).

Supplementary Figure 5. Inhibition of mTORC1 by ICSN3250 is responsible for its cytotoxicity in cancer cells. (**A**) Cell viability of both $TSC^{+/+}$ and $TSC^{-/-}$ MEFs incubated in the absence of ICSN3250. (**B-C**) HCT116 (B) or U2OS cells (C) were treated with several mTOR inhibitors, as indicated. Cell extracts were analysed by western blot to determine the activation of the mTORC1 pathway through the phosphorylation of its downstream targets S6K, S6, and 4EBP1. (**D**) IC50 values of different mTOR inhibitors in U2OS cells. Graphs show mean values ± s.e.m. (n=3).

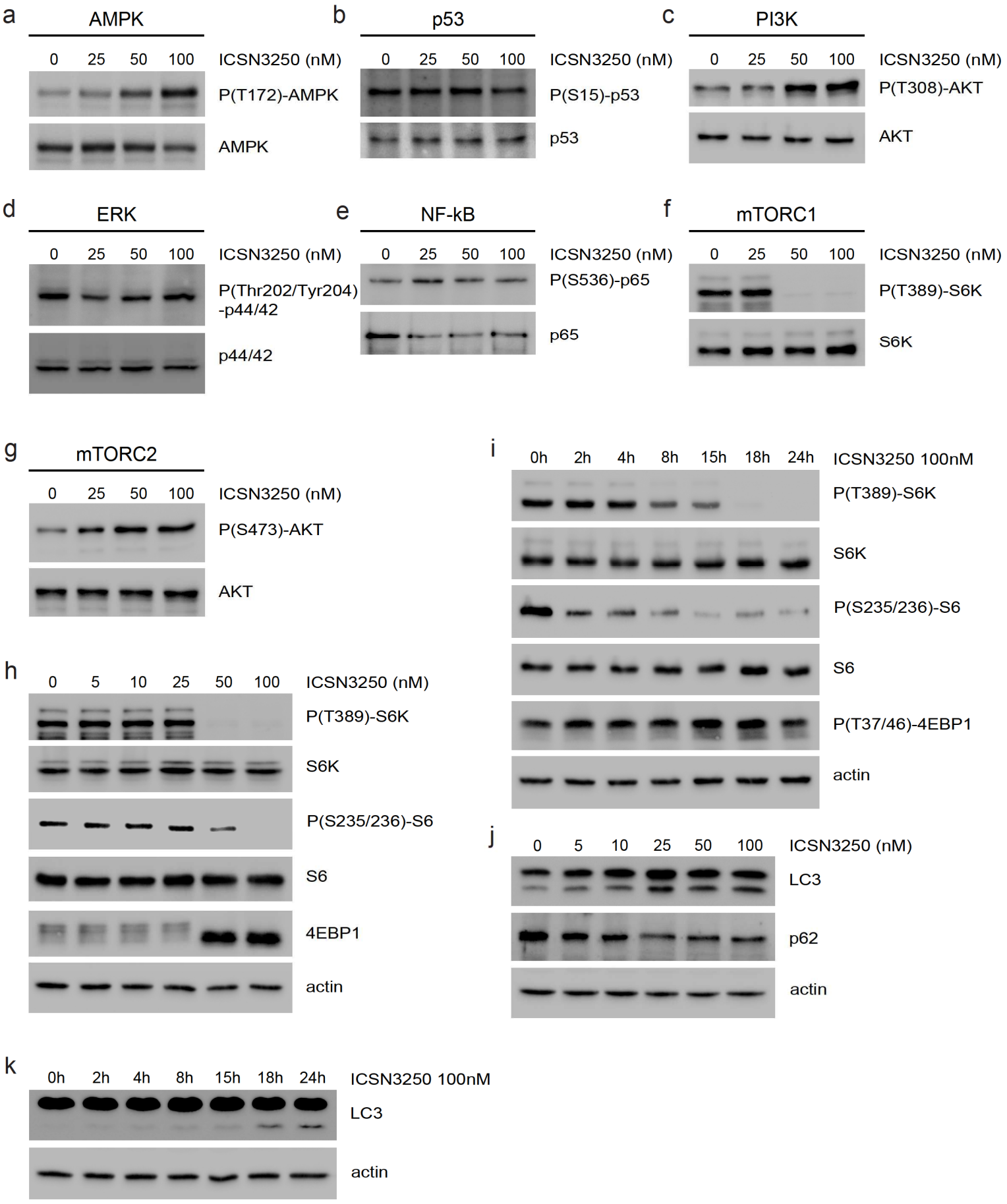

Supplementary Figure 1

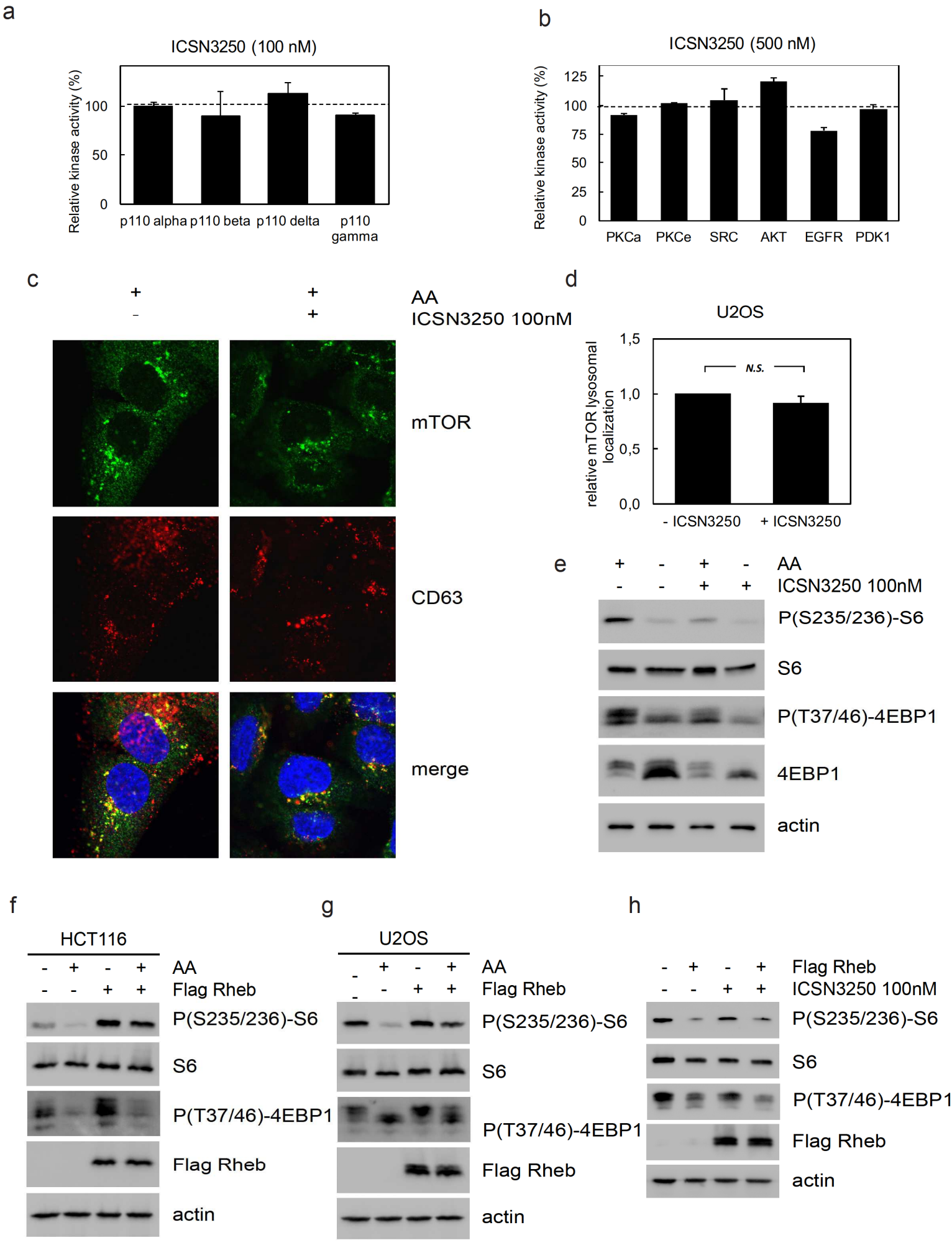

Supplementary Figure 2

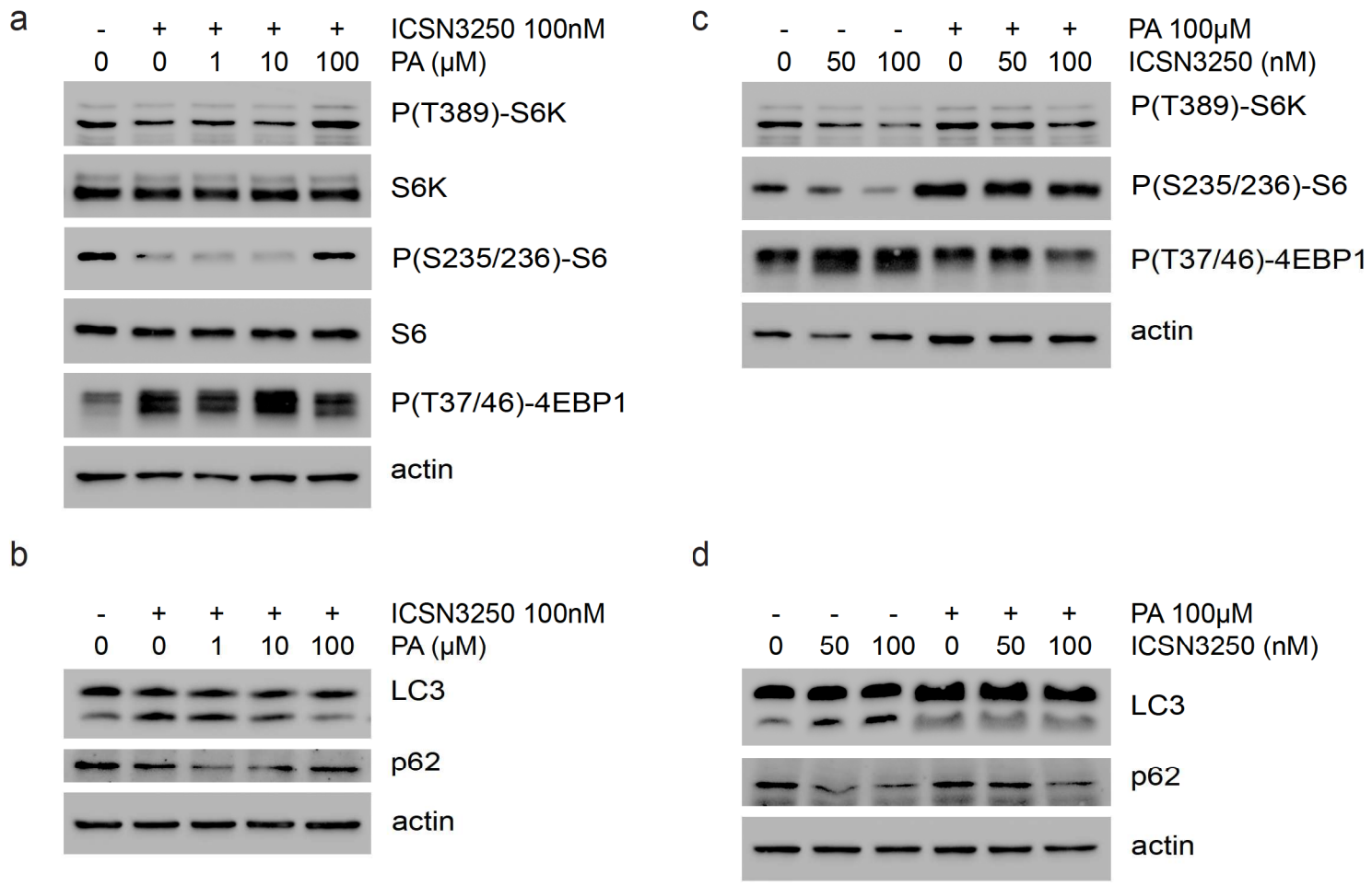

Supplementary Figure 3

a

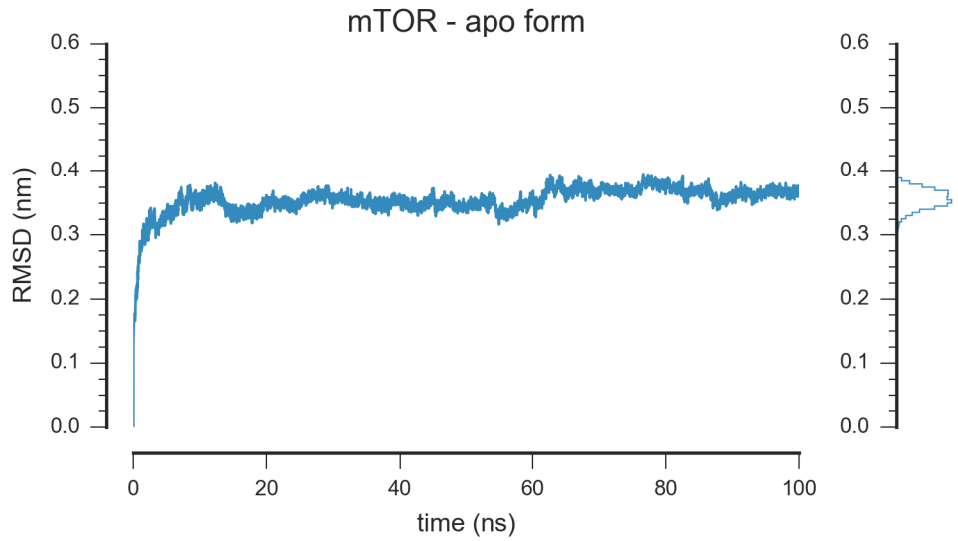

b

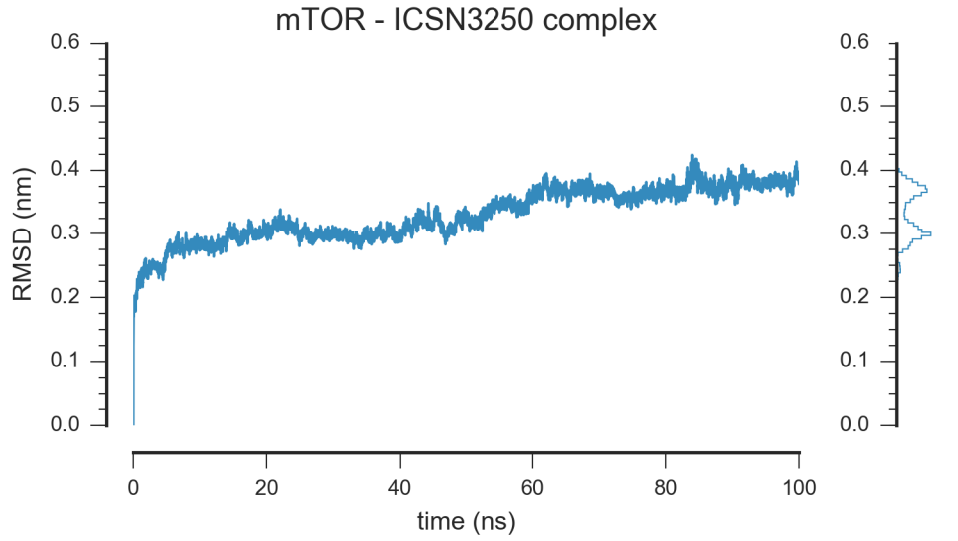

c

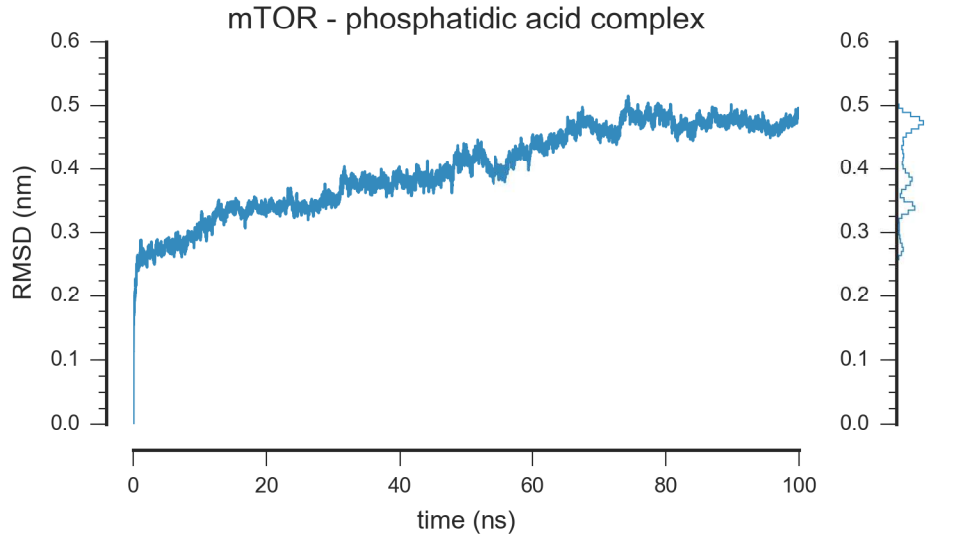

Supplementary Figure 4

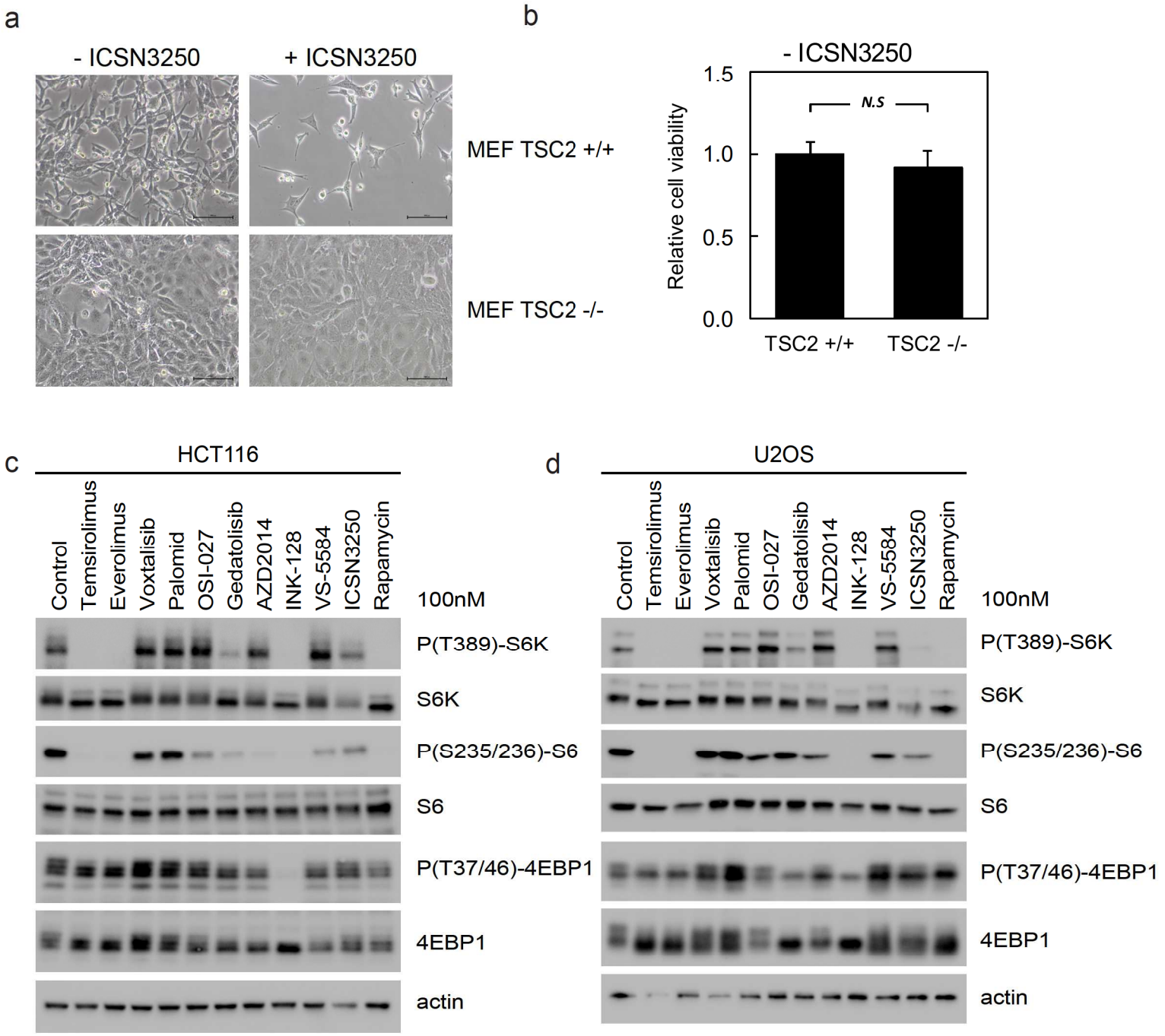

Supplementary Figure 5

Chapter two: Glutamine addiction induced by Notch1 activation in T-cell acute lymphoblastic leukemia.

Aims of the project

The aim of the research presented in this article is to understand the role of dysregulated Notch1 signaling in T-cell acute lymphoblastic leukemia (T-ALL) metabolism. As discussed, the interplay between glutamine metabolism and Notch1 signaling is poorly understood. This project will describe the molecular mechanism of this connection in the context of T-ALL, which have highly upregulated Notch1 pathway. Using *in vitro* and *in vivo* approaches, we have showed that Notch1-driven leukemic cells are dependent of extracellular glutamine level and they undergo apoptotic cell death upon glutamine withdrawal, which is called “glutamine addiction” phenotype. Moreover, Notch1 overexpression in Notch1-negative leukemic cells is sufficient to induce glutamine dependence. Mechanistically, Notch1 is able to regulate metabolic enzymes of glutamine metabolism, leading to increased glutamine catabolism and decreased glutamine anabolism. Accordingly, targeting glutamine metabolism could be considered as a therapeutic strategy against Notch1-driven leukemia.

This work is under preparation for submission.

Notch1 induces glutamine addiction in acute lymphoblastic leukemia

Tra Ly Nguyen[1,*], Silvia Terés[1,*], Marie-Julie Nokin[1], Mercedes Tomé[2], Oriane Galmar[1], Jean-Max Pasquet[3], Benoit Rousseau[4], Juan Manuel Falcon[5], Elodie Richard[6], Hamid-Reza Rezvani[7], Muriel Priault[8], Marion Bouchecareilh[8], Isabelle Redonnet[9], Patricia Fuentes[10], Maria Luisa Toribio[10], Abdel-Majid Khatib[2], Pierre Soubeyran[6] and Raúl V. Durán[1,11]

[1] *Institut Européen de Chimie et Biologie, INSERM U1218, Université de Bordeaux, 2 Rue Robert Escarpit, 33607 Pessac, France*

[2] *Angiogenesis and Cancer Microenvironment Laboratory INSERM U1029, Université de Bordeaux, Allée Geoffroy St Hilaire, 33615 Pessac, France*

[3] *INSERM-U876, Hématopoïèse Leucémique et Cible Thérapeutique, Université de Bordeaux, Laboratoire d'hématologie CHU de Bordeaux, Bordeaux, France.*

[4] *Service Commun des Animaleries, University of Bordeaux, Bordeaux, France*

[5] *Platform of Metabolomics, CIC bioGUNE, Ikerbasque, Derio, Spain*

[6] *Institut Bergonié, INSERM U1218, University of Bordeaux, 229 Cours de l'Argonne, 33076 Bordeaux, France*

[7] *Centre de Référence des Maladies Rares de la Peau, CHU de Bordeaux, INSEM U1035, Université de BordeauxBordeaux, France*

[8] *Institut de Biochimie et Génétique Cellulaires, CNRS UMR 5095, Université de Bordeaux, 1 Rue Camille Saint-Saëns, 33077 Bordeaux, France*

[9] *Maladies Héréditaires du Métabolisme, Laboratoire de Biochimie, Hôpital Pellegrin, CHU Bordeaux, Bordeaux France*

[10] *Centro de Biología Molecular "Severo Ochoa", Consejo Superior de Investigaciones Científicas, Universidad Autónoma de Madrid, 28049, Madrid, Spain*

[11] *To whom correspondence should be addressed:* Raúl V. Durán: raul.duran@inserm.fr

[*] *These authors contributed equally to this work*

Key words: Notch1, glutamine, mTOR, T-ALL, metabolic addiction

Conflict of interest: The authors declare no conflict of interest.

Abstract

The cellular receptor Notch1 is a central regulator of T-cell development, and as a consequence, Notch1 pathway appears upregulated in 50% of the cases of T-cell acute lymphoblastic leukemia (T-ALL). However, strategies targeting Notch signaling render only modest results in the clinic due to treatment resistance and severe side effects. While many investigations reported the different aspects of tumor cell growth and leukemia progression controlled by Notch1, very little is known regarding the modifications of cellular metabolism induced by Notch1 upregulation in T-ALL. In this work, we reported that Notch1 upregulation in T-ALL induced a change in the metabolism of the important amino acid glutamine, inducing glutaminolysis and preventing glutamine synthesis. This change ultimately leaded to glutamine addiction in Notch1-driven T-ALL both *in vitro* and *in vivo*. Our results also indicated that the increase in glutaminolysis mediated by Notch1 resulted in the activation of the mTORC1 pathway, a central controller of cell growth. Thus, we observed that the combined treatment targeting mTORC1 and limiting glutamine availability had synergistic effects to induce apoptotic cell death in Notch1-driven T-ALL cells. These results propose that the specific limitation of the amino acid glutamine could constitute a potential therapy to treat Notch1-driven leukemia.

Introduction

T-cell acute lymphoblastic leukemia (T-ALL) appears upon the malignant transformation of a T-cell progenitor. T-ALL is frequently driven by the oncogenic receptor Notch1. However, treatments targeting Notch signaling result in resistant or relapsed disease, and still 20% of childhood patients and 40% of adult patients do not survive[1]. Thus, a better understanding of the molecular basis of T-ALL origin and progression is essential for the proposal, design and validation of more specific, highly effective treatments against this type of leukemia.

Notch receptors (Notch1-4) are heterodimeric peptides, including an extracellular subunit and a transmembrane and intracellular subunit which interact through a heterodimerization domain present in both subunits. When a ligand of the DSL family located in the surface of a neighbor cell binds to the extracellular domain of the Notch receptor, it induces sequential cleavages in Notch by an ADAM metalloprotease and by a γ-secretase, releasing the Notch intracellular domain (NICD) from the membrane[2]. NCID then translocates to the nucleus, interacts with specific DNA-binding proteins (CBF1/Suppressor of Hairless/LAG-1 and Mastermind/SEL-8) and activates the transcription of target genes, such as the two families of transcriptional factors HES and HEY (including HES1, HES5, HEY1 and HEY2). The analysis of Notch1-target genes and gene expression programs controlled by Notch1 showed that Notch1 promotes leukemic cell growth via direct transcriptional upregulation of genes involved in ribosome biosynthesis, amino acid metabolism, protein translation, and nucleotide synthesis. However, Notch1 activation also follows an indirect mechanism to induce leukemic transformation through the upregulation of key target pathways, namely c-MYC pathway, PI3K/AKT pathway, and interleukin 7 receptor alpha chain. In addition, Notch1 activation increases G1/S cell cycle progression in T-ALL through the upregulation of CCND3, CDK4, and CDK6 cell cycle genes[3].

Although seminal works already showed the importance of glutamine in the control of metabolism of human leukemia long ago[4,5], still today we do not understand the role of glutamine metabolism in leukemia progression. Glutamine has been described as a crucial

nutrient for many types of tumor. This amino acid is metabolized within the mitochondria through an enzymatic process termed glutaminolysis, whereby glutamine is transformed into α-ketoglutarate (αKG), an intermediate of the tricarboxylic acid (TCA) cycle. Glutaminolysis is catalyzed by the enzymes glutaminase (GLS) and glutamate dehydrogenase (GDH)[6]. In addition to sustaining metabolism, glutaminolysis can also induce cell signaling deregulation in cancer cells through the hyper-activation of the mTORC1 pathway[7,8]. Conversely, glutamine synthesis through glutamine synthetase (GS) expression has been shown to be critical for the adaptation of certain types of solid tumors to glutamine scarcity[9].

In the case of Notch1-driven T-ALL, very little has been described regarding the participation of glutamine in Notch1-mediated T-cell malignant transformation or even in other types of cancer. Further, the mechanistic relationship between Notch1 and glutamine in the control of cellular homeostasis is not clear, as contradictory conclusions have been obtained. For instance, an *in vivo* study using T-ALL mouse models reported that glutaminolysis plays a critical role in leukemia progression downstream of Notch1. Glutaminolysis is thus proposed to be a key determinant of the response to anti-Notch1 therapies, as the inhibition of Notch1 blocks glutaminolysis[10]. Confirming the control of GLS by Notch1, an independent study in glioblastoma cells reached similar conclusions, showing a decrease of intracellular glutamate after Notch1 blockade[11]. However, a comparative metabolomic study performed in myeloid leukemic cells reported that the upregulation of Notch1 signaling decreases the expression of GLS and GDH, and decreases glutamine consumption[12]. This study also showed that an increase in glutamine utilization disrupts Notch signaling pathway, leading to a decrease in cleaved Notch1, in Notch activity, and in Hey1 expression.

Herein, we show that Notch1 activation induces glutamine addiction in T-ALL cells both *in vitro* and *in vivo*. We observed that Notch1 upregulation leads to proteosomal degradation of GS, responsible for glutamine addiction in Notch1-activated leukemic cells. Concomitantly, Notch1 also induces the upregulation of GLS and the subsequent activation

of mTORC1 signaling pathway. However, our results indicated that Notch1-driven glutamine addiction is mTORC1-independent. This study not only confirmed the model by which Notch1 induces glutaminolysis, but also proposed that Notch1 executes a program leading to the upregulation of glutamine catabolism, blocking glutamine anabolism, which ultimately leads to glutamine addiction in Notch1-driven leukemia. Our results also pointed at the potential therapeutic benefits of targeting glutamine metabolism specifically in Notch1-positive T-ALL patients.

Materials and methods

Reagents and antibodies

Antibodies against Notch1 total (#3608, dilution 1:1000), cleaved Notch1 (#4147, dilution 1:1000), c-myc (#13987, 1:1000), β-actin (#4967, dilution 1:1000), cleaved caspase 3 (#9664, dilution 1:1000), cleaved caspase 8 (#, 1:1000), cleaved PARP (#5625, dilution 1:1000), S6 (#2217, dilution 1:1000), phospho-S6 (Ser235/236) (#4856, dilution 1:1000), S6K (#2708, dilution 1:1000), phospho-S6K(T389) (#9205, dilution 1:1000), 4EBP1 (#9452, dilution 1:1000), phospho-4EBP1(T37/46) (#2855, dilution 1:1000), AKT (#4691, dilution 1:1000), phospho-AKT(Ser473) (#4060, dilution 1:1000), phospho-AKT(Thr308) (#13038, dilution 1:1000) were obtained from Cell Signaling Technology. Antibody against GS (#610517, dilution 1:1000) was obtained from BD Biosciences. Antibody against GLS (ab93434, dilution 1:1000) was purchased from Abcam. Antibody against hes1 (sc-165996, dilution 1:1000) is from Santa Cruz. The secondary antibodies anti-mouse (#7076, dilution 1:1000) and anti-rabbit (#7074, dilution 1:1000) were obtained from Cell Signaling Technology. The inhibitors Rapamycin (RAP), L-Methionine sulfoximine (MSO), Bis-2-(5-phenylacetamido-1,2,4-thiadiazol-2-yl)ethyl sulphide (BPTES) were obtained from Sigma. DAPT, Compound E, MG132 were purchased from Santa Cruz. SMARTvector Lentiviral Human GLUL shRNA were obtained from Dharmacon. The plasmid Glutamine Synthetase Human Tagged ORF Clone was purchased from Origene and the empty vector pJS27 MND-DEST SV40-Blasticidine is a gift from Dr. Richard Iggo (Institute Bergonié). The plasmid MND-LUC-IRES was obtained from the Vector Platform at the University of Bordeaux (France).

Cell lines and culture conditions

CUTLL1 and JURKAT were obtained from Marisa Toribio (Spain). HPB-ALL, LOUCY, MOLT4 were purchased from DMSZ. All the cells lines were grown in RPMI high glucose (4.5 g/l) (GIBCO) supplemented with 10% of fetal bovine serum (Dominique Dutscher), glutamine (2 mM), penicillin (100U/ml, Sigma) and streptomycin (100 mg/ml, Sigma), at

37°C, 5% CO_2 in humidified atmosphere. Mycoplasma contamination check was carried out using the PCR Mycoplasma Test Kit (PromoKine). For glutamine withdrawal experiments, cells are incubated in RPMI without glutamine (GIBCO) with dialyzed serum (Dutscher) during indicated time. Glutamine is added at 2mM final concentration. The different inhibitors were used as follows: BPTES (30 mM), Compound E (1 μM), DAPT (10 μM), MSO (1 mM), rapamycin (200 nM).

Metabolomics

After treatment, cells were centrifuged at 300g, 5 minutes and, freezed in liquid nitrogen and stored at -80°C. Cell pellets were lysed in 500 μl of a mixture of ice-cold water/methanol/acetic acid with a tissue homogenizer (Precellys) at 6000rpm for 20 seconds. Subsequently 400 μl of the homogenate was transferred to a new aliquot and shaken at 1400 rpm for 30 minutes at 4 °C. Next the aliquots were centrifuged for 15 minutes at 14000 rpm at 4 °C. 75 μl of the supernatant was transferred to a fresh aliquot and placed at -80°C for 20 minutes. The chilled supernatants were evaporated for 2 hours. The resulting pellets were suspended in 100 μl water/acetonitrile/formic acid. Concentrations of all metabolites were determined with a semi-quantitative method, using calibration curves. Samples were measured with a UPLC system (Acquity, Waters, Manchester) coupled to a Time of Flight mass spectrometer (ToF MS, SYNAPT G2, Waters). All samples were injected in duplicate.

Plasmids and shRNA transfections

The lentiviral production was carried out as described[13]. Subsequently, cells were seeded at a density of 500 000 cells per well in a 24-wells plate, infected using concentrated lentiviral supernatants at MOI5 for 24 hours. Then the cells were amplified and sorted by BD FACSAria sorting flow cytometer for GFP expression.

Western Blot

All cell lines were seeded in 10cm plates. After the treatment, cells were centrifuged at 300g, 5 minutes then washed with phosphate-buffered saline (PBS 1X) and lysed on ice using RIPA buffer, supplemented with protease inhibitors (Sigma), phosphatase inhibitors (Sigma) and PMSF 1mM (AppliChem). Protein quantification was performed with BCA assay kit (Thermo Fisher). After the electrophoresis, the proteins were transferred to a nitrocellulose membrane (BioRad) with Trans-Blot Turbo Transfer System (Bio-Rad). The membranes were incubated for 30 minutes in PBS 1X with 0.01% Tween-20 and 5% bovine serum albumin (BSA). Incubation with primary antibodies is overnight at 4°C and incubation with secondary antibodies is 2 hours at room temperature. Finally, membranes were imaged using the Chemi Doc MP Imager (Bio-Rad).

Cell viability

To assess cell proliferation, cells were seeded in 125 000 cells/ml in 24 wells plates for 7 days counting in triplicate. The number of cells were determined using the TC20 Automated Cell Counter (Bio-Rad) according to the manufacturer's instructions. Cells were counted every day with the counter with trypan blue 5% solution (Bio-Rad). After 7 days, proliferation curve has been established with the standard derivative. For cell viability, cells were seeded at 500 000 cells/ml in 24 wells plates and the number of total cell and alive cells were determined by the cell counter. Cell viability was the calculated as an end-point or for 7 days in triplicate.

Flow cytometry

For apoptotic cell death, after treatment, cells were stained with annexin V and propidium iodide (PI) (Annexin V-FITC Early Apoptosis Detection Kit, #6592 Cell Signaling Technology) following the manufacturer's protocol. Then, annexin V and PI staining were analysed using BDFACS Canto BD-Biosciences flow cytometer. The analysis of the data was performed using the software FACS Diva.

Real-time PCR

mRNA extraction was performed with Trizol (Invotrogen). One microgram of total mRNA was reverse transcribed using the GoScript Reverse Transcription system (Promega) following the manufacturer's protocol. Quantitative real-time PCR was performed using SSO Advanced Universal SYBR Green Supermix (Bio-Rad). Expression levels of each gene were evaluated using comparative threshold cycle (Ct) method using the $2^{-\Delta\Delta Ct}$ method with normalization to RPL29 and GAPDH housekeeping gene. Primers sequences of each gene are listed in supplementary table.

Xenograft mouse model

All animals are maintained in the Animal Facility A2 of the University of Bordeaux (institutional agreement number: A33063916), led by Dr. Benoît Rousseau. The project has received the agreement of the Ethic Committee under the number APAFiS #94212017032614365349v7. We used 8-weeks-old male NOD.Cg-*Prkdc*^{scid} *Il2rg*^{tm1Wjl}/SzJ immunodeficient mice which were randomly assigned to the different treatment groups. In the condition of glutamine withdrawal, the mice received glutamine-free diet from 5-weeks-old and at 8-weeks-old, mice received retro-orbital injections of cells which are luciferase positive. We performed the first imaging one week after the injection and twice per week. We evaluated disease progression and therapy response by *in vivo* luminescence bioimaging with the PhotonIMAGER (Biospace Lab, France). When mice were sacrificed after four weeks of injection, blood, bone marrow and spleen samples were collected and analyzed for further analyses (glutamine level, GFP expression by flow cytometry, Notch level by real time PCR).

Glutamine uptake

Uptake of glutamine uptake was assessed with ^{3}H-labelled glutamine. Cells were seeded at the concentration of 500 000 cells/ml in RPMI without glutamine for 4 hours. Labelled glutamine was added at the concentration of 2.5 µCi and incubated for 15 minutes. Cells

were collected, centrifuged at 1000g in 4°C for 5 minutes. Cell lysis was done after two washes in cold PBS with lysis solution (0.2N NaOH, 0.2% SDS) followed by HCl 2N. Protein concentration was quantified then the radioactivity was quantified in 5 mL of scintillation solution. We obtained the values that are normalized to protein content.

Statistics

The results are expressed as a mean ± SEM of at least three independent experiments. One-way ANOVA followed by bonferroni's comparison as a *post hoc* test was used to evaluate the statistical difference between more than two groups. *t*-test analysis was used to evaluate the statistical difference between two groups. Statistical significance was estimated when $p<0.05$.

Results

Glutamine is essential to sustain TCA cycle in T-ALL cells

To better understand the role of glutamine in sustaining the homeostatic metabolism of lymphoblastic leukemia, we performed a metabolomic analysis of two different T-ALL cell lines (Jurkat and Cutll1) in response to glutamine deprivation. As expected, the levels of glutamine, glutamate and α-ketoglutarate were decreased (in some cases even below detectable levels) in both cell lines when cells were incubated in the absence of glutamine (Figure 1A-C and Supplementary Figure 1A-B), confirming that glutaminolysis was abrogated in cells incubated in the absence of glutamine. However, we also observed a profound decrease in the levels of succinate, malate, fumarate, oxaloacetate, and citrate, all of them belonging to the TCA cycle (Figure 1D-H and Supplementary Figure 1C-G). These results further sustain the key role of glutamine in the support of TCA cycle through glutaminolysis in T-ALL cells, as previously suggested[4,5]. In contrast, levels of other metabolites not related to the TCA cycle, such as threonine, serine, and choline, were not decreased (Figure 1I-K and Supplementary Figure 1H-J). These results highlighted the specificity of glutamine in sustaining the TCA cycle in lymphoblastic leukemia, and led us to further investigate the addiction of T-ALL cells to glutamine availability.

Notch1 activation correlates with glutamine addiction in T-ALL cells

Next, we investigated glutamine addiction in T-ALL cells. Surprisingly, and despite the fact that glutamine was the key carbon source to sustain the TCA cycle in both T-ALL cell lines, only Cutll1 cells, but not Jurkat cells, showed an addiction to glutamine. As shown in Figure 2A, Cutll1 cells were unable to proliferate in glutamine-free conditions, while Jurkat cells could proliferate in these conditions (no major differences observed in glutamine-rich conditions among these cells, Supplementary Figure 2A). The lack of cell proliferation of Cutll1 cells incubated in the absence of glutamine correlated with a drastic increase in cell

death, not observed in Jurkat cells (Figure 2B, Supplementary Figure 2B). As one of the main genetic differences between these two cell lines are their differential activation of Notch1 (basal activity in Jurkat cells, high activity in Cutll1, Figure 2C), we further investigated the correlation between Notch1 activation and glutamine addiction using a broader panel of T-ALL cells. As shown in Figure 2D, glutamine addiction positively correlated with Notch1 activity in T-ALL cells (as determined by the levels of NICD and cell viability under glutamine restriction in a panel of T-ALL cell lines, Supplementary Figure 2C-D). Indeed, glutamine restriction induced apoptotic cell death in Notch1-positive T-ALL cells, such as Cutll1. As shown in Figure 2E, the incubation of Cutll1 cells in the absence of glutamine was sufficient to induce the cleavage of pro-apototic proteins including PARP, caspase 3, and caspase 8. In agreement with this result, the population of apoptotic cells as determined by annexin V/PI staining was increased in Cutll1 cells incubated in the absence of glutamine (Figure 2F-G). None of these apoptotic markers were observed in Notch1-negative T-ALL cells, such as Jurkat cells (Figure 2E-G). Further confirming that apoptosis induction mediated cell death upon glutamine withdrawal in Notch1-positive cells, treatment with zVAD, a caspase inhibitor, reduced caspase cleavage (both caspase 3 and caspase 8) and rescued cell viability (Supplementary Figure 2E-F). Apoptotic induction upon glutamine withdrawal also correlated with Notch1 activations using a broader panel of T-ALL cells (Supplementary Figure 2G-H).

Further confirming the positive role of Notch1 signaling in glutamine addiction of T-ALL cells, we observed that the induction of apoptotic cell death markers in Notch-positive glutamine-starved cells was strongly reduced upon gamma-secretase inhibitor (GSI) treatment, a Notch1 inhibitor (Figure 2H). The efficient inhibition of Notch1 signaling by GSI was confirmed by the reduced levels of NICD and by the reduced expression of the Notch1 downstream target genes Hes1 and Hey 1 (Supplementary Figure 2I). Notch1 inhibition using GSI also rescued significantly cell survival in glutamine starve cells (Figure 2I). Interestingly, the inability of Notch1-positive T-ALL cells to survive in glutamine-free

conditions correlated with their lack of induction of an appropriate UPR response in these conditions, a defect not seen in Notch1-negative cells (Supplementary Figure 2J). Altogether, these results clearly suggest that Notch1 upregulation correlates with an induced addiction to glutamine in T-ALL cells.

Notch1 upregulation induces glutamine addiction in T-ALL cells

The results shown above led us to investigate the sufficiency of Notch1 to induce glutamine addiction in T-ALL cells. The different T-ALL cells that we used so far present many genetic differences in addition to Notch1 activation. For this reason, we decided to induce Notch1 signaling in Notch1-negative cells, thus creating isogenic cell lines which only differ in their respective Notch1 signaling. For this purpose, we stably infected Jurkat cells (Notch1-negative cells) either with an empty vector (hereinafter referred as “EV cells”) or with a vector expressing NICD (hereinafter referred as “NICD cells”). The correct expression of NICD in infected cells was analyzed by qPCR (Figure 3A). To track them, both EV and NICD cells were co-infected with a GFP reporter and a luciferase reporter (Supplementary Figure 3A-B). The efficient upregulation of Notch1 signaling in NICD cells was further confirmed by the increased expression levels of the Notch1 downstream targets *c-myc*, *hes1*, and *hey1* (Supplementary Figure 3C). The upregulation of NICD did not affect the capacity of these leukemic cells to proliferate in rich media. As shown in Supplementary Figure 3D, both EV and NICD cells proliferate similarly in glutamine-rich conditions. However, the capacity of proliferation in glutamine-restrictive conditions was severely impaired upon the upregulation of the Notch1 pathway. Thus, EV cells were able to proliferate in the absence of glutamine, just as their parental counterpart (Jurkat cells). However, NICD-expressing cells lost dramatically their capacity to proliferate upon glutamine withdrawal (Figure 3B). The lost capacity to proliferate in glutamine-restricted conditions observed in NICD cells was accompanied by a dramatic increase in cells death, not observed in EV cells (Figure 3C-D). As previously observed for Notch1-positive leukemic cells, apoptosis induction accounted for

this increase in cell death. Thus, as shown in Figure 3E, NICD cells showed a prominent increase in pro-apoptotic markers, such as cleaved PARP and cleaved caspase 3, not observed in EV cells. Induction of apoptosis in NICD expressing cells upon glutamine withdrawal was again confirmed by annexin V / PI staining analysis by flow cytometry (Figure 3F-G). These results confirmed the sufficiency of Notch1 signaling to induce glutamine addiction in lymphoblastic leukemic cells.

Glutamine-free diet impairs Notch1-driven leukemia *in vivo*

To further validate the physiological relevance of glutamine addiction in T-ALL cells induced by Notch1 signaling observed *in vitro*, we investigated if Notch1-positive cells were addicted to glutamine also *in vivo*. For this purpose, we injected both EV and NICD cells (GFP and luciferase positive) into mice receiving either a normal complete diet or a diet in which both glutamine and glutamate content was eliminated (Figure 4A). Mice fed with a glutamine-free diet did not show any morphological or behavioral difference with respect to their complete diet fed littermates. No significant body weight decrease was observed in mice fed with either a complete or a glutamine-free diet (Figure 4B). Glutamine levels in the blood of mice fed with a glutamine-free diet decreased significantly with respect to the levels of glutamine in the blood of mice fed with a glutamine-rich diet, with no significant differences observed between mice injected with EV cells or NICD cells (Figure 4C). Upon implantation, NICD cells were able to induce leukemia progression (determined by *in vivo* luciferase analysis) in complete diet-fed mice even faster than EV cells (Figure 4D, left panels). However, disease progression of NICD leukemic cells was dramatically impaired in glutamine-free fed mice. In contrast, EV cells (Noch1-negative cells) were able to promote leukemia progression in both glutamine-free and glutamine-rich fed mice (Figure 4D, right panels). Thus, a glutamine-restricted diet did not affect the proliferation of the leukemia in mice injected with EV cells (Figure 4E), but it dramatically prevented leukemia progression in mice injected with NICD (Figure 4F). No differences between diets were observed in mice implanted with EV cells

(Figure 4D-F) A further necropsy analysis revealed the presence of NICD positive cells in the bow marrow of implanted mice fed in the presence of glutamine (Figure 4G). These results confirmed that Notch1-positive lymphoblastic leukemia is addicted to glutamine *in vivo*, and further validates the reduction of glutamine uptake as a potential approach to prevent leukemia progression in therapy.

Notch1 modulates glutamine metabolizing enzymes in T-ALL cells

In an attempt to understand the molecular mechanisms by which Notch1 signaling induces glutamine addiction in lymphoblastic leukemia, we investigated the effects of Notch1 induction towards glutamine metabolizing enzymes, particularly GLS as a key enzyme in the control of glutamine catabolism[6]. Our results showed that the induction of Notch1 signaling in NICD cells did not affect the levels of GLS in nutrient rich conditions (Supplementary Figure 4A). In contrast, the levels of GLS (both at the RNA and protein level) were enhanced in NICD cells with respect to EV cells when these cells were incubated in nutrient-restricted conditions (Figure 5A-B). This result suggested a role of Notch1 signaling in the upregulation of glutamine catabolism, as previously proposed[10]. The observed upregulation of GLS by Notch1 did not correlate with an increase in the transport of glutamine in these cells, as the upregulation of Notch1 in NICD cells did not increase (rather slightly decreased) the acute uptake of glutamine with respect to EV cells (Supplementary Figure 4B). Accordingly, the pharmacological inhibition of Notch1 signaling using GSI did not affect significantly the uptake of glutamine (Supplementary Figure 4C). Thus, Notch1 controls GLS expression, but does not seem to regulate glutamine transport in leukemic cells.

We reported recently that an increase in glutamine catabolism during nutritional imbalance induces apoptotic cell death in an autophagy-dependent manner that we named "glutamoptosis"[14,15]. Thus, we investigated if glutamoptosis induction during glutamine restriction was the reason of the addiction to glutamine induced by Notch1 in T-ALL cells.

Typically, glutamoptosis is inhibited by GLS inhibitors, such as BPTES, which reduce glutaminolysis[14]. In order to determine if the inhibition of glutaminolysis prevented cell death in glutamine-starved NICD cells, we inhibited GLS pharmacologically using BPTES in T-ALL cells with high levels of Notch1 (Cutll1 cells). However, the results shown in Supplementary Figure 4D-E indicated that BPTES treatment did not prevent the addiction to glutamine of Notch1-driven leukemic cells, as no decrease neither in cell death induction nor in apoptotic markers (cleaved PARP, cleaved caspase 3, and cleaved caspase 8) was observed upon BPTES treatment. These results discard glutamoptosis as a main reason for Notch1-mediated glutamine addiction. In addition, it is worth noting that the inhibition of GLS using BPTES in Notch1-positive cells during nutrient rich conditions did not induce the increase in apoptosis observed upon glutamine restriction (Supplementary Figure 4D-E). This results points at the very important conclusion that glutamine starvation and glutaminolysis inhibition render completely different responses in Notch1-driven leukemic cells.

In parallel, we also investigated if GS activity was necessary for the adaptation of T-ALL cells to conditions of low glutamine availability, as observed for other cancer types[9]. For this purpose, we inhibited GS activity pharmacologically using methionine sulfoximine (MSO). Our results showed that MSO treatment resulted in apoptotic cell death in T-ALL specifically in glutamine-restrictive conditions, showing increased cell death and increased apoptotic markers (cleaved PARP, cleaved caspase 3, and cleaved caspase 8) in these conditions (Figure 5C-D). These pharmacological results were confirmed by the genetic inhibition of GS using siRNA. Silencing of GS prevented cell proliferation of Notch1-negative cells in glutamine-free conditions (Figure 5E), and induced apoptotic markers such as cleaved PARP and cleaved caspase 3 (Figure 5F). Conversely, GS overexpression resulted in an attenuated apoptosis induction of Notch1-positive cells (Figure 5G).

Given the results obtained above, we investigated if Notch1 signaling regulates GS levels. Indeed, we observed that Notch1-negative T-ALL cells (Jurkat) presented an induction of GS at protein level during glutamine restriction, while this upregulation of GS

was strongly impaired in Notch1-positive T-ALL cells (Cutll1) (Figure 5H). A clear negative correlation between Notch1 and GS was observed when we analyzed a broader panel of T-ALL cell lines (Supplementary Figure 4F). However, no increase in GS, but rather a compensatory decrease was observed at RNA level was observed (Supplementary Figure 4G), suggesting that the induction of GS at the protein level in conditions upon glutamine withdrawal in Notch1-positive cells must be a post-transcriptional regulation mediated by Notch1. A recent publication suggested that GS levels are downregulated by glutamine availability due to its proteasomal degradation[16]. Indeed, in T-ALL cells we confirmed that the inhibition of the proteasome using MG132 treatment induced GS levels during glutamine sufficiency (Supplementary Figure 4H), confirming that GS is expressed but subsequently degraded in conditions of glutamine availability. Hence, the lack of proteasomal degradation seems to be responsible for the accumulation of GS during glutamine restriction in Notch1-negative cells. Further confirming that the upregulation of Notch1 signaling prevents GS accumulation during glutamine restriction in T-ALL cells, we observed that NICD cells showed a substantial decrease in the levels of GS with respect to their counterpart EV cells upon glutamine withdrawal (Figure 5I). Conversely, the inhibition of Notch1 signaling using GSI restored high levels of GS during glutamine restriction (Supplementary Figure 4I). These results confirm that Notch1 signaling is responsible for the lack of GS accumulation in glutamine-restrictive conditions, likely through the activation of the proteasomal degradation of GS in these conditions.

mTORC1 inhibition synergizes with glutamine starvation to induce cell death in Notch1-positive T-ALL cells

Glutamine metabolism is very closely connected with cell growth control. Indeed, glutamine metabolism is a major regulator of mTORC1[7,17]. mTORC1 is a master controller of cell growth and metabolism, and a therapeutic target for cancer cells[18]. As we found that Notch1 has a deep impact on enzymes implicated in glutamine metabolism in T-ALL cells, we investigated the potential connection between Notch1 and the activation of mTORC1 via

glutamine metabolism. We observed a moderate increase in mTORC1 activation (as determined by the phosphorylation status of the mTORC1 downstream target S6K) in Notch1-positive cells (Cutll1) with respect to Notch1-negative cells (Jurkat) cultured in the presence of glutamine (Supplementary Figure 5A). However, that difference was dramatically increased when these cells were incubated in the absence of glutamine. As shown in Figure 6A, we observed that mTORC1 activity was highly sustained during glutamine restriction in Cutll1 (Notch1-positive) cells, while mTORC1 was strongly inhibited in Jurkat (Notch1-negative) cells, suggesting a link between Notch1 activation and mTORC1 mediated by glutamine. Intriguingly, we observed that AKT phosphorylation at residue S473 was increased in Jurkat with respect to Cutll1, reflecting that, conversely to what was observed in mTORC1, an increase in mTORC2 activity in Jurkat cells with respect to Cutll1 cells was observed (Supplementary Figure 5A).

Next, we observed that Notch1 inhibition using GSI strongly reduced mTORC1 activity specifically in Cutll1 cells, while GSI treatment had no effect on mTORC1 in Jurkat cells (Figure 6B), indicating that Notch1 signaling was a main pathway to sustain mTORC1 activity in Notch1-positive cells, while Notch1-negative cells rely on other signaling pathways to sustain mTORC1 activation. On the other hand, mTORC1 inhibition using rapamycin induced a strong arrest of cell proliferation in Cutll1 cells, but it had almost no effect on Jurkat cells (Figure 6C-D). Thus, conversely, Notch1-positive cells are not only addicted to glutamine, but also require mTORC1 activation to sustain cell proliferation, a requirement not seen in Notch1-negative cells. To further sustain this conclusion, we compared mTORC1 activation and rapamycin response between EV and NICD cells. The induction of Notch1 signaling in NICD cells did not change the phosphorylation of mTORC1 downstream targets S6 and 4EBP1 in nutrient rich conditions (Supplementary Figure 5B). However, and in agreement with our previous observations, the activation of mTORC1 was sustained in NICD cells with respect to EV cells when these cells were incubated in nutrient-deprived conditions

(Figure 6E), strongly suggesting that Notch1 signaling sustains mTORC1 activation, even during nutrient-restrictive conditions.

As our results so far indicated that Notch1-driven lymphoblastic leukemia is both addicted to glutamine and rely on mTORC1 activation to proliferate, we next investigated if glutamine starvation and rapamycin treatment exerted a synergistic effect in the induction of cell death. Indeed, as shown in Supplementary Figure 5C, rapamycin treatment enhanced the activation of apoptosis (as determined by the cleavage of PARP) induced by glutamine starvation specifically in Notch1-positive leukemic cells (Cutll1). Confirming these results, we also observed that the upregulation of Notch1 signaling in NICD cells induced a sensitivity to rapamycin in glutamine starved cells (as determined by the cleavage of PARP), while it did not affect PARP cleavage in their counterpart EV cells (Figure 6F). Importantly, rapamycin effect alone did not affect apoptosis induction in glutamine rich conditions. These results indicated that rapamycin treatment enhances the sensitivity of Notch-driven leukemia to glutamine restriction, and suggested that the combination of glutamine starvation and rapamycin treatment could be an optimal approach to specifically kill Notch1-driven leukemia.

Discussion

Aberrant Notch signaling has been reported to play an important role in the tumorigenesis of different types of cancer[19–21]. However, the role of Notch1 in T-ALL metabolism is less evident. The present study about glutamine dependence of Notch1-driven lymphoblastic leukemia showed a connection between Notch1 signaling and glutamine metabolism. Indeed, the upregulation of Notch1 signaling in T-ALL induced apoptotic cell death upon glutamine withdrawal with an increase in the activation of apoptosis-related proteins (cleaved PARP, cleaved caspase 3, and cleaved caspase 8), leading to a glutamine addiction phenotype. Notch1 inhibition using GSI efficiently rescued cell viability and blocked apoptosis, and conversely Notch1 upregulation was sufficient to induce glutamine dependence in T-ALL cells, showing that Notch1 was both necessary and sufficient for glutamine addiction. Moreover, we confirmed this phenotype also *in vivo* using mouse models, as we observed that specifically Notch1-positive leukemia was unable to progress in mice fed with a glutamine-free diet. Finally, our results showed that Notch1-induction increased GLS expression at the mRNA level. In parallel, Notch1 blocked the accumulation of GS in glutamine-free conditions by enhancing the proteasomal degradation of GS, ultimately responsible for the addiction to glutamine (**Figure 6G**).

Mechanistically, how Notch1 induces the proteasomal degradation of GS is still unclear. Recently, it was reported that glutamine induces the degradation of GS through the activity of the cullin-RING ubiquitin ligase 4 (CRL4) complex. Thus, under glutamine-rich conditions GS is acetylated at lysines 11 and 14 by p300, which allows its interaction with CRL4(CRBN), and the subsequent ubiquitination and degradation of GS by the proteasome[16]. How Notch1 interferes with this system by enhancing the acetylation of GS by p300 or increasing the activity of CRL4(CRBN) remains an open question.

Although glutamine addiction has been reported in many cancer types[22–24], to the best of our knowledge this is the first time that glutamine addiction has been reported as a consequence of Notch1 activation in T-ALL. Previously, Herranz et al., showed that glutaminolysis is a

494 critical pathway for leukemia cell growth downstream of Notch1 and a key determinant of the
495 response to anti-Notch1 therapies *in vivo*[10]. This work showed that, mechanistically, the
496 inhibition of Notch1 induces glutaminolysis inhibition and triggers autophagy supporting
497 leukemic survival and cell growth by recycling essential metabolites required for leukemic
498 cell metabolism. Extending these results, our work showed that GLS inhibition did not have
499 the same effect than glutamine depletion on cell viability in Notch1-driven leukemia,
500 illustrating that glutamine is essential for Notch1-postivie T-ALL cells for reasons that exceed
501 just glutaminolysis. This conclusion was further supported by our observation that GS
502 degradation (and not GLS) was responsible for the glutamine-addiction phenotype.

503 The results obtained in this study highlighted the potential involvement of glutamine
504 restriction as a therapeutic approach for Notch1-positive T-ALL patients. In our model, we
505 used a glutamine/glutamate-free diet to fed mice bearing Notch1-induced leukemia.
506 Although the liver of mice can synthesize its own glutamine, our results showed that the
507 blood glutamine levels in mice fed with glutamine-free diet were actually decreased
508 significantly compare to the normal diet. Thus, the establishment of glutamine-free diets
509 could be considered to apply for patients bearing Notch1-driven leukemia. However, from
510 the practical point of view, preparation of such a diet might be not achievable, or at least not
511 affordable. Alternatively, the use of L-asparaginase could be envisioned in this situation. L-
512 asparaginase is an enzyme which catalyzes the conversion of L-asparagine to aspartic acid
513 and ammonia. However, it has been reported that L-asparaginase do not only degrade L-
514 asparagine, but also has a glutaminase activity although with lower affinity and lower
515 maximal rate, leading to decreased levels of glutamine in blood[25–27]. Considering that this
516 type treatment is already available for drug administration, it could be contemplated for the
517 treatment of T-ALL patients carrying Notch1 mutations.

518 Finally, our results showed that a treatment combining glutamine depletion with the
519 mTORC1 inhibitor reduces the viability specifically of Noch1-driven leukemic cells. The
520 mechanistic link observed between Notch1 and mTORC1 though glutaminolysis seems to

operate as a mechanism to potentiate cell growth and leukemia proliferation, sustaining high glutamine catabolism and high mTORC1 activity. Targeting this axis by attacking to main points (glutamine availability and mTORC1 activation) could be envisioned as a potential therapy to treat Notch1-positive T-ALL patients.

Acknowledgements

This work was supported by funds from the following institutions: Institut National de la Santé et de la Recherche Médicale - INSERM, Fondation pour la Recherche Médicale, the Conseil Régional d'Aquitaine, Ligue Contre le Cancer - Aquitaine, SIRIC-BRIO, and Institut Européen de Chimie et Biologie. We thank Vincent Pitard (Flow Cytometry Platform, Universite´ de Bordeaux, France) for technical assistance in flow cytometry experiments.

Conflict of Interest

The authors declare no competing financial interest.

References

1. Tremblay, C. S. & Curtis, D. J. The clonal evolution of leukemic stem cells in T-cell acute lymphoblastic leukemia. *Curr. Opin. Hematol.* **21,** 320–5 (2014).

2. Pancewicz, J. & Nicot, C. Current views on the role of Notch signaling and the pathogenesis of human leukemia. *BMC Cancer* **11,** 502 (2011).

3. Tzoneva, G. & Ferrando, A. A. Recent advances on NOTCH signaling in T-ALL. *Curr. Top. Microbiol. Immunol.* **360,** 163–82 (2012).

4. Raivio, K. O. & Andersson, L. C. Glutamine requirements for purine metabolism in leukemic lymphoblasts. *Leuk. Res.* **6,** 111–5 (1982).

5. Kitoh, T. *et al.* Metabolic basis for differential glutamine requirements of human leukemia cell lines. *J. Cell. Physiol.* **143,** 150–3 (1990).

6. Villar, V. H., Merhi, F., Djavaheri-Mergny, M. & Durán, R. V. Glutaminolysis and autophagy in cancer. *Autophagy* **11,** 1198–1208 (2015).

7. Durán, R. V. *et al.* Glutaminolysis Activates Rag-mTORC1 Signaling. *Mol. Cell* **47,** 349–358 (2012).

8. Durán, R. V *et al.* HIF-independent role of prolyl hydroxylases in the cellular response to amino acids. *Oncogene* **32,** 4549–4556 (2013).

9. Tardito, S. *et al.* Glutamine synthetase activity fuels nucleotide biosynthesis and supports growth of glutamine-restricted glioblastoma. *Nat. Cell Biol.* **17,** 1556–1568 (2015).

10. Herranz, D. *et al.* Metabolic reprogramming induces resistance to anti-NOTCH1 therapies in T cell acute lymphoblastic leukemia. *Nat. Med.* **21,** 1182–1189 (2015).

11. Kahlert, U. D. *et al.* Alterations in cellular metabolome after pharmacological inhibition of Notch in glioblastoma cells. *Int. J. Cancer* **138,** 1246–1255 (2016).

12. Basak, N. P., Roy, A. & Banerjee, S. Alteration of Mitochondrial Proteome Due to Activation of Notch1 Signaling Pathway. *J. Biol. Chem.* **289,** 7320–7334 (2014).

13. Iggo, R. & Richard, E. Lentiviral transduction of mammary epithelial cells. *Methods Mol. Biol.* **1293,** 137–60 (2015).

14. Villar, V. H. *et al.* mTORC1 inhibition in cancer cells protects from glutaminolysis-mediated apoptosis during nutrient limitation. *Nat. Commun.* **8,** 14124 (2017).

15. Villar, V. H. & Durán, R. V. Glutamoptosis: A new cell death mechanism inhibited by autophagy during nutritional imbalance. *Autophagy* **13,** 1078–1079 (2017).

16. Van Nguyen, T. *et al.* Glutamine Triggers Acetylation-Dependent Degradation of Glutamine Synthetase via the Thalidomide Receptor Cereblon. *Mol. Cell* **61,** 809–820 (2016).

17. Tan, H. W. S., Sim, A. Y. L. & Long, Y. C. Glutamine metabolism regulates autophagy-dependent mTORC1 reactivation during amino acid starvation. *Nat. Commun.* **8,** 338 (2017).

18. Saxton, R. A. & Sabatini, D. M. mTOR Signaling in Growth, Metabolism, and Disease. *Cell* **169,** 361–371 (2017).

19. Weng, A. P. *et al.* Activating mutations of NOTCH1 in human T cell acute lymphoblastic leukemia. *Science* **306,** 269–71 (2004).

20. Purow, B. W. *et al.* Expression of Notch-1 and its ligands, Delta-like-1 and Jagged-1, is critical for glioma cell survival and proliferation. *Cancer Res.* **65,** 2353–63 (2005).

21. Sikandar, S. S. *et al.* NOTCH signaling is required for formation and self-renewal of tumor-initiating cells and for repression of secretory cell differentiation in colon cancer. *Cancer Res.* **70,** 1469–78 (2010).

22. Petronini, P. G., Urbani, S., Alfieri, R., Borghetti, A. F. & Guidotti, G. G. Cell

susceptibility to apoptosis by glutamine deprivation and rescue: survival and apoptotic death in cultured lymphoma-leukemia cell lines. *J. Cell. Physiol.* **169,** 175–85 (1996).

23. Weinberg, F. *et al.* Mitochondrial metabolism and ROS generation are essential for Kras-mediated tumorigenicity. *Proc. Natl. Acad. Sci. U. S. A.* **107,** 8788–93 (2010).

24. Abu Aboud, O. *et al.* Glutamine Addiction in Kidney Cancer Suppresses Oxidative Stress and Can Be Exploited for Real-Time Imaging. *Cancer Res.* **77,** 6746–6758 (2017).

25. Distasio, J. A., Salazar, A. M., Nadji, M. & Durden, D. L. Glutaminase-free asparaginase from vibrio succinogenes: an antilymphoma enzyme lacking hepatotoxicity. *Int. J. cancer* **30,** 343–7 (1982).

26. Villa, P., Corada, M. & Bartosek, I. L-asparaginase effects on inhibition of protein synthesis and lowering of the glutamine content in cultured rat hepatocytes. *Toxicol. Lett.* **32,** 235–41 (1986).

27. Avramis, V. I. *et al.* A randomized comparison of native Escherichia coli asparaginase and polyethylene glycol conjugated asparaginase for treatment of children with newly diagnosed standard-risk acute lymphoblastic leukemia: a Children's Cancer Group study. *Blood* **99,** 1986–94 (2002).

Figure Legends

Figure 1. Metabolomic analysis showed that glutamine was essential to sustain TCA cycle in T-ALL cells. Cutll1 cells were incubated either in the presence (+Q) or the absence (-Q) of glutamine for 24h and the content of glutaminolysis intermediates (glutamine, glutamate, and αKG) (**A**-**C**), TCA cycle intermediates (succinate, fumarate, malate, oxaloacetate, and citrate) (**D**-**H**), and TCA cycle-independent metabolites (threonine, serine, and choline) (**I**-**K**) was analysed by mass spectrometry. Graphs show mean values ±S.E.M. (n≥3). "ND" indicates values below the detection level.

Figure 2. Notch1 activation correlated with glutamine addiction in T-ALL cells. (**A**) Cutll1 and Jurkat cells were incubated in the absence of glutamine for the indicated times and cell number was determined using a cell counter. (**B**) Cutll1 and Jurkat cells were incubated either in the presence (+Q) or the absence (-Q) of glutamine during 72h. Then, cell death was estimated using a trypan blue assay. (**C**) Cutll1 and Jurkat cells were incubated in complete medium for 24h. Cell extracts were collected and levels of NICD, Hes1, c-myc, and actin were estimated by western blot. (**D**) The relative levels of NICD and cell death induction during glutamine restriction for 72h were estimated for 5 different T-ALL cell lines. The values were represented in the graph, and the linear regression was calculated and represented. (**E**) Cutll1 and Jurkat cells were incubated as in B. Cell extracts were collected and levels of cleaved PARP, cleaved caspase 3, cleaved caspase 8, and actin were estimated by western blot. (**F**-**G**) Cutll1 and Jurkat cells were incubated as in B. Then late apoptotic cell percentage was estimated (F) through flow cytometry analysis of propidium iodide (PI) and annexin V content (G). (**H**-**I**) Cutll1 cells were incubated either in the presence or the absence of glutamine (Q) and GSI during 72h as indicated. Cell extracts were collected and levels of NICD, cleaved PARP, cleaved caspase 3, and actin were estimated by western blot (H), while cell death was estimated using a trypan blue assay (I). Graphs show mean values ±S.E.M. (n≥3, * $p<0.05$).

Figure 3. Notch1 upregulation induced glutamine addiction in T-ALL cells. (**A**) RNA content of EV and NICD cells was extracted from cells cultivated in complete medium. NICD RNA level was estimated by quantitative PCR. (**B**) EV and NICD cells were incubated in the absence of glutamine for the indicated times and cell number was determined using a cell counter. (**C**) EV and NICD cells were incubated either in the presence (+Q) or the absence (-Q) of glutamine during 72h as indicated. Then, cell death was estimated using a trypan blue assay. (**D**) EV and NICD cells were incubated as in B. Then, cell death was estimated using a trypan blue assay. (**E**) EV and NICD cells were incubated as in C. Cell extracts were collected and levels of cleaved PARP, cleaved caspase 3, and actin were estimated by western blot. (**F**-**G**) EV and NICD cells were incubated as in C. Then late apoptotic cell percentage was estimated (F) through flow cytometry analysis of propidium iodide (PI) and annexin V content (G). Graphs show mean values ±S.E.M. (n≥3, * p<0.05).

Figure 4. Glutamine-free diet impaired Notch1-driven leukemia *in vivo*. (**A**) Schematic representation of the strategy followed for *in vivo* experiments. (**B**) Graph representing the evolution of body weight of mice fed with a glutamine-free diet for the indicated time. (**C**) Graph representing the levels of glutamine in the blood of mice implanted with either EV or NICD cells fed under complete (+Q) or glutamine-free (-Q) diet at the end of the treatment, as indicated. (**D**-**F**) Representative luminescence images (D) and luminescence quantification (E-F) of mice implanted with either EV or NICD cells fed under complete (+Q) or glutamine-free (-Q) diet at the end of the treatment, as indicated. (**G**) RNA content was obtained from cells extracted from the bone marrow of mice implanted with either EV or NICD cells, fed in the presence of glutamine. NICD RNA level was estimated by quantitative PCR. Graphs show mean values ±S.E.M. (n≥3, * p<0.05).

Figure 5. Notch1 modulated glutamine metabolizing enzymes in T-ALL cells. (**A**) EV and NICD cells were incubated either in a complete medium (fed) or in a medium without amino acids (starved) during 72h as indicated. Then, RNA content of these cells was extracted and GLS RNA level was estimated by quantitative PCR. (**B**) EV and NICD cells were incubated in a medium without amino acids for the indicated time. Cell extracts were collected and levels of GLS and actin were estimated by western blot. (**C**-**D**) Jurkat cells were incubated either in the presence or the absence of glutamine (Q) and MSO during 72h as indicated. Cell extracts were collected and cell death was estimated using a trypan blue assay (C), while levels of cleaved PARP, cleaved caspase 3, cleaved caspase 8, and actin were estimated by western blot (D). (**E**) Jurkat cells were infected with either a plasmid expressing a control non-targeting shRNA (shRNA Control), or a plasmid expressing a shRNA against GS (shRNA GS). Cell proliferation of infected cells in glutamine-free conditions was determined by quantifying cell number using a cell counter. (**F**) Cell were infected as in E, and then incubated either in the presence (+Q) or the absence (-Q) of glutamine. Cell extracts were collected and levels of cleaved PARP, cleaved caspase 3, GS, and actin were estimated by western blot. (**G**) Cutll1 cells infected with either an empty vector plasmid (pJS27) or with a plasmid overexpressing GS (pJS27-GS). Then, cells were incubated either in the presence (+Q) or the absence (-Q) of glutamine. Cell extracts were collected and levels of cleaved PARP, GS, and actin were estimated by western blot. (**H**) Cutll1 and Jurkat cells were incubated either in the presence (+Q) or the absence (-Q) of glutamine. Cell extracts were collected and levels of cleaved PARP, GS, and actin were estimated by western blot. (**I**) EV and NICD cells were incubated either in the presence (+Q) or the absence (-Q) of glutamine. Cell extracts were collected and levels of GS, and actin were estimated by western blot. Graphs show mean values ±S.E.M. (n≥3, * p<0.05).

Figure 6. mTORC1 inhibition synergizes with glutamine starvation to induce cell death in Notch1-positive T-ALL cells. (**A**) Cutll1 and Jurkat cells were incubated in the presence of glutamine (-Q) during 4h as indicated. Cell extracts were collected and levels of NICD, phospho-S6K, total S6K, phospho-4EBP1, and total 4EBP1 were estimated by western blot. (**B**) Cutll1 and Jurkat cells were incubated either in the presence or the absence of GSI 500nM as indicated. Cell extracts were collected and levels of NICD, phospho-S6, and total S6 were estimated by western blot. (**C**-**D**) Cutll1 (C) and Jurkat (D) cells were incubated either in the presence or the absence of rapamycin (RAP) in complete medium as indicated. Cell proliferation was determined by quantifying cell number using a cell counter. (**E**) EV and NICD cells were incubated in starving conditions in the absence of amino acids for 6 hours. Cell extracts were collected and levels of phospho-S6, total S6, phospho-4EBP1, and total 4EBP1 were estimated by western blot. (**F**) EV and NICD cells where incubated either in the presence or the absence of glutamine (Q) and rapamycin (RAP) during 72h as indicated. Cell extracts were collected and levels of phospho-S6, cleaved PARP, and actin were estimated by western blot. (**G**) Model of the control of glutamine metabolism and mTORC1 activation by Notch1 in leukemic cells.

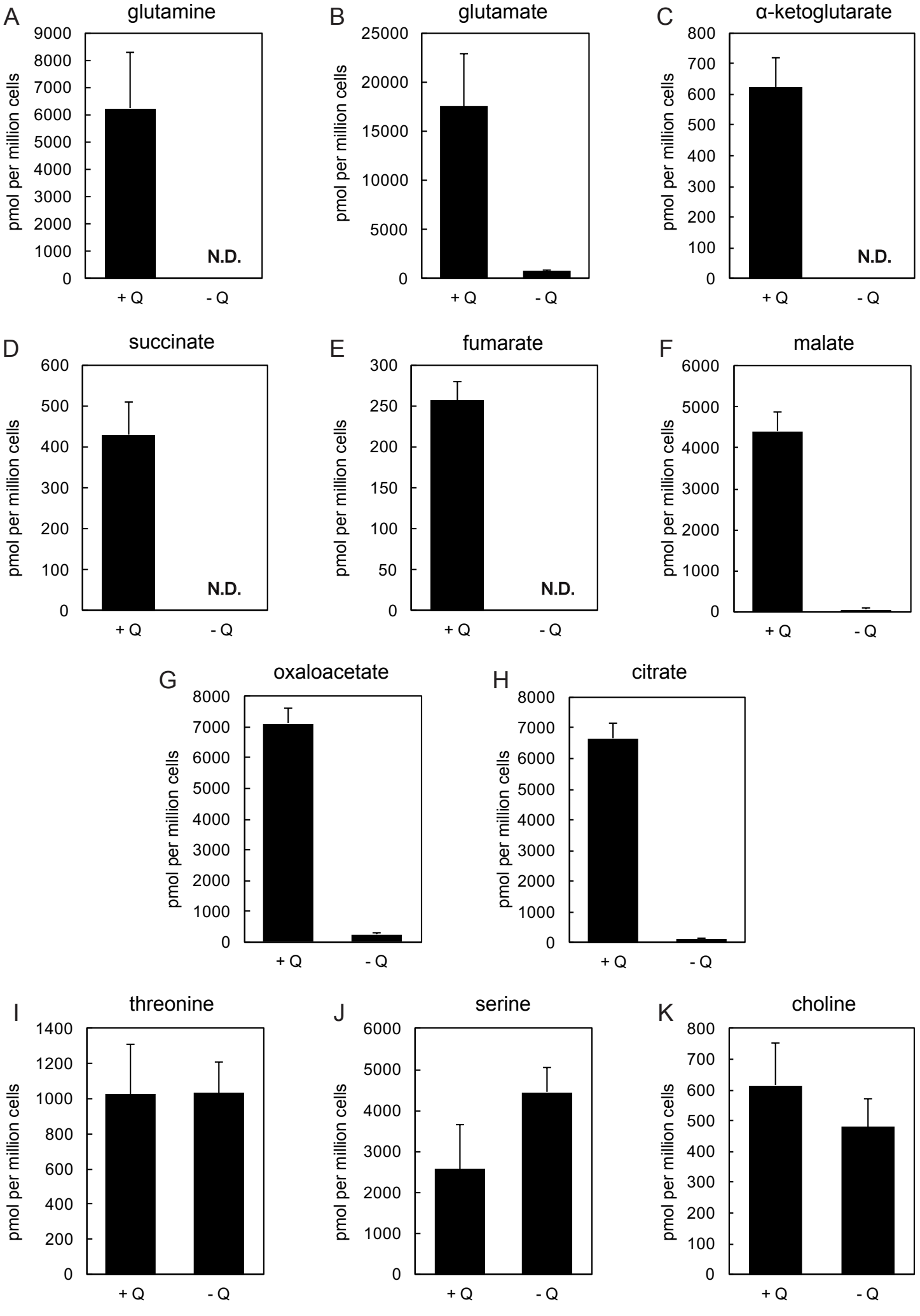
A
glutamine
pmol per million cells
9000
8000
7000
6000
5000
4000
3000
2000
1000
0
N.D.
+ Q
- Q
B
glutamate
pmol per million cells
25000
20000
15000
10000
5000
0
+ Q
- Q
C
α-ketoglutarate
pmol per million cells
800
700
600
500
400
300
200
100
0
N.D.
+ Q
- Q
D
succinate
pmol per million cells
600
500
400
300
200
100
0
N.D.
+ Q
- Q
E
fumarate
pmol per million cells
300
250
200
150
100
50
0
N.D.
+ Q
- Q
F
malate
pmol per million cells
6000
5000
4000
3000
2000
1000
0
+ Q
- Q
G
oxaloacetate
pmol per million cells
8000
7000
6000
5000
4000
3000
2000
1000
0
+ Q
- Q
H
citrate
pmol per million cells
8000
7000
6000
5000
4000
3000
2000
1000
0
+ Q
- Q
I
threonine
pmol per million cells
1400
1200
1000
800
600
400
200
0
+ Q
- Q
J
serine
pmol per million cells
6000
5000
4000
3000
2000
1000
0
+ Q
- Q
K
choline
pmol per million cells
800
700
600
500
400
300
200
100
0
+ Q
- Q

Figure 1

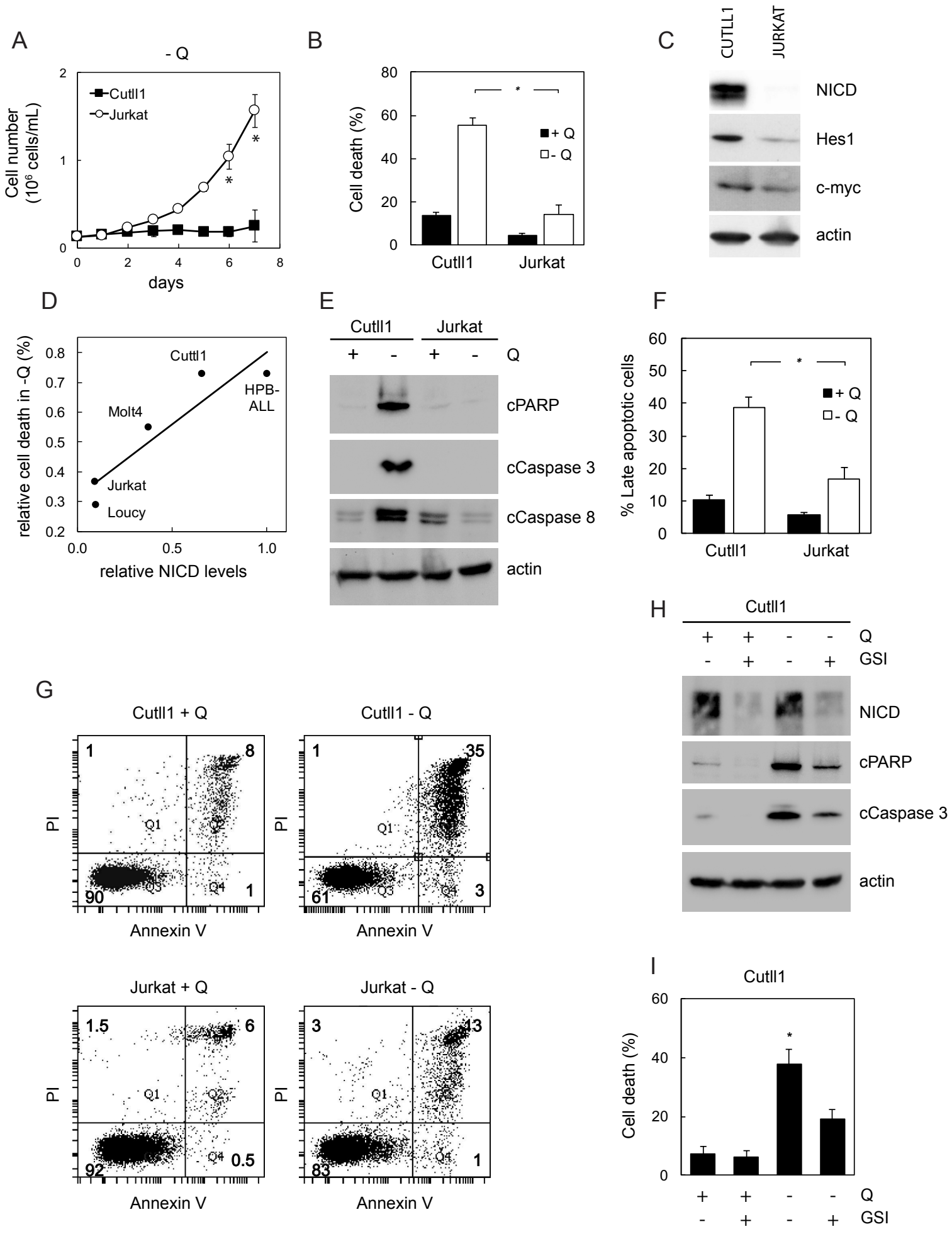
A
- Q
Cell number (10⁶ cells/mL)
Cutll1
Jurkat
days
B
Cell death (%)
+ Q
- Q
Cutll1
Jurkat
C
CUTLL1
JURKAT
NICD
Hes1
c-myc
actin
D
relative cell death in -Q (%)
relative NICD levels
Cuttl1
HPB-ALL
Molt4
Jurkat
Loucy
E
Cutll1
Jurkat
Q
cPARP
cCaspase 3
cCaspase 8
actin
F
% Late apoptotic cells
+ Q
- Q
Cutll1
Jurkat
G
Cutll1 + Q
Cutll1 - Q
Jurkat + Q
Jurkat - Q
PI
Annexin V
H
Cutll1
Q
GSI
NICD
cPARP
cCaspase 3
actin
I
Cutll1
Cell death (%)
Q
GSI

Figure 2

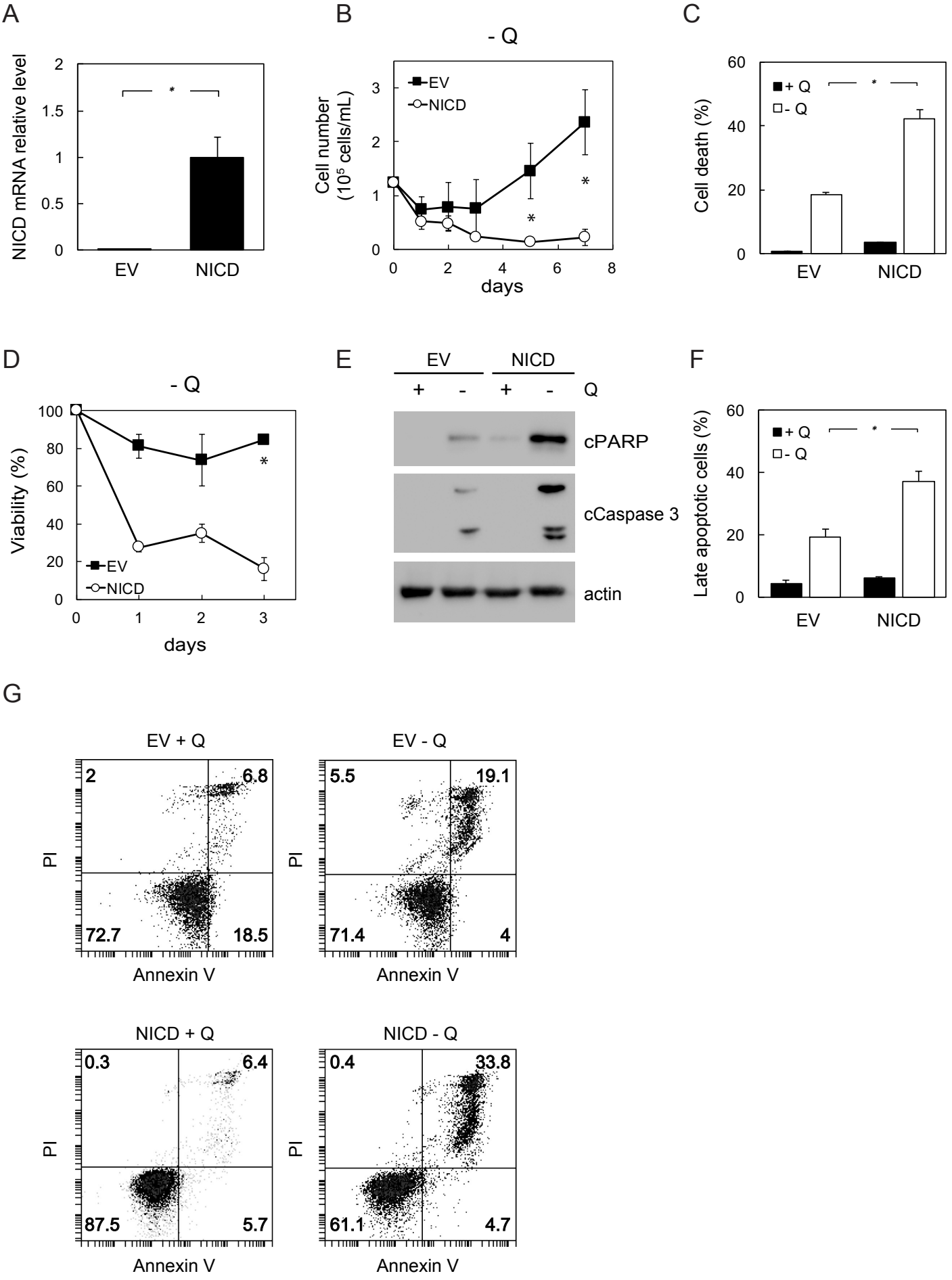
A
NICD mRNA relative level
2
1.5
1
0.5
0
*
EV
NICD
B
- Q
Cell number (10^5 cells/mL)
3
2
1
0
EV
NICD
*
*
0
2
4
6
8
days
C
Cell death (%)
60
40
20
0
+ Q
- Q
*
EV
NICD
D
- Q
Viability (%)
100
80
60
40
20
0
EV
NICD
*
0
1
2
3
days
E
EV
NICD
+
-
+
-
Q
cPARP
cCaspase 3
actin
F
Late apoptotic cells (%)
60
40
20
0
+ Q
- Q
*
EV
NICD
G
EV + Q
2
6.8
72.7
18.5
PI
Annexin V
EV - Q
5.5
19.1
71.4
4
PI
Annexin V
NICD + Q
0.3
6.4
87.5
5.7
PI
Annexin V
NICD - Q
0.4
33.8
61.1
4.7
PI
Annexin V

Figure 3

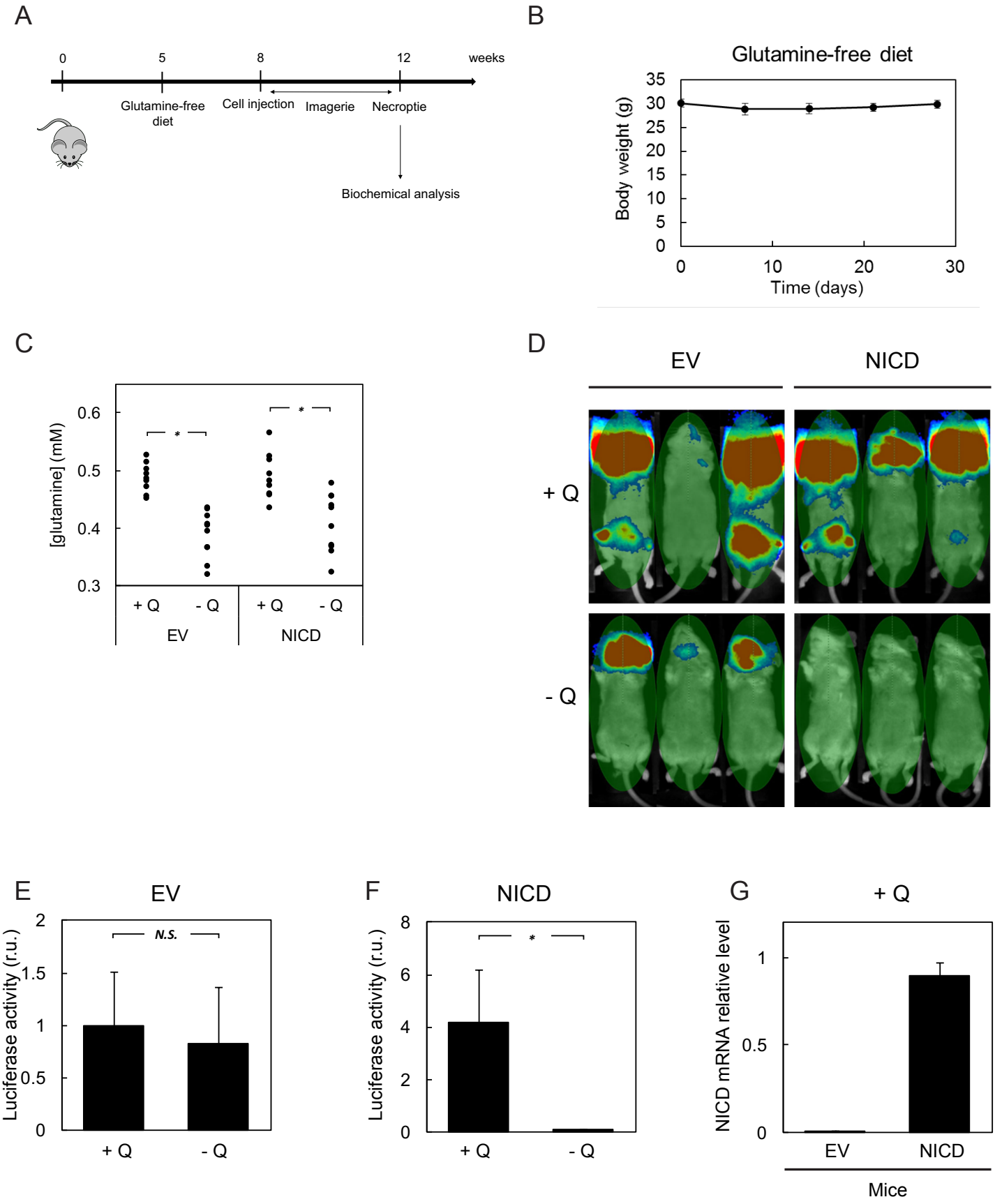
A
0
5
8
12
weeks
Glutamine-free diet
Cell injection
Imagerie
Necroptie
Biochemical analysis
B
Glutamine-free diet
Body weight (g)
Time (days)
C
[glutamine] (mM)
+ Q
- Q
+ Q
- Q
EV
NICD
D
EV
NICD
+ Q
- Q
E
EV
N.S.
Luciferase activity (r.u.)
+ Q
- Q
F
NICD
*
Luciferase activity (r.u.)
+ Q
- Q
G
+ Q
NICD mRNA relative level
EV
NICD
Mice

Figure 4

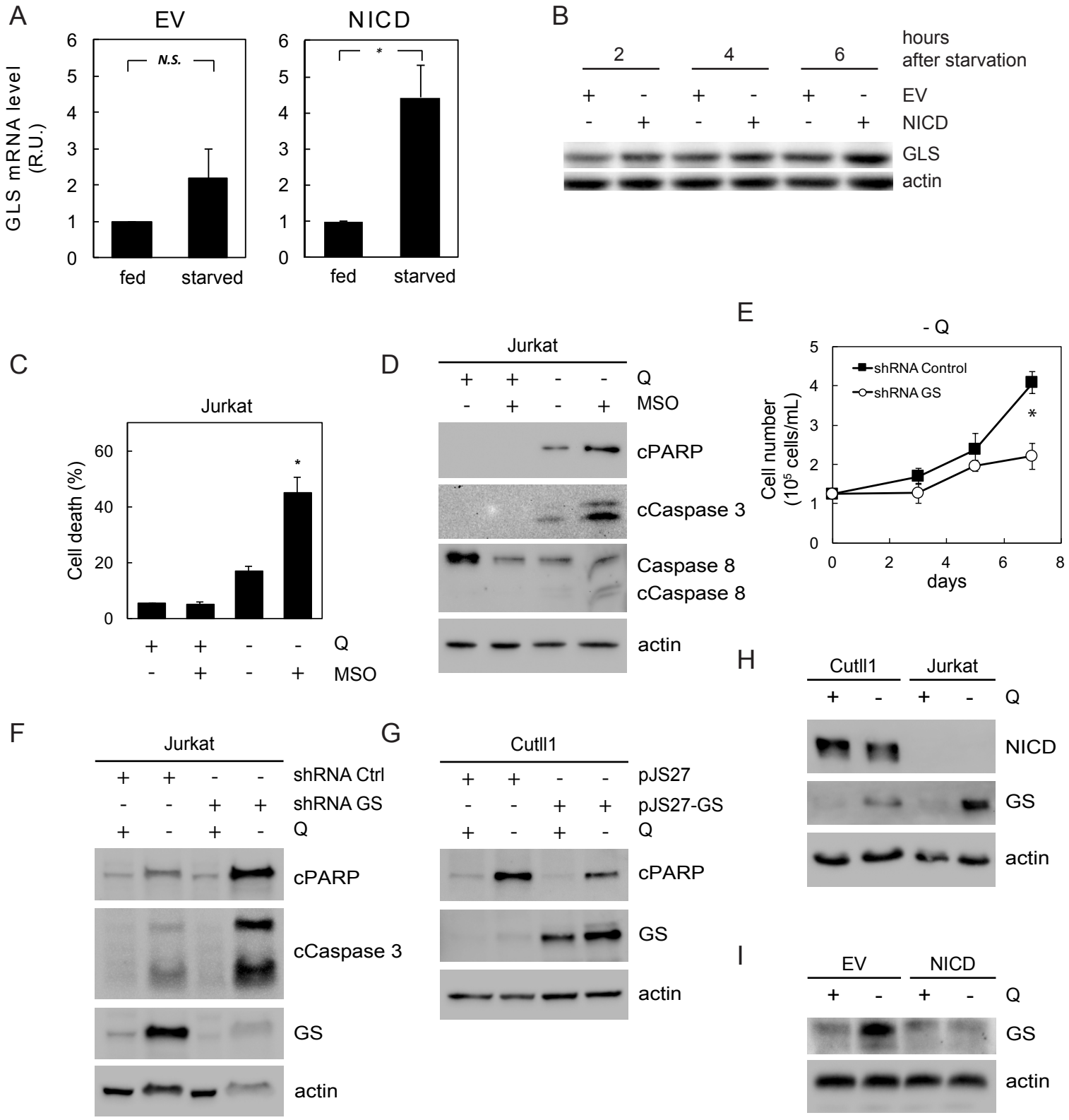
A
EV
NICD
GLS mRNA level (R.U.)
N.S.
*
fed
starved
B
hours after starvation
2
4
6
EV
NICD
GLS
actin
C
Jurkat
Cell death (%)
Q
MSO
D
Jurkat
Q
MSO
cPARP
cCaspase 3
Caspase 8
cCaspase 8
actin
E
- Q
shRNA Control
shRNA GS
Cell number (10^5 cells/mL)
days
F
Jurkat
shRNA Ctrl
shRNA GS
Q
cPARP
cCaspase 3
GS
actin
G
Cutll1
pJS27
pJS27-GS
Q
cPARP
GS
actin
H
Cutll1
Jurkat
Q
NICD
GS
actin
I
EV
NICD
Q
GS
actin

Figure 5

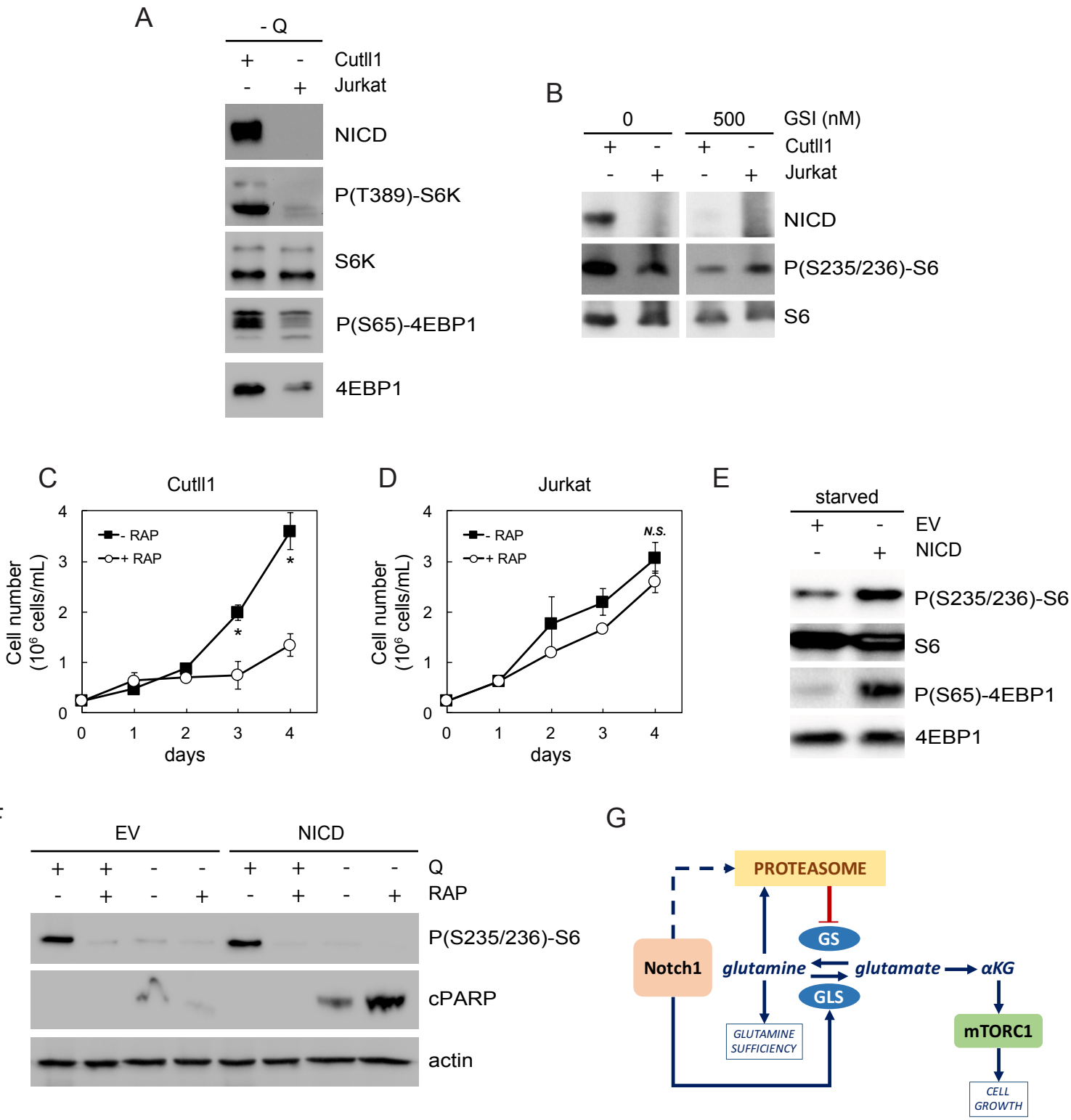
A
- Q
+ -
- +
Cutll1
Jurkat
NICD
P(T389)-S6K
S6K
P(S65)-4EBP1
4EBP1
B
0
500
GSI (nM)
+ - + -
Cutll1
- + - +
Jurkat
NICD
P(S235/236)-S6
S6
C
Cutll1
Cell number (10^6 cells/mL)
- RAP
+ RAP
days
D
Jurkat
N.S.
E
starved
+ -
EV
- +
NICD
P(S235/236)-S6
S6
P(S65)-4EBP1
4EBP1
F
EV
NICD
+ + - - + + - -
Q
- + - + - + - +
RAP
P(S235/236)-S6
cPARP
actin
G
PROTEASOME
GS
Notch1
glutamine
glutamate
αKG
GLS
GLUTAMINE SUFFICIENCY
mTORC1
CELL GROWTH

Figure 6

Supplementary Information

Notch1 induces glutamine addiction in acute lymphoblastic leukemia

Tra Ly Nguyen, Silvia Terés, Marie-Julie Nokin, Mercedes Tomé, Oriane Galmar, Jean-Max Pasquet, Benoit Rousseau, Juan Manuel Falcon, Elodie Richard, Hamid-Reza Rezvani, Muriel Priault, Marion Bouchecareilh, Isabelle Redonnet, Patricia Fuentes, Maria Luisa Toribio, Abdel-Majid Khatib, Pierre Soubeyran and Raúl V. Durán

Supplementary Figure legends

Supplementary Figure 1. Metabolomic analysis showed that glutamine was essential to sustain TCA cycle in T-ALL cells. Jurkat cells were incubated either in the presence (+Q) or the absence (-Q) of glutamine for 24h and the content of glutaminolysis intermediates (glutamine, and glutamate) (**A**-**B**), TCA cycle intermediates (succinate, fumarate, malate, oxaloacetate, and citrate) (**C**-**G**), and TCA cycle-independent metabolites (threonine, serine, and choline) (**H**-**J**) was analysed by mass spectrometry. Graphs show mean values ±S.E.M. (n≥3). “ND” indicates values below the detection level.

Supplementary Figure 2. Notch1 activation correlated with glutamine addiction in T-ALL cells. (**A**) Cutll1 and Jurkat cells were incubated in the presence of glutamine for the indicated times and cell number was determined using a cell counter. (**B**) Cutll1 and Jurkat cells were incubated either in the presence (+Q) or the absence (-Q) of glutamine for the indicated times. Then, cell viability was estimated using a trypan blue assay. (**C**) Cutll1, HBP-ALL, Molt4, Jurkat, and Loucy cells were incubated in complete medium for 24h. Cell extracts were collected and levels of NICD and actin were estimated by western blot. (**D**) Cutll1, HBP-ALL, Molt4, Jurkat and Loucy cells in the absence of glutamine for the indicated times and cell number was determined using a cell counter. (**E**-**F**) Cutll1 cells were where incubated either in the presence or the absence of glutamine (Q) and zVAD during 72h as

indicated. Cell extracts were collected and levels of cleaved PARP, cleaved caspase 3, cleaved caspase 8, and actin were estimated by western blot (E), while cell death was estimated using a trypan blue assay (F). (**G**) Cutll1, HBP-ALL, Molt4, Jurkat, and Loucy cells were incubated either in the presence (+Q) or the absence (-Q) of glutamine for 72h. Cell extracts were collected and levels of cleaved PARP and actin were estimated by western blot. (**H**) HBP-ALL, Molt4, and Loucy cells were incubated either in the presence (+Q) or the absence (-Q) of glutamine for 72h. Then late apoptotic cell percentage was estimated through flow cytometry analysis of propidium iodide (PI) and annexin V content. (**I**) Cutll1 cells were incubated in the presence or the absence of GSI during 24h in complete medium as indicated. RNA content of cells was extracted and Hes1 and Hey1 RNA level was estimated by quantitative PCR. (**J**) Cutll1 and Jurkat cells were incubated either in the presence or the absence of glutamine for 24h as indicated. RNA content of cells was extracted and RNA levels of ERN1, DDIT3, PPP1R15A, CEBPB, and DNAJB9 were estimated by quantitative PCR. Graphs show mean values ±S.E.M. (n≥3, * p<0.05).

Supplementary Figure 3. Notch1 upregulation induced glutamine addiction in T-ALL cells. (**A**) GFP content in EV and NICD cells was analyzed by flow cytometry. (**B**) Luciferase-dependent luminescence was estimated in EV (left panel) and NICD (right panel) using a luminometer after infection of parental Jurkat cells. (**C**) RNA content of EV and NICD cells was extracted from cells cultivated in complete medium. c-myc, Hes1, and Hey1 RNA levels were estimated by quantitative PCR. (**D**) EV and NICD cells were incubated in the presence of glutamine for the indicated times and cell number was determined using a cell counter. Graphs show mean values ±S.E.M. (n≥3, * p<0.05).

Supplementary Figure 4. Notch1 modulated glutamine metabolizing enzymes in T-ALL cells. (**A**) EV and NICD cells were incubated in a complete medium for 24h. Cell extracts were collected and levels of GLS and actin were estimated by western blot. (**B**) EV and NICD cells were incubated with radiolabeled ^{3}H-glutamine during 15 minutes. Cell content

was extracted and radiolabeled glutamine uptake was measured using a scintillation counter. (**C**) Cutll1 and Jurkat cells were incubated either in the presence or the absence of GSI for 24h. Then glutamine incorporation was determined as in B. (**D**-**E**) Cutll1 cells were incubated either in the presence or the absence of glutamine (Q) and BPTES during 72h as indicated. Cell death was estimated using a trypan blue assay (**D**), while cell extracts were collected and levels of, cleaved PARP, cleaved caspase 3, cleaved caspase 8, and actin were estimated by western blot (**E**). (**F**) Cutll1, HBP-ALL, Molt4, Jurkat, and Loucy cells were incubated either in the presence (+Q) or the absence (-Q) of glutamine for 72h. Cell extracts were collected and levels NICD, GS, and actin were estimated by western blot. (**G**) Cutll1 and Jurkat cells were incubated either in the presence (+Q) or the absence (-Q) of glutamine. RNA content was extracted and GS RNA level was estimated by quantitative PCR. (**H**) Jurkat cells where incubated either in the presence or the absence of glutamine (Q) and MG132 during 4h as indicated. Cell extracts were collected and levels of GS and actin were estimated by western blot. (**I**) Molt4 cells where incubated either in the presence or the absence of glutamine (Q) and GSI during 72h as indicated. Cell extracts were collected and levels of NICD, GS, and actin were estimated by western blot.

Supplementary Figure 5. mTORC1 inhibition synergizes with glutamine starvation to induce cell death in Notch1-positive T-ALL cells. (**A**) Cutll1 and Jurkat cells were incubated in a complete medium for 24h. Cell extracts were collected and levels of phospho-S6K, total S6K, phospho-AKT, and total AKT were estimated by western blot. (**B**) EV and NICD cells were incubated in a complete medium for 24h.Cell extracts were collected and levels of phospho-S6, total S6, phospho-4EBP1, and total 4EBP1 were estimated by western blot. (**C**) Cutll1 and Jurkat cells where incubated either in the presence or the absence of glutamine (Q) and rapamycin (RAP) during 72h as indicated. Cell extracts were collected and levels of NICD, cleaved PARP, and actin were estimated by western blot.

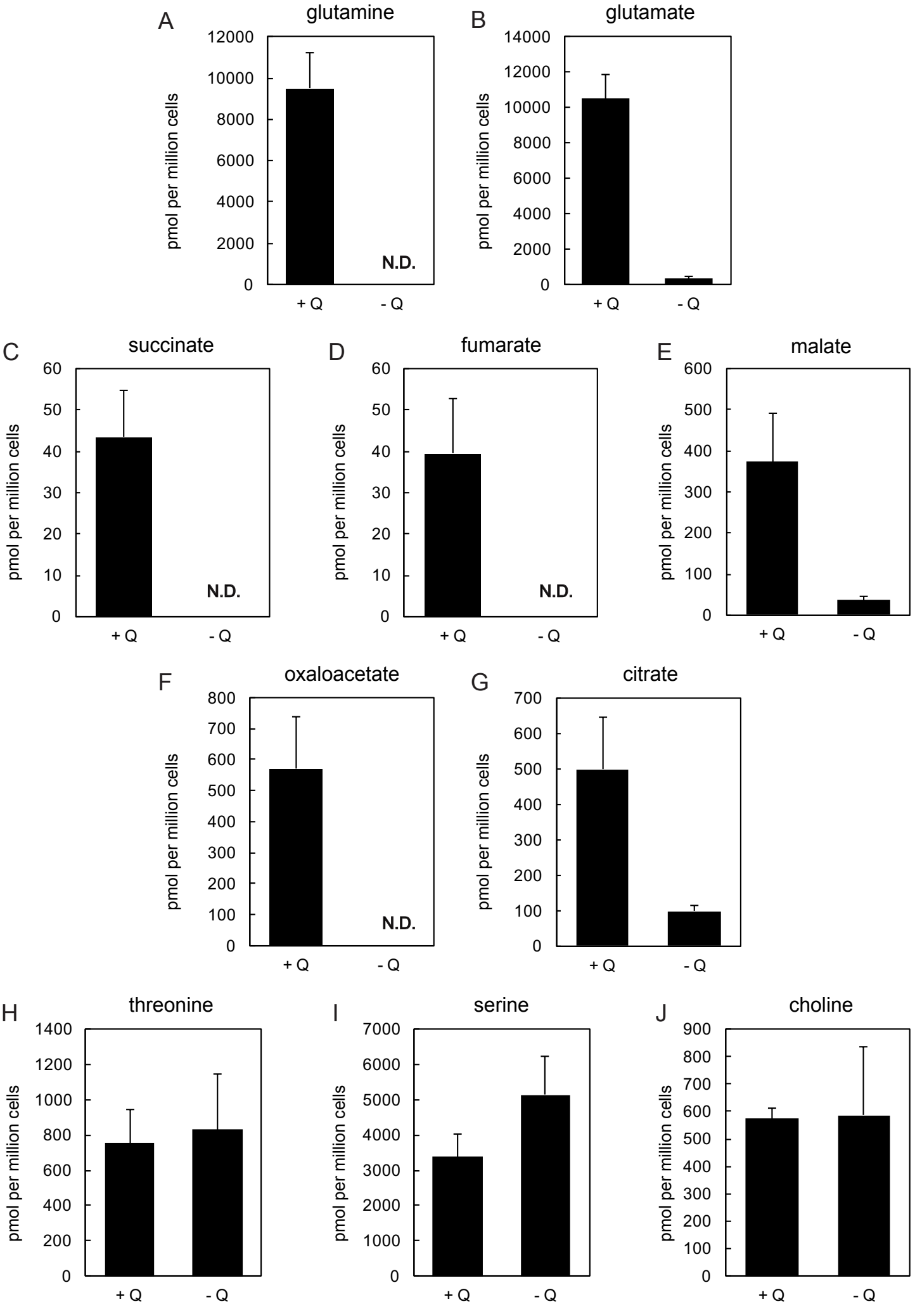

Supplementary Figure 1

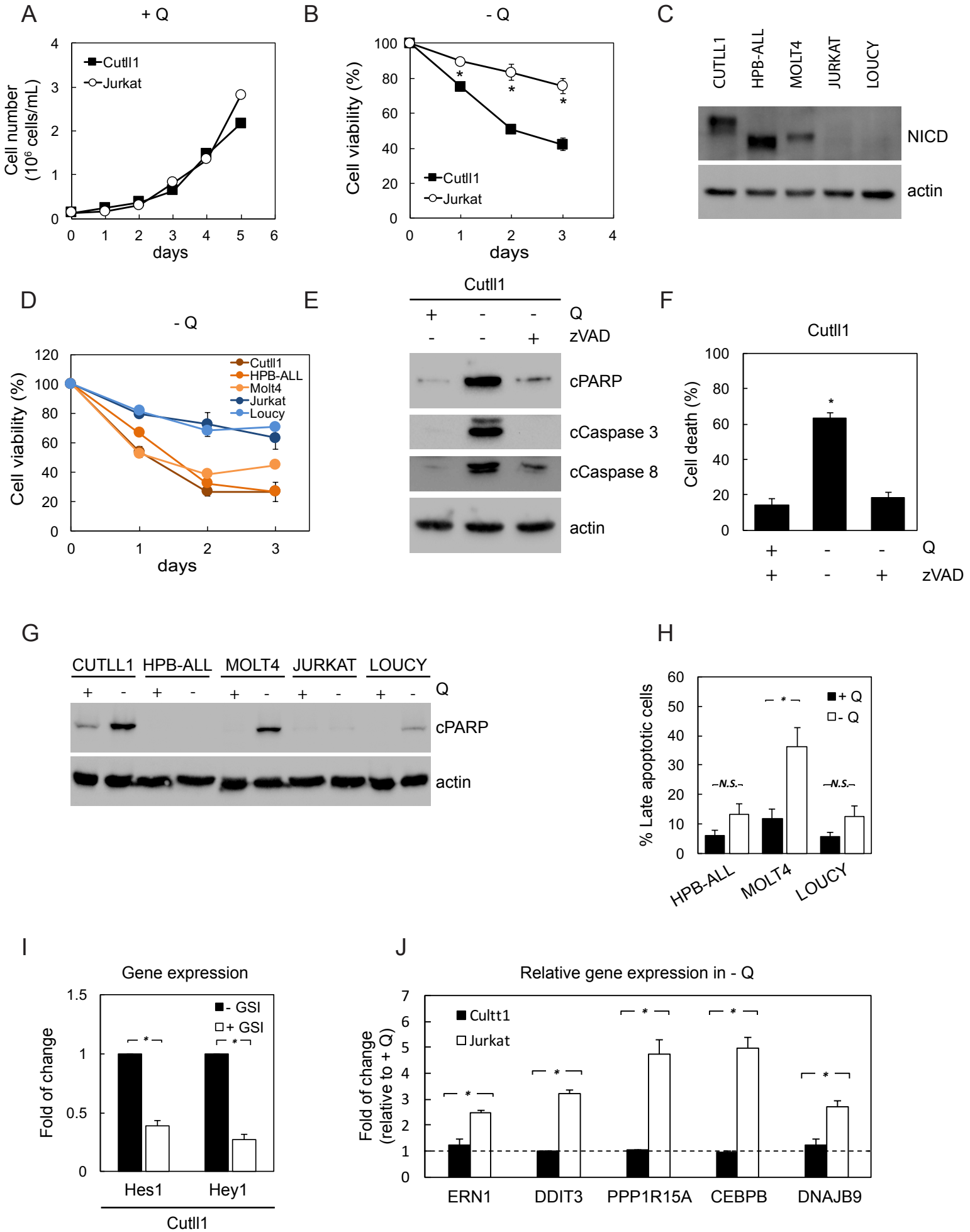

Supplementary Figure 2

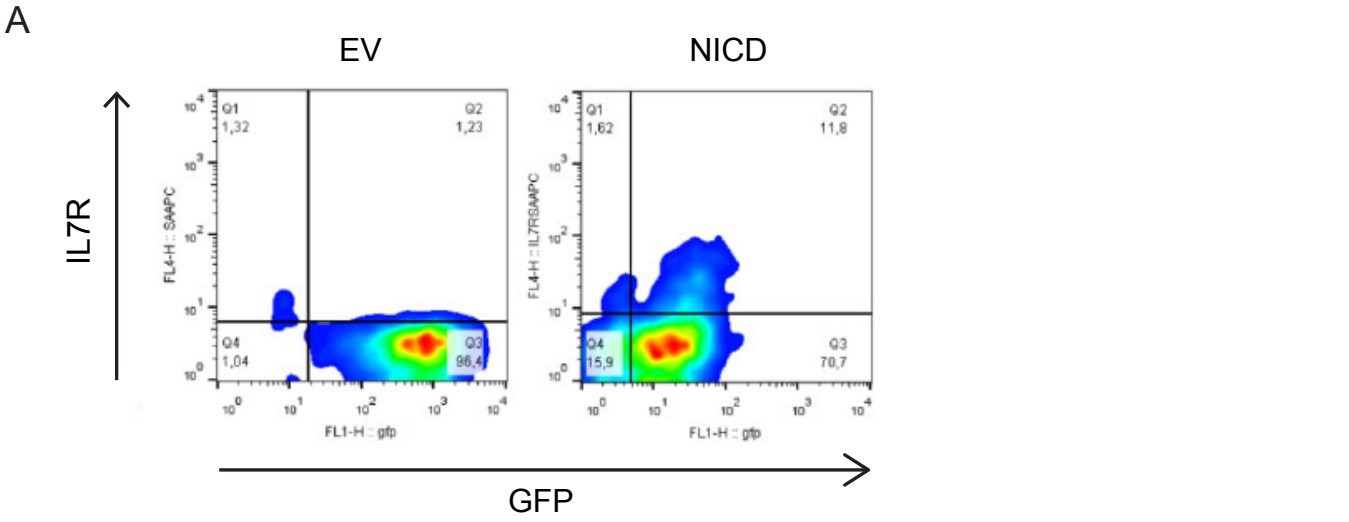

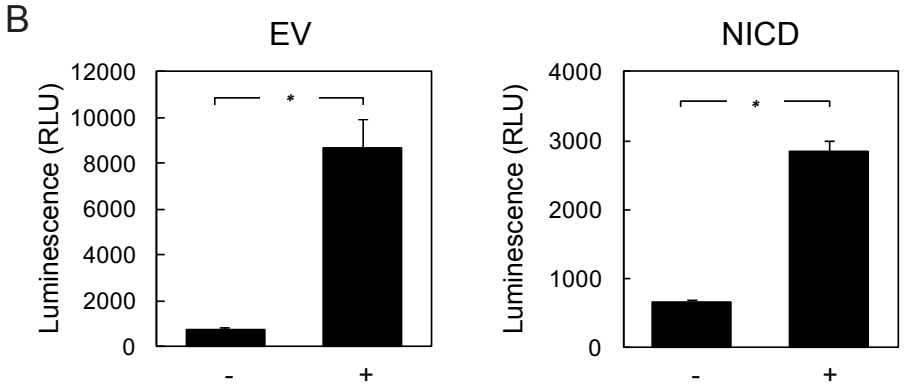

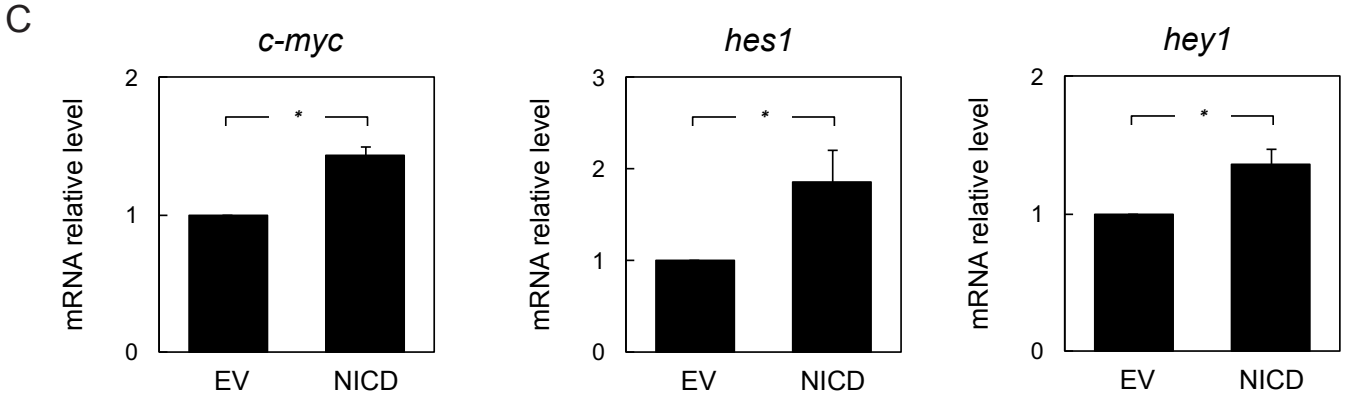

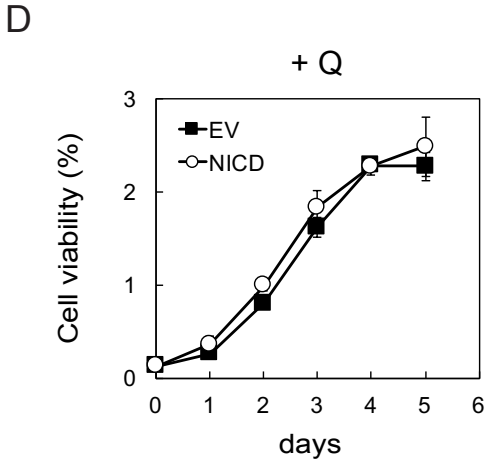

Supplementary Figure 3

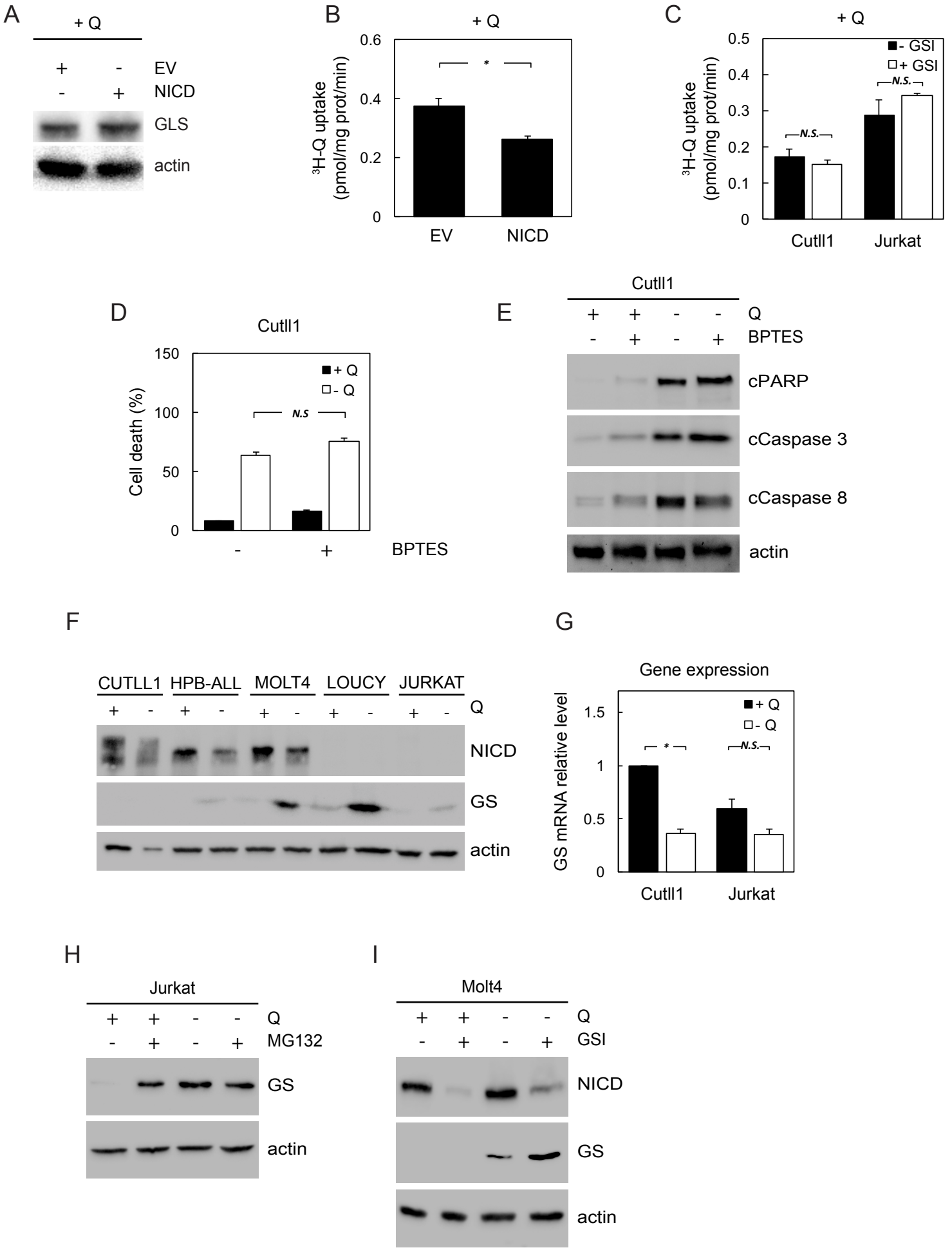

Supplementary Figure 4

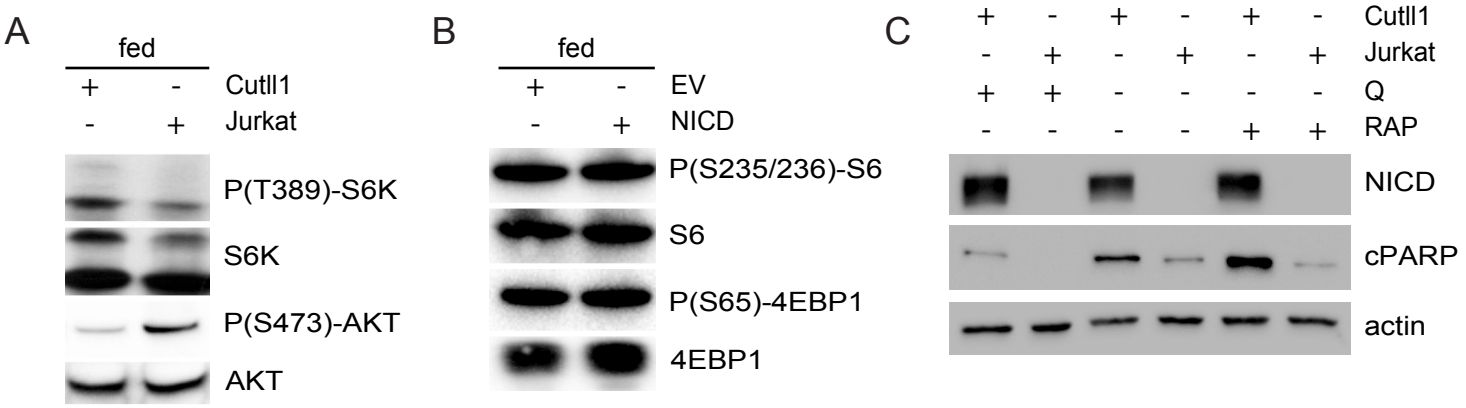

Supplementary Figure 5

Supplementary Table 1.List of primers used for RT-qPCR

Gene	Forward primer	Reverse primer
Notch1	AACAGCGAGGAAGAGGAGGA	GCATCAGAGCGTGAGTAGCG
NICD	AGTCCTCC GACAGACTGAGT	TCTTCTTGCTGGCCTCAGAC
Hes1	AGGCTGGAGAGGCGGCTAAG	TGGAAGGTGACACTGCGTTGG
Hey1	TGAGCTGAGAAGGCTGGTACCCA	TGCGCGTCAAAGTAACCTTTCCC
c-myc	CTTCTCTCCGTCCTCGGATTCT	GAAGGTGATCCAGACTCTGACCTT
GLS	TGGTGGCCTCAGGTGAAAAT	CCAAGCTAGGTAACAGACCCTGTT
GDH	CTCCAGACATGAGCACAGGTGA	CCAGTAGCAGAGATGCGTCCAT
GS	TCATCTTGCATCGTGTGTGTG	CTTCAGACCATTCTCCTCCCG
RPL29	GGCTATCAAGGCCCTCGTAAA	CGAGCTTGCGGCTGACA
GAPDH	CCATCTTCCAGGAGCGAGATC	GCCTTCTCCATGGTGGTGAA

SUMMARY & PERSPECTIVES

The works of this thesis evaluates new mechanisms to target the connection of metabolism with cell signaling, particularly mTORC1 and Notch1 signaling, in different cancer models. Due to the modest results of the current treatments targeting these two signaling pathways in cancer patients, new strategies need to be developed for future anti-cancer therapy. In one hand, we showed a new class of mTORC1 inhibitor, that displaces PA from the active site of mTOR, and that targets specifically cancer cells. Our results make emphasis in the important role played by lipid messenger PA in the control of mTORC1 activity. The dissociation of the PA-mTOR interaction showed a pronounced phenotype at the cell physiology level, resulting in cell death. In the other hand, Notch1 upregulation in T-ALL induces glutamine addiction through caspase-dependent activation of apoptosis. Notch1 induces the proteasome-mediated degradation of GS upon glutamine withdrawal, thus inhibiting glutamine production, necessary for cell survival. In both cases, interfering with link between metabolism (lipidic or amino acidic) and cell signlaing (mTOR or Notch1, respectively) resulted in the induction of cell death specifically on cancer cells.

Additional investigations will elucidate the mechanism of cell death induced by these metabolic challenges in cells with high mTORC1 or Notch1 signaling. In the case of mTORC1 inhibition using ICSN3250, we observed a caspase-independent mechanism, but yet how mTORC1 inhibition in these conditions (and not using other inhibitors) leads to cell death remain to be clarified. As mTORC1 integration operates at the lysosomal surface, it could be contemplated that the disruption of the PA-mTOR interaction might lead to a collapse in the lysosomal surface, causing lysosome-dependent cell death. In the case of Notch1-induced glutamine addiction, the observed

cell death is caspase-dependent. How GS degradation induce caspase cascade activation was not determined in this work. Notch1 signaling could mediate cell death upon glutamine starvation in a c-myc dependent manner, as described for other cancer models[226,282]. The absence specifically of glutamine in the presence of other cell growth inducers could result in the collapse of DNA synthesis during replication or even during transcription, as glutamine is a mains source for purine and pyrimidine *de novo* synthesis. Investigating the purine and pyrimidine levels/synthesis upon glutamine withdrawal in Notch1-driven leukemia could help to test this possibility.

Clarifying the role of mTORC1 in the glutamine dependence of Notch1-driven lymphoblastic leukemia appears as a major action line for future researches. We observed that the inhibition of mTORC1 enhances cell death upon glutamine withdrawal, underscoring the role of mTORC1 Notch1-induced glutamine addiction. Indeed, our work showed that mTORC1 inhibition blocks cell proliferation preferentially in Notch1-positive T-ALL. Although excluded from this work, we observed that the treatment of Notch1-positive cells with the mTORC1 activator DMKG, a cell-permeable analogue of α-ketoglutarate, reversed the effect of glutamine depletion and inhibited apoptotic cell death (data not shown). Genetic models of mTORC1 activations (upregulating Rheb or using overactive mTOR mutants) could help to further confirm the role of mTORC1 in the glutamine addiction phenotype. In the role of mTORC1 in Notch1-driven leukemia is confirmed, an attractive option could be to treat Notch1 positive-cells with ICSN3250, a compound with increased cytotoxicity in cancer cells.

Whether Notch1-induced glutamine addiction is a specific phenotype of T-ALL or, by contrast, it can be applied to other types of cancer, remains an open question. Notch1 is not only playing a role in T-ALL progression, but its deregulation occurs also in other types of cancer, including glioblastoma. Directly targeting Notch1 is an

effective therapeutic strategy in this type of cancer[327,442]. Moreover, glioblastoma avidly consume glutamine, showing a high addiction to this amino acid, and GS expression associates with poor prognosis in glioblastoma patients[232,274,283]. Still, no works has identified a connection between Notch1 and glutamine metabolism in glioblastoma cells.

Finally, as mTORC1 is not the only protein activated by PA, other additional mechanisms or pathways could mediate ICSN3250-induced cytotoxicity. Nevertheless, results from our work showed that mTORC1 re-activation by TSC2 inhibition is sufficient to rescue the cell viability, indicating that mTORC1 inhibition is at the basis of ICSN3250-induced cytotoxicity. Considering that PA is also required for the stabilization of mTORC2 complex[164], it was envisioned that ICSN3250 could inhibit mTORC2 in addition to mTORC1. However, our results showed that ICSN3250 does not inhibit but on the contrary, it increases mTORC2 activity. This increase would be in agreement with a specific inhibition of mTORC1 pathway, and the subsequent release of the negative feedback loop that leads to PI3K/mTORC2 re-activation. The absence of ICSN3250-mediated mTORC2 inhibition could be explained by a higher affinity of PA to bind to mTORC2 more strongly than to mTORC1[164]. Still, other PA-dependent pathways with implications in cancer biology, such as the LKB1/AMPK pathway[165], could be affected by ICSN3250, contributing to the potential anti-cancer activity of this compound.

Overall, this study has shown two clear examples targeting the link between cell metabolism and cell signaling to specifically eliminate cancer cells. Signal transduction reprograms cellular metabolism in order to fulfil the anabolic and energetic requirements of tumors, supporting cell growth and proliferation. However, the relationship between cellular signaling and metabolism is not unidirectional. By sensing

levels of intracellular metabolites which affect the status of key metabolic pathways, cells can exert a feedback control on their signaling networks. These mechanisms allow cells to growth and proliferate in agreement with their metabolic states and in function of the availability of the extracellular environment. Understanding the detailed molecular mechanism of this connection will help to understand how the viability of cancer cells is determined in response to variations in environmental nutrient levels. Nutrient restrictive-based therapy, as ICSN3250, glutamine depletion, or L-asparaginase, will be further developed to target the connection between metabolic states and cell signaling in cancer.

REFERENCES

1. Heitman, J., Movva, N. R. & Hall, M. N. Targets for cell cycle arrest by the immunosuppressant rapamycin in yeast. *Science* **253,** 905–9 (1991).
2. Jacinto, E. *et al.* Mammalian TOR complex 2 controls the actin cytoskeleton and is rapamycin insensitive. *Nat. Cell Biol.* **6,** 1122–1128 (2004).
3. Saxton, R. A. & Sabatini, D. M. mTOR Signaling in Growth, Metabolism, and Disease. *Cell* **169,** 361–371 (2017).
4. Cafferkey, R. *et al.* Dominant missense mutations in a novel yeast protein related to mammalian phosphatidylinositol 3-kinase and VPS34 abrogate rapamycin cytotoxicity. *Mol. Cell. Biol.* **13,** 6012–23 (1993).
5. Kunz, J. *et al.* Target of rapamycin in yeast, TOR2, is an essential phosphatidylinositol kinase homolog required for G1 progression. *Cell* **73,** 585–96 (1993).
6. Schalm, S. S. & Blenis, J. Identification of a conserved motif required for mTOR signaling. *Curr. Biol.* **12,** 632–9 (2002).
7. Schalm, S. S., Fingar, D. C., Sabatini, D. M. & Blenis, J. TOS motif-mediated raptor binding regulates 4E-BP1 multisite phosphorylation and function. *Curr. Biol.* **13,** 797–806 (2003).
8. Peterson, T. R. *et al.* DEPTOR is an mTOR inhibitor frequently overexpressed in multiple myeloma cells and required for their survival. *Cell* **137,** 873–86 (2009).
9. Wang, L., Harris, T. E., Roth, R. A. & Lawrence, J. C. PRAS40 regulates mTORC1 kinase activity by functioning as a direct inhibitor of substrate binding. *J. Biol. Chem.* **282,** 20036–44 (2007).
10. Guertin, D. A. *et al.* Ablation in mice of the mTORC components raptor, rictor, or mLST8 reveals that mTORC2 is required for signaling to Akt-FOXO and PKCalpha, but not S6K1. *Dev. Cell* **11,** 859–71 (2006).
11. Aylett, C. H. S. *et al.* Architecture of human mTOR complex 1. *Science* **351,** 48–52 (2016).
12. Baretić, D., Berndt, A., Ohashi, Y., Johnson, C. M. & Williams, R. L. Tor forms a dimer through an N-terminal helical solenoid with a complex topology. *Nat. Commun.* **7,** 11016 (2016).
13. Yip, C. K., Murata, K., Walz, T., Sabatini, D. M. & Kang, S. A. Structure of the human mTOR complex I and its implications for rapamycin inhibition. *Mol. Cell* **38,** 768–74 (2010).
14. Yang, H. *et al.* mTOR kinase structure, mechanism and regulation. *Nature* **497,**

217–23 (2013).

15. Barbet, N. C. *et al.* TOR controls translation initiation and early G1 progression in yeast. *Mol. Biol. Cell* **7,** 25–42 (1996).
16. Burnett, P. E., Barrow, R. K., Cohen, N. A., Snyder, S. H. & Sabatini, D. M. RAFT1 phosphorylation of the translational regulators p70 S6 kinase and 4E-BP1. *Proc. Natl. Acad. Sci. U. S. A.* **95,** 1432–7 (1998).
17. Fenton, T. R. & Gout, I. T. Functions and regulation of the 70kDa ribosomal S6 kinases. *Int. J. Biochem. Cell Biol.* **43,** 47–59 (2011).
18. Meyuhas, O. & Dreazen, A. Ribosomal protein S6 kinase from TOP mRNAs to cell size. *Prog. Mol. Biol. Transl. Sci.* **90,** 109–53 (2009).
19. Holz, M. K., Ballif, B. A., Gygi, S. P. & Blenis, J. mTOR and S6K1 mediate assembly of the translation preinitiation complex through dynamic protein interchange and ordered phosphorylation events. *Cell* **123,** 569–80 (2005).
20. Alessi, D. R., Kozlowski, M. T., Weng, Q. P., Morrice, N. & Avruch, J. 3-Phosphoinositide-dependent protein kinase 1 (PDK1) phosphorylates and activates the p70 S6 kinase in vivo and in vitro. *Curr. Biol.* **8,** 69–81 (1998).
21. Pullen, N. *et al.* Phosphorylation and activation of p70s6k by PDK1. *Science* **279,** 707–10 (1998).
22. Pende, M. *et al.* S6K1(-/-)/S6K2(-/-) mice exhibit perinatal lethality and rapamycin-sensitive 5'-terminal oligopyrimidine mRNA translation and reveal a mitogen-activated protein kinase-dependent S6 kinase pathway. *Mol. Cell. Biol.* **24,** 3112–24 (2004).
23. Thomas, G., Martin-Pérez, J., Siegmann, M. & Otto, A. M. The effect of serum, EGF, PGF2 alpha and insulin on S6 phosphorylation and the initiation of protein and DNA synthesis. *Cell* **30,** 235–42 (1982).
24. Raught, B. *et al.* Phosphorylation of eucaryotic translation initiation factor 4B Ser422 is modulated by S6 kinases. *EMBO J.* **23,** 1761–9 (2004).
25. Shahbazian, D. *et al.* The mTOR/PI3K and MAPK pathways converge on eIF4B to control its phosphorylation and activity. *EMBO J.* **25,** 2781–91 (2006).
26. Dorrello, N. V. *et al.* S6K1- and betaTRCP-mediated degradation of PDCD4 promotes protein translation and cell growth. *Science* **314,** 467–71 (2006).
27. Beretta, L., Gingras, A. C., Svitkin, Y. V, Hall, M. N. & Sonenberg, N. Rapamycin blocks the phosphorylation of 4E-BP1 and inhibits cap-dependent initiation of translation. *EMBO J.* **15,** 658–64 (1996).

28. Düvel, K. *et al.* Activation of a metabolic gene regulatory network downstream of mTOR complex 1. *Mol. Cell* **39,** 171–83 (2010).
29. Porstmann, T. *et al.* SREBP activity is regulated by mTORC1 and contributes to Akt-dependent cell growth. *Cell Metab.* **8,** 224–36 (2008).
30. Wang, C.-Y. *et al.* Tsc2, a positional candidate gene underlying a quantitative trait locus for hepatic steatosis. *J. Lipid Res.* **53,** 1493–501 (2012).
31. Yecies, J. L. *et al.* Akt stimulates hepatic SREBP1c and lipogenesis through parallel mTORC1-dependent and independent pathways. *Cell Metab.* **14,** 21–32 (2011).
32. Owen, J. L. *et al.* Insulin stimulation of SREBP-1c processing in transgenic rat hepatocytes requires p70 S6-kinase. *Proc. Natl. Acad. Sci. U. S. A.* **109,** 16184–9 (2012).
33. Han, J. *et al.* The CREB coactivator CRTC2 controls hepatic lipid metabolism by regulating SREBP1. *Nature* **524,** 243–6 (2015).
34. Peterson, T. R. *et al.* mTOR complex 1 regulates lipin 1 localization to control the SREBP pathway. *Cell* **146,** 408–20 (2011).
35. Ponugoti, B. *et al.* SIRT1 deacetylates and inhibits SREBP-1C activity in regulation of hepatic lipid metabolism. *J. Biol. Chem.* **285,** 33959–70 (2010).
36. Wan, W. *et al.* mTORC1 Phosphorylates Acetyltransferase p300 to Regulate Autophagy and Lipogenesis. *Mol. Cell* **68,** 323–335.e6 (2017).
37. Lefterova, M. I., Haakonsson, A. K., Lazar, M. A. & Mandrup, S. PPARγ and the global map of adipogenesis and beyond. *Trends Endocrinol. Metab.* **25,** 293–302 (2014).
38. Le Bacquer, O. *et al.* Elevated sensitivity to diet-induced obesity and insulin resistance in mice lacking 4E-BP1 and 4E-BP2. *J. Clin. Invest.* **117,** 387–96 (2007).
39. Kim, J. B., Wright, H. M., Wright, M. & Spiegelman, B. M. ADD1/SREBP1 activates PPARgamma through the production of endogenous ligand. *Proc. Natl. Acad. Sci. U. S. A.* **95,** 4333–7 (1998).
40. Settembre, C. *et al.* TFEB links autophagy to lysosomal biogenesis. *Science* **332,** 1429–33 (2011).
41. Settembre, C. *et al.* TFEB controls cellular lipid metabolism through a starvation-induced autoregulatory loop. *Nat. Cell Biol.* **15,** 647–58 (2013).
42. Martina, J. A., Chen, Y., Gucek, M. & Puertollano, R. MTORC1 functions as a

transcriptional regulator of autophagy by preventing nuclear transport of TFEB. *Autophagy* **8,** 903–914 (2012).

43. Roczniak-Ferguson, A. *et al.* The transcription factor TFEB links mTORC1 signaling to transcriptional control of lysosome homeostasis. *Sci. Signal.* **5,** ra42 (2012).
44. Settembre, C. *et al.* A lysosome-to-nucleus signalling mechanism senses and regulates the lysosome via mTOR and TFEB. *EMBO J.* **31,** 1095–108 (2012).
45. Ben-Sahra, I., Howell, J. J., Asara, J. M. & Manning, B. D. Stimulation of de novo pyrimidine synthesis by growth signaling through mTOR and S6K1. *Science* **339,** 1323–8 (2013).
46. Robitaille, A. M. *et al.* Quantitative phosphoproteomics reveal mTORC1 activates de novo pyrimidine synthesis. *Science* **339,** 1320–3 (2013).
47. Ben-Sahra, I., Hoxhaj, G., Ricoult, S. J. H., Asara, J. M. & Manning, B. D. mTORC1 induces purine synthesis through control of the mitochondrial tetrahydrofolate cycle. *Science* **351,** 728–733 (2016).
48. WARBURG, O. On the origin of cancer cells. *Science* **123,** 309–14 (1956).
49. Vander Heiden, M. G., Cantley, L. C. & Thompson, C. B. Understanding the Warburg effect: the metabolic requirements of cell proliferation. *Science* **324,** 1029–33 (2009).
50. Cheng, S.-C. *et al.* mTOR- and HIF-1α-mediated aerobic glycolysis as metabolic basis for trained immunity. *Science* **345,** 1250684 (2014).
51. Dodd, K. M., Yang, J., Shen, M. H., Sampson, J. R. & Tee, A. R. mTORC1 drives HIF-1α and VEGF-A signalling via multiple mechanisms involving 4E-BP1, S6K1 and STAT3. *Oncogene* **34,** 2239–50 (2015).
52. Hudson, C. C. *et al.* Regulation of hypoxia-inducible factor 1alpha expression and function by the mammalian target of rapamycin. *Mol. Cell. Biol.* **22,** 7004–14 (2002).
53. Land, S. C. & Tee, A. R. Hypoxia-inducible factor 1alpha is regulated by the mammalian target of rapamycin (mTOR) via an mTOR signaling motif. *J. Biol. Chem.* **282,** 20534–43 (2007).
54. Semenza, G. L., Roth, P. H., Fang, H. M. & Wang, G. L. Transcriptional regulation of genes encoding glycolytic enzymes by hypoxia-inducible factor 1. *J. Biol. Chem.* **269,** 23757–63 (1994).
55. Choo, A. Y. *et al.* Glucose addiction of TSC null cells is caused by failed

mTORC1-dependent balancing of metabolic demand with supply. *Mol. Cell* **38,** 487–99 (2010).

56. Poulain, L. *et al.* High mTORC1 activity drives glycolysis addiction and sensitivity to G6PD inhibition in acute myeloid leukemia cells. *Leukemia* **31,** 2326–2335 (2017).
57. Pusapati, R. V *et al.* mTORC1-Dependent Metabolic Reprogramming Underlies Escape from Glycolysis Addiction in Cancer Cells. *Cancer Cell* **29,** 548–562 (2016).
58. Durán, R. V *et al.* Glutaminolysis activates Rag-mTORC1 signaling. *Mol. Cell* **47,** 349–58 (2012).
59. Villar, V. H. *et al.* mTORC1 inhibition in cancer cells protects from glutaminolysis-mediated apoptosis during nutrient limitation. *Nat. Commun.* **8,** 14124 (2017).
60. Csibi, A. *et al.* The mTORC1 pathway stimulates glutamine metabolism and cell proliferation by repressing SIRT4. *Cell* **153,** 840–54 (2013).
61. Csibi, A. *et al.* The mTORC1/S6K1 pathway regulates glutamine metabolism through the eIF4B-dependent control of c-Myc translation. *Curr. Biol.* **24,** 2274–80 (2014).
62. Gao, P. *et al.* c-Myc suppression of miR-23a/b enhances mitochondrial glutaminase expression and glutamine metabolism. *Nature* **458,** 762–5 (2009).
63. Cunningham, J. T. *et al.* mTOR controls mitochondrial oxidative function through a YY1-PGC-1alpha transcriptional complex. *Nature* **450,** 736–40 (2007).
64. Morita, M. *et al.* mTORC1 controls mitochondrial activity and biogenesis through 4E-BP-dependent translational regulation. *Cell Metab.* **18,** 698–711 (2013).
65. Locasale, J. W. Serine, glycine and one-carbon units: cancer metabolism in full circle. *Nat. Rev. Cancer* **13,** 572–83 (2013).
66. Wang, D.-W. *et al.* A novel mechanism of mTORC1-mediated serine/glycine metabolism in osteosarcoma development. *Cell. Signal.* **29,** 107–114 (2017).
67. Zabala-Letona, A. *et al.* mTORC1-dependent AMD1 regulation sustains polyamine metabolism in prostate cancer. *Nature* **547,** 109–113 (2017).
68. Murray-Stewart, T. R., Woster, P. M. & Casero, R. A. Targeting polyamine metabolism for cancer therapy and prevention. *Biochem. J.* **473,** 2937–53 (2016).
69. Rabinowitz, J. D. & White, E. Autophagy and metabolism. *Science* **330,** 1344–8 (2010).

70. Kim, J., Kundu, M., Viollet, B. & Guan, K.-L. AMPK and mTOR regulate autophagy through direct phosphorylation of Ulk1. *Nat. Cell Biol.* **13,** 132–41 (2011).
71. Ganley, I. G. *et al.* ULK1.ATG13.FIP200 complex mediates mTOR signaling and is essential for autophagy. *J. Biol. Chem.* **284,** 12297–305 (2009).
72. Hosokawa, N. *et al.* Nutrient-dependent mTORC1 association with the ULK1-Atg13-FIP200 complex required for autophagy. *Mol. Biol. Cell* **20,** 1981–91 (2009).
73. Jung, C. H. *et al.* ULK-Atg13-FIP200 complexes mediate mTOR signaling to the autophagy machinery. *Mol. Biol. Cell* **20,** 1992–2003 (2009).
74. Russell, R. C. *et al.* ULK1 induces autophagy by phosphorylating Beclin-1 and activating VPS34 lipid kinase. *Nat. Cell Biol.* **15,** 741–50 (2013).
75. Yuan, H.-X., Russell, R. C. & Guan, K.-L. Regulation of PIK3C3/VPS34 complexes by MTOR in nutrient stress-induced autophagy. *Autophagy* **9,** 1983–95 (2013).
76. Ma, X. *et al.* MTORC1-mediated NRBF2 phosphorylation functions as a switch for the class III PtdIns3K and autophagy. *Autophagy* **13,** 592–607 (2017).
77. Koren, I., Reem, E. & Kimchi, A. DAP1, a novel substrate of mTOR, negatively regulates autophagy. *Curr. Biol.* **20,** 1093–8 (2010).
78. Takamura, A. *et al.* Autophagy-deficient mice develop multiple liver tumors. *Genes Dev.* **25,** 795–800 (2011).
79. Pilla, E. & Bertolotti, A. Decoding the Protein Destruction Code: A Panoramic View. *Mol. Cell* **63,** 915–7 (2016).
80. McNaught, K. S. P., Perl, D. P., Brownell, A.-L. & Olanow, C. W. Systemic exposure to proteasome inhibitors causes a progressive model of Parkinson's disease. *Ann. Neurol.* **56,** 149–162 (2004).
81. Bedford, L. *et al.* Depletion of 26S Proteasomes in Mouse Brain Neurons Causes Neurodegeneration and Lewy-Like Inclusions Resembling Human Pale Bodies. *J. Neurosci.* **28,** 8189–8198 (2008).
82. Petrocca, F. *et al.* A Genome-wide siRNA Screen Identifies Proteasome Addiction as a Vulnerability of Basal-like Triple-Negative Breast Cancer Cells. *Cancer Cell* **24,** 182–196 (2013).
83. D'Arcy, P. *et al.* Inhibition of proteasome deubiquitinating activity as a new cancer therapy. *Nat. Med.* **17,** 1636–1640 (2011).

84. Zhao, J., Zhai, B., Gygi, S. P. & Goldberg, A. L. mTOR inhibition activates overall protein degradation by the ubiquitin proteasome system as well as by autophagy. *Proc. Natl. Acad. Sci.* **112,** 15790–15797 (2015).
85. Rousseau, A. & Bertolotti, A. An evolutionarily conserved pathway controls proteasome homeostasis. *Nature* **536,** 184–9 (2016).
86. Zhang, Y. *et al.* Coordinated regulation of protein synthesis and degradation by mTORC1. *Nature* **513,** 440–3 (2014).
87. Bar-Peled, L., Schweitzer, L. D., Zoncu, R. & Sabatini, D. M. Ragulator Is a GEF for the Rag GTPases that Signal Amino Acid Levels to mTORC1. *Cell* **150,** 1196–1208 (2012).
88. de Araujo, M. E. G. *et al.* Crystal structure of the human lysosomal mTORC1 scaffold complex and its impact on signaling. *Science (80-.).* **358,** 377–381 (2017).
89. Sancak, Y. *et al.* Ragulator-Rag Complex Targets mTORC1 to the Lysosomal Surface and Is Necessary for Its Activation by Amino Acids. *Cell* **141,** 290–303 (2010).
90. Yonehara, R. *et al.* Structural basis for the assembly of the Ragulator-Rag GTPase complex. *Nat. Commun.* **8,** 1625 (2017).
91. Zhang, T. *et al.* Structural basis for Ragulator functioning as a scaffold in membrane-anchoring of Rag GTPases and mTORC1. *Nat. Commun.* **8,** 1394 (2017).
92. Hirose, E., Nakashima, N., Sekiguchi, T. & Nishimoto, T. RagA is a functional homologue of S. cerevisiae Gtr1p involved in the Ran/Gsp1-GTPase pathway. *J. Cell Sci.* **111 (Pt 1),** 11–21 (1998).
93. Schürmann, A., Brauers, A., Massmann, S., Becker, W. & Joost, H. G. Cloning of a novel family of mammalian GTP-binding proteins (RagA, RagBs, RagB1) with remote similarity to the Ras-related GTPases. *J. Biol. Chem.* **270,** 28982–8 (1995).
94. Sekiguchi, T., Hirose, E., Nakashima, N., Ii, M. & Nishimoto, T. Novel G Proteins, Rag C and Rag D, Interact with GTP-binding Proteins, Rag A and Rag B. *J. Biol. Chem.* **276,** 7246–7257 (2001).
95. Kogan, K., Spear, E. D., Kaiser, C. A. & Fass, D. Structural Conservation of Components in the Amino Acid Sensing Branch of the TOR Pathway in Yeast and Mammals. *J. Mol. Biol.* **402,** 388–398 (2010).

96. Powis, K. *et al.* Crystal structure of the Ego1-Ego2-Ego3 complex and its role in promoting Rag GTPase-dependent TORC1 signaling. *Cell Res.* **25,** 1043–59 (2015).
97. Binda, M. *et al.* The Vam6 GEF Controls TORC1 by Activating the EGO Complex. *Mol. Cell* **35,** 563–573 (2009).
98. Kim, E., Goraksha-Hicks, P., Li, L., Neufeld, T. P. & Guan, K.-L. Regulation of TORC1 by Rag GTPases in nutrient response. *Nat. Cell Biol.* **10,** 935–945 (2008).
99. Sancak, Y. *et al.* The Rag GTPases Bind Raptor and Mediate Amino Acid Signaling to mTORC1. *Science (80-.).* **320,** 1496–1501 (2008).
100. Long, X., Ortiz-Vega, S., Lin, Y. & Avruch, J. Rheb Binding to Mammalian Target of Rapamycin (mTOR) Is Regulated by Amino Acid Sufficiency. *J. Biol. Chem.* **280,** 23433–23436 (2005).
101. Saito, K., Araki, Y., Kontani, K., Nishina, H. & Katada, T. Novel role of the small GTPase Rheb: its implication in endocytic pathway independent of the activation of mammalian target of rapamycin. *J. Biochem.* **137,** 423–30 (2005).
102. Su, M.-Y. *et al.* Hybrid Structure of the RagA/C-Ragulator mTORC1 Activation Complex. *Mol. Cell* **68,** 835–846.e3 (2017).
103. Bar-Peled, L. *et al.* A Tumor Suppressor Complex with GAP Activity for the Rag GTPases That Signal Amino Acid Sufficiency to mTORC1. *Science (80-.).* **340,** 1100–1106 (2013).
104. Panchaud, N., Peli-Gulli, M.-P. & De Virgilio, C. Amino Acid Deprivation Inhibits TORC1 Through a GTPase-Activating Protein Complex for the Rag Family GTPase Gtr1. *Sci. Signal.* **6,** ra42-ra42 (2013).
105. Wolfson, R. L. *et al.* KICSTOR recruits GATOR1 to the lysosome and is necessary for nutrients to regulate mTORC1. *Nature* **543,** 438–442 (2017).
106. Peng, M., Yin, N. & Li, M. O. SZT2 dictates GATOR control of mTORC1 signalling. *Nature* **543,** 433–437 (2017).
107. Panchaud, N., Péli-Gulli, M.-P. & De Virgilio, C. SEACing the GAP that nEGOCiates TORC1 activation. *Cell Cycle* **12,** 2948–2952 (2013).
108. Petit, C. S., Roczniak-Ferguson, A. & Ferguson, S. M. Recruitment of folliculin to lysosomes supports the amino acid-dependent activation of Rag GTPases. *J. Cell Biol.* **202,** 1107–22 (2013).
109. Tsun, Z.-Y. *et al.* The folliculin tumor suppressor is a GAP for the RagC/D

GTPases that signal amino acid levels to mTORC1. *Mol. Cell* **52,** 495–505 (2013).

110. Zoncu, R. *et al.* mTORC1 senses lysosomal amino acids through an inside-out mechanism that requires the vacuolar H(+)-ATPase. *Science* **334,** 678–83 (2011).
111. Chantranupong, L. *et al.* The Sestrins interact with GATOR2 to negatively regulate the amino-acid-sensing pathway upstream of mTORC1. *Cell Rep.* **9,** 1–8 (2014).
112. Parmigiani, A. *et al.* Sestrins inhibit mTORC1 kinase activation through the GATOR complex. *Cell Rep.* **9,** 1281–91 (2014).
113. Saxton, R. A. *et al.* Structural basis for leucine sensing by the Sestrin2-mTORC1 pathway. *Science (80-.).* **351,** 53–58 (2016).
114. Wolfson, R. L. *et al.* Sestrin2 is a leucine sensor for the mTORC1 pathway. *Science (80-.).* **351,** 43–48 (2016).
115. Nicklin, P. *et al.* Bidirectional Transport of Amino Acids Regulates mTOR and Autophagy. *Cell* **136,** 521–534 (2009).
116. Chantranupong, L. *et al.* The CASTOR Proteins Are Arginine Sensors for the mTORC1 Pathway. *Cell* **165,** 153–164 (2016).
117. Saxton, R. A., Chantranupong, L., Knockenhauer, K. E., Schwartz, T. U. & Sabatini, D. M. Mechanism of arginine sensing by CASTOR1 upstream of mTORC1. *Nature* **536,** 229–233 (2016).
118. Jung, J., Genau, H. M. & Behrends, C. Amino Acid-Dependent mTORC1 Regulation by the Lysosomal Membrane Protein SLC38A9. *Mol. Cell. Biol.* **35,** 2479–94 (2015).
119. Rebsamen, M. *et al.* SLC38A9 is a component of the lysosomal amino acid sensing machinery that controls mTORC1. *Nature* **519,** 477–481 (2015).
120. Wang, S. *et al.* Metabolism. Lysosomal amino acid transporter SLC38A9 signals arginine sufficiency to mTORC1. *Science* **347,** 188–94 (2015).
121. Durán, R. V *et al.* HIF-independent role of prolyl hydroxylases in the cellular response to amino acids. *Oncogene* **32,** 4549–4556 (2013).
122. Jewell, J. L. *et al.* Differential regulation of mTORC1 by leucine and glutamine. *Science* **347,** 194–198 (2015).
123. Dibble, C. C. *et al.* TBC1D7 is a third subunit of the TSC1-TSC2 complex upstream of mTORC1. *Mol. Cell* **47,** 535–46 (2012).

124. Inoki, K., Li, Y., Xu, T. & Guan, K.-L. Rheb GTPase is a direct target of TSC2 GAP activity and regulates mTOR signaling. *Genes Dev.* **17,** 1829–34 (2003).
125. Tee, A. R., Manning, B. D., Roux, P. P., Cantley, L. C. & Blenis, J. Tuberous sclerosis complex gene products, Tuberin and Hamartin, control mTOR signaling by acting as a GTPase-activating protein complex toward Rheb. *Curr. Biol.* **13,** 1259–68 (2003).
126. Long, X., Lin, Y., Ortiz-Vega, S., Yonezawa, K. & Avruch, J. Rheb binds and regulates the mTOR kinase. *Curr. Biol.* **15,** 702–13 (2005).
127. Sancak, Y. *et al.* PRAS40 is an insulin-regulated inhibitor of the mTORC1 protein kinase. *Mol. Cell* **25,** 903–15 (2007).
128. Yang, H. *et al.* Mechanisms of mTORC1 activation by RHEB and inhibition by PRAS40. *Nature* **552,** 368–373 (2017).
129. Menon, S. *et al.* Spatial control of the TSC complex integrates insulin and nutrient regulation of mTORC1 at the lysosome. *Cell* **156,** 771–85 (2014).
130. Inoki, K., Li, Y., Zhu, T., Wu, J. & Guan, K.-L. TSC2 is phosphorylated and inhibited by Akt and suppresses mTOR signalling. *Nat. Cell Biol.* **4,** 648–657 (2002).
131. Vander Haar, E., Lee, S.-I., Bandhakavi, S., Griffin, T. J. & Kim, D.-H. Insulin signalling to mTOR mediated by the Akt/PKB substrate PRAS40. *Nat. Cell Biol.* **9,** 316–23 (2007).
132. Ma, L., Chen, Z., Erdjument-Bromage, H., Tempst, P. & Pandolfi, P. P. Phosphorylation and functional inactivation of TSC2 by Erk implications for tuberous sclerosis and cancer pathogenesis. *Cell* **121,** 179–93 (2005).
133. Roux, P. P., Ballif, B. A., Anjum, R., Gygi, S. P. & Blenis, J. Tumor-promoting phorbol esters and activated Ras inactivate the tuberous sclerosis tumor suppressor complex via p90 ribosomal S6 kinase. *Proc. Natl. Acad. Sci. U. S. A.* **101,** 13489–94 (2004).
134. Carrière, A. *et al.* Oncogenic MAPK signaling stimulates mTORC1 activity by promoting RSK-mediated raptor phosphorylation. *Curr. Biol.* **18,** 1269–77 (2008).
135. Carriere, A. *et al.* ERK1/2 phosphorylate Raptor to promote Ras-dependent activation of mTOR complex 1 (mTORC1). *J. Biol. Chem.* **286,** 567–77 (2011).
136. Inoki, K. *et al.* TSC2 integrates Wnt and energy signals via a coordinated phosphorylation by AMPK and GSK3 to regulate cell growth. *Cell* **126,** 955–68

(2006).

137. Lee, D.-F. *et al.* IKK beta suppression of TSC1 links inflammation and tumor angiogenesis via the mTOR pathway. *Cell* **130,** 440–55 (2007).
138. Inoki, K., Zhu, T. & Guan, K.-L. TSC2 mediates cellular energy response to control cell growth and survival. *Cell* **115,** 577–90 (2003).
139. Gwinn, D. M. *et al.* AMPK Phosphorylation of Raptor Mediates a Metabolic Checkpoint. *Mol. Cell* **30,** 214–226 (2008).
140. Zhang, C.-S. *et al.* The Lysosomal v-ATPase-Ragulator Complex Is a Common Activator for AMPK and mTORC1, Acting as a Switch between Catabolism and Anabolism. *Cell Metab.* **20,** 526–540 (2014).
141. Efeyan, A. *et al.* Regulation of mTORC1 by the Rag GTPases is necessary for neonatal autophagy and survival. *Nature* **493,** 679–683 (2012).
142. Kalender, A. *et al.* Metformin, independent of AMPK, inhibits mTORC1 in a rag GTPase-dependent manner. *Cell Metab.* **11,** 390–401 (2010).
143. Yoshida, S. *et al.* Redox regulates mammalian target of rapamycin complex 1 (mTORC1) activity by modulating the TSC1/TSC2-Rheb GTPase pathway. *J. Biol. Chem.* **286,** 32651–60 (2011).
144. Zheng, M. *et al.* Inactivation of Rheb by PRAK-mediated phosphorylation is essential for energy-depletion-induced suppression of mTORC1. *Nat. Cell Biol.* **13,** 263–72 (2011).
145. Wu, X.-N. *et al.* Phosphorylation of Raptor by p38beta participates in arsenite-induced mammalian target of rapamycin complex 1 (mTORC1) activation. *J. Biol. Chem.* **286,** 31501–11 (2011).
146. Liu, L. *et al.* Hypoxia-induced energy stress regulates mRNA translation and cell growth. *Mol. Cell* **21,** 521–31 (2006).
147. Brugarolas, J. *et al.* Regulation of mTOR function in response to hypoxia by REDD1 and the TSC1/TSC2 tumor suppressor complex. *Genes Dev.* **18,** 2893–904 (2004).
148. Sofer, A., Lei, K., Johannessen, C. M. & Ellisen, L. W. Regulation of mTOR and cell growth in response to energy stress by REDD1. *Mol. Cell. Biol.* **25,** 5834–45 (2005).
149. DeYoung, M. P., Horak, P., Sofer, A., Sgroi, D. & Ellisen, L. W. Hypoxia regulates TSC1/2-mTOR signaling and tumor suppression through REDD1-mediated 14-3-3 shuttling. *Genes Dev.* **22,** 239–51 (2008).

150. Elorza, A. *et al.* HIF2α acts as an mTORC1 activator through the amino acid carrier SLC7A5. *Mol. Cell* **48,** 681–91 (2012).
151. Chen, Y., Rodrik, V. & Foster, D. A. Alternative phospholipase D/mTOR survival signal in human breast cancer cells. *Oncogene* **24,** 672–679 (2005).
152. Hui, L. *et al.* Phospholipase D elevates the level of MDM2 and suppresses DNA damage-induced increases in p53. *Mol. Cell. Biol.* **24,** 5677–86 (2004).
153. Fang, Y., Vilella-Bach, M., Bachmann, R., Flanigan, A. & Chen, J. Phosphatidic acid-mediated mitogenic activation of mTOR signaling. *Science* **294,** 1942–5 (2001).
154. Xu, Y., Fang, Y., Chen, J. & Prestwich, G. D. Activation of mTOR signaling by novel fluoromethylene phosphonate analogues of phosphatidic acid. *Bioorg. Med. Chem. Lett.* **14,** 1461–1464 (2004).
155. Hornberger, T. A. *et al.* The role of phospholipase D and phosphatidic acid in the mechanical activation of mTOR signaling in skeletal muscle. *Proc. Natl. Acad. Sci. U. S. A.* **103,** 4741–6 (2006).
156. Tang, W. *et al.* Identification of a novel human lysophosphatidic acid acyltransferase, LPAAT-theta, which activates mTOR pathway. *J. Biochem. Mol. Biol.* **39,** 626–35 (2006).
157. Avila-Flores, A., Santos, T., Rincón, E. & Mérida, I. Modulation of the mammalian target of rapamycin pathway by diacylglycerol kinase-produced phosphatidic acid. *J. Biol. Chem.* **280,** 10091–9 (2005).
158. Menon, D. *et al.* Lipid sensing by mTOR complexes viade novosynthesis of phosphatidic acid. *J. Biol. Chem.* **292,** 6303–6311 (2017).
159. Sun, Y. *et al.* Phospholipase D1 is an effector of Rheb in the mTOR pathway. *Proc. Natl. Acad. Sci. U. S. A.* **105,** 8286–91 (2008).
160. Jiang, H. *et al.* Involvement of Ral GTPase in v-Src-induced phospholipase D activation. *Nature* **378,** 409–12 (1995).
161. Toda, K., Nogami, M., Murakami, K., Kanaho, Y. & Nakayama, K. Colocalization of phospholipase D1 and GTP-binding-defective mutant of ADP-ribosylation factor 6 to endosomes and lysosomes. *FEBS Lett.* **442,** 221–5 (1999).
162. Xu, L. *et al.* Elevated phospholipase D activity in H-Ras- but not K-Ras-transformed cells by the synergistic action of RalA and ARF6. *Mol. Cell. Biol.* **23,** 645–54 (2003).
163. Yoon, M.-S., Du, G., Backer, J. M., Frohman, M. A. & Chen, J. Class III PI-3-

kinase activates phospholipase D in an amino acid-sensing mTORC1 pathway. *J. Cell Biol.* **195,** 435–47 (2011).

164. Toschi, A. *et al.* Regulation of mTORC1 and mTORC2 Complex Assembly by Phosphatidic Acid: Competition with Rapamycin. *Mol. Cell. Biol.* **29,** 1411–1420 (2009).
165. Dogliotti, G. *et al.* Membrane-binding and activation of LKB1 by phosphatidic acid is essential for development and tumour suppression. *Nat. Commun.* **8,** 15747 (2017).
166. Sehgal, S. N., Baker, H. & Vézina, C. Rapamycin (AY-22,989), a new antifungal antibiotic. II. Fermentation, isolation and characterization. *J. Antibiot. (Tokyo).* **28,** 727–32 (1975).
167. Sabatini, D. M., Erdjument-Bromage, H., Lui, M., Tempst, P. & Snyder, S. H. RAFT1: a mammalian protein that binds to FKBP12 in a rapamycin-dependent fashion and is homologous to yeast TORs. *Cell* **78,** 35–43 (1994).
168. Chen, J., Zheng, X. F., Brown, E. J. & Schreiber, S. L. Identification of an 11-kDa FKBP12-rapamycin-binding domain within the 289-kDa FKBP12-rapamycin-associated protein and characterization of a critical serine residue. *Proc. Natl. Acad. Sci. U. S. A.* **92,** 4947–51 (1995).
169. Sabers, C. J. *et al.* Isolation of a protein target of the FKBP12-rapamycin complex in mammalian cells. *J. Biol. Chem.* **270,** 815–22 (1995).
170. Koltin, Y. *et al.* Rapamycin sensitivity in Saccharomyces cerevisiae is mediated by a peptidyl-prolyl cis-trans isomerase related to human FK506-binding protein. *Mol. Cell. Biol.* **11,** 1718–23 (1991).
171. Kim, D.-H. *et al.* mTOR interacts with raptor to form a nutrient-sensitive complex that signals to the cell growth machinery. *Cell* **110,** 163–75 (2002).
172. Oshiro, N. *et al.* Dissociation of raptor from mTOR is a mechanism of rapamycin-induced inhibition of mTOR function. *Genes Cells* **9,** 359–66 (2004).
173. Shor, B. *et al.* A new pharmacologic action of CCI-779 involves FKBP12-independent inhibition of mTOR kinase activity and profound repression of global protein synthesis. *Cancer Res.* **68,** 2934–43 (2008).
174. Sarbassov, D. D. *et al.* Prolonged rapamycin treatment inhibits mTORC2 assembly and Akt/PKB. *Mol. Cell* **22,** 159–68 (2006).
175. Rosner, M. & Hengstschläger, M. Cytoplasmic and nuclear distribution of the protein complexes mTORC1 and mTORC2: rapamycin triggers

dephosphorylation and delocalization of the mTORC2 components rictor and sin1. *Hum. Mol. Genet.* **17,** 2934–48 (2008).

176. Kapoor, A. & Figlin, R. A. Targeted inhibition of mammalian target of rapamycin for the treatment of advanced renal cell carcinoma. *Cancer* **115,** 3618–30 (2009).
177. Mita, M. M. *et al.* Phase I trial of the novel mammalian target of rapamycin inhibitor deforolimus (AP23573; MK-8669) administered intravenously daily for 5 days every 2 weeks to patients with advanced malignancies. *J. Clin. Oncol.* **26,** 361–7 (2008).
178. Bissler, J. J. *et al.* Sirolimus for Angiomyolipoma in Tuberous Sclerosis Complex or Lymphangioleiomyomatosis. *N. Engl. J. Med.* **358,** 140–151 (2008).
179. Marsh, D. J. *et al.* Rapamycin treatment for a child with germline PTEN mutation. *Nat. Clin. Pract. Oncol.* **5,** 357–61 (2008).
180. Choo, A. Y., Yoon, S.-O., Kim, S. G., Roux, P. P. & Blenis, J. Rapamycin differentially inhibits S6Ks and 4E-BP1 to mediate cell-type-specific repression of mRNA translation. *Proc. Natl. Acad. Sci. U. S. A.* **105,** 17414–9 (2008).
181. Harrington, L. S. *et al.* The TSC1-2 tumor suppressor controls insulin-PI3K signaling via regulation of IRS proteins. *J. Cell Biol.* **166,** 213–23 (2004).
182. Shah, O. J., Wang, Z. & Hunter, T. Inappropriate activation of the TSC/Rheb/mTOR/S6K cassette induces IRS1/2 depletion, insulin resistance, and cell survival deficiencies. *Curr. Biol.* **14,** 1650–6 (2004).
183. Mondesire, W. H. *et al.* Targeting mammalian target of rapamycin synergistically enhances chemotherapy-induced cytotoxicity in breast cancer cells. *Clin. Cancer Res.* **10,** 7031–42 (2004).
184. Baumann, P., Hagemeier, H., Mandl-Weber, S., Franke, D. & Schmidmaier, R. Myeloma cell growth inhibition is augmented by synchronous inhibition of the insulin-like growth factor-1 receptor by NVP-AEW541 and inhibition of mammalian target of rapamycin by Rad001. *Anticancer. Drugs* **20,** 259–66 (2009).
185. Feldman, M. E. *et al.* Active-site inhibitors of mTOR target rapamycin-resistant outputs of mTORC1 and mTORC2. *PLoS Biol.* **7,** e38 (2009).
186. García-Martínez, J. M. *et al.* Ku-0063794 is a specific inhibitor of the mammalian target of rapamycin (mTOR). *Biochem. J.* **421,** 29–42 (2009).
187. Thoreen, C. C. *et al.* An ATP-competitive mammalian target of rapamycin inhibitor reveals rapamycin-resistant functions of mTORC1. *J. Biol. Chem.* **284,**

8023–32 (2009).

188. Yu, K. *et al.* Biochemical, cellular, and in vivo activity of novel ATP-competitive and selective inhibitors of the mammalian target of rapamycin. *Cancer Res.* **69,** 6232–40 (2009).
189. Di Nicolantonio, F. *et al.* Deregulation of the PI3K and KRAS signaling pathways in human cancer cells determines their response to everolimus. *J. Clin. Invest.* **120,** 2858–66 (2010).
190. Chiarini, F., Evangelisti, C., McCubrey, J. A. & Martelli, A. M. Current treatment strategies for inhibiting mTOR in cancer. *Trends Pharmacol. Sci.* **36,** 124–135 (2015).
191. Kim, A. *et al.* Coexistent mutations of KRAS and PIK3CA affect the efficacy of NVP-BEZ235, a dual PI3K/MTOR inhibitor, in regulating the PI3K/MTOR pathway in colorectal cancer. *Int. J. cancer* **133,** 984–96 (2013).
192. Shepherd, C. *et al.* PI3K/mTOR inhibition upregulates NOTCH-MYC signalling leading to an impaired cytotoxic response. *Leukemia* **27,** 650–60 (2013).
193. Veverka, V. *et al.* Structural characterization of the interaction of mTOR with phosphatidic acid and a novel class of inhibitor: compelling evidence for a central role of the FRB domain in small molecule-mediated regulation of mTOR. *Oncogene* **27,** 585–95 (2008).
194. McMahon, L. P., Yue, W., Santen, R. J. & Lawrence, J. C. Farnesylthiosalicylic acid inhibits mammalian target of rapamycin (mTOR) activity both in cells and in vitro by promoting dissociation of the mTOR-raptor complex. *Mol. Endocrinol.* **19,** 175–83 (2005).
195. Bunpo, P. *et al.* GCN2 protein kinase is required to activate amino acid deprivation responses in mice treated with the anti-cancer agent L-asparaginase. *J. Biol. Chem.* **284,** 32742–9 (2009).
196. Hanahan, D. & Weinberg, R. A. Hallmarks of Cancer: The Next Generation. *Cell* **144,** 646–674 (2011).
197. Almuhaideb, A., Papathanasiou, N. & Bomanji, J. 18F-FDG PET/CT imaging in oncology. *Ann. Saudi Med.* **31,** 3–13 (2011).
198. Barthel, A. *et al.* Regulation of GLUT1 gene transcription by the serine/threonine kinase Akt1. *J. Biol. Chem.* **274,** 20281–6 (1999).
199. Wieman, H. L., Wofford, J. A. & Rathmell, J. C. Cytokine stimulation promotes glucose uptake via phosphatidylinositol-3 kinase/Akt regulation of Glut1 activity

and trafficking. *Mol. Biol. Cell* **18,** 1437–46 (2007).

200. Deprez, J., Vertommen, D., Alessi, D. R., Hue, L. & Rider, M. H. Phosphorylation and activation of heart 6-phosphofructo-2-kinase by protein kinase B and other protein kinases of the insulin signaling cascades. *J. Biol. Chem.* **272,** 17269–75 (1997).
201. Gottlob, K. *et al.* Inhibition of early apoptotic events by Akt/PKB is dependent on the first committed step of glycolysis and mitochondrial hexokinase. *Genes Dev.* **15,** 1406–1418 (2001).
202. Lee, J.-H. *et al.* Stabilization of phosphofructokinase 1 platelet isoform by AKT promotes tumorigenesis. *Nat. Commun.* **8,** 949 (2017).
203. Murakami, T. *et al.* Identification of two enhancer elements in the gene encoding the type 1 glucose transporter from the mouse which are responsive to serum, growth factor, and oncogenes. *J. Biol. Chem.* **267,** 9300–6 (1992).
204. EAGLE, H. The minimum vitamin requirements of the L and HeLa cells in tissue culture, the production of specific vitamin deficiencies, and their cure. *J. Exp. Med.* **102,** 595–600 (1955).
205. Nicklin, P. *et al.* Bidirectional transport of amino acids regulates mTOR and autophagy. *Cell* **136,** 521–34 (2009).
206. Kaira, K. *et al.* Prognostic significance of L-type amino acid transporter 1 expression in resectable stage I-III nonsmall cell lung cancer. *Br. J. Cancer* **98,** 742–8 (2008).
207. Sakata, T. *et al.* L-type amino-acid transporter 1 as a novel biomarker for high-grade malignancy in prostate cancer. *Pathol. Int.* **59,** 7–18 (2009).
208. Lieberman, B. P. *et al.* PET imaging of glutaminolysis in tumors by 18F-(2S,4R)4-fluoroglutamine. *J. Nucl. Med.* **52,** 1947–55 (2011).
209. Venneti, S. *et al.* Glutamine-based PET imaging facilitates enhanced metabolic evaluation of gliomas in vivo. *Sci. Transl. Med.* **7,** 274ra17 (2015).
210. Wang, R. *et al.* The transcription factor Myc controls metabolic reprogramming upon T lymphocyte activation. *Immunity* **35,** 871–82 (2011).
211. Wise, D. R. *et al.* Myc regulates a transcriptional program that stimulates mitochondrial glutaminolysis and leads to glutamine addiction. *Proc. Natl. Acad. Sci.* **105,** 18782–18787 (2008).
212. Eberhardy, S. R. & Farnham, P. J. c-Myc mediates activation of the cad promoter via a post-RNA polymerase II recruitment mechanism. *J. Biol. Chem.* **276,**

48562–71 (2001).
213. Gao, P. *et al.* c-Myc suppression of miR-23a/b enhances mitochondrial glutaminase expression and glutamine metabolism. *Nature* **458,** 762–5 (2009).
214. Mannava, S. *et al.* Direct role of nucleotide metabolism in C-MYC-dependent proliferation of melanoma cells. *Cell Cycle* **7,** 2392–400 (2008).
215. Reynolds, M. R. *et al.* Control of glutamine metabolism by the tumor suppressor Rb. *Oncogene* **33,** 556–66 (2014).
216. Kuo, W., Lin, J. & Tang, T. K. Human glucose-6-phosphate dehydrogenase (G6PD) gene transforms NIH 3T3 cells and induces tumors in nude mice. *Int. J. cancer* **85,** 857–64 (2000).
217. Wang, C. *et al.* Identification of transaldolase as a novel serum biomarker for hepatocellular carcinoma metastasis using xenografted mouse model and clinic samples. *Cancer Lett.* **313,** 154–66 (2011).
218. Locasale, J. W. *et al.* Phosphoglycerate dehydrogenase diverts glycolytic flux and contributes to oncogenesis. *Nat. Genet.* **43,** 869–74 (2011).
219. Possemato, R. *et al.* Functional genomics reveal that the serine synthesis pathway is essential in breast cancer. *Nature* **476,** 346–50 (2011).
220. Bauer, D. E., Hatzivassiliou, G., Zhao, F., Andreadis, C. & Thompson, C. B. ATP citrate lyase is an important component of cell growth and transformation. *Oncogene* **24,** 6314–22 (2005).
221. Hatzivassiliou, G. *et al.* ATP citrate lyase inhibition can suppress tumor cell growth. *Cancer Cell* **8,** 311–21 (2005).
222. Berwick, D. C., Hers, I., Heesom, K. J., Moule, S. K. & Tavare, J. M. The identification of ATP-citrate lyase as a protein kinase B (Akt) substrate in primary adipocytes. *J. Biol. Chem.* **277,** 33895–900 (2002).
223. Birsoy, K. *et al.* An Essential Role of the Mitochondrial Electron Transport Chain in Cell Proliferation Is to Enable Aspartate Synthesis. *Cell* **162,** 540–51 (2015).
224. Sullivan, L. B. *et al.* Supporting Aspartate Biosynthesis Is an Essential Function of Respiration in Proliferating Cells. *Cell* **162,** 552–563 (2015).
225. DeBerardinis, R. J. *et al.* Beyond aerobic glycolysis: transformed cells can engage in glutamine metabolism that exceeds the requirement for protein and nucleotide synthesis. *Proc. Natl. Acad. Sci. U. S. A.* **104,** 19345–50 (2007).
226. Yuneva, M., Zamboni, N., Oefner, P., Sachidanandam, R. & Lazebnik, Y. Deficiency in glutamine but not glucose induces MYC-dependent apoptosis in

human cells. *J. Cell Biol.* **178,** 93–105 (2007).
227. Metallo, C. M. *et al.* Reductive glutamine metabolism by IDH1 mediates lipogenesis under hypoxia. *Nature* **481,** 380–4 (2011).
228. Wang, J.-B. *et al.* Targeting mitochondrial glutaminase activity inhibits oncogenic transformation. *Cancer Cell* **18,** 207–19 (2010).
229. Krebs, H. A. Metabolism of amino-acids: The synthesis of glutamine from glutamic acid and ammonia, and the enzymic hydrolysis of glutamine in animal tissues. *Biochem. J.* **29,** 1951–69 (1935).
230. YIELDING, K. L. & TOMKINS, G. M. An effect of L-leucine and other essential amino acids on the structure and activity of glutamic dehydrogenase. *Proc. Natl. Acad. Sci. U. S. A.* **47,** 983–9 (1961).
231. Long, J. *et al.* Glutamine synthetase as an early marker for hepatocellular carcinoma based on proteomic analysis of resected small hepatocellular carcinomas. *Hepatobiliary Pancreat. Dis. Int* **9,** 296–305 (2010).
232. Rosati, A. *et al.* Glutamine synthetase expression as a valuable marker of epilepsy and longer survival in newly diagnosed glioblastoma multiforme. *Neuro. Oncol.* **15,** 618–25 (2013).
233. Gameiro, P. A. *et al.* In vivo HIF-mediated reductive carboxylation is regulated by citrate levels and sensitizes VHL-deficient cells to glutamine deprivation. *Cell Metab.* **17,** 372–85 (2013).
234. Jiang, L. *et al.* Reductive carboxylation supports redox homeostasis during anchorage-independent growth. *Nature* **532,** 255–8 (2016).
235. Mullen, A. R. *et al.* Reductive carboxylation supports growth in tumour cells with defective mitochondria. *Nature* **481,** 385–8 (2011).
236. Patel, D. *et al.* Aspartate Rescues S-phase Arrest Caused by Suppression of Glutamine Utilization in KRas-driven Cancer Cells. *J. Biol. Chem.* **291,** 9322–9329 (2016).
237. Zhang, J. *et al.* Asparagine plays a critical role in regulating cellular adaptation to glutamine depletion. *Mol. Cell* **56,** 205–18 (2014).
238. Hao, Y. *et al.* Oncogenic PIK3CA mutations reprogram glutamine metabolism in colorectal cancer. *Nat. Commun.* **7,** 11971 (2016).
239. Xu, P. *et al.* LRH-1-dependent programming of mitochondrial glutamine processing drives liver cancer. *Genes Dev.* **30,** 1255–1260 (2016).
240. Vié, N. *et al.* Overexpression of phosphoserine aminotransferase PSAT1

stimulates cell growth and increases chemoresistance of colon cancer cells. *Mol. Cancer* **7,** 14 (2008).

241. Liu, W. *et al.* Reprogramming of proline and glutamine metabolism contributes to the proliferative and metabolic responses regulated by oncogenic transcription factor c-MYC. *Proc. Natl. Acad. Sci. U. S. A.* **109,** 8983–8 (2012).
242. Li, H., Meininger, C. J., Bazer, F. W. & Wu, G. Intracellular sources of ornithine for polyamine synthesis in endothelial cells. *Amino Acids* **48,** 2401–10 (2016).
243. Altman, B. J., Stine, Z. E. & Dang, C. V. From Krebs to clinic: glutamine metabolism to cancer therapy. *Nat. Rev. Cancer* **16,** 619–634 (2016).
244. Hosios, A. M. *et al.* Amino Acids Rather than Glucose Account for the Majority of Cell Mass in Proliferating Mammalian Cells. *Dev. Cell* **36,** 540–9 (2016).
245. Xiang, L. *et al.* Knock-down of glutaminase 2 expression decreases glutathione, NADH, and sensitizes cervical cancer to ionizing radiation. *Biochim. Biophys. Acta* **1833,** 2996–3005 (2013).
246. Timmerman, L. A. *et al.* Glutamine sensitivity analysis identifies the xCT antiporter as a common triple-negative breast tumor therapeutic target. *Cancer Cell* **24,** 450–65 (2013).
247. Tsuchihashi, K. *et al.* The EGF Receptor Promotes the Malignant Potential of Glioma by Regulating Amino Acid Transport System xc(-). *Cancer Res.* **76,** 2954–63 (2016).
248. Son, J. *et al.* Glutamine supports pancreatic cancer growth through a KRAS-regulated metabolic pathway. *Nature* **496,** 101–5 (2013).
249. Figueroa, M. E. *et al.* Leukemic IDH1 and IDH2 mutations result in a hypermethylation phenotype, disrupt TET2 function, and impair hematopoietic differentiation. *Cancer Cell* **18,** 553–67 (2010).
250. Ward, P. S. *et al.* The common feature of leukemia-associated IDH1 and IDH2 mutations is a neomorphic enzyme activity converting alpha-ketoglutarate to 2-hydroxyglutarate. *Cancer Cell* **17,** 225–34 (2010).
251. Letouzé, E. *et al.* SDH mutations establish a hypermethylator phenotype in paraganglioma. *Cancer Cell* **23,** 739–52 (2013).
252. Xiao, M. *et al.* Inhibition of -KG-dependent histone and DNA demethylases by fumarate and succinate that are accumulated in mutations of FH and SDH tumor suppressors. *Genes Dev.* **26,** 1326–1338 (2012).
253. Pan, M. *et al.* Regional glutamine deficiency in tumours promotes

dedifferentiation through inhibition of histone demethylation. *Nat. Cell Biol.* **18,** 1090–101 (2016).

254. van Geldermalsen, M. *et al.* ASCT2/SLC1A5 controls glutamine uptake and tumour growth in triple-negative basal-like breast cancer. *Oncogene* **35,** 3201–8 (2016).
255. Bröer, A., Rahimi, F. & Bröer, S. Deletion of Amino Acid Transporter ASCT2 (SLC1A5) Reveals an Essential Role for Transporters SNAT1 (SLC38A1) and SNAT2 (SLC38A2) to Sustain Glutaminolysis in Cancer Cells. *J. Biol. Chem.* **291,** 13194–205 (2016).
256. Polletta, L. *et al.* SIRT5 regulation of ammonia-induced autophagy and mitophagy. *Autophagy* **11,** 253–70 (2015).
257. Masamha, C. P. *et al.* CFIm25 links alternative polyadenylation to glioblastoma tumour suppression. *Nature* **510,** 412–6 (2014).
258. Redis, R. S. *et al.* Allele-Specific Reprogramming of Cancer Metabolism by the Long Non-coding RNA CCAT2. *Mol. Cell* **61,** 520–534 (2016).
259. Colombo, S. L. *et al.* Molecular basis for the differential use of glucose and glutamine in cell proliferation as revealed by synchronized HeLa cells. *Proc. Natl. Acad. Sci.* **108,** 21069–21074 (2011).
260. Fahien, L. A. & Kmiotek, E. Regulation of glutamate dehydrogenase by palmitoyl-coenzyme A. *Arch. Biochem. Biophys.* **212,** 247–53 (1981).
261. FRIEDEN, C. GLUTAMATE DEHYDROGENASE. V. THE RELATION OF ENZYME STRUCTURE TO THE CATALYTIC FUNCTION. *J. Biol. Chem.* **238,** 3286–99 (1963).
262. Tomita, T., Kuzuyama, T. & Nishiyama, M. Structural basis for leucine-induced allosteric activation of glutamate dehydrogenase. *J. Biol. Chem.* **286,** 37406–13 (2011).
263. Haigis, M. C. *et al.* SIRT4 inhibits glutamate dehydrogenase and opposes the effects of calorie restriction in pancreatic beta cells. *Cell* **126,** 941–54 (2006).
264. Wang, Y. *et al.* GLUL Promotes Cell Proliferation in Breast Cancer. *J. Cell. Biochem.* **118,** 2018–2025 (2017).
265. van der Vos, K. E. *et al.* Modulation of glutamine metabolism by the PI(3)K-PKB-FOXO network regulates autophagy. *Nat. Cell Biol.* **14,** 829–37 (2012).
266. Bott, A. J. *et al.* Oncogenic Myc Induces Expression of Glutamine Synthetase through Promoter Demethylation. *Cell Metab.* **22,** 1068–77 (2015).

267. Cox, A. G. *et al.* Yap reprograms glutamine metabolism to increase nucleotide biosynthesis and enable liver growth. *Nat. Cell Biol.* **18,** 886–896 (2016).
268. Arad, G., Freikopf, A. & Kulka, R. G. Glutamine-stimulated modification and degradation of glutamine synthetase in hepatoma tissue culture cells. *Cell* **8,** 95–101 (1976).
269. DEMARS, R. The inhibition by glutamine of glutamyl transferase formation in cultures of human cells. *Biochim. Biophys. Acta* **27,** 435–6 (1958).
270. Nguyen, T. Van *et al.* Glutamine Triggers Acetylation-Dependent Degradation of Glutamine Synthetase via the Thalidomide Receptor Cereblon. *Mol. Cell* **61,** 809–20 (2016).
271. Abu Aboud, O. *et al.* Glutamine Addiction in Kidney Cancer Suppresses Oxidative Stress and Can Be Exploited for Real-Time Imaging. *Cancer Res.* **77,** 6746–6758 (2017).
272. Petronini, P. G., Urbani, S., Alfieri, R., Borghetti, A. F. & Guidotti, G. G. Cell susceptibility to apoptosis by glutamine deprivation and rescue: survival and apoptotic death in cultured lymphoma-leukemia cell lines. *J. Cell. Physiol.* **169,** 175–85 (1996).
273. Weinberg, F. *et al.* Mitochondrial metabolism and ROS generation are essential for Kras-mediated tumorigenicity. *Proc. Natl. Acad. Sci. U. S. A.* **107,** 8788–93 (2010).
274. Tardito, S. *et al.* Glutamine synthetase activity fuels nucleotide biosynthesis and supports growth of glutamine-restricted glioblastoma. *Nat. Cell Biol.* **17,** 1556–68 (2015).
275. Pavlova, N. N. *et al.* As Extracellular Glutamine Levels Decline, Asparagine Becomes an Essential Amino Acid. *Cell Metab.* **27,** 428–438.e5 (2018).
276. Krall, A. S., Xu, S., Graeber, T. G., Braas, D. & Christofk, H. R. Asparagine promotes cancer cell proliferation through use as an amino acid exchange factor. *Nat. Commun.* **7,** 11457 (2016).
277. Robinson, M. M. *et al.* Novel mechanism of inhibition of rat kidney-type glutaminase by bis-2-(5-phenylacetamido-1,2,4-thiadiazol-2-yl)ethyl sulfide (BPTES). *Biochem. J.* **406,** 407–14 (2007).
278. Gross, M. I. *et al.* Antitumor activity of the glutaminase inhibitor CB-839 in triple-negative breast cancer. *Mol. Cancer Ther.* **13,** 890–901 (2014).
279. Jacque, N. *et al.* Targeting glutaminolysis has antileukemic activity in acute

myeloid leukemia and synergizes with BCL-2 inhibition. *Blood* **126,** 1346–56 (2015).

280. Korangath, P. *et al.* Targeting Glutamine Metabolism in Breast Cancer with Aminooxyacetate. *Clin. Cancer Res.* **21,** 3263–73 (2015).
281. Li, M., Allen, A. & Smith, T. J. High throughput screening reveals several new classes of glutamate dehydrogenase inhibitors. *Biochemistry* **46,** 15089–102 (2007).
282. Qing, G. *et al.* ATF4 regulates MYC-mediated neuroblastoma cell death upon glutamine deprivation. *Cancer Cell* **22,** 631–44 (2012).
283. Cheng, T. *et al.* Pyruvate carboxylase is required for glutamine-independent growth of tumor cells. *Proc. Natl. Acad. Sci. U. S. A.* **108,** 8674–9 (2011).
284. Christen, S. *et al.* Breast Cancer-Derived Lung Metastases Show Increased Pyruvate Carboxylase-Dependent Anaplerosis. *Cell Rep.* **17,** 837–848 (2016).
285. Linares, J. F. *et al.* ATF4-Induced Metabolic Reprograming Is a Synthetic Vulnerability of the p62-Deficient Tumor Stroma. *Cell Metab.* **26,** 817–829.e6 (2017).
286. Tanaka, K. *et al.* Compensatory glutamine metabolism promotes glioblastoma resistance to mTOR inhibitor treatment. *J. Clin. Invest.* **125,** 1591–602 (2015).
287. Tan, H. W. S., Sim, A. Y. L. & Long, Y. C. Glutamine metabolism regulates autophagy-dependent mTORC1 reactivation during amino acid starvation. *Nat. Commun.* **8,** 338 (2017).
288. Jeong, S. M. *et al.* SIRT4 has tumor-suppressive activity and regulates the cellular metabolic response to DNA damage by inhibiting mitochondrial glutamine metabolism. *Cancer Cell* **23,** 450–63 (2013).
289. Coloff, J. L. *et al.* Differential Glutamate Metabolism in Proliferating and Quiescent Mammary Epithelial Cells. *Cell Metab.* **23,** 867–80 (2016).
290. White, M. A. *et al.* Glutamine Transporters Are Targets of Multiple Oncogenic Signaling Pathways in Prostate Cancer. *Mol. Cancer Res.* **15,** 1017–1028 (2017).
291. Scalise, M., Pochini, L., Galluccio, M. & Indiveri, C. Glutamine transport. From energy supply to sensing and beyond. *Biochim. Biophys. Acta* **1857,** 1147–1157 (2016).
292. Kondo, M. *et al.* Biology of hematopoietic stem cells and progenitors: implications for clinical application. *Annu. Rev. Immunol.* **21,** 759–806 (2003).

293. Akashi, K., Traver, D., Miyamoto, T. & Weissman, I. L. A clonogenic common myeloid progenitor that gives rise to all myeloid lineages. *Nature* **404,** 193–7 (2000).
294. Lind, E. F., Prockop, S. E., Porritt, H. E. & Petrie, H. T. Mapping precursor movement through the postnatal thymus reveals specific microenvironments supporting defined stages of early lymphoid development. *J. Exp. Med.* **194,** 127–34 (2001).
295. Anderson, G., Jenkinson, E. J., Moore, N. C. & Owen, J. J. MHC class II-positive epithelium and mesenchyme cells are both required for T-cell development in the thymus. *Nature* **362,** 70–3 (1993).
296. Scimone, M. L., Aifantis, I., Apostolou, I., von Boehmer, H. & von Andrian, U. H. A multistep adhesion cascade for lymphoid progenitor cell homing to the thymus. *Proc. Natl. Acad. Sci. U. S. A.* **103,** 7006–11 (2006).
297. Belver, L. & Ferrando, A. The genetics and mechanisms of T cell acute lymphoblastic leukaemia. *Nat. Rev. Cancer* **16,** 494–507 (2016).
298. Marks, D. I. *et al.* T-cell acute lymphoblastic leukemia in adults: clinical features, immunophenotype, cytogenetics, and outcome from the large randomized prospective trial (UKALL XII/ECOG 2993). *Blood* **114,** 5136–45 (2009).
299. Ferrando, A. A. *et al.* Gene expression signatures define novel oncogenic pathways in T cell acute lymphoblastic leukemia. *Cancer Cell* **1,** 75–87 (2002).
300. Thalhammer-Scherrer, R. *et al.* The immunophenotype of 325 adult acute leukemias: relationship to morphologic and molecular classification and proposal for a minimal screening program highly predictive for lineage discrimination. *Am. J. Clin. Pathol.* **117,** 380–9 (2002).
301. Greaves, M. F., Janossy, G., Peto, J. & Kay, H. Immunologically defined subclasses of acute lymphoblastic leukaemia in children: their relationship to presentation features and prognosis. *Br. J. Haematol.* **48,** 179–97 (1981).
302. Pui, C. H. *et al.* Long-term results of St Jude Total Therapy Studies 11, 12, 13A, 13B, and 14 for childhood acute lymphoblastic leukemia. *Leukemia* **24,** 371–82 (2010).
303. Goldstone, A. H. *et al.* In adults with standard-risk acute lymphoblastic leukemia, the greatest benefit is achieved from a matched sibling allogeneic transplantation in first complete remission, and an autologous transplantation is less effective than conventional consolidation/maintenance chemotherapy in all patients: final

results of the International ALL Trial (MRC UKALL XII/ECOG E2993). *Blood* **111,** 1827–33 (2008).

304. Ferrando, A. A. *et al.* Prognostic importance of TLX1 (HOX11) oncogene expression in adults with T-cell acute lymphoblastic leukaemia. *Lancet (London, England)* **363,** 535–6 (2004).
305. Mansour, M. R. *et al.* Oncogene regulation. An oncogenic super-enhancer formed through somatic mutation of a noncoding intergenic element. *Science* **346,** 1373–7 (2014).
306. Van Vlierberghe, P. *et al.* The recurrent SET-NUP214 fusion as a new HOXA activation mechanism in pediatric T-cell acute lymphoblastic leukemia. *Blood* **111,** 4668–4680 (2008).
307. Bar-Eli, M., Ahuja, H., Foti, A. & Cline, M. J. N-RAS mutations in T-cell acute lymphocytic leukaemia: analysis by direct sequencing detects a novel mutation. *Br. J. Haematol.* **72,** 36–9 (1989).
308. Zhang, J. *et al.* The genetic basis of early T-cell precursor acute lymphoblastic leukaemia. *Nature* **481,** 157–63 (2012).
309. Gutierrez, A. *et al.* The BCL11B tumor suppressor is mutated across the major molecular subtypes of T-cell acute lymphoblastic leukemia. *Blood* **118,** 4169–73 (2011).
310. Hebert, J., Cayuela, J. M., Berkeley, J. & Sigaux, F. Candidate tumor-suppressor genes MTS1 (p16INK4A) and MTS2 (p15INK4B) display frequent homozygous deletions in primary cells from T- but not from B-cell lineage acute lymphoblastic leukemias. *Blood* **84,** 4038–44 (1994).
311. De Keersmaecker, K. *et al.* Exome sequencing identifies mutation in CNOT3 and ribosomal genes RPL5 and RPL10 in T-cell acute lymphoblastic leukemia. *Nat. Genet.* **45,** 186–90 (2013).
312. Weng, A. P. *et al.* Activating mutations of NOTCH1 in human T cell acute lymphoblastic leukemia. *Science* **306,** 269–71 (2004).
313. Felli, M. P. *et al.* Expression pattern of notch1, 2 and 3 and Jagged1 and 2 in lymphoid and stromal thymus components: distinct ligand-receptor interactions in intrathymic T cell development. *Int. Immunol.* **11,** 1017–25 (1999).
314. Pui, J. C. *et al.* Notch1 expression in early lymphopoiesis influences B versus T lineage determination. *Immunity* **11,** 299–308 (1999).
315. Radtke, F. *et al.* Deficient T cell fate specification in mice with an induced

inactivation of Notch1. *Immunity* **10,** 547–58 (1999).

316. Artavanis-Tsakonas, S., Rand, M. D. & Lake, R. J. Notch signaling: cell fate control and signal integration in development. *Science* **284,** 770–6 (1999).
317. Raya, A. *et al.* Notch activity acts as a sensor for extracellular calcium during vertebrate left-right determination. *Nature* **427,** 121–8 (2004).
318. Rebay, I. *et al.* Specific EGF repeats of Notch mediate interactions with Delta and Serrate: implications for Notch as a multifunctional receptor. *Cell* **67,** 687–99 (1991).
319. Gordon, W. R. *et al.* Structural basis for autoinhibition of Notch. *Nat. Struct. Mol. Biol.* **14,** 295–300 (2007).
320. Sanchez-Irizarry, C. *et al.* Notch subunit heterodimerization and prevention of ligand-independent proteolytic activation depend, respectively, on a novel domain and the LNR repeats. *Mol. Cell. Biol.* **24,** 9265–73 (2004).
321. Fortini, M. E. & Artavanis-Tsakonas, S. The suppressor of hairless protein participates in notch receptor signaling. *Cell* **79,** 273–82 (1994).
322. Tamura, K. *et al.* Physical interaction between a novel domain of the receptor Notch and the transcription factor RBP-J kappa/Su(H). *Curr. Biol.* **5,** 1416–23 (1995).
323. Gupta-Rossi, N. *et al.* Functional interaction between SEL-10, an F-box protein, and the nuclear form of activated Notch1 receptor. *J. Biol. Chem.* **276,** 34371–8 (2001).
324. Oberg, C. *et al.* The Notch intracellular domain is ubiquitinated and negatively regulated by the mammalian Sel-10 homolog. *J. Biol. Chem.* **276,** 35847–53 (2001).
325. Aster, J. *et al.* Functional analysis of the TAN-1 gene, a human homolog of Drosophila notch. *Cold Spring Harb. Symp. Quant. Biol.* **59,** 125–36 (1994).
326. Ellisen, L. W. *et al.* TAN-1, the human homolog of the Drosophila notch gene, is broken by chromosomal translocations in T lymphoblastic neoplasms. *Cell* **66,** 649–61 (1991).
327. Purow, B. W. *et al.* Expression of Notch-1 and Its Ligands, Delta-Like-1 and Jagged-1, Is Critical for Glioma Cell Survival and Proliferation. *Cancer Res.* **65,** 2353–2363 (2005).
328. Sikandar, S. S. *et al.* NOTCH signaling is required for formation and self-renewal of tumor-initiating cells and for repression of secretory cell differentiation in colon

cancer. *Cancer Res.* **70,** 1469–78 (2010).

329. Maraver, A. *et al.* NOTCH pathway inactivation promotes bladder cancer progression. *J. Clin. Invest.* **125,** 824–30 (2015).
330. Nicolas, M. *et al.* Notch1 functions as a tumor suppressor in mouse skin. *Nat. Genet.* **33,** 416–21 (2003).
331. Sriuranpong, V. *et al.* Notch signaling induces cell cycle arrest in small cell lung cancer cells. *Cancer Res.* **61,** 3200–5 (2001).
332. Rampias, T. *et al.* A new tumor suppressor role for the Notch pathway in bladder cancer. *Nat. Med.* **20,** 1199–205 (2014).
333. De Strooper, B. *et al.* A presenilin-1-dependent gamma-secretase-like protease mediates release of Notch intracellular domain. *Nature* **398,** 518–22 (1999).
334. Schroeter, E. H., Kisslinger, J. A. & Kopan, R. Notch-1 signalling requires ligand-induced proteolytic release of intracellular domain. *Nature* **393,** 382–6 (1998).
335. Seegar, T. C. M. *et al.* Structural Basis for Regulated Proteolysis by the α-Secretase ADAM10. *Cell* **171,** 1638–1648.e7 (2017).
336. Struhl, G. & Greenwald, I. Presenilin is required for activity and nuclear access of Notch in Drosophila. *Nature* **398,** 522–5 (1999).
337. Lu, F. M. & Lux, S. E. Constitutively active human Notch1 binds to the transcription factor CBF1 and stimulates transcription through a promoter containing a CBF1-responsive element. *Proc. Natl. Acad. Sci. U. S. A.* **93,** 5663–7 (1996).
338. Wu, L. *et al.* MAML1, a human homologue of Drosophila mastermind, is a transcriptional co-activator for NOTCH receptors. *Nat. Genet.* **26,** 484–9 (2000).
339. Bailey, A. M. & Posakony, J. W. Suppressor of hairless directly activates transcription of enhancer of split complex genes in response to Notch receptor activity. *Genes Dev.* **9,** 2609–22 (1995).
340. Jarriault, S. *et al.* Signalling downstream of activated mammalian Notch. *Nature* **377,** 355–8 (1995).
341. Palomero, T. *et al.* NOTCH1 directly regulates c-MYC and activates a feed-forward-loop transcriptional network promoting leukemic cell growth. *Proc. Natl. Acad. Sci. U. S. A.* **103,** 18261–6 (2006).
342. Dongre, A. *et al.* Non-Canonical Notch Signaling Drives Activation and Differentiation of Peripheral CD4(+) T Cells. *Front. Immunol.* **5,** 54 (2014).
343. Jin, S. *et al.* Non-canonical Notch signaling activates IL-6/JAK/STAT signaling in

breast tumor cells and is controlled by p53 and IKKα/IKKβ. *Oncogene* **32,** 4892–902 (2013).

344. Lee, K.-S. *et al.* Roles of PINK1, mTORC2, and mitochondria in preserving brain tumor-forming stem cells in a noncanonical Notch signaling pathway. *Genes Dev.* **27,** 2642–7 (2013).
345. Liao, W.-R. *et al.* The CBF1-independent Notch1 signal pathway activates human c-myc expression partially via transcription factor YY1. *Carcinogenesis* **28,** 1867–76 (2007).
346. Glittenberg, M., Pitsouli, C., Garvey, C., Delidakis, C. & Bray, S. Role of conserved intracellular motifs in Serrate signalling, cis-inhibition and endocytosis. *EMBO J.* **25,** 4697–706 (2006).
347. Henderson, S. T., Gao, D., Christensen, S. & Kimble, J. Functional domains of LAG-2, a putative signaling ligand for LIN-12 and GLP-1 receptors in Caenorhabditis elegans. *Mol. Biol. Cell* **8,** 1751–62 (1997).
348. Parks, A. L. *et al.* Structure-function analysis of delta trafficking, receptor binding and signaling in Drosophila. *Genetics* **174,** 1947–61 (2006).
349. de Celis, J. F. & Bray, S. Feed-back mechanisms affecting Notch activation at the dorsoventral boundary in the Drosophila wing. *Development* **124,** 3241–51 (1997).
350. Fleming, R. J. *et al.* An extracellular region of Serrate is essential for ligand-induced cis-inhibition of Notch signaling. *Development* **140,** 2039–49 (2013).
351. LeBon, L., Lee, T. V, Sprinzak, D., Jafar-Nejad, H. & Elowitz, M. B. Fringe proteins modulate Notch-ligand cis and trans interactions to specify signaling states. *Elife* **3,** (2014).
352. Palmer, W. H., Jia, D. & Deng, W.-M. Cis-interactions between Notch and its ligands block ligand-independent Notch activity. *Elife* **3,** (2014).
353. Seugnet, L., Simpson, P. & Haenlin, M. Requirement for dynamin during Notch signaling in Drosophila neurogenesis. *Dev. Biol.* **192,** 585–98 (1997).
354. Thompson, B. J. *et al.* Tumor suppressor properties of the ESCRT-II complex component Vps25 in Drosophila. *Dev. Cell* **9,** 711–20 (2005).
355. Vaccari, T., Lu, H., Kanwar, R., Fortini, M. E. & Bilder, D. Endosomal entry regulates Notch receptor activation in Drosophila melanogaster. *J. Cell Biol.* **180,** 755–62 (2008).
356. Acar, M. *et al.* Rumi Is a CAP10 Domain Glycosyltransferase that Modifies Notch

and Is Required for Notch Signaling. *Cell* **132,** 247–258 (2008).

357. Okajima, T. & Irvine, K. D. Regulation of notch signaling by o-linked fucose. *Cell* **111,** 893–904 (2002).
358. Luca, V. C. *et al.* Notch-Jagged complex structure implicates a catch bond in tuning ligand sensitivity. *Science* **355,** 1320–1324 (2017).
359. Logeat, F. *et al.* The Notch1 receptor is cleaved constitutively by a furin-like convertase. *Proc. Natl. Acad. Sci. U. S. A.* **95,** 8108–12 (1998).
360. Panin, V. M., Papayannopoulos, V., Wilson, R. & Irvine, K. D. Fringe modulates Notch-ligand interactions. *Nature* **387,** 908–12 (1997).
361. Schneider, M. *et al.* Inhibition of Delta-induced Notch signaling using fucose analogs. *Nat. Chem. Biol.* **14,** 65–71 (2018).
362. Foltz, D. R., Santiago, M. C., Berechid, B. E. & Nye, J. S. Glycogen synthase kinase-3beta modulates notch signaling and stability. *Curr. Biol.* **12,** 1006–11 (2002).
363. Gupta-Rossi, N. *et al.* Monoubiquitination and endocytosis direct gamma-secretase cleavage of activated Notch receptor. *J. Cell Biol.* **166,** 73–83 (2004).
364. Fryer, C. J., White, J. B. & Jones, K. A. Mastermind recruits CycC:CDK8 to phosphorylate the Notch ICD and coordinate activation with turnover. *Mol. Cell* **16,** 509–20 (2004).
365. Tsunematsu, R. *et al.* Mouse Fbw7/Sel-10/Cdc4 is required for notch degradation during vascular development. *J. Biol. Chem.* **279,** 9417–23 (2004).
366. Wu, G. *et al.* SEL-10 is an inhibitor of notch signaling that targets notch for ubiquitin-mediated protein degradation. *Mol. Cell. Biol.* **21,** 7403–15 (2001).
367. Yeh, C.-H., Bellon, M., Pancewicz-Wojtkiewicz, J. & Nicot, C. Oncogenic mutations in the FBXW7 gene of adult T-cell leukemia patients. *Proc. Natl. Acad. Sci. U. S. A.* **113,** 6731–6 (2016).
368. Akhoondi, S. *et al.* FBXW7/hCDC4 is a general tumor suppressor in human cancer. *Cancer Res.* **67,** 9006–12 (2007).
369. King, B. *et al.* The ubiquitin ligase FBXW7 modulates leukemia-initiating cell activity by regulating MYC stability. *Cell* **153,** 1552–66 (2013).
370. Yada, M. *et al.* Phosphorylation-dependent degradation of c-Myc is mediated by the F-box protein Fbw7. *EMBO J.* **23,** 2116–25 (2004).
371. Kumar, V. *et al.* Notch and NF-kB signaling pathways regulate miR-223/FBXW7 axis in T-cell acute lymphoblastic leukemia. *Leukemia* **28,** 2324–35 (2014).

372. Thompson, B. J. *et al.* Control of hematopoietic stem cell quiescence by the E3 ubiquitin ligase Fbw7. *J. Exp. Med.* **205,** 1395–408 (2008).
373. Weng, A. P. *et al.* c-Myc is an important direct target of Notch1 in T-cell acute lymphoblastic leukemia/lymphoma. *Genes Dev.* **20,** 2096–109 (2006).
374. Bonnet, M. *et al.* Posttranscriptional deregulation of MYC via PTEN constitutes a major alternative pathway of MYC activation in T-cell acute lymphoblastic leukemia. *Blood* **117,** 6650–9 (2011).
375. Ortega, M. *et al.* A microRNA-mediated regulatory loop modulates NOTCH and MYC oncogenic signals in B- and T-cell malignancies. *Leukemia* **29,** 968–76 (2015).
376. Demarest, R. M., Dahmane, N. & Capobianco, A. J. Notch is oncogenic dominant in T-cell acute lymphoblastic leukemia. *Blood* **117,** 2901–2909 (2011).
377. Murata, K. *et al.* Hes1 directly controls cell proliferation through the transcriptional repression of p27Kip1. *Mol. Cell. Biol.* **25,** 4262–71 (2005).
378. Sang, L., Coller, H. A. & Roberts, J. M. Control of the reversibility of cellular quiescence by the transcriptional repressor HES1. *Science* **321,** 1095–100 (2008).
379. Schnell, S. A. *et al.* Therapeutic targeting of HES1 transcriptional programs in T-ALL. *Blood* **125,** 2806–14 (2015).
380. Wendorff, A. A. *et al.* Hes1 Is a Critical but Context-Dependent Mediator of Canonical Notch Signaling in Lymphocyte Development and Transformation. *Immunity* **33,** 671–684 (2010).
381. Palomero, T. *et al.* Mutational loss of PTEN induces resistance to NOTCH1 inhibition in T-cell leukemia. *Nat. Med.* **13,** 1203–10 (2007).
382. D'Altri, T., Gonzalez, J., Aifantis, I., Espinosa, L. & Bigas, A. Hes1 expression and CYLD repression are essential events downstream of Notch1 in T-cell leukemia. *Cell Cycle* **10,** 1031–6 (2011).
383. Espinosa, L. *et al.* The Notch/Hes1 pathway sustains NF-κB activation through CYLD repression in T cell leukemia. *Cancer Cell* **18,** 268–81 (2010).
384. Vilimas, T. *et al.* Targeting the NF-kappaB signaling pathway in Notch1-induced T-cell leukemia. *Nat. Med.* **13,** 70–7 (2007).
385. Zenatti, P. P. *et al.* Oncogenic IL7R gain-of-function mutations in childhood T-cell acute lymphoblastic leukemia. *Nat. Genet.* **43,** 932–9 (2011).
386. Flex, E. *et al.* Somatically acquired JAK1 mutations in adult acute lymphoblastic

leukemia. *J. Exp. Med.* **205,** 751–8 (2008).

387. González-García, S. *et al.* CSL-MAML-dependent Notch1 signaling controls T lineage-specific IL-7R{alpha} gene expression in early human thymopoiesis and leukemia. *J. Exp. Med.* **206,** 779–91 (2009).
388. Dibirdik, I. *et al.* Engagement of interleukin-7 receptor stimulates tyrosine phosphorylation, phosphoinositide turnover, and clonal proliferation of human T-lineage acute lymphoblastic leukemia cells. *Blood* **78,** 564–70 (1991).
389. Joshi, I. *et al.* Notch signaling mediates G1/S cell-cycle progression in T cells via cyclin D3 and its dependent kinases. *Blood* **113,** 1689–98 (2009).
390. Dohda, T. *et al.* Notch signaling induces SKP2 expression and promotes reduction of p27Kip1 in T-cell acute lymphoblastic leukemia cell lines. *Exp. Cell Res.* **313,** 3141–52 (2007).
391. Bretones, G., Delgado, M. D. & León, J. Myc and cell cycle control. *Biochim. Biophys. Acta* **1849,** 506–16 (2015).
392. Bi, P. & Kuang, S. Notch signaling as a novel regulator of metabolism. *Trends Endocrinol. Metab.* **26,** 248–55 (2015).
393. Herranz, D. *et al.* Metabolic reprogramming induces resistance to anti-NOTCH1 therapies in T cell acute lymphoblastic leukemia. *Nat. Med.* **21,** 1182–9 (2015).
394. Landor, S. K.-J. *et al.* Hypo- and hyperactivated Notch signaling induce a glycolytic switch through distinct mechanisms. *Proc. Natl. Acad. Sci. U. S. A.* **108,** 18814–9 (2011).
395. Jitschin, R. *et al.* Stromal cell-mediated glycolytic switch in CLL cells involves Notch-c-Myc signaling. *Blood* **125,** 3432–3436 (2015).
396. Basak, N. P., Roy, A. & Banerjee, S. Alteration of mitochondrial proteome due to activation of Notch1 signaling pathway. *J. Biol. Chem.* **289,** 7320–34 (2014).
397. Avellino, R. *et al.* Rapamycin stimulates apoptosis of childhood acute lymphoblastic leukemia cells. *Blood* **106,** 1400–6 (2005).
398. Gutierrez, A. *et al.* High frequency of PTEN, PI3K, and AKT abnormalities in T-cell acute lymphoblastic leukemia. *Blood* **114,** 647–50 (2009).
399. Cardoso, B. A. *et al.* Interleukin-4 stimulates proliferation and growth of T-cell acute lymphoblastic leukemia cells by activating mTOR signaling. *Leukemia* **23,** 206–8 (2009).
400. Silva, A. *et al.* Intracellular reactive oxygen species are essential for PI3K/Akt/mTOR-dependent IL-7-mediated viability of T-cell acute lymphoblastic

leukemia cells. *Leukemia* **25,** 960–7 (2011).

401. Hoshii, T. *et al.* Loss of mTOR complex 1 induces developmental blockage in early T-lymphopoiesis and eradicates T-cell acute lymphoblastic leukemia cells. *Proc. Natl. Acad. Sci. U. S. A.* **111,** 3805–10 (2014).
402. Bressanin, D. *et al.* Harnessing the PI3K/Akt/mTOR pathway in T-cell acute lymphoblastic leukemia: eliminating activity by targeting at different levels. *Oncotarget* **3,** 811–23 (2012).
403. Chiarini, F. *et al.* Dual inhibition of class IA phosphatidylinositol 3-kinase and mammalian target of rapamycin as a new therapeutic option for T-cell acute lymphoblastic leukemia. *Cancer Res.* **69,** 3520–8 (2009).
404. Evangelisti, C. *et al.* Targeted inhibition of mTORC1 and mTORC2 by active-site mTOR inhibitors has cytotoxic effects in T-cell acute lymphoblastic leukemia. *Leukemia* **25,** 781–91 (2011).
405. Ma, J. *et al.* Mammalian target of rapamycin regulates murine and human cell differentiation through STAT3/p63/Jagged/Notch cascade. *J. Clin. Invest.* **120,** 103–14 (2010).
406. Bhola, N. E. *et al.* Treatment of Triple-Negative Breast Cancer with TORC1/2 Inhibitors Sustains a Drug-Resistant and Notch-Dependent Cancer Stem Cell Population. *Cancer Res.* **76,** 440–52 (2016).
407. Muellner, M. K. *et al.* A chemical-genetic screen reveals a mechanism of resistance to PI3K inhibitors in cancer. *Nat. Chem. Biol.* **7,** 787–93 (2011).
408. Shepherd, C. *et al.* PI3K/mTOR inhibition upregulates NOTCH-MYC signalling leading to an impaired cytotoxic response. *Leukemia* **27,** 650–60 (2013).
409. Song, J., Park, S., Kim, M. & Shin, I. Down-regulation of Notch-dependent transcription by Akt in vitro. *FEBS Lett.* **582,** 1693–9 (2008).
410. Mo, J.-S. *et al.* Serum- and glucocorticoid-inducible kinase 1 (SGK1) controls Notch1 signaling by downregulation of protein stability through Fbw7 ubiquitin ligase. *J. Cell Sci.* **124,** 100–12 (2011).
411. Espinosa, L., Inglés-Esteve, J., Aguilera, C. & Bigas, A. Phosphorylation by Glycogen Synthase Kinase-3β Down-regulates Notch Activity, a Link for Notch and Wnt Pathways. *J. Biol. Chem.* **278,** 32227–32235 (2003).
412. Guha, S. *et al.* Glycogen synthase kinase 3 beta positively regulates Notch signaling in vascular smooth muscle cells: role in cell proliferation and survival. *Basic Res. Cardiol.* **106,** 773–85 (2011).

413. Androutsellis-Theotokis, A. *et al.* Notch signalling regulates stem cell numbers in vitro and in vivo. *Nature* **442,** 823–6 (2006).
414. Mungamuri, S. K., Yang, X., Thor, A. D. & Somasundaram, K. Survival signaling by Notch1: mammalian target of rapamycin (mTOR)-dependent inhibition of p53. *Cancer Res.* **66,** 4715–24 (2006).
415. Efferson, C. L. *et al.* Downregulation of Notch pathway by a gamma-secretase inhibitor attenuates AKT/mammalian target of rapamycin signaling and glucose uptake in an ERBB2 transgenic breast cancer model. *Cancer Res.* **70,** 2476–84 (2010).
416. Pajvani, U. B. *et al.* Inhibition of Notch uncouples Akt activation from hepatic lipid accumulation by decreasing mTorc1 stability. *Nat. Med.* **19,** 1054–60 (2013).
417. Chan, S. M., Weng, A. P., Tibshirani, R., Aster, J. C. & Utz, P. J. Notch signals positively regulate activity of the mTOR pathway in T-cell acute lymphoblastic leukemia. *Blood* **110,** 278–86 (2007).
418. Cullion, K. *et al.* Targeting the Notch1 and mTOR pathways in a mouse T-ALL model. *Blood* **113,** 6172–81 (2009).
419. Kahlert, U. D. *et al.* Alterations in cellular metabolome after pharmacological inhibition of Notch in glioblastoma cells. *Int. J. cancer* **138,** 1246–55 (2016).
420. Swamy, M. *et al.* Glucose and glutamine fuel protein O-GlcNAcylation to control T cell self-renewal and malignancy. *Nat. Immunol.* **17,** 712–20 (2016).
421. Palomero, T. *et al.* CUTLL1, a novel human T-cell lymphoma cell line with t(7;9) rearrangement, aberrant NOTCH1 activation and high sensitivity to gamma-secretase inhibitors. *Leukemia* **20,** 1279–87 (2006).
422. De Keersmaecker, K. *et al.* In vitro validation of gamma-secretase inhibitors alone or in combination with other anti-cancer drugs for the treatment of T-cell acute lymphoblastic leukemia. *Haematologica* **93,** 533–42 (2008).
423. Milano, J. *et al.* Modulation of notch processing by gamma-secretase inhibitors causes intestinal goblet cell metaplasia and induction of genes known to specify gut secretory lineage differentiation. *Toxicol. Sci.* **82,** 341–58 (2004).
424. van Es, J. H. *et al.* Notch/gamma-secretase inhibition turns proliferative cells in intestinal crypts and adenomas into goblet cells. *Nature* **435,** 959–63 (2005).
425. Tammam, J. *et al.* Down-regulation of the Notch pathway mediated by a gamma-secretase inhibitor induces anti-tumour effects in mouse models of T-cell leukaemia. *Br. J. Pharmacol.* **158,** 1183–95 (2009).

426. Rao, S. S. *et al.* Inhibition of NOTCH signaling by gamma secretase inhibitor engages the RB pathway and elicits cell cycle exit in T-cell acute lymphoblastic leukemia cells. *Cancer Res.* **69,** 3060–8 (2009).
427. Thompson, B. J. *et al.* The SCFFBW7 ubiquitin ligase complex as a tumor suppressor in T cell leukemia. *J. Exp. Med.* **204,** 1825–35 (2007).
428. Agnusdei, V. *et al.* Therapeutic antibody targeting of Notch1 in T-acute lymphoblastic leukemia xenografts. *Leukemia* **28,** 278–88 (2014).
429. Qiu, M. *et al.* Specific inhibition of Notch1 signaling enhances the antitumor efficacy of chemotherapy in triple negative breast cancer through reduction of cancer stem cells. *Cancer Lett.* **328,** 261–70 (2013).
430. Wu, Y. *et al.* Therapeutic antibody targeting of individual Notch receptors. *Nature* **464,** 1052–7 (2010).
431. Aste-Amézaga, M. *et al.* Characterization of Notch1 antibodies that inhibit signaling of both normal and mutated Notch1 receptors. *PLoS One* **5,** e9094 (2010).
432. Noguera-Troise, I. *et al.* Blockade of Dll4 inhibits tumour growth by promoting non-productive angiogenesis. *Nature* **444,** 1032–7 (2006).
433. Ridgway, J. *et al.* Inhibition of Dll4 signalling inhibits tumour growth by deregulating angiogenesis. *Nature* **444,** 1083–7 (2006).
434. Scehnet, J. S. *et al.* Inhibition of Dll4-mediated signaling induces proliferation of immature vessels and results in poor tissue perfusion. *Blood* **109,** 4753–60 (2007).
435. Moellering, R. E. *et al.* Direct inhibition of the NOTCH transcription factor complex. *Nature* **462,** 182–8 (2009).
436. Pinnell, N. *et al.* The PIAS-like Coactivator Zmiz1 Is a Direct and Selective Cofactor of Notch1 in T Cell Development and Leukemia. *Immunity* **43,** 870–883 (2015).
437. He, Y., Chen, D. & Zheng, W. An enhanced functional interrogation/manipulation of intracellular signaling pathways with the peptide ‘stapling’ technology. *Oncogene* **34,** 5685–98 (2015).
438. Loosveld, M. *et al.* Therapeutic targeting of c-Myc in T-cell acute lymphoblastic leukemia, T-ALL. *Oncotarget* **5,** 3168–72 (2014).
439. Roderick, J. E. *et al.* c-Myc inhibition prevents leukemia initiation in mice and impairs the growth of relapsed and induction failure pediatric T-ALL cells. *Blood*

123, 1040–50 (2014).

440. Wolfe, A. L. *et al.* RNA G-quadruplexes cause eIF4A-dependent oncogene translation in cancer. *Nature* **513,** 65–70 (2014).
441. Medyouf, H. *et al.* High-level IGF1R expression is required for leukemia-initiating cell activity in T-ALL and is supported by Notch signaling. *J. Exp. Med.* **208,** 1809–22 (2011).
442. Fassl, A. *et al.* Notch1 signaling promotes survival of glioblastoma cells via EGFR-mediated induction of anti-apoptotic Mcl-1. *Oncogene* **31,** 4698–708 (2012).

ANNEXES

During my thesis, I have participated also to other publications of the team and have presented my projects in different conferences. Please find enclosed all the publications that I have contributed.

1. **Escaping mTOR inhibition for cancer therapy: Tumor suppressor functions of mTOR**. *Mol Cell Oncol. 2017 Mar 3;4(3):e1297284*.

   Villar VH, Nguyen TL, Terés S, Bodineau C, Durán RV.

   This comment highlighted the tumor suppressor role of mTORC1, which is a well-known tumor promoter. Thus, this observation explained the modest results of rapamycin obtained in the clinic by inhibiting mTORC1. In other words, mTORC1-mediated glutamoptosis could be a potential alternative to improve the outcome of mTORC1-targeted therapy.

2. **mTORC1 inhibition in cancer cells protects from glutaminolysis-mediated apoptosis during nutrient limitation**. *Nat Commun. 2017 Jan 23;8:14124.*

   Villar VH, Nguyen TL, Delcroix V, Terés S, Bouchecareilh M, Salin B, Bodineau C, Vacher, P, Priault M, Soubeyran P, Durán RV.

   This work described the tumor suppressor role of mTORC1 during nutrient restrictive conditions. Indeed, anomalous activation of mTORC1 by glutaminolysis upon amino acid starvation inhibited autophagy, which leads to an accumulation of p62 and an activation of apoptosis through the interaction of p62 and caspase 8.

3. **Metabolic Transformation in Notch-Driven Acute Lymphoblastic Leukemia**. *J Mol Med Clin Appl 1(1): doi http://dx.doi.org/10.16966/ijmbm.102.*

   Terés S, Nguyen TL, Durán RV.

   This mini review made a summarize about the upregulation of Notch1 signaling in T-cell acute lymphoblastic leukemia and its consequences into cancer cell growth and cancer metabolism.

4. **Prolyl hydroxylase domain enzymes and their role in cell signaling and cancer metabolism**. *Int J Biochem Cell Biol. 2016 Nov;80:71-80*.

   Nguyen TL & Durán RV.

   This review made a state-of-the-art of the roles of the prolyl hydroxylase domain enzymes in the control of different cellular pathways and also its regulation in cancer signaling and cell metabolism.

MOLECULAR & CELLULAR ONCOLOGY
2017, VOL. 4, NO. 3, e1297284 (2 pages)
https://doi.org/10.1080/23723556.2017.1297284

Taylor & Francis
Taylor & Francis Group

AUTHOR'S VIEW

OPEN ACCESS Check for updates

Escaping mTOR inhibition for cancer therapy: Tumor suppressor functions of mTOR

Victor H. Villar[a,b,c], Tra Ly Nguyen[a,b,c], Silvia Terés[a,b,c], Clément Bodineau[a,b,c], and Raúl V. Durán[a,b,c]

[a]Institut Européen de Chimie et Biologie, Pessac, France; [b]Institut Bergonié, ACTION Unit U1218 INSERM, Bordeaux, France; [c]University of Bordeaux, Bordeaux, France

ABSTRACT
A master promoter of cell growth, mammalian target of rapamycin (mTOR) is upregulated in a large percentage of cancer cells. Still, targeting mTOR using rapamycin has a limited outcome in patients. Our recent results highlight the additional role of mTOR as a tumor suppressor, explaining these modest results in the clinic.

ARTICLE HISTORY
Received 13 February 2017
Revised 16 February 2017
Accepted 16 February 2017

KEYWORDS
α-ketoglutarate; autophagy; cancer metabolism; glutamoptosis; mTORC1; rapamycin

The serine/threonine kinase mammalian target of rapamycin (mTOR) is a central regulator of mammalian cell growth. mTOR forms 2 complexes, termed mTOR complex 1 (mTORC1) and mTOR complex 2 (mTORC2). While both complexes are stimulated by growth factors, only mTORC1 can be activated by amino acids ([1]Cell Res). Particularly, the catabolism of glutamine (glutaminolysis), which yields α-ketoglutarate (αKG), activates the lysosomal translocation and subsequent activation of mTORC1 ([2]Mol Cell). Recently, our work revealed an unexpected mechanism by which the unbalanced activation of glutaminolysis in the absence of other amino acids induces a particular type of mTORC1-dependent cell death that we are naming "glutamoptosis" ([3]Nat Comm). During glutamoptosis, abnormally high levels of glutaminolytic αKG during nutrient restriction activates mTORC1, which in turn inhibits autophagy ([4]Autophagy). The inhibition of autophagy during glutamoptosis results in the accumulation of the autophagic protein sequestosome 1 (SQSTM1/p62), as SQSTM1/p62 is degraded during autophagy ([5]Cell). Our results showed that the increasing levels of SQSTM1/p62 in these restrictive conditions induce its interaction with caspase 8 to trigger apoptosis. The inhibition of mTORC1 reactivates autophagy and decreases SQSTM1/p62 levels, abrogating the induction of apoptosis by glutaminolysis. Thus, surprisingly, the inhibition of mTORC1 prevents glutamoptosis-mediated cell death, representing a tumor suppressor function of mTORC1 during nutritional imbalance.

For a long time, mTORC1 is known to be hyperactive in a large variety of different types of human cancer ([6]Cell). Therefore, this pathway has been considered as a major target for cancer therapy. However, for unclear reasons, the inhibition of mTORC1 as a therapeutic strategy has only modestly improved the outcome of patients ([7]N Engl J Med). Several reasons have been invoked to explain this lack of success in the use of rapamycin and analogues (rapalogues) in the clinic. The most accepted reason is the existence of a negative feedback loop downstream of mTORC1 which, upon its inhibition, upregulates the phosphoinositide 3-kinase (PI3K) signaling ([8]Curr Biol). The upregulation of the PI3K pathway would result in a deleterious effect of rapamycin treatment, as it promotes cancer growth, including the activation of mTORC2. To overcome this issue, dual inhibitors targeting both mTOR complexes have been designed, although it is unclear that they can actually improve the outcome of rapamycin in patients.

Our recent results suggest that additional fundamental reasons might explain the capacity of cancer cells to escape rapamycin treatment. As explained above, the inhibition of mTORC1 or the dual inhibition of both mTORC1 and mTORC2 during nutritional imbalance prevents glutamoptosis and promotes cell survival. Considering the restrictive nature of tumors (particularly solid tumors) due to their abnormal vasculature, and their general avidity to consume glutamine, tumors might constitute favorable microenvironments to induce glutamoptosis. In these conditions, the inhibition of mTORC1 during cancer therapy would prevent tumor growth, but at the same time would provide with an opportunity to cancer cells to avoid cell death. In other words, rapamycin treatment will result in a merely cytostatic effect, sustaining the survival of tumor cells. Upon treatment discontinuation, tumors will resume their growth. As a result, cancer progression will be only delayed during the period of rapamycin treatment or until the acquisition of rapamycin resistance mechanism by the cytostatic tumor cell.

These tumor suppressor functions of mTORC1 highlight the complexity of the action mechanisms of central cell growth regulators, such as mTOR, and how microenvironmental cues influence their function (Fig. 1). The assumption that the inhibition of these cell growth regulators will inevitably result in

CONTACT Raúl V. Durán raul.duran@inserm.fr Institut Européen de Chimie et Biologie, 2 Rue Robert Escarpit, 33607 Pessac, France.

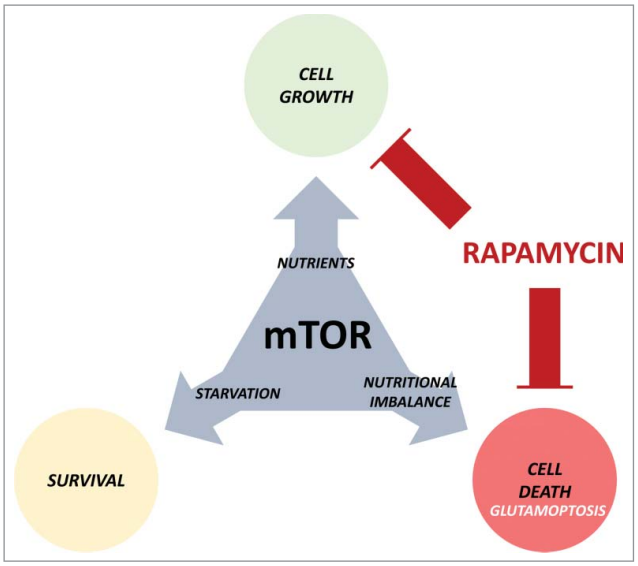

Figure 1. The many faces of the mammalian target of rapamycin (mTOR). mTOR promotes cell growth during nutrient availability, and its inactivation allows cell survival in nutrient-restrictive conditions. However, its anomalous activation induces cell death (glutamoptosis). Rapamycin treatment blocks cell growth, but at the same time guarantees cell survival during nutritional imbalance, a detrimental effect for cancer therapy.

the arrest of tumor growth seems to be a too simplistic view of the complex mechanism of cell growth control. Further, it confirms that strategies to beat cancer based on targeted monotherapies, at least in the case of mTOR, will probably require further reconsideration to mitigate those adverse consequences. In the case of glutamoptosis, our results indicated that the re-stimulation of autophagy mediates the pre-survival effect of rapamycin. Thus, it can be envisioned that autophagy inhibition could certainly improve the outcome of rapamycin treatment by re-activating glutamoptosis. Indeed, treatments targeting both mTOR signaling and autophagy have been previously proposed and are already under clinical evaluation ([9]Autophagy). The lack of efficient and specific inhibitors of autophagy is a major limitation for the implementation of this strategy. The central role played by the autophagic protein SQSTM1/p62 during glutamoptosis and its close connection with mTORC1 suggest that SQSTM1/p62 upregulation might be a key element to overcome rapamycin-mediated cell survival. Our results already indicate that SQSTM1/p62 upregulation can indeed induce cell death even in rapamycin-treated cells.

Finally, our results open a new opportunity to explore the translational involvement of glutamoptosis for cancer therapy. In other words, can we induce glutamoptosis in tumors to specifically kill cancer cells? Microenvironments with a high concentration glutamine, or tumor types with a particular avidity for glutamine, might be particularly sensitive to glutamoptosis. Simulating glutaminolysis by artificially increasing the intracellular levels of αKG is known to induce tumor cell death *in vivo* ([10]Oncogene), although the involvement of mTORC1 and SQSTM1/p62 in this phenotype remains elusive.

In conclusion, the tumor suppressor function of mTORC1 during nutritional imbalance points at the necessity of finding alternatives to improve the outcome of mTORC1 inhibition in the clinics and questions the pertinence of the use of rapamycin as monotherapy in cancer patients.

Disclosure of potential conflicts of interest

No potential conflicts of interest were disclosed.

Funding

This work was supported by funds from the following institutions: Institut National de la Santé et de la Recherche Médicale - INSERM, Fondation pour la Recherche Médicale, Conseil Régional d'Aquitaine, Fondation ARC pour la Recherche sur le Cancer, SIRIC-BRIO, and Institut Européen de Chimie et Biologie.

References

1. Shimobayashi M, Hall MN. Multiple amino acid sensing inputs to mTORC1. Cell Res 2016; 26:7-20; PMID:26658722; https://doi.org/10.1038/cr.2015.146
2. Durán RV, Oppliger W, Robitaille AM, Heiserich L, Skendaj R, Gottlieb E, Hall MN. Glutaminolysis activates Rag-mTORC1 signaling. Mol Cell 2012; 47:349-58; PMID:22749528; https://doi.org/10.1016/j.molcel.2012.05.043
3. Villar VH, Nguyen TL, Delcroix V, Terés S, Bouchecareilh M, Salin B, Bodineau C, Vacher P, Priault M, Soubeyran P, et al. mTORC1 inhibition in cancer cells protects from glutaminolysis-mediated apoptosis during nutrient limitation. Nature Comm 2017; 8:14124; https://doi.org/10.1038/ncomms14124
4. Villar VH, Merhi F, Djavaheri-Mergny M, Durán RV. Glutaminolysis and autophagy in cancer. Autophagy 2015; 11:1198-208; PMID:26054373; https://doi.org/10.1080/15548627.2015.1053680
5. Moscat J, Karin M, Diaz-Meco MT. p62 in Cancer: Signaling Adaptor Beyond Autophagy. Cell 2016; 167:606-9; PMID:27768885; https://doi.org/10.1016/j.cell.2016.09.030
6. Guertin DA, Sabatini DM. Defining the role of mTOR in cancer. Cancer Cell 2007; 12:9-22; PMID:17613433; https://doi.org/10.1016/j.ccr.2007.05.008
7. Hudes G, Carducci M, Tomczak P, Dutcher J, Figlin R, Kapoor A, Staroslawska E, Sosman J, McDermott D, Bodrogi I, et al. Temsirolimus, interferon alfa, or both for advanced renal-cell carcinoma. N Engl J Med 2007; 356:2271-81; PMID:17538086; https://doi.org/10.1056/NEJMoa066838
8. Shah OJ, Wang Z, Hunter T. Inappropriate activation of the TSC/Rheb/mTOR/S6K cassette induces IRS1/2 depletion, insulin resistance, and cell survival deficiencies. Curr Biol 2004; 14:1650-6; PMID:15380067; https://doi.org/10.1016/j.cub.2004.08.026
9. Rangwala R, Chang YC, Hu J, Algazy KM, Evans TL, Fecher LA, Schuchter LM, Torigian DA, Panosian JT, Troxel AB, et al. Combined MTOR and autophagy inhibition: phase I trial of hydroxychloroquine and temsirolimus in patients with advanced solid tumors and melanoma. Autophagy 2014; 10:1391-402; PMID:24991838; https://doi.org/10.4161/auto.29119
10. Tennant DA, Frezza C, MacKenzie ED, Nguyen QD, Zheng L, Selak MA, Roberts DL, Dive C, Watson DG, Aboagye EO, et al. Reactivating HIF prolyl hydroxylases under hypoxia results in metabolic catastrophe and cell death. Oncogene 2009; 28:4009-21; PMID:19718054; https://doi.org/10.1038/onc.2009.250

nature COMMUNICATIONS

ARTICLE

Received 20 Apr 2016 | Accepted 1 Dec 2016 | Published 23 Jan 2017

DOI: 10.1038/ncomms14124 OPEN

mTORC1 inhibition in cancer cells protects from glutaminolysis-mediated apoptosis during nutrient limitation

Victor H. Villar[1], Tra Ly Nguyen[1], Vanessa Delcroix[2], Silvia Terés[1], Marion Bouchecareilh[3], Bénédicte Salin[3], Clément Bodineau[1], Pierre Vacher[2], Muriel Priault[3], Pierre Soubeyran[2] & Raúl V. Durán[1]

A master coordinator of cell growth, mTORC1 is activated by different metabolic inputs, particularly the metabolism of glutamine (glutaminolysis), to control a vast range of cellular processes, including autophagy. As a well-recognized tumour promoter, inhibitors of mTORC1 such as rapamycin have been approved as anti-cancer agents, but their overall outcome in patients is rather poor. Here we show that mTORC1 also presents tumour suppressor features in conditions of nutrient restrictions. Thus, the activation of mTORC1 by glutaminolysis during nutritional imbalance inhibits autophagy and induces apoptosis in cancer cells. Importantly, rapamycin treatment reactivates autophagy and prevents the mTORC1-mediated apoptosis. We also observe that the ability of mTORC1 to activate apoptosis is mediated by the adaptor protein p62. Thus, the mTORC1-mediated upregulation of p62 during nutrient imbalance induces the binding of p62 to caspase 8 and the subsequent activation of the caspase pathway. Our data highlight the role of autophagy as a survival mechanism upon rapamycin treatment.

[1] Institut Européen de Chimie et Biologie, INSERM U1218, Université de Bordeaux, 2 Rue Robert Escarpit, Pessac 33607, France. [2] Institut Bergonié, INSERM U1218, 229 Cours de l'Argonne, Bordeaux 33076, France. [3] Institut de Biochimie et Génétique Cellulaires, CNRS UMR 5095, Université de Bordeaux, 1 Rue Camille Saint-Saëns, Bordeaux 33077, France. Correspondence and requests for materials should be addressed to R.V.D. (email: raul.duran@inserm.fr).

mTORC1 (mammalian target of rapamycin complex 1) is a highly conserved serine/threonine kinase complex that integrates several inputs, including amino acid availability, to regulate different cellular processes such as cell growth, anabolism and autophagy[1,2]. mTORC1 pathway is aberrantly activated in 80% of human cancers[3]. Thus, the inhibition of this pathway was considered a relevant approach to treat cancer. However, for still unclear reasons, rapamycin analogues have shown only modest effects in clinical trials[4–6]. Hence, understanding the molecular mechanism by which tumour cells escape from mTORC1 inhibition is a main objective to design new targeted therapies that efficiently eliminate cancer cells. As mTORC1 is strongly regulated by the metabolism of certain amino acids, particularly glutamine, leucine and arginine, there is an intense research nowadays to elucidate how the altered metabolism of amino acids during malignant transformation might play a role in mTORC1 upregulation and in rapamycin treatment resistance.

Glutamine is the most abundant amino acid in the blood and a nitrogen source for cells[7,8]. This amino acid has been described as a crucial nutrient for tumour proliferation, and indeed a vast number of different types of tumour cells consume abnormally high quantities of glutamine and develop glutamine addiction[9–12]. Glutamine is mostly degraded in the cell through glutaminolysis. Glutaminolysis comprises two-step enzymatic reactions, whereby glutamine is first deamidated to glutamate, in a reaction catalysed by glutaminase (GLS), and then glutamate is deaminated to α-ketoglutarate (αKG), in a reaction catalysed by glutamate dehydrogenase. In addition, leucine, another important amino acid from a signalling point of view, activates allosterically glutamate dehydrogenase and promotes the production of glutaminolitic αKG (refs 8,13). Therefore, leucine and glutamine cooperate to produce αKG, an intermediate of the tricarboxylic acid cycle. Besides this anaplerotic role of glutamine, glutaminolysis also activates mTORC1 pathway and inhibits macroautophagy[14]. Macroautophagy (hereafter simply autophagy) is a catabolic process regulated by mTORC1 pathway, through which lysosomal-degradation of cellular components provides cells with recycled nutrients[15–18].

Although it is known that glutaminolysis is a source to replenish tricarboxylic acid cycle and also activates mTORC1, the capacity of glutaminolysis to sustain mTORC1 activation and cell growth in the long term in the absence of other nitrogen sources has not been elucidated. Here we report that, surprisingly, the long-term activation of glutaminolysis in the absence of other amino acids induces the aberrant inhibition of autophagy in an mTORC1-dependent manner. This inhibition of autophagy during amino acid restriction led to apoptotic cell death due to the accumulation of the autophagic protein p62 and the subsequent activation of caspase 8. Of note, the inhibition of mTORC1 restores autophagy and blocks the apoptosis induced by glutaminolysis activation. Our results highlight the tumour suppressor features of mTORC1 during nutrient restriction and provide with an alternative explanation for the poor outcome obtained using mTORC1 inhibitors as an anticancer therapy.

Results

Long-term glutaminolysis decreased cell viability. As we have previously shown that short-term glutaminolysis (15–60 min) is sufficient and necessary to activate mTORC1 and to sustain cell growth (ref. 14), we first explored the capacity of glutaminolysis to serve as a metabolic fuel during amino acid starvation at long term in cancer cells. For the long-term activation of glutaminolysis, we added glutamine (the source of glutaminolysis) and leucine (the allosteric activator of glutaminolysis) to otherwise amino acid-starved cells as previously described[14], and the cells were incubated in these conditions during 24–72 h. As previously observed, the incubation of a panel of different cancer cell lines, including U2OS, A549 and JURKAT, in the absence of all amino acids arrested cell proliferation, but it did not affect cell viability significantly (Fig. 1a,b and Supplementary Fig. 1A). Strikingly, the activation of glutaminolysis by adding leucine and glutamine (LQ treatment) caused a strong decrease in the number of cells incubated in these conditions (Fig. 1a,b and Supplementary Fig. 1B). Similar results were obtained in HEK293 cells (Fig. 1a,b). To confirm whether this decrease in the number of cells was related to an increase in cell death or a decrease in cell proliferation, we measured the percentage of cell death using the trypan blue exclusion assay, and we determined cell viability using a clonogenic assay. We observed that glutaminolysis activation using LQ treatment increased the percentage of cell death in all the tested cell lines (Fig. 1c and Supplementary Fig. 1C). In addition, LQ treatment during amino acid restriction strongly reduced the number of colonies formed in a clonogenic assay (Fig. 1d,e and Supplementary Fig. 1D). Further confirming that glutaminolysis was responsible for cell death induction upon LQ treatment, we used a cell-permeable derivative of αKG, dimethyl-α-ketoglutarate (DMKG), and we observed that the addition of DMKG to amino acid-starved cells induced cell death to a similar extent than LQ treatment (Fig. 1a–c). As αKG is the final product of glutaminolysis, and we previously showed that LQ treatment efficiently increases the intracellular levels of αKG (ref. 14), this result suggested that the ability of LQ treatment to induce cell death correlates with the activation of glutaminolysis and αKG production. To finally confirm the active role of glutaminolysis in LQ-induced cell death, we inhibited the enzyme GLS1 (both genetically using siRNA and pharmacologically using the inhibitors DON and BPTES), responsible for the first step of glutaminolysis. As shown in Fig. 1f–i and in Supplementary Fig. 1E,F, both the genetic and the pharmacologic inhibition of GLS1 prevented the LQ-induced cell death in U2OS and HEK293 cells, with no effect on the viability of the cells during amino acid starvation. Of note, GLS1 inhibition using DON or GLS1 silencing using siRNA did not prevent the induction of cell death mediated by DMKG treatment (Supplementary Fig. 1G,H), as DMKG bypasses the inhibition of GLS1 to produce αKG. Taken together, these results strongly support the conclusion that the unbalanced production of αKG by glutaminolysis during amino acid restriction decreases cell viability. The specificity of glutaminolysis in the observed cell death was confirmed as the addition of all the amino acids did not decrease cell viability (Supplementary Fig. 1I,J). Thus, glutaminolysis (a well-known pro-proliferative process) causes cell death if it is activated during nutrient restriction, a result that pointed at the importance of nutritional balance in the control of cancer cell viability.

Unbalanced glutaminolysis induced apoptosis. We next investigated whether the cell death induced by glutaminolysis was apoptosis. For this purpose, we analysed several apoptotic markers, such as the cleavage of caspases 3, 8 and 9, the cleavage of PARP, and the expression of the pro-apoptotic protein BAX after 72 h of amino acid restriction in several tumour cell lines, by western blot and by immunofluorescence. We also analysed the expression of the anti-apoptotic proteins Bcl-XL and MCL-1. We observed that LQ treatment or DMKG treatment increased the levels of cleaved caspase 3, cleaved PARP and BAX in U2OS (Fig. 2a–c), A549 (Supplementary Fig. 2A), JURKAT (Supplementary Fig. 2B) and HEK293A cells (Supplementary Fig. 2D,F), in a dose-dependent manner (Supplementary Fig. 2C). We also observed an increase in the cleavage of caspase 8, while we

did not detect any changes in cleaved caspase 9 (Fig. 2a). Similarly, we did not see any decrease in the levels of the anti-apoptotic proteins Bcl-XL and MCL-1 (Fig. 2a). In agreement with these results, both LQ and DMKG treatment significantly increased the late apoptotic population compared to amino acid-starved cells as determined by the double positive annexin V/PI staining observed by flow cytometry (Fig. 2d,e). Further confirming that LQ-induced cell death is mediated by an activation of apoptosis, we used zVAD-FMK, a specific inhibitor of caspases. As shown in Fig. 2f,g, the treatment of cells with zVAD-FMK completely abolished the LQ-mediated cell death and activation of the apoptotic markers, supporting that LQ-induced cell death can be explained by an increase in apoptosis.

We next assayed whether αKG was a necessary byproduct for the induction of apoptosis upon LQ treatment. For this purpose, we inhibited glutaminolysis either genetically (siRNA GLS1) and pharmacologically (using DON or BPTES). Following this approach, we confirmed that the silencing of GLS1 or the inhibition of GLS1 drastically reduced the induction of cleaved caspase 3, cleaved PARP and BAX by LQ treatment (Fig. 2h,i and Supplementary Fig. 2E,F). Likewise, the pharmacological inhibition of GLS1 blocked the increase in the population of annexin V/PI-positive cells induced by LQ (Supplementary Fig. 2G,H). In contrast to LQ treatment, and as expected, the addition of all amino acids did not induce apoptosis (Supplementary Fig. 2I). Therefore, we concluded that the

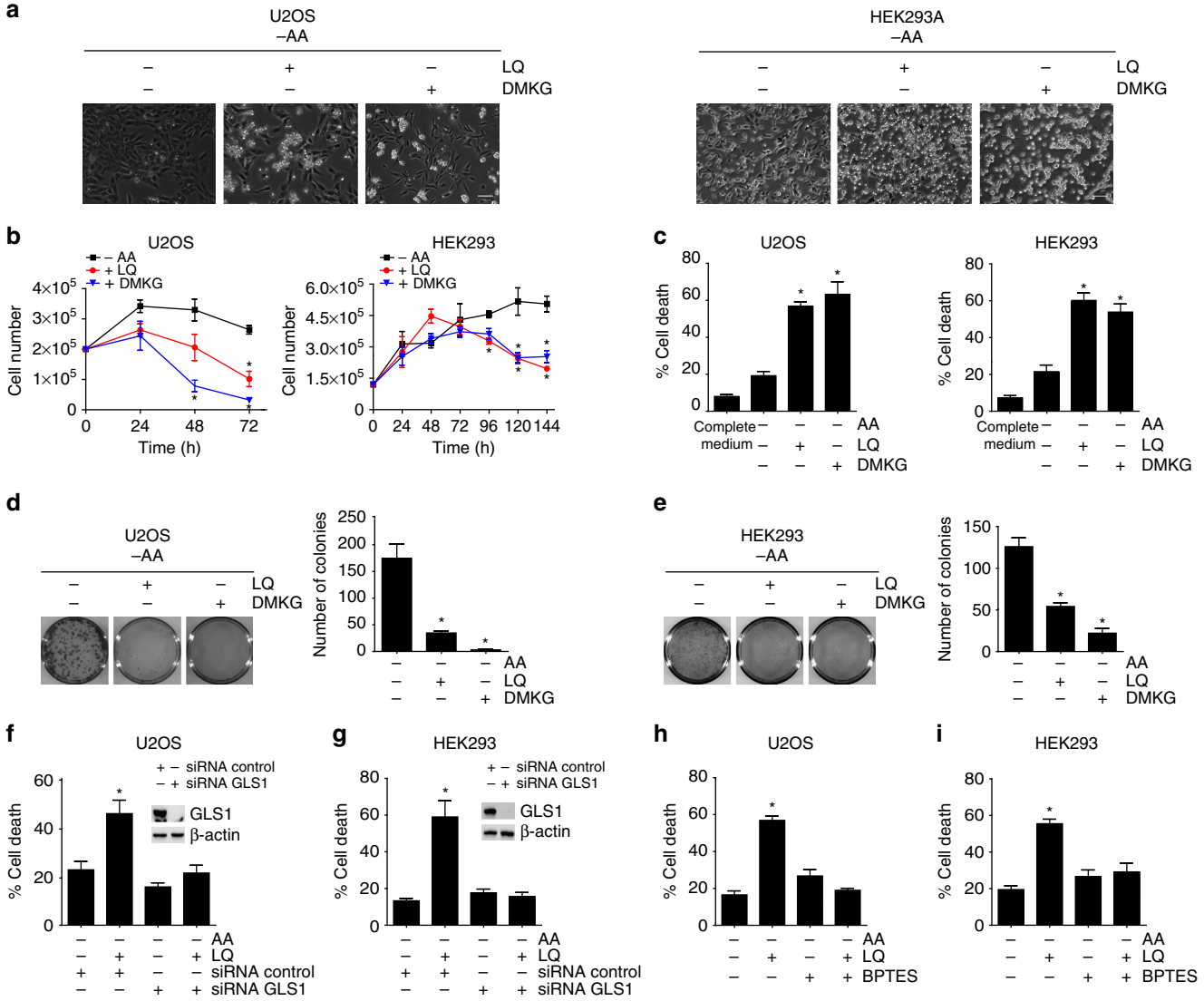

Figure 1 | Long-term glutaminolysis activation during amino acid restriction decreased cell viability. (**a**) U2OS (left panel) and HEK923 (right panel) cells were starved for all the amino acids (− AA) in the presence or absence of LQ or DMKG (2 mM) for 72 h (U2OS) or 144 h (HEK293). Representative microscopy images of the cells are shown for the indicated conditions. The scale bar represents 100 μm. (**b**) Proliferation curves for U2OS and HEK293 were determined upon − AA, in the presence or the absence of LQ and DMKG after 24–144 h. (**c**) Percentage of cell death was estimated using trypan blue exclusion assay upon LQ or DMKG treatment after 72 h for U2OS or 144 h for HEK293, as indicated. (**d**,**e**) A representative image of a clonogenic assay (left panel) and the quantification of the colonies formed in three independent experiments (right panel) are shown for U2OS (**d**) and HEK293 (**e**). (**f**,**g**) Percentage of cell death was estimated in cells depleted of GLS1 (siRNA GLS1) upon amino acids starvation either in the presence or the absence of LQ after 72 h for U2OS (**f**) and 144 h for HEK293 (**g**). (**h**,**i**) Percentage of cell death was estimated upon amino acids starvation either in the presence or the absence of LQ and BPTES (30 μM) after 72 h for U2OS and 144 h for HEK293 cells. Graphs show mean values ± s.e.m. ($n=3$). *$P<0.05$ (Anova *post hoc* Bonferroni).

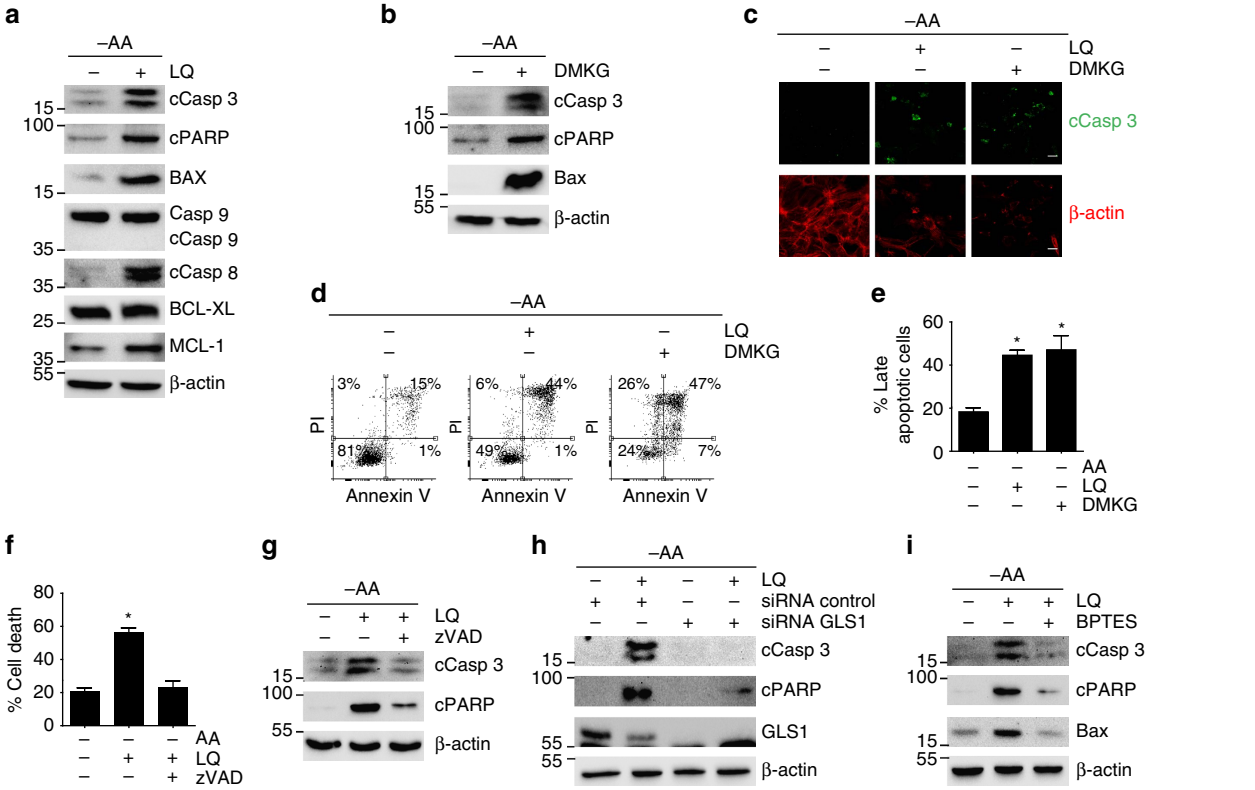

Figure 2 | Glutaminolysis activation during amino acid restriction induced apoptosis. (**a**,**b**) U2OS cells were starved for amino acid either in the presence or the absence of LQ (**a**) or DMKG (2 mM) (**b**). The level of the pro-apoptotic proteins (caspase 3, PARP, BAX, Caspase 8 and caspase 9) and anti-apoptotic member of the Bcl-2 family (Bcl-XL and MCL-1) were determined by western blot for U2OS cells treated as indicated. The scale bar represents 20 μm. (**c**) Immunofluorescence analysis of cleaved caspase 3 and actin filaments are shown for LQ-treated and DMKG-treated cells upon amino acid starvation after 72 h in U2OS cells. (**d**) Flow cytometry analysis of annexin V/PI staining of U2OS cells treated with LQ or DMKG as indicated. (**e**) Quantification of late apoptosis (annexin V/PI-positive cells) for the indicated conditions in U2OS cells. (**f**,**g**) Effect of the inhibition of apoptosis using zVAD-FMK (1 μM) on the percentage of cell death (**f**) and apoptotic markers (**g**) in LQ-treated U2OS cells. (**h**,**i**) Western blot analysis of apoptotic markers upon GLS1 silencing using siRNA (**h**) or upon GLS inhibition using BPTES (**i**) in LQ-treated U2OS cells. Graphs show mean values ± s.e.m. ($n=3$). *$P<0.05$ (Anova *post hoc* Bonferroni).

increase in glutaminolytic αKG production during amino acids restriction induced apoptotic cell death.

In order to gain some insights in the mechanism of apoptosis induction mediated by LQ, we investigated if the observed increased levels of the pro-apoptotic protein BAX played a mechanistic role in the induction of apoptosis. Indeed, the downregulation of BAX using siRNA reduced cell death, caspase 3/8 cleavage, and PARP cleavage in LQ-treated cells (Supplementary Fig. 2J,K), suggesting that BAX upregulation is necessary for the activation of apoptosis by LQ treatment. This was a rather surprising result, as we previously observed an activation of caspase 8, and not caspase 9 (Fig. 2a), as canonically described for BAX (ref. 19). Indeed, the increased protein levels of BAX observed in LQ treated cells did not correlate with an increase in BAX transcription, as no significant differences in BAX mRNA levels were observed upon LQ addition (Supplementary Fig. 2L). Accordingly, both the levels and activity of p53 (as determined by p21 as a readout), a major transcriptional regulator of BAX (ref. 20), were decreased upon glutaminolysis activation (Supplementary Fig. 2M), further discarding an increase in the transcription of BAX in LQ-treated cells. Finally, we also investigated if LQ-treated cells showed a BAX-mediated induction of the intrinsic pathway of apoptosis that promotes the release of cytochrome c from the mitochondria, which in turn activates the caspase 9. As shown in Supplementary Fig. 2N, LQ treatment did not induce the release of cytochrome c from the mitochondria, in agreement with the lack of caspase 9 cleavage previously observed. Thus, we concluded that BAX played a non-canonical mechanistic role in LQ-induced apoptosis.

mTORC1 inhibition prevented glutaminolysis induced apoptosis. We have shown previously that short-term (15 min) glutaminolysis is sufficient and necessary to activate mTORC1 pathway[14]. However, whether glutaminolysis is sufficient to activate mTORC1 at long term (72 h) was not clear. Hence, we investigated if the induction of apoptosis mediated by the activation of glutaminolysis in the absence of other amino acids correlated with the activation of mTORC1. Indeed, the activation of glutaminolysis adding LQ to amino acid-starved cells, or the treatment with DMKG, increased the phosphorylation S6K (Thre389), S6 (Ser235/236) and 4EBP1 (Ser37/46), all of them downstream targets of mTORC1, after 72 h (Supplementary Fig. 2A–I). In contrast, LQ treatment did not affect the activation of mTORC2, as the phosphorylation of its downstream target AKT at Ser473 (refs 2,21) was not affected (Fig. 3d). These results confirmed that long-term activation of glutaminolysis adding glutamine and leucine, even in the absence of other amino acids, is sufficient to activate mTORC1, but has not effect towards mTORC2, upon amino acid starvation. In addition, the pharmacological inhibition of GLS (using DON or BPTES) abrogated the activation of mTORC1 induced by LQ treatment, supporting a mechanistic role of glutaminolytic αKG

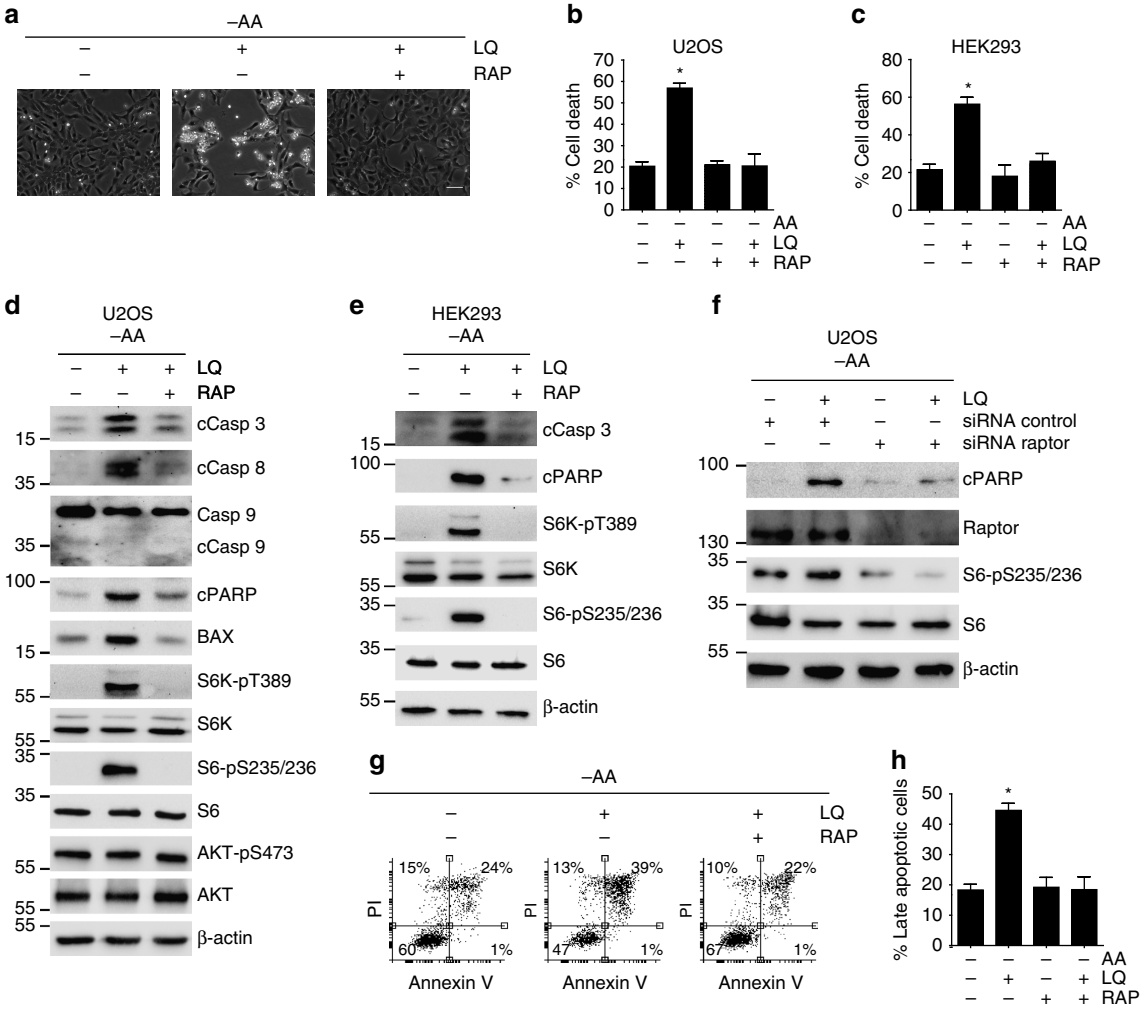

Figure 3 | mTORC1 inhibition prevented the glutaminolysis induced apoptosis. (**a**) Representative microscopy image of U2OS cells upon LQ treatment either in the presence or the absence of rapamycin after 72 h. The scale bar represents 100 μm. (**b**,**c**) Percentage of cell death as estimated using trypan blue exclusion assay is U2OS cells (**b**) or HEK293 cells (**c**) upon LQ treatment either in the presence or the absence of rapamycin for 72 h (U2OS) or 144 h (HEK293). (**d**,**e**) Western blot analysis of apoptotic markers and mTORC1 downstream targets upon rapamycin (RAP) addition in LQ-treated U2OS cells (**d**) and HEK293 cells (**e**). (**f**) Western blot analysis of apoptotic markers and mTORC1 downstream targets upon the silencing of Raptor using siRNA (thus inhibiting mTORC1 activity) in LQ-treated U2OS cells. (**g**) Flow cytometry analysis of annexin V/PI staining of U2OS cells treated with LQ and rapamycin as indicated. (**h**) Quantification of late apoptosis (annexin V/PI-positive cells) for the U2OS cells treated as in **g**, as indicated. Graphs show mean values ± s.e.m. ($n = 3$). *$P < 0.05$ (Anova *post hoc* Bonferroni).

levels in the activation of mTORC1 at long term, as previously demonstrated for short-term glutaminolysis[14] (Supplementary Fig. 2E–H).

The translocation of mTORC1 to the surface of the lysosome is a crucial step for its activation[22], and indeed, we previously showed that short-term glutaminolysis was sufficient to induce the lysosomal translocation of mTORC1 (ref. 14). Hence, we evaluated whether long-term glutaminolysis was also sufficient to sustain the localization of mTORC1 at the surface of the lysosome. For this purpose, we determined the colocalization between mTOR and CD63, a late endosomal and lysosomal marker, by confocal microscopy. As shown in Supplementary Fig. 3C, mTOR showed a disperse distribution throughout the cytoplasm when cancer cells were incubated in the absence of amino acids. In contrast, the activation of glutaminolysis by either LQ treatment or DMKG treatment in amino acid-restricted cells was sufficient to sustain the co-localization of mTOR and CD63 even after 72 h of treatment, again confirming that long-term glutaminolysis is sufficient to induce the lysosomal localization of mTORC1, prior to its activation. Furthermore, as mTORC1 activity regulates cell size[23], we also confirmed that the activation of mTORC1 by long-term glutaminolysis increased cell size. As shown in Supplementary Fig. 3D, while the withdrawal of amino acids decreased cell size, the activation of glutaminolysis (LQ treatment) maintained the size of the cells to a similar level than cells grown in a complete medium. As expected, the inhibition of mTORC1 using rapamycin in LQ-treated cells decreased the cell size to a similar extent than amino acids starvation. Altogether, these results strongly support that glutaminolysis is sufficient to maintain mTORC1 active upon amino acid deprivation at long term (72 h). This is an abnormal activation of mTORC1, as the mTORC1-dependent activation of cell growth does not seem viable for a prolonged time in conditions of amino acid restriction. Indeed, it is already known that the hyperactivation of mTORC1 in TSC2 −/− MEFs leads to cell death upon nutrient deprivation[24–26]. Therefore, we hypothesized that this unbalanced activation of mTORC1 may be mechanistically linked to the glutaminolysis-mediated apoptosis.

To evaluate the mechanistic link between the activation of mTORC1 and glutaminolysis-induced apoptosis, we followed

both a genetic and pharmacological approach to inhibit mTORC1 upon LQ treatment to determine whether the induction of apoptosis was affected. First, we observed that mTORC1 inhibition using rapamycin efficiently prevented the increase in cell death mediated by glutaminolysis in U2OS, and HEK293 cells (Fig. 3a–c). We next confirmed that the activation of glutaminolysis adding LQ to amino acid-starved cells induced the concomitant activation of mTORC1, as determined by S6K phosphorylation and S6 phosphorylation, and the activation of apoptosis, as determined by the cleavage of caspase 3, caspase 8 and PARP, in several cellular models (Fig. 3d,e and Supplementary Fig. 3E). Very importantly, the efficient pharmacological inhibition of mTORC1 using rapamycin (assessed by the reduction in the phosphorylation of mTORC1 downstream targets S6K, S6 and 4EBP1) completely prevented the activation of caspase pathway by glutaminolysis, as rapamycin treatment in LQ-induced cells was sufficient to drastically reduce the cleavage of caspase 3, caspase 8 and PARP, and to prevent the upregulation of BAX (Fig. 3d,e and Supplementary Fig. 3E). Similar results were obtained with a different inhibitor of mTORC1 (PP242, which is a dual inhibitor of both mTORC1 and mTORC2), and with the genetic inhibition of mTORC1 using an siRNA that efficiently silenced Raptor, a mTORC1-specific component[27,28] (Fig. 3f and Supplementary Fig. 3F). In contrast, the genetic inhibition of mTORC2 using an siRNA against Rictor did not block apoptosis induction (Supplementary Fig. 3G). Furthermore, mTORC1 inhibition using rapamycin abrogated the increase in the late apoptotic population mediated by LQ treatment. Thus, as shown in Fig. 3g,h, although rapamycin treatment did not affect the percentage of annexin V/PI-positive population in amino acid-starved cells, it prevented the increase in the percentage of annexin V/PI-positive cells induced by LQ.

The results presented above strongly suggest that glutaminolysis-induced apoptosis is mediated by the aberrant activation of mTORC1 during amino acid limitation. This very important observation suggests that mTORC1, besides its well-known function as a tumour promoter, also exhibits tumour suppressor features during nutritional limitation, a conclusion with important consequences in terms of targeting mTOR as anticancer-therapy. Of note, the capacity of unbalanced glutaminolysis to induce cell death was also evident in a genetic background showing mTORC1 upregulation, such as the case of TSC2 −/− MEFs. Indeed, we observed that LQ-treatment-induced caspase 3 cleavage in TSC2 −/− MEFs, and rapamycin treatment efficiently abrogated this effect (Supplementary Fig. 3H), underscoring the physiological relevance of our finding in a genetic context of mTORC1 overactivation.

UPR did not participate in glutaminolysis mediated apoptosis. In order to understand the cellular mechanism by which the unbalanced activation of mTORC1 induced apoptosis during nutrient limitation, we first investigated the potential role of endoplasmic reticulum (ER) stress and unfolded protein response (UPR) (refs 24,29,30) upon glutaminolysis activation. As shown in Supplementary Fig. 3I, we did not observe any change in the levels of Bip/GRP78, elF2α-pS52, HErpud1 or PDI upon LQ treatment as determined by western blot, all of them being markers of ER stress and UPR. Similarly, the inhibition of mTORC1 using rapamycin in these conditions did not affect the levels of those proteins. This result suggests that the activation of glutaminolysis and mTORC1 during amino acid restriction did not induce an ER stress, neither activated UPR by the time at which apoptosis was already activated. This result does not support an active role of UPR and ER stress in the mechanism of apoptosis activation mediated by mTORC1.

As we observed that LQ-treatment induced the activation of caspase 8, we investigated if the extrinsic pathway of apoptosis (activated by apoptosis-inducing ligands such as FasL, TRAIL or TNFα, and leading to the activation of caspase 8 (ref. 31)) was involved in LQ-mediated apoptosis, and whether rapamycin treatment had an effect on the capacity of the extrinsic pathway to induce apoptosis. However, we did not observe any change in the levels of FasL, TRAIL or TNFα upon LQ treatment either in the presence or the absence of rapamycin (indeed, no detectable levels of FasL or TNFα were appreciated in WB). Similarly, we did not observe any change in the levels of the death receptor Fas (Supplementary Fig. 3J). This result discards that mTORC1 inhibition restricted translation of TNFα, FasL or TRAIL as a mechanism to explain cell death via caspase 8. Further sustaining this conclusion, rapamycin treatment did not block the capacity of FasL or TRIAL to induce apoptotic cell death (Supplementary Fig. 3K–N), discarding that the protective effect of rapamycin treatment involved the modulation of ligand-induced apoptosis.

Autophagy inhibition associated to unbalanced glutaminolysis. The activation of mTORC1 is known to inhibit the initiation of autophagy[32–36]. Autophagy is a degradative process that maintains metabolism and survival in condition of nutrient limitation[8,16]. Previously we have reported that the short-term activation of glutaminolysis inhibits autophagy in an mTORC1-dependent manner[14]. Now, we wanted to explore whether the activation of apoptosis observed upon the unbalanced activation of glutaminolysis/mTORC1 during nutrient restriction correlated with an inhibition of autophagy. First, and as previously shown, we observed that the inhibition of mTORC1 induced by long-term amino acids withdrawal (8–72 h) led to the induction of autophagy. As shown in Fig. 4a,b and Supplementary Fig. 4A,B, U2OS cells stably expressing a GFP-LC3 construct displayed an increase in the number of GFP-LC3 aggregates after 8–72 h of amino acids starvation with respect to cells incubated in the presence of amino acids, clearly suggesting an increase in autophagosome formation[37]. In contrast, LQ and αKG treatment strongly decreased the number of GFP-LC3 aggregates in U2OS cells, suggesting that glutaminolysis is sufficient to inactivate autophagy during amino acids restriction. In agreement with this conclusion, LQ and αKG treatments were also sufficient to increase the expression of p62 and to decrease the formation of LC3II (Fig. 4b,c), indicating a decrease in autophagy[37]. We also evaluated the autophagic flux using chloroquine (CQ) to trap the formation of autophagosomes. Whereas the addition of CQ to amino acid-starved cells increased GFP-LC3 punctate and the levels of LC3II, LQ or αKG treatments were able to reduce GFP-LC3 punctate, to reduce the levels of LC3II and to increase the levels of p62 even in the presence of CQ (Supplementary Fig. 4A–D), suggesting that indeed glutaminolysis reduced the autophagic flux. Finally, we also determined autophagy activation through the analysis of autophagy-related vesicles by transmission electron microscopy. While cells exposed to amino acid starvation for 72 h displayed an increase in the autophagy-related vesicles, the activation of glutaminolysis upon LQ treatment blocked the formation of those vesicles (Fig. 4d), again suggesting an inhibition of autophagy. Thus, the apoptotic cell death induced by the activation of glutaminolysis in the absence of amino acids correlated with an inhibition of autophagy.

To elucidate the role of mTORC1 on the blockage of autophagy by glutaminolysis, we inhibited mTORC1 pathway using rapamycin. As shown in Fig. 4a,b and Supplementary Fig. 4A–C, the inhibition of mTORC1 using rapamycin prevented the

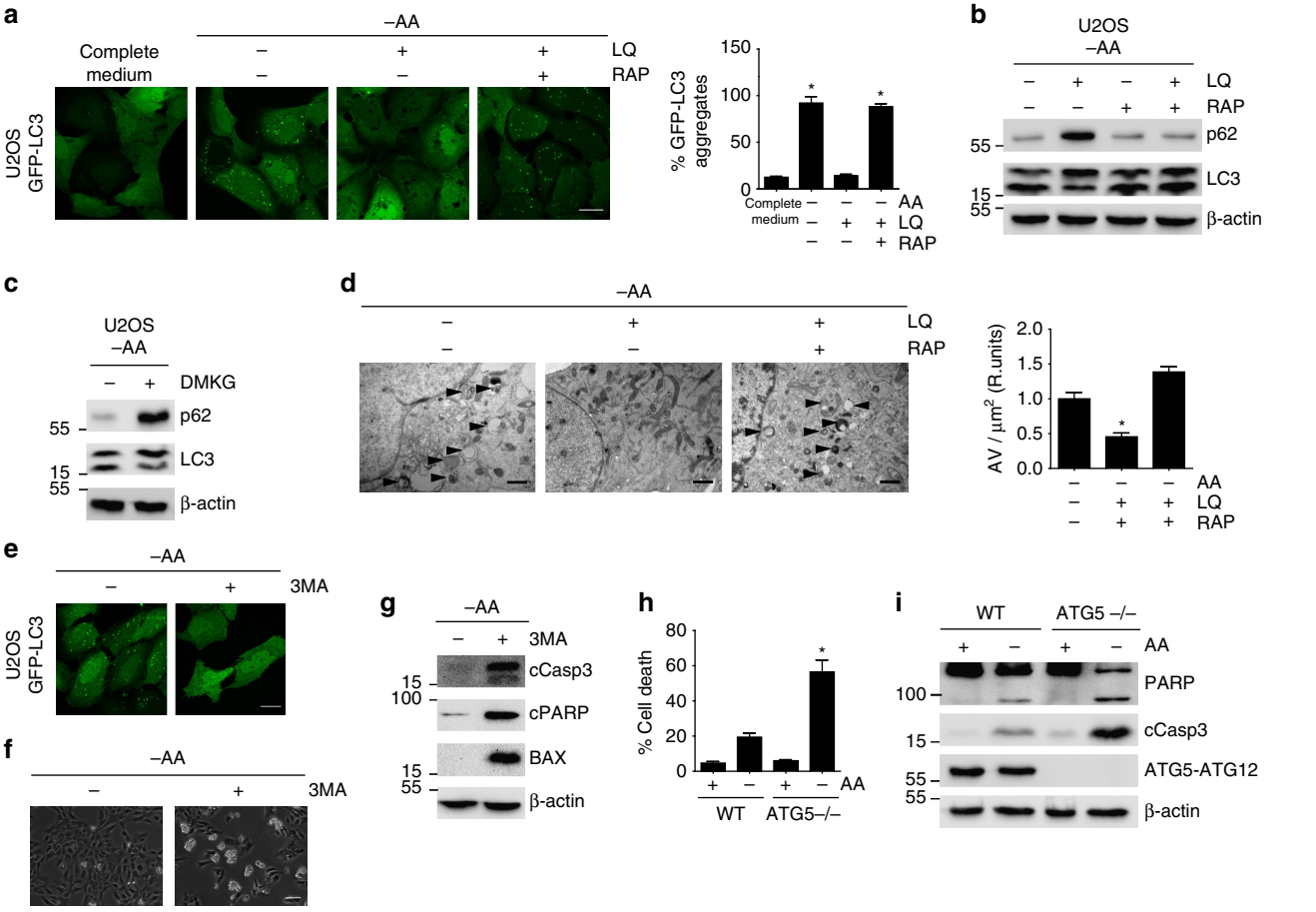

Figure 4 | Glutaminolysis activated cells showed an mTORC1 dependent inhibition of autophagy during amino acid restriction. (**a**) GFP-LC3 expressing U2OS cells were starved for amino acids in the presence or absence of LQ and RAP for 72 h as indicated. Autophagosome formation upon GFP-LC3 aggregation was determined (left panel) and quantified (right panel) using confocal microscopy. The scale bar represents 20 μm. (**b**,**c**) Western blot analysis of U2OS cells treated with LQ, DMKG and RAP as indicated to determine the levels of p62 and LC3II after 72 h. (**d**) Transmission electron microscopy (TEM) images of U2OS cells starved for amino acid in the presence or absence of LQ and RAP after 72 h. The number of autophagy-related vesicles per μm^2 was quantified for each indicated condition. The scale bar represents 1 μm. (**e**) GFP-LC3 expressing U2OS cells were starved for amino acids in the presence or absence of 3MA (5 mM) during 72 h. Autophagosome formation upon GFP-LC3 aggregation was determined using confocal microscopy. The scale bar represents 20 μm. (**f**,**g**) Representative microscopy image (**f**) and western blot analysis of apoptotic markers (**g**) in U2OS cells upon 3MA treatment during 72 h as indicated. The scale bar represents 100 μm. (**h**,**i**) WT and ATG5 −/− MEFs were incubated either in the presence (+AA) or the absence (−AA) of amino acids (+AA) for 24 h. Cell viability using trypan blue exclusion assay (**h**) and western blot analysis of apoptotic markers (**i**) are shown. Graphs show mean values ± s.e.m. ($n=3$). *$P<0.05$ (Anova *post hoc* Bonferroni).

LQ-mediated inhibition of autophagy flux, as determined by the increasing number of GFP-LC3 aggregates, the decreasing levels of p62 protein and the increasing formation of LC3II. Furthermore, the inhibition of mTORC1 using rapamycin also blocked the capacity of glutaminolysis to reduce the number of autophagy-related vesicles (Fig. 4d). Similar results were observed upon the genetic inhibition of mTORC1 using an siRNA that efficiently silenced Raptor protein. As shown in Supplementary Fig. 4E,F, Raptor (but not Rictor) depletion blocked the inhibition of autophagy by glutaminolysis, as assessed by the increasing levels of the GFP-LC3 aggregates and the decreasing levels of p62. Finally, to confirm that the glutaminolitic flux inhibits autophagy, we inhibited glutaminolysis using either DON or BPTES, and using an siRNA that efficiently silenced GLS1. In all the cases, the inhibition of GLS prevented the inhibition of autophagy by LQ treatment, assessed by the decrease of GFP-LC3 aggregates, the decrease in p62 levels and the increase in LC3II (Supplementary Fig. 4G–I). All those results confirmed that the capacity of long-term LQ treatment to inhibit autophagy required glutaminolysis and the activation of mTORC1.

Next, we wanted to investigate whether the inhibition of autophagy mediated by the activation of glutaminolysis/mTORC1 plays a mechanistic role in the induction of apoptosis during amino acid restriction. For this purpose, we first investigated whether autophagy is necessary to sustain cell viability upon nutrient restriction. Hence, we inhibited autophagy pharmacologically using 3-methyladenine (3MA) during amino acid withdrawal. 3MA treatment efficiently inhibited autophagy in amino acid-starved cells, decreasing the formation of GFP-LC3 aggregates (Fig. 4e), and induced apoptotic cell death as determined by the levels of cleaved caspase 3, cleaved PARP and BAX (Fig. 4f,g). Similarly, the inhibition of autophagy using CQ, also induced apoptotic cell death in amino acid-restricted cells (Supplementary Fig. 4J,K). These results confirmed that autophagy is necessary to sustain cell viability in conditions of amino acid restriction. We confirmed the results obtained with 3MA and CQ using ATG5 −/− MEFS and ATG5 knock down in U2OS cells. The ablation/downregulation of ATG5 prevented the capacity of the cells to survive upon amino acid withdrawal (Fig. 4h,i and Supplementary Fig. 5C).

This conclusion led us to investigate whether autophagy inhibition is the mechanistic link between the activation of glutaminolysis/mTORC1 during amino acid restriction and apoptosis.

Autophagy mediated cell survival upon rapamycin treatment. To elucidate if autophagy inhibition is the mechanistic link between the activation of glutaminolysis/mTORC1 and apoptosis during amino acid restriction, we tested whether the inhibition of autophagy prevents the rapamycin-dependent restoration of cell viability upon LQ treatment. The treatment of cells with 3MA was sufficient to inhibit autophagy in rapamycin-treated cells (Fig. 5a). Importantly, the inhibition of autophagy using 3MA or CQ also prevented the rapamycin-mediated inhibition of apoptosis in glutaminolysis-activated cells, as determined by trypan blue exclusion assay (Fig. 5b,c) and apoptotic markers such as cleaved caspase 3, cleaved PARP and BAX (Fig. 5d and Supplementary Fig. 5A), while no reactivation of mTORC1 was detected. Similarly, 3MA treatment completely abolished the capacity of rapamycin to restore colony number in a clonogenic assay (Fig. 5e,f). These results were confirmed using ATG5 knock down in U2OS cells and ATG5 −/− MEFs, in which the impairment of autophagy completely abolished the capacity of rapamycin to promote cell survival during amino acids starvation (Fig. 5g,h and Supplementary Fig. 5C–E). As expected, in ATG5 −/− MEFs, neither LQ treatment nor rapamycin modulated autophagy, as assessed by the levels of p62, which remained high due to the inactivation of autophagy (Supplementary Fig. 5B). All these results confirmed that the ability of rapamycin to promote apoptosis resistance necessarily requires autophagy re-activation, confirming that the mechanism of glutaminolysis-induced apoptosis is mediated by autophagy inhibition.

p62 mediated caspase 8 activation and apoptosis induction. While the previous results strongly suggested that mTORC1 inhibition prevented apoptotic cell death in an autophagy-dependent manner, we wanted to elucidate the precise molecular mechanism of apoptosis induction resulting from the unbalanced activation of mTORC1. The contribution of p62 to the activation of caspase 8, caspase 3 and apoptosis under certain stress conditions has been described previously[38–40]. Indeed, the interaction between p62 and caspase 8 has been reported to activate caspase pathway and apoptosis[41]. p62 levels are normally downregulated in amino acid-restricted conditions due to the activation of autophagy[42]. However, the activation of glutaminolysis/mTORC1

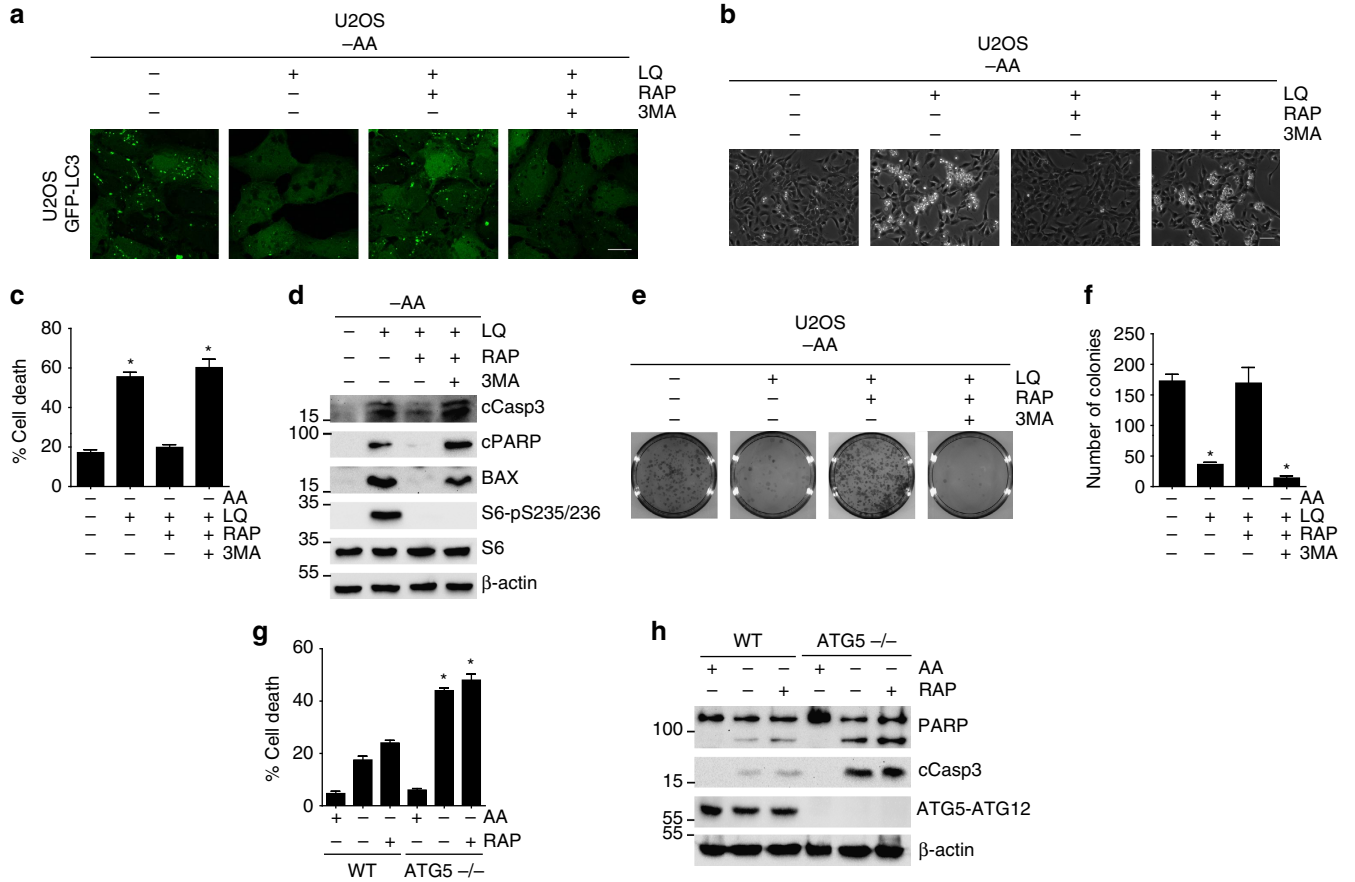

Figure 5 | Autophagy was necessary for the ability of rapamycin treatment to prevent glutaminolysis and mTORC1 induced apoptosis. (**a**) GFP-LC3 expressing U2OS cells were starved for amino acids in the presence or absence of LQ, RAP and 3MA for 72 h as indicated. Autophagosome formation upon GFP-LC3 aggregation was determined using confocal microscopy. The scale bar represents 20 μm. (**b**) U2OS cells were starved for all the amino acids in the presence or absence of LQ, RAP and 3MA for 72 h as indicated. A representative microscopy image of the cells for the indicated conditions is shown. The scale bar represents 100 μm. (**c**) Percentage of cell death as estimated using trypan blue exclusion assay in U2OS treated as in **b**. (**d**) Western blot analysis of apoptotic markers and mTORC1 downstream targets was assessed for U2OS cells treated as in **b**. (**e**,**f**) Clonogenic assay of U2OS cells treated as in **b** (**e**). The number of colonies in three independent experiments was quantified (**f**). (**g**,**h**) WT and ATG5 −/− MEFs were incubated either in the presence (+AA) or the absence (−AA) of amino acids (+AA) and rapamycin as indicated for 24 h. Cell viability using trypan blue exclusion assay (**g**) and western blot analysis of apoptotic markers (**h**) are shown. Graphs show mean values ± s.e.m. ($n=3$). *$P<0.05$ (Anova *post hoc* Bonferroni).

clearly sustained high levels of p62 in amino acid-restrictive conditions (Figs 4b,c and 6a). Moreover, the anti-apoptotic capacity of rapamycin correlated with its ability to reduce p62 levels (Fig. 4b). Finally, the results shown in Figs 2a and 3d demonstrated that the activation of mTORC1 during nutrient restriction activated caspase 3 and caspase 8, but it did not affect caspase 9 activation. Thus, we decided to investigate whether p62 plays a mechanistic role in mTORC1-mediated apoptosis induction. Supporting this hypothesis, we first observed that silencing p62 (using siRNA) was sufficient to prevent the activation of apoptosis mediated by LQ treatment, as determined by caspase 8 and PARP cleavage (Fig. 6a). It is noteworthy that, despite the role assigned to p62 in the activation of mTORC1 (ref. 43), silencing p62 did not affect the LQ-induced activation of mTORC1 (Fig. 6a), which placed p62 downstream of mTORC1 in the glutaminolysis-induced apoptosis. Conversely, the upregulation (exogenous overexpression) of p62 was sufficient to strongly increase cell death and to activate the cleavage of caspase 8, caspase 3 and PARP specifically in cells incubated in the absence of amino acids, but to a much lesser extent in amino acid fed cells (Fig. 6b,c). Confirming the specific role p62 in the activation of caspase 8 and caspase 3, p62 upregulation did not increase the cleavage of caspase 9 (Fig. 6b). Again, the overexpression of p62 did not affect the inactivation of mTORC1 during amino acid starvation (Fig. 6b), confirming that in our conditions p62 operates downstream of mTORC1. In addition, we corroborated that the upregulation of p62 induced its interaction with caspase 8 specifically when cells are incubated in the absence of amino acids. As shown in Fig. 6d, endogenous caspase 8 co-immunoprocipitated with p62-HA only when cells where incubated in the absence of amino acids. These results strongly suggest that the abnormally high levels of p62 during amino acid restriction are sufficient to promote the interaction of p62 with caspase 8 to induce the cleavage of caspase 8. These results sustain a model in which the unbalanced activation of glutaminolysis inhibits autophagy in an mTORC1-dependent manner. Autophagy inhibition induces high levels of p62, which in turn promotes the activation of caspase 8 and apoptosis upon amino acid imbalance (Fig. 6e).

Discussion

The results presented herein propose a complete molecular mechanism to explain how the activation of glutaminolysis in the absence of other amino acids induces an unbalanced activation of mTORC1, which promotes apoptosis upon amino acid deprivation. This unprecedented function of both glutamine metabolism and mTORC1 (two well-known pro-proliferative inducers) as activators of cell death in tumour cells place both elements with a potential tumour suppressor functionality that could be exploited in therapy. We observed that the addition of glutamine and leucine at similar concentrations than used in a complete culture medium to amino acid-starved cells (what we called 'LQ treatment') promoted the activation of apoptotic cell death through glutaminolysis, as the inhibition of this process abrogated this cell death induction. The unexpected role of glutaminolysis as a cell death inducing mechanism during nutrient restriction also pointed at the importance of nutritional balance in the control of cancer cell viability and the potential use of this metabolic disequilibrium to identify new metabolic addictions. Further sustaining this concept, previous reports showed that increasing intracellular αKG levels induce apoptosis *in vivo*, although no clear mechanism was provided[44,45]. On the other hand, a recent report showed that glutaminolysis is crucial

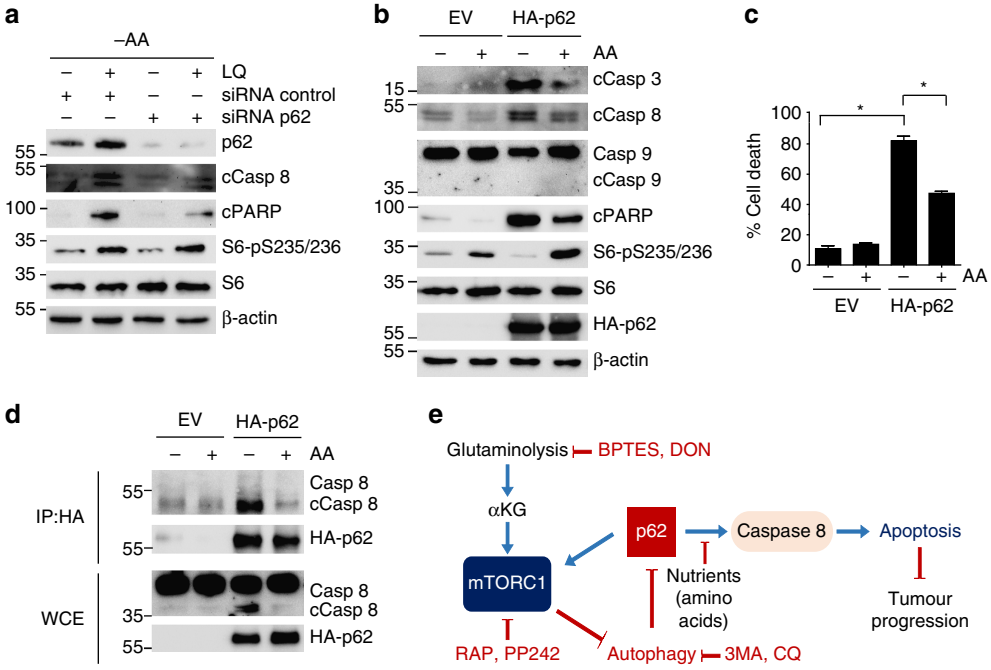

Figure 6 | p62 interacts with and activates caspase 8 and apoptosis. (**a**) U2OS cells were transfected either with a non-targeting siRNA (control) or siRNA against p62. Then cells were treated with LQ for 72 h. The activation of apoptotic markers and mTORC1 downstream targets were assessed by western blot analysis. (**b**,**c**) U2OS cells were transfected with HA-p62 for 24 h and then incubated in the presence or the absence of all the amino acids for 48 h as indicated. The expression of apoptotic markers and mTORC1 downstream targets were assessed by western blot (**b**), and cell viability was estimated using trypan blue exclusion assay (**c**). Graphs show mean values ± s.e.m. ($n=3$). *$P<0.05$ (Anova *post hoc* Bonferroni). (**d**) U2OS cells were transfected with HA-p62 and the interaction of HA-p62 with endogenous caspase 8 was evaluated by immunoprecipitation upon amino acid starvation (− AA) or amino acid sufficiency (+ AA). The co-precipitation of bot HA-p62 and caspase 8 was determined by western blot analysis. (**e**) Working model summarizing the results obtained in this work.

for the induction of ferroptosis, a non-apoptotic type of cell death[46].

As we previously described, glutaminolysis activates mTORC1 in a short-term setting[14]. Now, we have corroborated this observation in a long-term setting, showing that the activation of glutaminolysis or its end-up product αKG maintain the activity of mTORC1 for 72 h at least, which correlated with the activation of apoptosis. Strikingly, the inhibition of mTORC1 promoted cell survival upon amino acid starvation. Regarding this observation, it is important to mention here that an abnormally high activity of mTORC1 in nutrient limiting conditions is a stressful situation that many tumour cells (particularly solid tumours) are subjected to, as mTORC1 is aberrantly activated in 80% of human cancer, and the tumour environment is restrictive *per se*[3,8]. According to our results, the addition of rapamycin in these conditions constitutes an opportunity for the cancer cell to resist apoptosis. Indeed, this anti-apoptotic effect of rapamycin might explain, at least in part, the lack of efficacy observed in patients treated with mTORC1 inhibitors: mTORC1 inhibition in patients will indeed restrict tumour growth, but at the same time allows tumour survival and apoptosis resistance, which might lead to an increase in therapy resistance. A number of reports suggest that one of the reasons to explain the limited efficacy of rapamycin to target tumour growth is the specificity of rapamycin to target mTORC1 and not mTORC2 (refs 47–50). As a result, dual inhibitors of both complexes have been developed in the last years. However, we observed that a double inhibitor of mTORC1/mTORC2 (PP242) also promoted cell survival in these conditions, implying that a double mTORC1/mTORC2 inhibition might present similar problems of apoptosis resistance in patients.

In our study, we have dissected the mechanism that promotes cell death by the unbalanced activation of mTORC1 induced by glutaminolysis in the absence of amino acids. Thus, we tested the potential role of UPR, ER stress and autophagy, all processes related with apoptosis and mTORC1 activation[1,2,8,15,16,18,24,29,30]. We observed that none of the tested markers of UPR and ER stress were affected in these conditions. By contrast, the glutaminolysis-mediated activation of mTORC1 inhibited autophagy, a process crucial for the survival of the cells upon nutrient deprivation. Indeed, the inhibition of autophagy was sufficient to induce cell death. We also demonstrated that rapamycin requires autophagy to promote cell survival in glutaminolysis activated cells. Finally, we observed that autophagy-dependent reduction of p62 levels during amino acid withdrawal is a necessary step to prevent apoptosis. Hence, any tested condition that induced high levels of p62 during amino acid restriction (LQ treatment, DMKG treatment, 3MA treatment, ATG5 −/−, p62 overexpression) led to the activation of apoptosis. Therefore, this upregulation of p62 during nutrient restriction seems to be the ultimate mechanism detected by the cell to recognize an anomalous activation of cell growth signalling in restrictive conditions, and that situation prompts the cell to undergo apoptosis. This model (Fig. 6e) was corroborated by the direct interaction of p62 with cleaved caspase 8, a mechanism that has been previously described to activate apoptosis in other stressful circumstances[38–41]. However, the physiological and biochemical control of the interaction between p62 and caspase 8 needs further investigation. Mainly, how amino acid sufficiency prevents this interaction is a question that remains to be answered. Interestingly, the overexpression of p62 in conditions of amino acid sufficiency led to a higher activation of mTORC1, compared to cells expressing normal levels of p62 (Fig. 6b). This corroborates the partial role of p62 in the activation of mTORC1, as described elsewhere[43,51]. This evidence highlights the dual role of p62 either promoting cell growth through mTORC1 pathway or acting as an apoptotic signal depending on the presence or absence of amino acids.

Altogether, these results points towards autophagy as an 'addiction' in rapamycin-treated tumours, and therefore highlight the potential of autophagy as a therapeutic target to overcome rapamycin-resistant problems in tumour therapy[8,52]. Some clinical trials using the inhibition of both mTORC1 and autophagy have already shown promising results[53,54]. Here, we propose a complete molecular mechanism highlighting the functionality of mTORC1 not only as a major tumour promoter as it has been extensively characterized, but also exhibiting tumour suppressor features during nutrient restrictive conditions. Our results provide with a molecular explanation for the modest results obtained when mTOR inhibitors are used as anti-tumour therapy, as rapamycin treatment promotes survival during nutrient-restricted conditions. Discontinuation of the treatment will be then followed by a relapsed growth of tumour cells that resisted apoptosis induction. In this context, other independent reports support the notion that the inhibition of mTORC1 promotes malignancy in solid tumours. Indeed, Mikaelian *et al.* reported that mTORC1 inhibition promotes the epithelial-mesenchymal transition, increasing the migration of cancer cells[55]. In addition, recently Palm *et al.*[56] observed that the inhibition of mTORC1 increases the use of extracellular sources of nutrients, thus, sustaining the growth of cancer cells exposed to nutrient-restricted conditions. Finally, the results here exposed unveil both the crucial role played by autophagy and p62 in the anti-apoptotic effect of rapamycin and their potential use as therapeutic co-targets in rapamycin therapies.

Methods

Reagents and antibodies. Antibodies against mTOR (#2983, dilution 1:150), S6 (#2217, dilution 1:1,000), phospho-S6 (Ser235/236) (#4856, dilution 1:1,000), S6K (#2708, dilution 1:1,000), phospho-S6K(T389) (#9205, dilution 1:1,000), 4EBP1 (#9452, dilution 1:1,000), phospho-4EBP1(T37/46) (#2855, dilution 1:1,000), AKT (#4691, dilution 1:1,000), phospho-AKT(Ser473) (#4060, dilution 1:1,000), p62 (#5114, dilution 1:1,000), LC3 AB (#12741, dilution 1:1,000), β-actin (#4967, dilution 1:1,000), RAPTOR (#2280, dilution 1:1,000), RICTOR (#2140, dilution 1:1,000), cleaved caspase 3 (#9664, dilution 1:1,000), cleaved PARP (#5625, dilution 1:1,000), Bax (#5023, dilution 1:1,000), caspase 8 (#9746, dilution 1:1,000), caspase 9 (#9508, dilution 1:1,000), ATG5 (#12994, dilution 1:1,000), TNF-α (#3707, dilution 1:1,000), FasL (#4273, dilution 1:1,000), cytocrhome c (#4272, dilution 1:1,000), TSC2 (#4308, dilution 1:1,000) and Cox4 (#4850, dilution 1:1,000) were obtained from Cell Signaling Technology. Antibodies against CD63 (SAB4700215, dilution 1:400) and HA (H3663, dilution 1:5,000) were obtained from Sigma. Antibodies against GLS (ab93434, dilution 1:1,000) and Herpud1 (ab155778, dilution 1:1,000) were purchased from Abcam. Antibodies against Fas (sc-715, dilution 1:1,000), BiP (sc-15897, dilution 1:1,000) and Hsp90 (sc-69703, dilution 1:1,000) were obtained from Santa Cruz. Antibody against phospho-EIF2A (Ser52) (44-728G, dilution 1:1,000) was purchased from Thermo Fisher Scientific. Antibody against PDI (ADI-SPA-890, dilution 1:1,000) was obtained from Enzo Life Sciences. The secondary antibodies anti-mouse (#7076, dilution 1:1,000) and anti-rabbit (#7074, dilution 1:1,000) were obtained from Cell Signaling Technology. The apoptotic ligand FasL was kindly provided by Patrick Legembre (INSERM, Rennes, France), while TRAIL mAb (HS501) was obtained from Adipogen. The Permeable αKG (dimethyl-α-ketoglutarate), Diazo-5-oxo-L-norleucine (DON), Bis-2-(5-phenylacetamido-1,2,4-thiadiazol-2-yl)ethyl sulphide (BPTES), Rapamycin (RAP), paraformaldehyde, violet crystal, 3MA, chloroquine (CQ), PP242 were obtained from Sigma. siRNA against GLS1, RAPTOR, RICTOR, p62, ATG5, BAX and non-targeting siRNA control were obtained from Dharmacon. EGFP-LC3 plasmid was a gift from Karla Kirkegaard (Addgene plasmid #11546). HA-p62 plasmid was a gift from Qing Zhong (Addgene plasmid #28027).

Cell culture. U2OS, HEK293A, A549 and JURKAT cells were obtained from ATTC. WT and ATG5 −/− MEFs were kindly provided by Patricia Boya (Centro de Investigaciones Biologicas, Madrid, Spain). GFP-LC3 expressing U2OS cells were obtained from Eyal Gottlieb (Cancer research UK, Glasgow, UK). Except for JURKAT (RPMI GIBCO), all the cells lines were grown in DMEM high glucose (4.5 g l^{-1}) (GIBCO) supplemented with 10% of fetal bovine serum (Dominique Dutscher), glutamine (2 mM), penicillin (Sigma, 100 U ml^{-1}) and streptomycin (Sigma, 100 μg ml^{-1}), at 37 °C, 5% CO_2 in humidified atmosphere. Mycoplasma contamination check was carried out using the VenorGeM Kit (Minerva Biolabs GmbH, Germany). Standard starvation medium was EBSS (GIBCO) containing

4.5 g l^{-1} of glucose. The activation of glutaminolysis was performed by adding glutamine (2 mM final concentration) and leucine (0.8 mM final concentration). When indicated, DMKG was added to a final concentration of 0.2–2 mM. The different inhibitors were used concomitantly with the activation of glutaminolysis as follows: DON (40 μM), BPTES (30 μM), rapamycin (100 nM) and PP242 (100 nM).

Plasmids and siRNA transfections. The plasmid transfections were carried out using Jetpei (Polyplus Transfection) according to the manufacturer's instructions. Briefly, 70% confluent cells were transfected with 2-3 μg of plasmid. Twenty-four hours later cells were starved in the presence or absence of LQ for 48 h more. siRNA transfections were performed using Interferin@ (Polyplus Transfection) according to the manufacturer's instructions: cells at 50% of confluence were transfected with siRNA (final concentration 10 nM) in complete medium for 48 h and then starved with different treatments for another 72 h.

All siRNAs were obtained from Dharmacon (on-target plus smartpool siRNA). Sequences of the siRNAs were as follows:

Non-targeting control (D-001810-02-05): (1) UGGUUUACAUGUCGACUAA, (2) UGGUUUACAUGUUGUGUGA, (3) UGGUUUACAUGUUUUCUGA, (4) UGGUUUACAUGUUUUCCUA; BAX (L-003308-01-0005): (1) GUGCGGA ACUGAUCAGAA, (2) ACAUGUUUUCUGACGGCAA, (3) CUGAGCAGAU CAUGAAGAC, (4) UGGGCUGGAUCCAAGACCA; ATG5 (L-004374-00-0005): (1) GGCAUUAUCCAAUUGGUUU, (2) GCAGAACCAUACUAUUUGC, (3) UGACAGAUUUGACCAGUUU, (4) ACAAAGAUGUGCUUCGAGA; p62 (L-010230-00-0005): (1) GAACAGAUGGAGUCGGAUA, (2) GCAUUGAAGUU GAUAUCGA, (3) CCACAGGGCUGAAGGAAGC, (4) GGACCCAUCUGUCUU CAAA; Raptor (L-004107-00-0010): (1) UGGCUAGUCUGUUUCGAAA, (2) CACGGAAGAUGUUCGACAA, (3) AGAAGGGCAUUACGAGAUU, (4) UGGAGAAGCGUGUCAGAUA; Rictor (L-016984-00-0010): (1) GACACAA GCACUUCGAUUA, (2) GAAGAUUUAUUGAGUCCUA, (3) GCGAGCUGAUG UAGAAUUA, (4) GGGAAUACAACUCCAAAUA; GLS (L-004548-01-0010): (1) CCUGAAGCAGUUCGAAAUA, (2) CUGAAUAUGUGCAUCGAUA, (3) AGAAAGUGGAGAUCGAAAU, (4) GCACAGACAUGGUUGGUAU.

Immunoblots. 5×10^6 JURKAT cells or 2×10^6 U2OS, A549, HEK293 cells were seeded in 10 cm plates. After the respective treatments cells were washed two times with phosphate-buffered saline (PBS) and lysed with RIPA buffer containing a cocktail of protease inhibitor (P8340 Sigma), inhibitors of phosphatases (P0044 and P5726 Sigma) and PMSF 1 mM. Protein quantification was performed using BCA kit (Pierce). After the electrophoresis, the proteins were transferred to a nitrocellulose membrane (midi kit, Bio-Rad) with Trans-Blot Turbo Transfer System (Bio-Rad). Finally, membranes were imaged using the ChemiDoc MP imager (Bio-Rad). Uncropped Western Blot scan is reported in Supplementary Fig. 6.

Immunoprecipitation. After the transfection with p62-HA, the cells were starved for 48 h. After two washes with cold PBS, cells were lysed with lP lysis buffer (40 mM Hepes pH 7.5, 120 mM NaCl, 1 mM EDTA, 0.3% CHAPS, protease inhibitor cocktail P8340 Sigma and 1 mM PMSF). Protein extracts were incubated overnight at 4 °C with anti-HA magnetic beads (Pierce Anti-HA Magnetic Beads, Thermo Fisher #88836). Thereafter beads were washed twice with cold PBS and eluted with Laemmli buffer for immunoblot analysis.

Cell proliferation and cell viability. 1.2×10^5 cells were seeded for all the cell lines (U2OS, A549, HEK293A, JURKAT) and the number of viable cells was determined after 24–144 h, using the TC20 Automated Cell Counter (Bio-Rad) according to the manufacturer's protocol. Briefly, after the respective treatments cells were detached with trypsin/EDTA and 10 μl of the cells suspension were mixed with 10 μl trypan blue 5% solution (Bio-Rad) and analysed with the TC20 cell counter (Bio-rad). To estimate the percentage of cell death, cells were seeded at 1×10^6 in 6 cm plates and after the treatments (72–144 h), the viability and cell size was assessed with the TC20 cell counter.

Real-time PCR. The mRNAs from cells were isolated using Trisol (Invitrogen). One microgram of total mRNA was reverse transcribed using GoScript Reverse Transcription System (Promega). Real-time PCR was performed using SSO Advanced Universal SYBR Green Supermix (Bio-Rad). Specific primers for BAX (forward: CATGTTTTCTGACGGCCAACTTC; reverse: AGGGCCTTGAGCAC CAGTTT, PMM1 (forward: GACAGCTTGACACCATCCA; reverse: CGGCAAA GATCTCAAAGTCGTT) and RPL29 (forward: GGCTATCAAGGCCCTCGT AAA; reverse: CGAGCTTGCGGCTGACA) were purchased from Sigma-Aldrich.

Subcellular fractionation. 25×10^6 cells were seeded in two 25 cm plates for each condition and after the respective treatment the cells were subjected to a subcellular fractionation using the Cell Fractionation Kit (#9038) of Cell Signaling Technology, following the manufacturer's recommendations.

Flow cytometry. After treatment, cells were stained with annexin V and propidium iodide (PI) (Annexin V—early apoptosis detection kit, #6592 Cell Signaling Technology) following the manufacturer's instructions. Then, cells were analysed using BDFACS Canto BD-Biosciences flow cytometer. The analysis of the data was performed using the free software Flowing.

Confocal microscopy. 1.2×10^5 cells were grown in coverslips with the respective treatments for 72 h. Thereafter, cells were fixed with 4% paraformaldehyde in PBS during 30 min at room temperature. GFP-LC3 expressing U2OS cell lines were mounted after the fixation with Prolong containing DAPI (Invitrogen). For the co-localization experiments, after the fixation, cells were permeabilized using Triton-X 0.05% during 10 min, and then blocked with BSA 5% in PBS for 30 min. Finally, cells were incubated with the primary antibodies for 1 h at 37 °C. After three washes with PBS, the cover slide was incubated for 1 h at 37 °C with the appropriate secondary antibody (anti-rabbit Alexa488, dilution 1:400 or anti-mouse Alexa555, dilution 1:400, both from Invitrogen). Finally, coverslips were mounted with Prolong (invitrogen). Samples were imaged with a Leica Confocal microscope.

Clonogenic assay. Cell were starved in EBSS (glucose 4.5 g l^{-1}) with or without leucine/glutamine or DMKG during 72 h for U2OS and A549, and during 144 h for HEK293A. Similarly, U2OS cells were starved for amino acids, treated with LQ, RAP (100 nM) and/or 3MA (5 mM) as indicated for 72 h. After the treatment, 1.5×10^3 cells (U2OS, A549) or 3×10^4 (HEK293A) were seeded in a 3 cm plate containing complete media. After 14 days cells were fixed with paraformaldehyde 4% in PBS (30 min) and stained with violet crystal 5% for 15 min. Then, the plates were washed with water and imaged using ChemiDoc MP Imager (Bio Rad).

Transmission electron microscopy. After the respective treatment, cells were fixed for 1 h at 4 °C in 4% paraformaldehyde in PBS, washed and fixed again 1 h at room temperature in aqueous 2% osmium tetroxide in 0.2 M sodium cacodylate (pH 7.4). Dehydration was performed with ethanol (50%, 70%, 95% and absolute ethanol). Thereafter, the samples were embedded in Epon/Ethanol and evaporated overnight at room temperature. The samples were processed for ultra-microtomy according to standard procedures. Finally sample imaging was performed using a Hitachi H7650 microscope operated at − 80 KV with a camera Gatan—11 MPx.

Autophagosome formation was quantified counting the number of autophagy-related vesicles per area in several images for each condition and the data are represented as the average number of vesicles per μm^2.

Statistics. The results are expressed as a mean ± s.e.m. of at least three independent experiments. One-way ANOVA followed by Bonferroni's comparison as a *post hoc* test were used to evaluate the statistical difference of the results. Statistical significance was estimated when $P < 0.05$.

Data availability. The authors declare that all the data supporting the findings of this study are available within the article and its Supplementary Information files and from the corresponding author on reasonable request.

References

1. Bar-Peled, L. & Sabatini, D. M. Regulation of mTORC1 by amino acids. *Trends Cell Biol.* **24,** 1–7 (2014).
2. Liko, D. & Hall, M. N. mTOR in health and in sickness. *J. Mol. Med. (Berl)* **93,** 1061–1073 (2015).
3. Howell, J. J., Ricoult, S. J., Ben-Sahra, I. & Manning, B. D. A growing role for mTOR in promoting anabolic metabolism. *Biochem. Soc. Trans.* **41,** 906–912 (2013).
4. Efeyan, A. & Sabatini, D. M. mTOR and cancer: many loops in one pathway. *Curr. Opin. Cell Biol.* **22,** 169–176 (2010).
5. Sun, S. Y. mTOR kinase inhibitors as potential cancer therapeutic drugs. *Cancer Lett.* **340,** 1–8 (2013).
6. Chiarini, F., Evangelisti, C., McCubrey, J. A. & Martelli, A. M. Current treatment strategies for inhibiting mTOR in cancer. *Trends Pharmacol. Sci.* **36,** 124–135 (2015).
7. DeBerardinis, R. J. & Cheng, T. Q's next: the diverse functions of glutamine in metabolism, cell biology and cancer. *Oncogene* **29,** 313–324 (2010).
8. Villar, V. H., Merhi, F., Djavaheri-Mergny, M. & Durán, R. V. Glutaminolysis and autophagy in cancer. *Autophagy* **11,** 1198–1208 (2015).
9. Souba, W. W. Glutamine and cancer. *Ann. Surg.* **218,** 715–728 (1993).
10. Kovacevic, Z. & Morris, H. P. The role of glutamine in the oxidative metabolism of malignant cells. *Cancer Res.* **32,** 326–333 (1972).
11. Matés, J. M., Pérez-Gómez, C., Núñez de Castro, I., Asenjo, M. & Márquez, J. Glutamine and its relationship with intracellular redox status, oxidative stress and cell proliferation/death. *Int. J. Biochem. Cell Biol.* **34,** 439–458 (2002).
12. Newsholme, E. A., Crabtree, B. & Ardawi, M. S. The role of high rates of glycolysis and glutamine utilization in rapidly dividing cells. *Biosci. Rep.* **5,** 393–400 (1985).

13. Li, M., Li, C., Allen, A., Stanley, C. A. & Smith, T. J. Glutamate dehydrogenase: structure, allosteric regulation, and role in insulin homeostasis. *Neurochem. Res.* **39,** 433–445 (2014).
14. Durán, R. V. *et al.* Glutaminolysis activates Rag-mTORC1 signaling. *Mol. Cell* **47,** 349–358 (2012).
15. Russell, R. C., Yuan, H. X. & Guan, K. L. Autophagy regulation by nutrient signaling. *Cell Res.* **24,** 42–57 (2014).
16. Jiang, X., Overholtzer, M. & Thompson, C. B. Autophagy in cellular metabolism and cancer. *J. Clin. Invest.* **125,** 47–54 (2015).
17. Kroemer, G., Mariño, G. & Levine, B. Autophagy and the integrated stress response. *Mol. Cell* **40,** 280–293 (2010).
18. Meijer, A. J., Lorin, S. S., Blommaart, E. F. & Codogno, P. Regulation of autophagy by amino acids and MTOR-dependent signal transduction. *Amino Acids* **47,** 2037–2063 (2014).
19. Fulda, S. & Debatin, K.-M. Extrinsic versus intrinsic apoptosis pathways in anticancer chemotherapy. *Oncogene* **25,** 4798–4811 (2006).
20. Selvakumaran, M. *et al.* Immediate early up-regulation of bax expression by p53 but not TGF beta 1: a paradigm for distinct apoptotic pathways. *Oncogene* **9,** 1791–1798 (1994).
21. Alessi, D. R. *et al.* Mechanism of activation of protein kinase B by insulin and IGF-1. *EMBO J.* **15,** 6541–6551 (1996).
22. Sancak, Y. *et al.* Ragulator-Rag complex targets mTORC1 to the lysosomal surface and is necessary for its activation by amino acids. *Cell* **141,** 290–303 (2010).
23. Fingar, D. C., Salama, S., Tsou, C., Harlow, E. & Blenis, J. Mammalian cell size is controlled by mTOR and its downstream targets S6K1 and 4EBP1/eIF4E. *Genes Dev.* **16,** 1472–1487 (2002).
24. Young, R. M. *et al.* Dysregulated mTORC1 renders cells critically dependent on desaturated lipids for survival under tumor-like stress. *Genes Dev.* **27,** 1115–1131 (2013).
25. Choo, A. Y. *et al.* Glucose addiction of TSC null cells is caused by failed mTORC1-dependent balancing of metabolic demand with supply. *Mol. Cell* **38,** 487–499 (2010).
26. Ng, S., Wu, Y.-T., Chen, B., Zhou, J. & Shen, H.-M. Impaired autophagy due to constitutive mTOR activation sensitizes TSC2-null cells to cell death under stress. *Autophagy* **7,** 1173–1186 (2011).
27. Hara, K. *et al.* Raptor, a binding partner of target of rapamycin (TOR), mediates TOR action. *Cell* **110,** 177–189 (2002).
28. Kim, D. H. *et al.* mTOR interacts with raptor to form a nutrient-sensitive complex that signals to the cell growth machinery. *Cell* **110,** 163–175 (2002).
29. Chevet, E., Hetz, C. & Samali, A. Endoplasmic reticulum stress-activated cell reprogramming in oncogenesis. *Cancer Discov.* **5,** 586–597 (2015).
30. Kokame, K., Agarwal, K. L., Kato, H. & Miyata, T. Herp, a new ubiquitin-like membrane protein induced by endoplasmic reticulum stress. *J. Biol. Chem.* **275,** 32846–32853 (2000).
31. Mariño, G., Niso-Santano, M., Baehrecke, E. H. & Kroemer, G. Self-consumption: the interplay of autophagy and apoptosis. *Nat. Rev. Mol. Cell Biol.* **15,** 81–94 (2014).
32. Noda, T. Tor, a phosphatidylinositol kinase homologue, controls autophagy in yeast. *J. Biol. Chem.* **273,** 3963–3966 (1998).
33. Mortimore, G. E. & Schworer, C. M. Induction of autophagy by amino-acid deprivation in perfused rat liver. *Nature* **270,** 174–176 (1977).
34. Li, J. B. & Jefferson, L. S. Influence of amino acid availability on protein turnover in perfused skeletal muscle. *BBA—Gen. Subj.* **544,** 351–359 (1978).
35. Seglen, P. O., Grinde, B. & Solheim, A. E. Inhibition of the lysosomal pathway of protein degradation in isolated rat hepatocytes by ammonia, methylamine, chloroquine and leupeptin. *Eur. J. Biochem.* **95,** 215–225 (1979).
36. Blommaart, E. F., Luiken, J. J., Blommaart, P. J., van Woerkom, G. M. & Meijer, A. J. Phosphorylation of ribosomal protein S6 is inhibitory for autophagy in isolated rat hepatocytes. *J. Biol. Chem.* **270,** 2320–2326 (1995).
37. Klionsky, D. J. *et al.* Guidelines for the use and interpretation of assays for monitoring autophagy (3rd edition). *Autophagy* **12,** 1–222 (2016).
38. Zhang, Y.-B., Gong, J.-L., Xing, T.-Y., Zheng, S.-P. & Ding, W. Autophagy protein p62/SQSTM1 is involved in HAMLET-induced cell death by modulating apotosis in U87MG cells. *Cell Death Dis.* **4,** e550 (2013).
39. Young, M. M. *et al.* Autophagosomal membrane serves as platform for intracellular death-inducing signaling complex (iDISC)-mediated caspase-8 activation and apoptosis. *J. Biol. Chem.* **287,** 12455–12468 (2012).
40. Kim, E. *et al.* Activation of caspase-8 contributes to 3,3-Diindolylmethane-induced apoptosis in colon cancer cells. *J. Nutr.* **137,** 31–36 (2007).
41. Jin, Z. *et al.* Cullin3-based polyubiquitination and p62-dependent aggregation of caspase-8 mediate extrinsic apoptosis signaling. *Cell* **137,** 721–735 (2009).
42. Bjørkøy, G. *et al.* p62/SQSTM1 forms protein aggregates degraded by autophagy and has a protective effect on huntingtin-induced cell death. *J. Cell Biol.* **171,** 603–614 (2005).
43. Duran, A. *et al.* p62 is a key regulator of nutrient sensing in the mTORC1 pathway. *Mol. Cell* **44,** 134–146 (2011).
44. Tennant, D. A. *et al.* Reactivating HIF prolyl hydroxylases under hypoxia results in metabolic catastrophe and cell death. *Oncogene* **28,** 4009–4021 (2009).
45. Tennant, D. A. & Gottlieb, E. HIF prolyl hydroxylase-3 mediates alpha-ketoglutarate-induced apoptosis and tumor suppression. *J. Mol. Med. (Berl)* **88,** 839–849 (2010).
46. Gao, M., Monian, P., Quadri, N., Ramasamy, R. & Jiang, X. Glutaminolysis and transferrin regulate ferroptosis. *Mol. Cell* **59,** 298–308 (2015).
47. O'Reilly, K. E. *et al.* mTOR inhibition induces upstream receptor tyrosine kinase signaling and activates Akt. *Cancer Res.* **66,** 1500–1508 (2006).
48. Carracedo, A. *et al.* Inhibition of mTORC1 leads to MAPK pathway activation through a PI3K-dependent feedback loop in human cancer. *J. Clin. Invest.* **118,** 3065–3074 (2008).
49. Chandarlapaty, S. *et al.* AKT inhibition relieves feedback suppression of receptor tyrosine kinase expression and activity. *Cancer Cell* **19,** 58–71 (2011).
50. Tabernero, J. *et al.* Dose- and schedule-dependent inhibition of the mammalian target of rapamycin pathway with everolimus: a phase I tumor pharmacodynamic study in patients with advanced solid tumors. *J. Clin. Oncol.* **26,** 1603–1610 (2008).
51. Linares, J. F. *et al.* Amino acid activation of mTORC1 by a PB1-domain-driven kinase complex cascade. *Cell Rep.* **12,** 1339–1352 (2015).
52. Medvetz, D., Priolo, C. & Henske, E. P. Therapeutic targeting of cellular metabolism in cells with hyperactive mTORC1: a paradigm shift. *Mol. Cancer Res.* **13,** 3–8 (2015).
53. Chi, K.-H. *et al.* Addition of rapamycin and hydroxychloroquine to metronomic chemotherapy as a second line treatment results in high salvage rates for refractory metastatic solid tumors: a pilot safety and effectiveness analysis in a small patient cohort. *Oncotarget* **6,** 16735–16745 (2015).
54. Rangwala, R. *et al.* Combined MTOR and autophagy inhibition: phase I trial of hydroxychloroquine and temsirolimus in patients with advanced solid tumors and melanoma. *Autophagy* **10,** 1391–1402 (2014).
55. Mikaelian, I. *et al.* Genetic and pharmacologic inhibition of mTORC1 promotes EMT by a TGF-β-independent mechanism. *Cancer Res.* **73,** 6621–6631 (2013).
56. Palm, W. *et al.* The utilization of extracellular proteins as nutrients is suppressed by mTORC1. *Cell* **162,** 259–270 (2015).

Acknowledgements

This work was supported by funds from the following institutions: Institut National de la Santé et de la Recherche Médicale—INSERM, Fondation pour la Recherche Médicale, the Conseil Régional d'Aquitaine, Fondation ARC pour la Recherche sur le Cancer, SIRIC-BRIO, Institut Européen de Chimie et Biologie. We thank Vincent Pitard and Santiago Gonzalez (Flow Cytometry Platform, Université de Bordeaux, France) for technical assistance in flow cytometry experiments. MEFs WT and ATG5 −/− were kindly provided by Prof. Patricia Boya (Centro de Investigaciones Biologicas, Madrid, Spain). FasL was a gift from Patrick Legembre (INSERM, Rennes, France). EGFP-LC3 plasmid was a gift from Karla Kirkegaard. HA-p62 plasmid was a gift from Qing Zhong.

Author contributions

V.H.V. and R.V.D. conceived the project. V.H.V., M.B., P.V., M.P., and R.V.D. designed experiments. V.H.V., T.L.N., S.T., V.D., M.B., C.B., B.S. and M.P. performed experiments and analysed data. R.V.D. and P.S. secured funding. V.H.V. and R.V.D. wrote the manuscript. All the authors read and approved the manuscript.

Additional information

Supplementary Information accompanies this paper at http://www.nature.com/naturecommunications

Competing financial interests: The authors declare no competing financial interests.

Reprints and permission information is available online at http://npg.nature.com/reprintsandpermissions/

How to cite this article: Villar, V. H. *et al.* mTORC1 inhibition in cancer cells protects from glutaminolysis-mediated apoptosis during nutrient limitation. *Nat. Commun.* **8,** 14124 doi: 10.1038/ncomms14124 (2017).

Publisher's note: Springer Nature remains neutral with regard to jurisdictional claims in published maps and institutional affiliations.

SciForschen
Open HUB for Scientific Research

ISSN 2575-0305

Journal of Molecular Medicine and Clinical Applications

Mini Review | Volume: 1.1 | Open Access

Metabolic Transformation in Notch-Driven Acute Lymphoblastic Leukemia

Silvia Terés[1,2,3], Tra Ly Nguyen[1,2,3] and Raúl V Durán[1,2,3,*]

[1]*Institut Européen de Chimie et Biologie, 2 Rue Robert Escarpit, 33607 Pessac, France*
[2]*INSERM U916 VINCO, Institut Bergonié, 229 Cours de l'Argonne, 33076 Bordeaux, France*
[3]*University of Bordeaux, Bordeaux, France*

[*]**Corresponding author:** Raúl V Durán, Institut Européen de Chimie et Biologie, 2 Rue Robert Escarpit, 33607 Pessac, France, **E-mail:** raul.duran@u-bordeaux.fr

Received date: 01 Dec 2015; **Accepted date:** 04 Jan 2016; **Published date:** 10 Jan 2016.

Citation: Terés S, Nguyen TL, Durán RV (2016) Metabolic Transformation in Notch-Driven Acute Lymphoblastic Leukemia. J Mol Med Clin Appl 1(1): doi http://dx.doi.org/10.16966/2575-0305.102

Abstract

T-cell acute lymphoblastic leukemia (T-ALL) is an aggressive, highly frequent type of hematologic tumor. Current treatments against T-ALL are recurrently associated with treatment resistance, severe toxicity and side effects. For the proposal and validation of more effective treatments, great efforts are dedicated to elucidate the molecular mechanisms leading to the origin and progression of this type of leukemia. In this short review, we briefly summarize some aspects of those molecular mechanisms, with an especial emphasis in the upregulation of the Notch signaling pathway and its consequences into cancer cell growth and cancer metabolism.

Keywords: Notch1; T-ALL; mTOR; Metabolic transformation

T-cell Acute Lymphoblastic Leukemia

T-cell acute lymphoblastic leukemia (T-ALL) is a genetically heterogeneous malignancy which appears upon the malignant transformation of a T-cell progenitor. It is an aggressive type of hematologic tumor which accounts for 15% of pediatric and 25% of adult acute lymphoblastic leukemia [1]. T-ALL patients present aggressive clinical features, including an increase in the level of circulating white blood cells and affected central nervous system. Nowadays, the regular treatment of T-ALL patients is based on high-doses of multi-agent chemotherapy, recurrently associated with severe toxicity and side effects. Although these protocols of intensified chemotherapy have significantly improved the outcome of patients, still 20% of childhood patients and the majority of adult patients do not survive due to resistant or relapsed disease [2]. Thus, a better understanding of the molecular basis of T-ALL origin and progression is essential for the proposal, design and validation of more specific, highly effective treatments against this type of leukemia. The main objective of contemporary research in pathobiology of T-ALL is to understand how frequently arising genetic lesions affect malignant transformation hallmarks, including cell growth and proliferation, cell survival and cellular bioenergetics [3]. The final goal should be to identify selectively targeted treatments against those elements to which the transformed T-cell have become addicted, including signaling pathways and metabolic processes.

The malignant transformation process of T-cells is very complex. It involves different genetic alterations during thymocyte development leading to the deregulation of cell growth, proliferation, differentiation, migration and survival of the T-cell. Originating mutations might arise in a haemopoietic stem cell, leading to multilineage developmental capacity. Transformed T-cells present clonal rearrangements in their T-cell receptor genes, and express antigen-receptor molecules resembling immature lymphoid progenitor cells within the early developmental stages of normal T lymphocytes. Genome-wide sequencing studies showed that, while some somatic mutations in T-ALL correlate preferentially with either children or adults, other genetic alterations are uniformly identified both in pediatric and adult T-ALL [4]. One example is the constitutive activation of Notch1 signaling, present in a majority of T-ALL patients. First discovered in Drosophila, Notch1 was identified in humans through a t(7;9)(q34;q34.3) chromosomal translocation observed in some patients with T-ALL [5]. Since only 1% to 3% of patients of T-ALL were found to carry this translocation, the mechanistic role of Notch1 in the origin and development this malignancy was not clear. Later, it was found that other activating mutations leading to the upregulation of Notch1 pathway are present in more than 50% of the patients with T-ALL, underscoring the direct implication of Notch1 in the proliferation and survival of leukemia cells.

Notch and mTOR Signaling in T-ALL

Notch signaling plays an active role in many biological processes, including embryonic development, vascular formation, cell proliferation and cell survival. The human Notch family is constituted by four receptors (Notch1-4) located in the surface of the cell membrane, and five ligands (Dll1, Dll3, Dll4, Jagged1 and Jagged2) located on the surface of the neighboring cell, all ligands belonging to the Delta/Serrate/LAG-2 (DSL) family [6]. Notch receptors are expressed as heterodimeric peptides, including an extracellular subunit and a transmembrane subunit which interact through a heterodimerization domain present in both subunits. When a ligand of the DSL family binds to the extracellular domain of the Notch receptor, it induces sequential cleavages in Notch by an ADAM metalloprotease and by a γ-secretase, releasing the Notch intracellular domain (NICD) from the membrane [7]. NCID then translocates to the nucleus, interacts with specific DNA-binding proteins (CBF1/Suppressor of Hairless/LAG-1 and Mastermind/SEL-8) and activates the transcription of target genes, such as the two families of transcriptional factors HES and HEY (including HES1, HES5, HEY1 and HEY2). The analysis of Notch1-target genes and gene expression programs controlled by Notch1 showed that Notch1 promotes leukemic cell growth via direct transcriptional upregulation of genes involved in ribosome biosynthesis, amino acid metabolism including glutamine, protein translation, and nucleotide synthesis. However, Notch1 activation also follows an indirect mechanism to induce leukemic transformation through the upregulation of key target pathways, namely c-MYC pathway, PI3K/AKT/mTOR

pathway, and interleukin 7 receptor alpha chain. In addition, Notch1 activation increases G1/S cell cycle progression in T-ALL (through the upregulation of CCND3, CDK4, and CDK6 cell cycle genes) [8].

Despite the prominent oncogenic role of Notch signaling in T-ALL, the inhibition of Notch signaling using γ-secretase inhibitors (GSI) have only limited anti-leukemic activity against human T-ALL cell lines, exerting primarily a cytostatic effect with minimal or no apoptosis. Furthermore, early trials were hampered by excessive toxicity from off-target effects on the intestinal epithelial differentiation, resulting in dose-limiting diarrhea. GSI resistance can be induced by mutational loss of PTEN which leads to constitutive activation of the PI3K/AKT/mTOR pathway. Several lines of evidence connect Notch signaling with mTOR activation in T-ALL. mTOR is a conserved serine/threonine kinase which integrates several stimuli to regulate cell growth and metabolism. mTOR forms two functionally and structurally distinct complexes termed mTORC1 and mTORC2. mTORC1 regulates protein synthesis, ribosome biogenesis, nutrient uptake and autophagy in response to growth factors, amino acids, and cellular energy [9]. In response to amino acids, mTORC1 is activated by its translocation to the surface of the lysosomes, a process regulated by the Rag GTPases. Due to its central role in controlling cell growth and metabolism, mTORC1 is upregulated in many different types of tumors to sustain tumor growth. This upregulation of mTORC1 constitutes a critical step for the deregulation of cell signaling during malignant transformation. Intriguingly, GSI treatment suppresses the phosphorylation of multiple signaling proteins in the mTORC1 pathway, suggesting a mechanistic role of Notch signaling in the activation of mTORC1. Of note, simultaneous blockade of the mTORC1 and Notch pathway with small molecule inhibitors resulted in synergistic suppression of T-ALL growth [10]. Thus, this simultaneous inhibition has gathered some attention as a potential co-treatment strategy against T-ALL. However, the mechanistic connection between both pathways is not clear. While some results suggest a PTEN-dependent mechanism involving AKT activation [11], other results showed that the mechanism of mTORC1 activation is independent of both PTEN and AKT, and rather involves c-MYC activation [10].

Metabolic Transformation in Notch-driven T-ALL

The origin, development and progression of cancer require a set of modifications in the normal homeostasis of the cell known as malignant transformation. Among these modifications, changes in cellular metabolism and in cellular signaling are key elements. While signaling deregulation in cancer has been deeply studied during many years, metabolic changes during malignant transformation become a matter of intense research. However, most of the studies concerned the role of p53, cMYC, MYCN and AKT, and the metabolic impact of Notch signaling in cancer has not been investigated deeply yet. To date, several reports have shown bioenergetic changes in leukemic models, but no molecular explanation has been provided yet [12-14]. These reports highlighted the importance of aerobic glycolysis (the so-called "Warburg Effect") to sustain ATP production in T-ALL cells, showing a potentiation between glycolysis inhibition via 3-BrOP and mTOR inhibition by rapamycin in their ability to reduce T-ALL cell viability [12]. In addition, a recent report also showed that PTEN loss upregulates glycolysis and consequently rescues leukemic cell metabolism [15]. This report also identified glutaminolysis as a major node in cancer metabolism in T-ALL. Nowadays, a proper integration between metabolism and cell signaling in cancer cells is required to really understand the mechanisms by which these two components of malignant transformation interact, and ultimately, to find potential candidates that could be used for targeted therapies to specifically kill cancer cells.

As described above, Notch signaling is a major target in a very large percentage of lymphoblastic leukemia, as it is upregulated in more than 50% of the patients with T-ALL. Still, anti-cancer treatments targeting Notch signaling fail due to treatment resistance and tumor relapse. Indeed, it is becoming clear that inherent or acquired resistance of tumor cells to treatment has limited the effectiveness of the majority of targeted therapies. A proposed solution to overcome this limitation is the use of molecular co-treatments, targeting more than one critical element for the tumor growth and survival. In this direction, one potential solution that has not received enough attention during the last years is the possibility of targeting essential aspects of both cell signaling and cell metabolism of the tumor. The main reason to explain why these kinds of therapies have been disregarded during the past years is simple: our knowledge about the crosstalk between cell signaling and cell metabolism in both normal and tumor cells is limited, and therefore the proposal of rationally designed co-treatments is currently inaccessible.

Concluding Remarks

In summary, much more effort is necessary to understand the molecular and cellular implications of Notch upregulation in T-ALL. The inter-connection between Notch pathway and other major signaling pathways, such as mTOR, and with metabolic re-programing open the door to the definition of new "addictions" in Notch-driven T-ALL cells that might be used for the specific treatment of this type of leukemia. Further research should elucidate if metabolic reprograming is not only a hallmark, but also an Achilles heel of Notch-driven leukemia.

Acknowledgements

This work was supported by funds from the following institutions: *Institut National de la Santé et de la Recherche Médicale* - INSERM, *Université de Bordeaux*, *Fondation pour la Recherche Médicale*, *Conseil Régional d'Aquitaine*, *Institut Européen de Chimie et Biologie*, and *Ligue Contre le Cancer - Comité de la Gironde*.

References

1. Van Vlierberghe P, Ferrando A (2012) The molecular basis of T cell acute lymphoblastic leukemia. J Clin Invest 122: 3398-3406.
2. Tremblay CS, Curtis DJ (2014) The clonal evolution of leukemic stem cells in T-cell acute lymphoblastic leukemia. Curr Opin Hematol 21: 320-325.
3. Pui CH, Robison LL, Look AT (2008) Acute lymphoblastic leukemia. Lancet 371: 1030-1043.
4. Peirs S, Van der Meulen J, Van de Walle I, Taghon T, Speleman F, et al. (2015) Epigenetics in T-cell acute lympho blastic leukemia. Immunol Rev 263: 50-67.
5. Ellisen LW, Bird J, West DC, Soreng AL, Reynolds TC, et al. (1991) TAN-1, the humanhomolog of the Drosophila notchgene, isbroken by chromosomal translocations in T lymphoblastic neoplasms. Cell 66: 649-61.
6. D'Souza B, Meloty-Kapella L, Weinmaster G (2010) Canonical and non-canonical Notch ligands. Curr Top Dev Biol 92: 73-129.
7. Pancewicz J, Nicot C (2011) Current views on the role of Notch signaling and the pathogenesis of human leukemia. BMC Cancer 11: 502.
8. Tzoneva G, Ferrando AA (2012) Recent advances on NOTCH signaling in T-ALL. Curr Top Microbiol Immunol 360: 163-182.
9. Duran RV, Hall MN (2012) Regulation of TOR by small GTPases. EMBO Rep 13: 121-128.
10. Chan SM, Weng AP, Tibshirani R, Aster JC, Utz PJ (2007) Notch signals positively regulate activity of the mTOR pathway in T-cell acute lymphoblastic leukemia. Blood 110: 278-86.
11. Palomero T, Sulis ML, Cortina M, Real PJ, Barnes K, et al. (2007) Mutational loss of PTEN inducesresistance to NOTCH1 inhibition in T-cell leukemia. Nat Med 13: 1203-1210.

12. Akers LJ, Fang W, Levy AG, Franklin AR, Huang P, et al. (2011) Targeting glycolysis in leukemia: a novel inhibitor 3-BrOP in combination with rapamycin. Leuk Res 35: 814-820.

13. Renner K, Kofler R, Gnaiger E (2002) Mitochondrial function in glucocorticoid triggered T-ALL cells with transgenic bcl-2 expression. Mol Biol Rep 29: 97-101.

14. Ursini MV, Parrella A, Rosa G, Salzano S, Martini G (1997) Enhanced expression of glucose-6-phosphate dehydrogenase in human cells sustaining oxidative stress. Biochem J 323: 801-806.

15. Herranz D, Ambesi-Impiombato A, Sudderth J, Sánchez-Martín M, Belver L, et al. (2015) Metabolic reprogramming induces resistance to anti-NOTCH1 therapies in T cell acute lymphoblastic leukemia. Nat Med 21: 1182-1189.

16. Son J, Lyssiotis CA, Ying H, Wang X, Hua S, Ligorio M, et al. (2013) Glutamine supports pancreatic cancer growth through a KRAS-regulated metabolic pathway. Nature 496: 101-115.

The International Journal of Biochemistry & Cell Biology 80 (2016) 71–80

Contents lists available at ScienceDirect

The International Journal of Biochemistry & Cell Biology

journal homepage: www.elsevier.com/locate/biocel

Review article

Prolyl hydroxylase domain enzymes and their role in cell signaling and cancer metabolism

Tra Ly Nguyen[a,b,c], Raúl V. Durán[a,b,c,*]

[a] Institut Européen de Chimie et Biologie, 2 Rue Robert Escarpit, 33607 Pessac, France
[b] INSERM U1218 Unit, Institut Bergonié, 229 Cours de l'Argonne, 33076 Bordeaux, France
[c] University of Bordeaux, Bordeaux, France

ARTICLE INFO

Article history:
Received 29 July 2016
Received in revised form
28 September 2016
Accepted 30 September 2016
Available online 1 October 2016

Keywords:
2-Oxoglutarate
Cancer
Metabolism
mTOR
PHD

ABSTRACT

The prolyl hydroxylase domain (PHD) enzymes regulate the stability of the hypoxia-inducible factor (HIF) in response to oxygen availability. During oxygen limitation, the inhibition of PHD permits the stabilization of HIF, allowing the cellular adaptation to hypoxia. This adaptation is especially important for solid tumors, which are often exposed to a hypoxic environment. However, and despite their original role as the oxygen sensors of the cell, PHD are currently known to display HIF-independent and hydroxylase-independent functions in the control of different cellular pathways, including mTOR pathway, NF-kB pathway, apoptosis and cellular metabolism. In this review, we summarize the recent advances in the regulation and functions of PHD in cancer signaling and cell metabolism.

Contents

Abbreviations: αKG, 2-oxoglutarate; AMPK, AMP-activated protein kinase; ATF4, activating transcription factor 4; DDR, DNA damage response; DMOG, dimethyloxaloylglycine; eEF2, eukaryotic elongation factor 2; EGFR, epidermal growth factor receptor; HCLK2, Caenorhabditis elegans biological clock protein CLK-2; HIF, hypoxia inducible factor; HRE, hypoxia-response element; Hsp90, heat shock protein 90; KIF1Bβ, kinesin-like protein; mTOR, mammalian target of rapamycin; NF-kB, nuclear factor-kappa B; ODD, oxygen dependent degradation; PCBP, poly-r(C)-binding protein 1; PDH, pyruvate dehydrogenase; PKM2, pyruvate kinase isozymes M2; PHD, prolyl hydroxylase; pVHL, von Hippel-Lindau tumor suppressor; ROS, reactive oxygen species; TCA, tricarboxylic acid cycle.

* Corresponding author at: Institut Européen de Chimie et Biologie, 2 Rue Robert Escarpit, 33607 Pessac, France.
E-mail address: raul.duran@inserm.fr (R.V. Durán).

http://dx.doi.org/10.1016/j.biocel.2016.09.026
1357-2725/

1. Introduction

Among the different hallmarks of cancer (Hanahan and Weinberg, 2011), metabolic transformation plays a key role in the adaptation of cancer cells to a changing environment. Due to the rapid proliferation of cancer cells, solid tumors are often exposed to low oxygen and nutrient availabilities. The stabilization of the hypoxia-inducible factor (HIF) upon oxygen restriction in the cancer cell coordinates the transcriptional response to low oxygen levels. Known as the oxygen sensors of the cell in metazoans, the prolyl hydroxylase domain (PHD) protein family plays a central role in the regulation of HIF stability. PHD enzymes were first described about 10 years after HIF discovery. This family belongs to a family of 2-oxoglutarate(αKG)-dependent, non-haem iron-binding dioxygenases. PHD were discovered in *Caenorhabditis elegans* (EGL-9), and since then they have been described in different organisms, such as mammals (EGLN1-4), rat (SM-20), *Drosophila melanogaster* (CG1114), *Dictyostelium*, the fission yeast (*Schizosaccharomyces pombe*), or even in photosynthetic organisms such as *Chlamydomonas reinhardtii* (Boulahbel et al., 2009). In mammalian cells, there are three different genes encoding three isoforms of PHD, called EGLN1 (encoding PHD2), EGLN2 (encoding PHD1), and EGLN3 (encoding PHD3). An endoplasmic reticulum transmembrane prolyl hydroxylase (TM-HIF-P4H) has also been identified with an activity similar to HIF prolyl hydroxylase but the C-terminal catalytic region is closely related to collagen prolyl hydroxylase (Koivunen et al., 2007b; Oehme et al., 2002). PHD1 and PHD2 are two longer isoforms with respectively 407 and 426 amino acids in humans. They share a highly conserved hydroxylase domain at their C-terminal domain, but a divergent and poorly characterized N-terminal domain. The shorter isoform PHD3, with only 239 amino acids, has the hydroxylase domain and also a divergent N-terminal sequence (Bruick and Mcknight, 2001; Epstein et al., 2001; Ivan et al., 2002).

All three isoforms are expressed in all tissues but at different levels. PHD2 is found in most tissues, whereas PHD1 is more expressed in testes, brain, kidney, heart, and liver, and PHD3 is present mostly in the heart (Cioffi et al., 2003). Although three main isoforms are reported and studied, different alternatively spliced isoforms have been also described (Hirsilä et al., 2003). For example, gain or loss of function of different splicing forms of the PHD3 gene are reported to regulate the hypoxia response pathway (Cervera et al., 2006). Besides, two different isoforms of PHD1, produced by alternative translational initiation, have very similar activity on the HIF system, raising a question of the regulation of other non-HIF targets (Tian et al., 2006). So far, alternatively spliced PHD2 transcripts encode catalytically inactive polypeptides (Hirsilä et al., 2003). The reason of the presence of different splicing isoforms of PHD family is still unclear.

The hydroxylation activity of PHD is oxygen-dependent. As mentioned above, the main target is the transcription factor HIFα, (three main subunits described, HIF-1α, HIF-2α and HIF-3α) that regulates cell response to hypoxic conditions. In the presence of oxygen, PHD (mostly PHD2, at least *in vivo*) hydroxylate HIF-1α in its oxygen-dependent degradation (ODD) domain at two proline residues (P402 and P564). Both proline residues are found in a conserved motif with a sequence like −Leu-X-X-Leu-Ala-Pro, and the substitution of flanking leucine or alanine residues has little effect on prolyl hydroxylation (Epstein et al., 2001; Huang et al., 2002). The hydroxylation leads to the binding of HIFα to the von Hippel–Lindau (pVHL) tumor suppressor protein and induces its ubiquitination and subsequent proteolytic degradation by the E3 ubiquitin ligase complex (Berra et al., 2006). Under hypoxia, PHD are inactivated and HIFα is stabilized, thus interacting with HIFβ, allowing the expression of target genes (Kaelin and Ratcliffe, 2008).

Despite the important role of PHD in oxygen sensing and HIF regulation, there is now strong evidences that PHD have additional functions in different pathways. Various publications have reported non-HIF substrates and also hydroxylase-independent functions of PHD. In this review, we will summarize both the HIF-dependent and HIF-independent functions and regulation of PHD inside the eukaryotic cell.

2. Upstream of PHD: metabolic components controlling PHD activity

PHD activity depends on different upstream inputs, such as oxygen and αKG as co-substrates, or iron and ascorbate as co-factors (Fig. 1).

2.1. Oxygen

A member of the dioxygenase family, PHD are able to incorporate both atoms of dioxygen into their products, and they are, as a consequent, sensitive to oxygen level. The isotopic study using ^{18}O showed that one oxygen atom from dioxygen is used in the oxidative decarboxylation of αKG to generate succinate and CO_2, and the other oxygen atom is used for the hydroxylation of a proline residue of the targeted HIFα molecule (McNeill et al., 2002). The presence of oxygen is crucial for PHD activity and it cannot be substituted by an H_2O molecule. Different studies have measured the affinity of PHD by oxygen using HIFα peptide substrates. The apparent K_M for oxygen (the concentration of oxygen that supports a half-maximal initial catalytic rate) is closer to 100 μM (Ehrismann et al., 2007; Koivunen et al., 2006). Compared with others dioxygenases, this K_M is particularly high, and certainly higher than the intracellular oxygen level (10–30 μM). It means that PHD activity relies on oxygen levels when all other substrates and co-factors are available. This is the biochemical basis of the function of PHD as oxygen sensors. PHD are also regulated by O_2 availability through E3 ubiquitin ligases Siah1a and Siah2 activity. Under hypoxia, Siah2 transcription is stimulated, leading to PHD1 and PHD3 proteasomal degradation (Nakayama et al., 2004). This study present an additional layer of complexity in the regulation of PHD in response to oxygen level.

Low oxygen levels lead to the production of Reactive Oxygen Species (ROS) generated by complex III of the mitochondrial electron transport chain (Chandel et al., 1998). Several works confirmed the role of ROS in the control of HIFα stability by genetic or pharmacological inhibition of mitochondria activity (Brunelle et al., 2005; Chandel et al., 2000; Guzy et al., 2005; Mansfield et al., 2005; Pan et al., 2006). According to this, ROS production inhibits PHD enzymes by regulating the level of Fe(II), ascorbate or Krebs cycle intermediates which have an impact on PHD activity (Gerald et al., 2004; Hagen, 2012; Li et al., 2014). Nonetheless, different works denied the role of ROS in HIF accumulation. In mitochondria-deficient HeLa cells, ROS production is very low and HIF can still be stabilized under hypoxia (Enomoto et al., 2002). Another result showed that mitochondria regulate HIF-1α protein stabilization and accumulation by regulating the intracellular oxygen availability not by producing ROS from complex III (Chua et al., 2010).

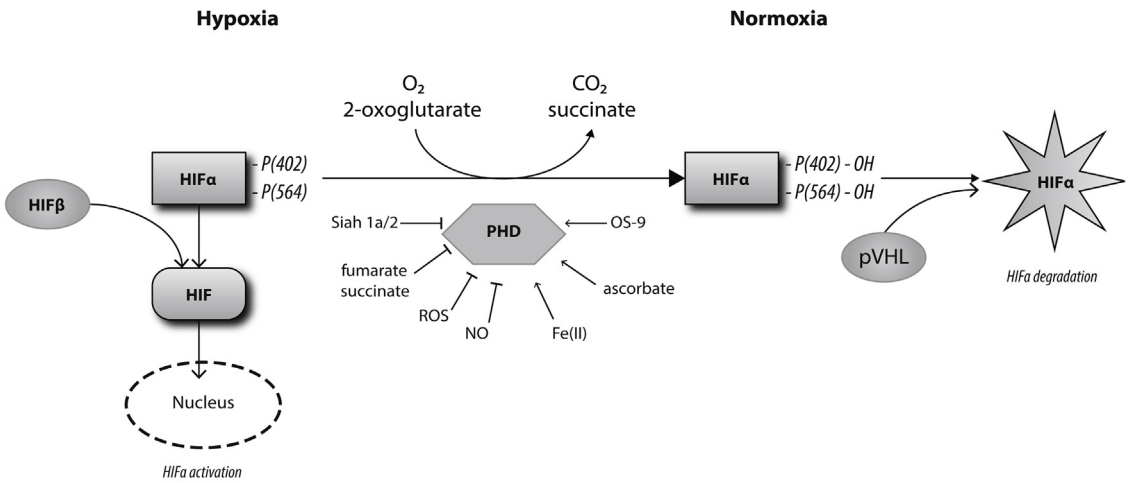

Fig. 1. The hydroxylation of HIFα by PHD proteins depends on oxygen level. Under normoxia, PHD hydroxylate HIFα in its oxygen-dependent degradation (ODD) domain at two proline residues (P402 and P564 in the case of HIF-1α). This hydroxylation leads to the binding of HIFα subunit to the von Hippel–Lindau (pVHL) protein and induces the ubiquitination of HIFα and its subsequent proteolytic degradation by the E3 ubiquitin ligase complex. When oxygen levels decrease under hypoxic conditions, PHD activity is inhibited and HIFα is accumulated. Then, stable HIFα interacts with HIFβ to induce the expression of different target genes. PHD are also sensitive to different upstream inputs which regulate their activity is response to environmental changes.

An additional inhibitor of PHD is nitric oxide (NO), which is known to compete with O2 for binding to iron at the active site of αKG-dependent oxygenases (Zhang et al., 2002). Besides, NO is also an endogenous inhibitor of cytochrome c oxidase. Inhibition of mitochondrial respiration by NO can lead to HIFα destabilization under hypoxia (Hagen et al., 2003). There are different explanations. Nitric oxide can prevent ROS production in the mitochondria under hypoxia. An alternative explanation could be that a redistribution of intracellular oxygen, from the inactivated mitochondria to the cytosol, activates PHD family and causes HIFα degradation. Under normoxic conditions, mitochondria inhibitors do not increase PHD activity (Doege et al., 2005; Kaelin, 2005). Overall, NO has different effects on PHD activity in function of the environment.

2.2. 2-Oxoglutarate

As mentioned above, αKG, an intermediate of the tricarboxylic acid (TCA) cycle, is a co-substrate of PHD, serving as an electron donor for prolyl hydroxylation. In addition, αKG is needed for the coordination of Fe(II) in the catalytic center of PHD (Epstein et al., 2001). Produced mostly in the mitochondria, αKG shuttles from the mitochondria to the cytosol through a malate—αKG transporter. Non-metabolizable analogues of αKG, such as dimethyloxallyl glycine (DMOG), competitively inhibit the PHD activity and stabilize HIF-1α both *in vitro* and *in vivo*. In addition to that, TCA cycle intermediates, such as citrate, isocitrate, succinate, fumarate, malate, oxaloacetate and pyruvate, are also reported to inhibit PHD (Dalgard et al., 2004; Hewitson et al., 2007; Koivunen et al., 2007a; Selak et al., 2005). Fumarate, succinate and oxaloacetate are identified as competitive inhibitors of all three PHD isoforms *in vitro* with similar IC_{50}, being fumarate the most effective inhibitor and oxaloacetate the weakest. Succinate, as the product of the hydroxylation reaction catalyzed by PHD, can also inhibit its activity. Citrate is an effective inhibitor of PHD3, but not of two others (Koivunen et al., 2007a). Under normal conditions, these molecules cannot compete against αKG in PHD activity because they are produced and consumed mostly in the mitochondria. However, succinate dehydrogenase and fumarate hydratase deficiencies result in a cytosolic accumulation of succinate and fumarate respectively, leading to the inhibition of PHD (Isaacs et al., 2005; Selak et al., 2005). Interestingly, addition of exogenous αKG, in cells with succinate or fumarate accumulation, can reactivate PHD and destabilize HIF-1α (MacKenzie et al., 2007), which supports the model of a competitive relationship between αKG and TCA intermediates in the activation of PHD. Other molecules of the TCA cycle or glucose metabolites are also reported to modulate HIF hydroxylation, but this regulation is not completely clear and seems to depend on the experimental systems, and therefore requires a more detailed investigation.

The production of αKG during normoxia is critical for the activity of PHD, following a mechanism that seems to involve the metabolism of certain amino acids (Duran et al., 2013). In highly proliferating cells, αKG is produced mostly from glutamine through glutaminolysis, a two steps process catalyzed by glutaminase and glutamate dehydrogenase. Thus, glutaminolysis is necessary to produce αKG and to re-feed the TCA cycle. Indeed, αKG levels are dependent on amino acid availability. Under amino acid deprivation, αKG levels decrease, leading to an inactivation of PHD. The addition of a cell-permeable αKG derivative replenishes the αKG levels during amino acid restriction and restores PHD activity. Intriguingly, the inhibition of PHD activity during amino acid deprivation does not cause HIFα accumulation and activation of HIF target genes, due to an inhibition of HIFα expression during these conditions.

2.3. Iron

PHD belong to the non-haem, Fe(II)-dependent enzyme family that uses a conserved two-histidine, one carboxylate motif to coordinate Fe(II) at the catalytic site. Iron is firstly bound to the enzyme allowing the binding of other reactants (αKG, HIFα and oxygen) (Schofield and Ratcliffe, 2004). The incorporation Fe(II) into the active site depends on the PCBP family of iron chaperones/RNA-binding proteins activity (Nandal et al., 2011). Iron chelators (such as deferoxamine mesylate) or iron antagonists (such as cobalt chloride) can inhibit PHD by stabilizing HIFα and HIFα-transcriptional activity. Structural and spectroscopic studies have shown that the active-site Fe(II) can be substituted by Co(II), Cu(II), Zn(II) and Mn(II) (Epstein et al., 2001). Moreover, cobalt also binds directly to HIFα and prevents its degradation (Yuan et al., 2003, 2001). Besides, nitric oxide chelates Fe(II) and ROS oxidizes the ferrous iron Fe(II) to the ferric state Fe(III),

inducing PHD inactivation. Additionally, iron level plays a role in inflammation-driven, normoxic HIF-1α accumulation. In dendritic cells, lipopolysaccharide-triggered inflammation blocks PHD activity through NF-kB-mediated decrease of intracellular available iron, then leads to HIF-1α stabilization and activation of immune system (Siegert et al., 2015). In turn, HIF activity is also involved in iron metabolism and homeostasis. Thus, expressions of transferrin, an iron transporter, and the transferrin receptor 1 (TfR1), necessary for iron uptake, are regulated by HIF under hypoxia (Lok and Ponka, 1999; Rolfs et al., 1997; Tacchini et al., 1999). Therefore, there is a complex crosstalk between HIF regulation and iron metabolism.

2.4. Ascorbate

As other αKG-dependent dioxygenases, PHD also need ascorbate for full catalytic activity. The detailed role of ascorbate is not very well known, as it is not needed during the majority of the catalytic cycle. Ascorbate can reduce Fe(III) to Fe(II) in solution, and prevent, at the active site, its oxidation for a full activity of the enzyme. The current model proposes that ascorbate participates in the completion of uncoupled cycles. In the complete reaction, the oxidative decarboxylation of αKG to succinate leads to the formation of a ferryl ion (Fe(IV) = 0). But in the uncoupled reaction, Fe(II) is converted to Fe(III) which remains bound to the active site, making the enzyme unavailable for a new catalytic cycle. Thus, ascorbate is needed to reduce the ferric state Fe(III) and reactivate the enzyme (Myllyla et al., 1984). The presence of nickel (II) and cobalt (II) in the environment can inhibit PHD activity through the reduction of intracellular ascorbate concentrations (Salnikow et al., 2004). The addition of higher concentrations of ascorbate to the cell can restore the catalytic activity of PHD.

3. Downstream of PHD: metabolic and singnaling functions controlled by PHD

3.1. HIF-dependent regulation of metabolism

HIF is a heterodimer consisting of one alpha subunit (three isoforms present in humans, HIF-1α, HIF-2α or HIF-3α) and one beta subunit (only one isoform, HIFβ, also known as Aryl Hydrocarbon Nuclear Translocator, ARNT). The heterodimeric HIF binds to DNA of different target genes at the hypoxia response elements (HREs), which present the specific sequence G/ACGTG. These target genes are involved in glucose metabolism, angiogenesis, cell proliferation and cell survival (Semenza, 2012). Among them, vascular endothelial growth factor (VEGF) expression is enhanced for the angiogenesis activation in colorectal, gastric, and pancreatic cancer (Forsythe et al., 1996). Moreover, HIF can increase glucose metabolism by inducing glucose transporters (GLUT1 and GLUT3) and glycolytic enzymes that convert glucose to lactate, at the same time inhibiting mitochondrial oxidative metabolism (Semenza, 2012). Thus, HIF overexpression is advantageous in the hypoxic regions of solid tumors in many different types of cancer. Among the three isoforms of HIFα, HIF-1α and HIF-2α are the best characterized, while HIF-3α regulation is less understood (Schofield and Ratcliffe, 2004). The control of metabolism by HIF has been indeed extensively reviewed previously (Masson and Ratcliffe, 2014; Semenza, 2013).

The activity of HIF depends on the stabilization of the alpha subunits. HIFα subunits are rapidly degraded in the presence of oxygen. HIF-1α and HIF-2α have two independently functioning oxygen-dependent degradation domains (NODDD and CODDD) that play a central role in the proteolytic regulation mediated by PHD (Kaelin and Ratcliffe, 2008). Thus, PHD mediate this stabilization in function of oxygen availability, linking oxygen availability and HIF stabilization. Among the three isoforms of PHD, PHD2 is known to be the main oxygen sensor for HIF stabilization in vivo. Thus, silencing PHD2 using siRNA is sufficient to upregulate the protein concentration of HIF-1α, and to increase the nuclear accumulation of HIF, and to induce HIF-dependent transcription during normoxia (Berra et al., 2003). Nevertheless, PHD1 and PHD3 also regulate HIF but under specific conditions as prolonged hypoxia (Appelhoffl et al., 2004) or specific tissues. In a negative feedback loop, both PHD2, and PHD3 expression can be induced during hypoxia in a HIF-dependent manner (Berra et al., 2003; D'Angelo et al., 2003; Del Peso et al., 2003; Marxsen et al., 2004). Indeed, *phd2/egln-1* gene contains a *cis*-regulatory HRE motif, which converts PHD2 in a direct HIF target gene (Metzen et al., 2005).

The interplay between PHD and HIF, however, seems to involve additional elements, which are not completely understood. For instance, a recent report highlighted the control of HIF by PHD3 in a hydroxylase-independent manner (Núñez-O'Mara et al., 2015). Thus, PHD3 sumoylation contributes to the repression of HIF-dependent transcriptional activity, without affecting PHD3 hydroxylase activity or HIF stability. In addition to that, alternative splicing isoforms of the PHD family members have been reported (Hirsilä et al., 2003). Those spliced isoforms present an altered structure of the catalytic core, and therefore their hydroxylase activity is thought to be impaired. However, the function and the regulation of these isoforms remain unclear.

3.2. HIF-independent functions of PHD

In addition to the well-characterized function of PHD as regulators of HIF stability, PHD have been also reported to control metabolism, cell signaling, gene expression and apoptosis in a HIF-independent fashion.

3.2.1. Control of cellular metabolism by PHD

3.2.1.1. Glycolysis. In addition to HIF, PHD control glycolysis through the hydroxylation of pyruvate kinase M2 (PKM2), an isoform of the glycolytic enzyme pyruvate kinase. In cancer cells, PKM2 is more abundant than PKM1, and exists mainly as dimer/monomer (the less active conformation), rather than as a tetramer (the most active conformation). PKM2 isoform has been thus related with the Warburg effect (anaerobic glycolysis) and with tumorigenesis (Christofk et al., 2008; Hitosugi et al., 2009). Interestingly, the downregulation of PHD3 increases the tetrameric conformation of PKM2, resulting in an increase in pyruvate production (Chen et al., 2011). In addition, PHD3 was shown to interact with and hydroxylates PKM2 on two proline residues, enhancing the interaction between PKM2 and HIF-1α. In the same work, it was shown that this interaction happens within multiple domain, including the transactivation domain and the PAS domain of HIF-1α. Interestingly, this direct interaction between PKM2 and HIF-1α promotes the transactivation of HIF-target genes, thus reprograming glucose metabolism in cancer cells (Luo et al., 2011).

Pyruvate dehydrogenase (PDH) catalyzes the conversion of pyruvate in acetyl-coA and regulates the connection between glycolysis and the TCA cycle. PDH is one of the key enzymes in glycolysis, containing four main subunits: E1α, E1β, E2, and E3. Its activity depends on the phosphorylation status of E1α that is regulated by pyruvate dehydrogenase kinase, which in turn is upregulated by HIF. When E1α is phosphorylated, PDH activity is inhibited, leading to a metabolic shift from mitochondrial respiration to glycolysis (Kim et al., 2006). Recently, it has been reported that PDH activity was significantly decreased in PHD3-depleted cells both in normoxia and in hypoxia (Kikuchi et al., 2014). While PHD3 ablation does not affect the phosphorylation of E1α, E1α, E2 subunits, PHD3-deficient cells display a destabilization of the PDH complex, which impairs its functionality. Further investigations are

required to determine the molecular mechanism of the regulation of the PDH complex by PHD3. Altogether, these results suggest that PHD3 can control glycolytic rate both in HIF-dependent and HIF-independent manner, through the regulation of PKM2 and PDH activities.

3.2.1.2. Mitochondrial physiology. The HIF-independent role of PHD in energy metabolism is described in neonatal cardiomyocytes (Sridharan et al., 2007, 2008). PHD inhibition with DMOG suppresses actively respiration in a PHD/HIF-dependent way, and decreases ATP consumption for contractile activity via a HIF-independent mechanism. In addition, DMOG treatment activates the conversion of succinate into fumarate by mitochondrial complex II to maintain ATP levels upon cytochrome c oxidase inactivation, which happens often during anoxia in cardiac tissue. Thus, PHD inhibition using DMOG offers protection to the cell from the blockade of oxidative phosphorylation by maintaining mitochondrial membrane potential.

Moreover, DMOG has been shown to have a direct effect on mitochondrial function in a PHD/HIF-independent manner (Zhdanov et al., 2015). Zhdanov et al. (2015) showed that DMOG suppresses cellular respiration, inhibits ATP production and decreases histone H4 lysine 16 acetylation before activation of the HIF pathway, through a direct inhibition of the mitochondrial enzymes. In addition, DMOG-treated cells are more sensitive to glycolysis inhibition or glucose deprivation. Thus, the double treatment targeting both PHD and glycolysis could be an interesting therapy to be considered against cancer.

3.2.1.3. Neuronal metabolism. Recently, Quaegebeur et al. showed a HIF-independent function of PHD1 in neuronal metabolism (Quaegebeur et al., 2016). PHD1 deficiency provides neuroprotection against brain ischemic stroke, which is the fourth leading cause of death in humans. In murine model, these authors showed that PHD1-/- neurons induced a reprograming of glucose metabolism during ischemic conditions, without vascular changes. Glucose flux is diverted towards the oxidative pentose phosphate pathway instead of glycolysis, which helps to scavenge oxygen radicals and protect against neuronal death. The proposed mechanism involves NF-kB signaling pathway downstream of PHD1 in the reprogramming of glucose metabolism.

Thus, PHD1 deficiency increases NF-kB promoter activity via reduced hydroxylation. Being a regulator of neuronal metabolism, PHD1 could be a potential therapeutic target to prevent ischemic stroke.

3.2.2. Control of cell signaling by PHD

3.2.2.1. mTOR signaling. PHD have been involved in the activation of mTORC1 by amino acids in a HIF-independent manner (Duran et al., 2013). The mammalian target of rapamycin (mTOR) is a serine/threonine kinase highly conserved from unicellular eukaryotes to humans. mTOR is organized in two functionally and structurally distinct complexes: mTOR complex 1 (mTORC1) and mTOR complex 2 (mTORC2). As rapamycin specifically inhibits mTORC1, this complex has been more studied than mTORC2. mTORC1 receives several inputs, including intracellular and extracellular signals: growth factors, amino acids, stress, oxygen availability and the bioenergetics status of the cell. In function of those inputs, mTORC1 can regulate different major cellular processes such as protein and lipid synthesis, and autophagy (Soulard et al., 2009; Wullschleger et al., 2006). Whereas the mechanisms by which growth factors, oxygen and energetic status control mTORC1 activity are well understood, the pathway by which amino acids activate mTORC1 activity has been the focus of an intense debate in the last years. Amino acids allow mTORC1 to translocate to the surface of the lysosome to interact with its co-activator, Rheb, a GTPase activated by growth factors. The lysosomal translocation of mTORC1 is necessary for mTORC1 activation and requires the activation of Rag GTPase, an heterodimer located in the surface of the lysosome (Bar-Peled et al., 2012). There are four members in Rag family RagA, RagB, RagC and RagD which are coupled in heterodimers: RagA or RagB interacts with RagC or RagD. Amino acids induce the exchange of GDP by GTP in RagA/B, allowing the Rag heterodimer to bind and thereby recruit mTORC1 to the lysosome (Durán et al., 2012). The exchange of GDP by GTP in RagA/B is catalyzed by the GEF activity of Ragulator, a pentameric complex that tethers the Rag to the lysosome.

Glutamine is the most abundant free amino acid in the blood and is highly consumed by proliferative cells. As explained above, glutamine sustain αKG levels through glutaminolysis. This production of αKG is necessary for the translocation of mTORC1 to the lysosomal surface and is subsequent activation (Durán et al., 2012; Lorin et al., 2013), but it is also necessary for the activation of PHD (Duran et al., 2013). Importantly, the inhibition of PHD impairs the ability of glutaminolysis to activate mTORC1, suggesting an active role of PHD in the activation of mTORC1. However, the direct substrate(s) of PHD which are mediating this mechanism are not known, neither which isoform of the PHD family plays the role in mTORC1 activation.

3.2.2.2. NF-kB signaling. The nuclear factor kappa-light chain-enhancer of activated B cells (NF-kB), which is involved in inflammatory and innate immune responses, is also regulated by PHD activity. Indeed, both PHD1 and PHD3 are negative regulators of NF-kB through IkB kinase β (IKKβ). The molecular mechanism is not known, but some hypotheses are reported. IKKβ could be hydroxylated by PHD1 and PHD3 on a putative hydroxylation motif (Cummins et al., 2006; Fu and Taubman, 2010). Alternatively, PHD3 could block the interaction between IKKβ and heat shock protein 90 (Hsp90) in a hydroxylation-independent manner. This interaction is required for the phosphorylation and activation of IKKβ, and thus for the activation of the NF-kB pathway (Xue et al., 2010).

Moreover, PHD2 also plays a role in NF-kB pathway regulation in macrophage (Takeda et al., 2011). Macrophage expressing low level of PHD2 displays an arteriogenic phenotype which enhances the formation of collateral vessels and protects the skeletal muscle from ischaemic necrosis through angiopoietin receptor signaling. In conditions of ischemia, angiopoietin-mediated repression of PHD2 induces angiopoietin receptor upregulation in macrophages, following a NF-kB-dependent mechanism. In turn, angiopoietin receptor promotes the proarteriogenic functions of macrophages (Hamm et al., 2013).

3.2.2.3. Epidermal growth factor receptor signaling. Solid tumors are often subjected to low oxygen and nutrient availability that can damage cell metabolism. In response to hypoxia and nutrient starvation, cells enter to a dormant state with a decreased proliferation, cell cycle arrest and cell death escape, enabling cell survival. In glioblastoma, PHD3 upregulation has been found as an additional mechanism to promote growth inhibition through EGFR (epidermal growth factor receptor) internalization and signaling (Garvalov et al., 2014; Henze et al., 2014). This function of PHD3 is independent of HIF regulation, NF-kB or hydroxylation-dependent degradation. In high-grade human gliomas, PHD3 is downregulated by genetic deletion and promoter hyper-methylation, even in hypoxic conditions. Loss of PHD3 results in hyper-phosphorylation of EGFR and its internalization impairment. This results in the upregulation of EGFR signaling, promoting cell growth and escaping the growth inhibition of hypoxia. In this context, the regulation of EGFR by PHD3 identifies PHD3 as a regulator of cell growth.

3.2.2.4. Erythropoietin receptor signaling. Erythropoietin receptor is a member of the cytokine receptor family that plays a role in the cell differentiation and cell survival of erythroid progenitor cells. Upon erythropoietin binding, erythropoietin receptor activates JAK2-STAT5 signal transduction cascade. Erythropoiesis is dependent of the erythropoietin concentration that is regulated by an oxygen-sensitive PHD2-HIF-2α-VHL axis (Kapitsinou et al., 2010). Heir et al. have recently reported that erythropoietin receptor is hydroxylated by PHD3 on prolines at position 419 and 426 of the cytoplasmic region. This hydroxylation, especially at Pro419, is oxygen dependent and targeted for VHL-mediated ubiquitination and subsequent degradation. Hypoxia or inhibition of PHD3 or VHL lead to an aberrant expression level of erythropoietin receptor and erythropoietin-dependent downstream signaling. Moreover, the accumulation of truncated erythropoietin receptor at the plasma membrane, associated with primary familial and congenital polycythemia, could be the consequent of the absence of Pro419 (and/or Pro426) then PHD3-VHL-mediated degradation. Further experiments are needed to better understand the control and the important role of the hydroxylation of Pro419 and 426 for the erythropoietin receptor turnover in erythropoiesis (Heir et al., 2016).

3.2.3. Control of transcription and translation by PHD

3.2.3.1. RNA polymerase II. The large subunit of RNA polymerase II has been reported to be a target of both PHD1 and PHD2 in renal clear cell carcinoma. The hydroxylation of a proline residue (Pro-1465) within an LXXLAP motif is necessary for the phosphorylation of Ser-5 in the C-terminal domain of Rpb1, which in turn leads to the ubiquitination of the complex in low-grade oxidative stress (Mikhaylova et al., 2008). PHD1 is necessary for this hydroxylation, while PHD2 has an inhibitory effect on this modification. This hydroxylation on Pro-1465 was suggested to have an oncogenic effect, as the expression of a P1465A mutant of the large subunit of RNA polymerase II does not stimulate kidney tumor growth.

3.2.3.2. Activating transcription factor 4. Activating transcription factor 4 (ATF4), also known as CREB2, TAXREB67 or C/ATF, is a transcription factor that regulates gene expression in mitochondrial function, amino acid metabolism and redox chemistry, in response to metabolic stress (such as glucose and amino acid deprivation), oxidative stress, and ER stress (Ameri and Harris, 2008). ATF4 is highly activated in hypoxia conditions, promoting tumor growth. Both PHD3 and PHD1 participate in this hypoxia-dependent regulation of ATF4. However, this PHD-dependent regulation of ATF4 does not require pVHL-mediated ubiquitination (Hiwatashi et al., 2011; Köditz et al., 2007). Although both enzymes repress the transcriptional activity of ATF4, whether ATF4 is hydroxylated by PHD has not been demonstrated.

3.2.3.3. Eukaryotic elongation factor 2 kinase. Eukaryotic elongation factor 2 (eEF2) kinase is reported to be hydroxylated by PHD on proline-98 which are inactivated during hypoxia (Moore et al., 2015). eEF2 kinase regulates indirectly the translation elongation step of protein synthesis by phosphorylating and inhibiting the activity the eukaryotic elongation factor 2 and then slowing down elongation. It is a high energy-consuming process, which is regulated in function of nutrient availability by mTORC1 or AMPK pathways to conserve energy (ATP or GTP) and to adapt low nutrient conditions. Moore and al. have described a new regulation of eEF2 kinase by oxygen-dependent proline hydroxylation catalyzed by PHD. This hydroxylation leads to an impairment of the interaction of eEF2 kinase with calmodulin, and therefore to a decrease in the calmodulin-mediated activation of eEF2 kinase. The regulation of eEF2 kinase by proline hydroxylation allows cells to adapt to low oxygen conditions, not only to nutrient availability. According to its regulation in response to different inputs of environment, eEF2 kinase is playing a cytoprotective role to the cells, especially in poorly vascularized solid tumors.

3.2.4. Control of apoptosis by PHD

The hydroxylation activity of PHD3 regulates apoptosis in a HIF-independent manner. In neuronal cells, PHD3 is the unique enzyme of the PHD family responsible for apoptosis induced by nerve growth factor deprivation (Lee et al., 2005; Lipscomb et al., 1999). Its possible downstream target is the kinesin-like protein KIF1Bβ, a microtubule motor (Schlisio et al., 2008). However, it is unclear whether KIF1Bβ is a direct substrate hydroxylated by PHD3, and how KIF1Bβ could regulate mechanistically apoptosis in cancer. In addition, PHD3 plays an important role in the DNA Damage Response (DDR) and in apoptosis induced by DNA damage (Xie et al., 2012). In this context, the direct hydroxylation target of PHD3 is HCLK2 (human homologue of the *Caenorhabditis elegans* biological clock protein Clk2), an essential component of the ATR/CHK1/p53 signaling pathway leading to the association between HCLK2 and ATR, and to the subsequent activation of the pathway. Moreover, the interaction between PHD3 and HCLK2 seems to be involved also in cell cycle regulation, as the depletion of either PHD3 or HCLK2 blocks the cell cycle and reduces S phase (Högel et al., 2011; Takai et al., 2007; Xie et al., 2012). Another direct target of PHD3 is beta(2)-adrenergic receptor, a prototypic G-protein coupled receptor that plays a role in cardiovascular and pulmonary regulation (Xie et al., 2009). Hydroxylation of beta(2)-adrenergic receptor by PHD3 allows its interaction with the pVHL-E3 ligase complex and its subsequent ubiquitin-mediated degradation. Furthermore, this receptor is involved in apoptosis in thymocytes (Gu et al., 2000). However, despite of many established links between PHD3 and apoptosis, the direct targets of PHD3 and the mechanism of PHD3-mediated apoptosis are not completely understood. In any case, the role of PHD3 in apoptosis induction seems to be tissue-specific.

4. PHD and diseases

Due to a number of identified downstream targets, PHD become a new target for drug design in the treatment of cancer or cardiovascular diseases. So far, more than 200 HIF-target genes have been identified involved in glucose metabolism, angiogenesis, erythropoiesis, cell proliferation and cell survival. Several diseases are associated with HIF pathway regulation, such as ischemia, peripheral artery disease, anemia, pulmonary hypertension, stroke and many types of cancer. In the case of anemia, stroke or myocardial infarction that are linked with low oxygenation, HIF stabilization is an advantage by inducing angiogenesis, vasodilatation, red blood cell production and tissue survival. The development of new inhibitors of PHD that can stabilize HIF and enhance its activity constitute an attractive strategy to treat these diseases (Bernhardt, 2006; Hsieh et al., 2007; Kasiganesan et al., 2007; Ratan et al., 2007; Shohet and Garcia, 2007).

Different inhibitors of PHD have been reported with diverse results. For example, TM60008 is an inhibitor that binds to PHD active site and chelates Fe(II). It has an effect against ischemia-induced cerebral lesions by reducing neuronal cell death without affecting angiogenesis (Nangaku et al., 2007). FG-2216, an orally bioavailable PHD inhibitor that is currently in clinical development to treat anemia, effectively and reversibly promotes erythropoiesis in rhesus macaques and prevents anemia by inducing erythropoietin induction (Hsieh et al., 2007). Moreover, PHD2 inhibitors can also be useful to protect against obesity or metabolic dysfunction, by improving glucose and lipid metabolism. PHD2 hypomorphic mice that have a decreased wild-type PHD2 mRNA, showed improved glucose tolerance and insulin sensitivity, reduced serum

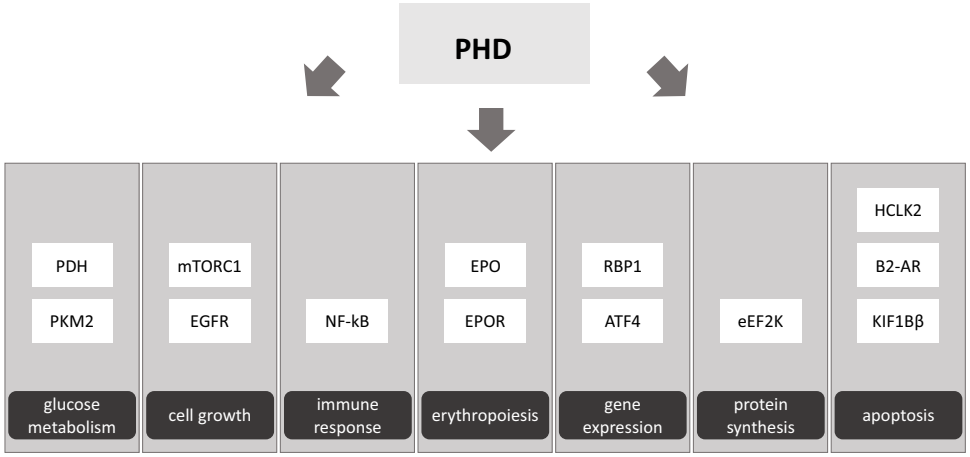

Fig. 2. HIF-independent functions of PHD family. Summary of the cellular processes regulated by PHD in a HIF-independent manner.

cholesterol levels, and protection against hepatic steatosis even in high-fat diet (Rahtu-Korpela et al., 2014).

The presence of HIF in many solid tumors is well documented (Semenza, 2012). In addition to hypoxia, cancer-associated mutations can also lead to HIFα accumulation even under normoxic conditions. This can be due to the higher mTORC1-dependent translation or impaired HIFα degradation (Maxwell, 2005). Loss-activity mutations of TSC1, TSC2, LKB1 or gain-activity mutations of AKT can induce the mTORC1-dependent translation of HIFα (Inoki et al., 2005; Plas and Thompson, 2005). Impaired HIFα degradation is principally due to PHD inactivation or VHL deficiency (Kim and Kaelin, 2004). PHD inactivation results from the accumulation of succinate and fumarate, which is caused by mutations of the two mitochondrial enzymes succinate dehydrogenase and fumarate hydratase, leading to a pseudohypoxic phenotype due to the inactivation of PHD and the subsequent stabilization of HIFα. This stabilization of HIFα plays an important role in the tumorigenic phenotype associated to succinate dehydrogenase and fumarate hydratase mutations (Isaacs et al., 2005; Pollard et al., 2005; Selak et al., 2005). As HIF presents tumor promoting features, and PHDs act as negative regulators of HIF, PHD might display tumor suppressor features. Indeed, overexpression of PHD1 can suppress HIF-1α accumulation and inhibit tumor growth (Erez et al., 2003). Reintroduction of PHD2 in human endometrial cancer cells leads to senescence (Kato et al., 2006). Low expression in PHD3 in colon carcinomas cells is explained by its role in NF-kB signaling inhibition, whereas this pathway is a survival prerequisite of these cells (Xue et al., 2010). PHD3 has also been related with apoptosis and tumor suppression through αKG in xenograft models (Tennant and Gottlieb, 2010). Because of its role in tumor suppression, long-term exposure to PHD inhibitors may increase the probability to develop tumor. Paradoxically, PHD are reported to participate in tumor growth or tumor chemoresistance (Fox et al., 2011; Klotzsche-Von Ameln et al., 2011). Thus, using PHD as therapeutic target needs to be considered carefully in function of cancer type and characterization.

As discussed above, PHD might play an intermediate role in the activation of mTORC1 by glutaminolysis, leading to subsequent inhibition of autophagy. Clinical trials using different analogues of rapamycin have shown modest effects, which could be explained by the activation of autophagy upon mTORC1 inhibition. Autophagy could be a survival strategy of cancer cells against rapamycin treatment. The molecular mechanism of autophagy regulation of mTORC1 through PHD activity needs more investigations, but targeting PHD and autophagy together could be an promising therapy to improve the patient outcome (Villar et al., 2015).

5. Concluding remarks

In conclusion, PHD family becomes so far, not only an oxygen sensor, but also a center of regulation of different signaling pathways (Fig. 2). How PHD can accomplish this central role is still unclear. We still do not understand of the reason of the presence of different splicing isoforms of PHD, neither the structure of the divergent N-terminal domain. Hydroxylase-independent functions are also under discussion because no other enzymatic activity has been identified. Moreover, as PHD functions are isoform-dependent, the drug design needs to be more precise to target the specific isoform, to avoid side effects of treatments. Understanding the PHD functions and its regulation inside the cell will provide new insights for therapeutic strategies.

Declarations of interest

The authors declare no conflict of interest.

Funding information

This research has been funded by INSERM, Conseil Régional d'Aquitaine, and the Fondation pour la Recherche Médicale.

Acknowledgements

We thank Clément Bodineau, Victor H. Villar and Angela Rubio for critically reading the manuscript.

References

Ameri, K., Harris, A.L., 2008. Activating transcription factor 4. Int. J. Biochem. Cell Biol. 40, 14–21, http://dx.doi.org/10.1016/j.biocel.2007.01.020.

Appelhoffl, R.J., Tian, Y.M., Raval, R.R., Turley, H., Harris, A.L., Pugh, C.W., Ratcliffe, P.J., Gleadle, J.M., 2004. Differential function of the prolyl hydroxylases PHD1, PHD2, and PHD3 in the regulation of hypoxia-inducible factor. J. Biol. Chem. 279, 38458–38465, http://dx.doi.org/10.1074/jbc.M406026200.

Bar-Peled, L., Schweitzer, L.D., Zoncu, R., Sabatini, D.M., 2012. Ragulator is a GEF for the rag GTPases that signal amino acid levels to mTORC1. Cell 150, 1196–1208, http://dx.doi.org/10.1016/j.cell.2012.07.032.

Bernhardt, W.M., 2006. Preconditional activation of hypoxia-inducible factors ameliorates ischemic acute renal failure. J. Am. Soc. Nephrol. 17, 1970–1978, http://dx.doi.org/10.1681/ASN.2005121302.

Berra, E., Benizri, E., Ginouvès, A., Volmat, V., Roux, D., Pouysségur, J., 2003. HIF prolyl-hydroxylase 2 is the key oxygen sensor setting low steady-state levels of HIF-1è in normoxia. EMBO J. 22, 4082–4090, http://dx.doi.org/10.1093/emboj/cdg392.

Berra, E., Ginouvès, A., Pouysségur, J., 2006. The hypoxia-inducible-factor hydroxylases bring fresh air into hypoxia signalling. EMBO Rep. 7, 41–45, http://dx.doi.org/10.1038/sj.embor.7400598.

Boulahbel, H., Durán, R.V., Gottlieb, E., 2009. Prolyl hydroxylases as regulators of cell metabolism. Biochem. Soc. Trans. 37, 291–294, http://dx.doi.org/10.1042/BST0370291.

Bruick, R.K., Mcknight, S.L., 2001. A conserved family of prolyl-4-hydroxylases that modify HIF. Science 294, 1337–1340, http://dx.doi.org/10.1126/science.1066373.

Brunelle, J.K., Bell, E.L., Quesada, N.M., Vercauteren, K., Tiranti, V., Zeviani, M., Scarpulla, R.C., Chandel, N.S., 2005. Oxygen sensing requires mitochondrial ROS but not oxidative phosphorylation. Cell Metab. 1, 409–414, http://dx.doi.org/10.1016/j.cmet.2005.05.002.

Cervera, A.M., Apostolova, N., Luna-Crespo, F., Sanjuan-Pla, A., Garcia-Bou, R., McCreath, K.J., 2006. An alternatively spliced transcript of the PHD3 gene retains prolyl hydroxylase activity. Cancer Lett. 233, 131–138, http://dx.doi.org/10.1016/j.canlet.2005.03.004.

Chandel, N.S., Maltepe, E., Goldwasser, E., Mathieu, C.E., Simon, M.C., Schumacker, P.T., 1998. Mitochondrial reactive oxygen species trigger hypoxia-induced transcription. Proc. Natl. Acad. Sci. U. S. A. 95, 11715–11720, http://dx.doi.org/10.1073/pnas.95.20.11715.

Chandel, N.S., McClintock, D.S., Feliciano, C.E., Wood, T.M., Melendez, J.A., Rodriguez, A.M., Schumacker, P.T., 2000. Reactive oxygen species generated at mitochondrial complex III stabilize hypoxia-inducible factor-1α during hypoxia: a mechanism of O2 sensing. J. Biol. Chem. 275, 25130–25138, http://dx.doi.org/10.1074/jbc.M001914200.

Chen, N., Rinner, O., Czernik, D., Nytko, K.J., Zheng, D., Stiehl, D.P., Zamboni, N., Gstaiger, M., Frei, C., 2011. The oxygen sensor PHD3 limits glycolysis under hypoxia via direct binding to pyruvate kinase. Cell Res. 21, 983–986, http://dx.doi.org/10.1038/cr.2011.66.

Christofk, H.R., Vander Heiden, M.G., Harris, M.H., Ramanathan, A., Gerszten, R.E., Wei, R., Fleming, M.D., Schreiber, S.L., Cantley, L.C., 2008. The M2 splice isoform of pyruvate kinase is important for cancer metabolism and tumour growth. Nature 452, 230–233, http://dx.doi.org/10.1038/nature06734.

Chua, Y.L., Dufour, E., Dassa, E.P., Rustin, P., Jacobs, H.T., Taylor, C.T., Hagen, T., 2010. Stabilization of hypoxia-inducible factor-1α protein in hypoxia occurs independently of mitochondrial reactive oxygen species production. J. Biol. Chem. 285, 31277–31284, http://dx.doi.org/10.1074/jbc.M110.158485.

Cioffi, C.L., Liu, X.Q., Kosinski, P.A., Garay, M., Bowen, B.R., 2003. Differential regulation of HIF-1α prolyl-4-hydroxylase genes by hypoxia in human cardiovascular cells. Biochem. Biophys. Res. Commun. 303, 947–953, http://dx.doi.org/10.1016/S0006-291X(03)00453-4.

Cummins, E.P., Berra, E., Comerford, K.M., Ginouves, A., Fitzgerald, K.T., Seeballuck, F., Godson, C., Nielsen, J.E., Moynagh, P., Pouyssegur, J., Taylor, C.T., 2006. Prolyl hydroxylase-1 negatively regulates IkB kinase-β, giving insight into hypoxia-induced NFkB activity. PNAS 103, 18154–18159, http://dx.doi.org/10.1073/pnas.0602235103.

D'Angelo, G., Duplan, E., Boyer, N., Vigne, P., Frelin, C., 2003. Hypoxia up-regulates prolyl hydroxylase activity. A feedback mechansim that limits HIF-1 responses during reoxygenation. J. Biol. Chem. 278, 38183–38187, http://dx.doi.org/10.1074/jbc.M302244200.

Dalgard, C.L., Lu, H., Mohyeldin, A., Verma, A., 2004. Endogenous 2-oxoacids differentially regulate expression of oxygen sensors. Biochem. J. 380, 419–424, http://dx.doi.org/10.1042/BJ20031647.

Del Peso, L., Castellanos, M.C., Temes, E., Martín-Puig, S., Cuevas, Y., Olmos, G., Landázuri, M.O., 2003. The von Hippel Lindau/hypoxia-inducible factor (HIF) pathway regulates the transcription of the HIF-proline hydroxylase genes in response to low oxygen. J. Biol. Chem. 278, 48690–48695, http://dx.doi.org/10.1074/jbc.M308862200.

Doege, K., Heine, S., Jensen, I., Jelkmann, W., Metzen, E., 2005. Inhibition of mitochondrial respiration elevates oxygen concentration but leaves regulation of hypoxia-inducible factor (HIF) intact. Blood 106, 2311–2317, http://dx.doi.org/10.1182/blood-2005-03-1138.

Durán, R.V., Oppliger, W., Robitaille, A.M., Heiserich, L., Skendaj, R., Gottlieb, E., Hall, M.N., 2012. Glutaminolysis activates Rag-mTORC1 signaling. Mol. Cell 47, 349–358, http://dx.doi.org/10.1016/j.molcel.2012.05.043.

Duran, R., Mackenzie, V., Boulahbel, E.D., Frezza, H., Heiserich, C., Tardito, L., Bussolati, S., Rocha, O., Hall, S., Gottlieb, M.N., 2013. HIF-independent role of prolyl hydroxylases in the cellular response to amino acids. Oncogene 32, 4549–4556, http://dx.doi.org/10.1038/onc.2012.465.

Ehrismann, D., Flashman, E., Genn, D.N., Mathioudakis, N., Hewitson, K.S., Ratcliffe, P.J., Schofield, C.J., 2007. Studies on the activity of the hypoxia-inducible-factor hydroxylases using an oxygen consumption assay. Biochem. J. 401, 227–234, http://dx.doi.org/10.1042/BJ20061151.

Enomoto, N., Koshikawa, N., Gassmann, M., Hayashi, J.I., Takenaga, K., 2002. Hypoxic induction of hypoxia-inducible factor-1α and oxygen-regulated gene expression in mitochondrial DNA-depleted HeLa cells. Biochem. Biophys. Res. Commun. 297, 346–352, http://dx.doi.org/10.1016/S0006-291X(02)02186-1.

Epstein, A.C.R., Gleadle, J.M., McNeill, L.A., Hewitson, K.S., O'Rourke, J., Mole, D.R., Mukherji, M., Metzen, E., Wilson, M.I., Dhanda, A., Tian, Y.M., Masson, N., Hamilton, D.L., Jaakkola, P., Barstead, R., Hodgkin, J., Maxwell, P.H., Pugh, C.W., Schofield, C.J., Ratcliffe, P.J., 2001. C. elegans EGL-9 and mammalian homologs define a family of dioxygenases that regulate HIF by prolyl hydroxylation. Cell 107, 43–54, http://dx.doi.org/10.1016/s0092-8674(01)00507-4.

Erez, N., Milyavsky, M., Eilam, R., Shats, I., Goldfinger, N., Rotter, V., 2003. Expression of prolyl-hydroxylase-1 (PHD1/EGLN2) suppresses hypoxia inducible factor-1alpha activation and inhibits tumor growth. Cancer Res. 63, 8777–8783.

Forsythe, J.A., Jiang, B.H., Iyer, N., Agani, V., Leung, F., Koos, S.W., Semenza, R.D., 1996. Activation of vascular endothelial growth factor gene transcription by hypoxia-inducible factor 1. Mol. Cell. Biol. 16, 4604–4613, http://dx.doi.org/10.1128/MCB.16.9.4604.

Fox, S.B., Generali, D., Berruti, A., Brizzi, M.P., Campo, L., Bonardi, S., Bersiga, A., Allevi, G., Milani, M., Aguggini, S., Mele, T., Dogliotti, L., Bottini, A., Harris, A.L., 2011. The prolyl hydroxylase enzymes are positively associated with hypoxia-inducible factor-1α and vascular endothelial growth factor in human breast cancer and alter in response to primary systemic treatment with epirubicin and tamoxifen. Breast Cancer Res. 13, R16, http://dx.doi.org/10.1186/bcr2825.

Fu, J., Taubman, M.B., 2010. Prolyl hydroxylase EGLN3 regulates skeletal myoblast differentiation through an NF-kB-dependent pathway. J. Biol. Chem. 285, 8927–8935, http://dx.doi.org/10.1074/jbc.M109.078600.

Garvalov, B.K., Foss, F., Henze, A.-T., Bethani, I., Gräf-Höchst, S., Singh, D., Filatova, A., Dopeso, H., Seidel, S., Damm, M., Acker-Palmer, A., Acker, T., 2014. PHD3 regulates EGFR internalization and signalling in tumours. Nat. Commun. 5, 5577, http://dx.doi.org/10.1038/ncomms6577.

Gerald, D., Berra, E., Frapart, Y.M., Chan, D.A., Giaccia, A.J., Mansuy, D., Pouysségur, J., Yaniv, M., Mechta-Grigoriou, F., 2004. JunD reduces tumor angiogenesis by protecting cells from oxidative stress. Cell 118, 781–794, http://dx.doi.org/10.1016/j.cell.2004.08.025.

Gu, C., Ma, Y.C., Benjamin, J., Littman, D., Chao, M.V., Huang, X.Y., 2000. Apoptotic signaling through the β-adrenergic receptor: a new G(s) effector pathway. J. Biol. Chem. 275, 20726–20733, http://dx.doi.org/10.1074/jbc.M000152200.

Guzy, R.D., Hoyos, B., Robin, E., Chen, H., Liu, L., Mansfield, K.D., Simon, M.C., Hammerling, U., Schumacker, P.T., 2005. Mitochondrial complex III is required for hypoxia-induced ROS production and cellular oxygen sensing. Cell Metab. 1, 401–408, http://dx.doi.org/10.1016/j.cmet.2005.05.001.

Högel, H., Rantanen, K., Jokilehto, T., Grenman, R., Jaakkola, P.M., 2011. Prolyl hydroxylase PHD3 enhances the hypoxic survival and G1 to S transition of carcinoma cells. PLoS One 6, e27112, http://dx.doi.org/10.1371/journal.pone.0027112.

Hagen, T., Taylor, C.T., Lam, F., Moncada, S., 2003. Redistribution of intracellular oxygen in hypoxia by nitric oxide: effect on HIF1α. Science (80) 302, 1975–1978, http://dx.doi.org/10.1126/science.1088805.

Hagen, T., 2012. Oxygen versus reactive oxygen in the regulation of HIF-1α: the balance tips. Biochem. Res. Int. 2012, 1–5, http://dx.doi.org/10.1155/2012/436981.

Hamm, A., Veschini, L., Takeda, Y., Costa, S., Delamarre, E., Squadrito, M.L., Henze, A.-T., Wenes, M., Serneels, J., Pucci, F., Roncal, C., Anisimov, A., Alitalo, K., De Palma, M., Mazzone, M., 2013. PHD2 regulates arteriogenic macrophages through TIE2 signalling. EMBO Mol. Med. 5, 843–857, http://dx.doi.org/10.1002/emmm.201302695.

Hanahan, D., Weinberg, R.A., 2011. Hallmarks of cancer: the next generation. Cell 144, 646–674, http://dx.doi.org/10.1016/j.cell.2011.02.013.

Heir, P., Srikumar, T., Bikopoulos, G., Bunda, S., Poon, B.P., Lee, J.E., Raught, B., Ohh, M., 2016. Oxygen-dependent regulation of erythropoietin receptor turnover and signaling. J. Biol. Chem., 7357–7372, http://dx.doi.org/10.1074/jbc.m115.694562.

Henze, A.-T., Garvalov, B.K., Seidel, S., Cuesta, A.M., Ritter, M., Filatova, A., Foss, F., Dopeso, H., Essmann, C.L., Maxwell, P.H., Reifenberger, G., Carmeliet, P., Acker-Palmer, A., Acker, T., 2014. Loss of PHD3 allows tumours to overcome hypoxic growth inhibition and sustain proliferation through EGFR. Nat. Commun. 5, 5582, http://dx.doi.org/10.1038/ncomms6582.

Hewitson, K.S., Lienard, B.M.R., McDonough, M.A., Clifton, I.J., Butler, D., Soares, A.S., Oldham, N.J., McNeill, L.A., Schofield, C.J., 2007. Structural and mechanistic studies on the inhibition of the hypoxia-inducible transcription factor hydroxylases by tricarboxylic acid cycle intermediates. J. Biol. Chem. 282, 3293–3301, http://dx.doi.org/10.1074/jbc.M608337200.

Hirsilä, M., Koivunen, P., Günzler, V., Kivirikko, K.I., Myllyharju, J., 2003. Characterization of the human prolyl 4-hydroxylases that modify the hypoxia-inducible factor. J. Biol. Chem. 278, 30772–30780, http://dx.doi.org/10.1074/jbc.M304982200.

Hitosugi, T., Kang, S., Vander Heiden, M.G., Chung, T.-W., Elf, S., Lythgoe, K., Dong, S., Lonial, S., Wang, X., Chen, G.Z., Xie, J., Gu, T.-L., Polakiewicz, R.D., Roesel, J.L., Boggon, T.J., Khuri, F.R., Gilliland, D.G., Cantley, L.C., Kaufman, J., Chen, J., 2009. Tyrosine phosphorylation inhibits PKM2 to promote the Warburg effect and tumor growth. Sci. Signal. 2, http://dx.doi.org/10.1126/scisignal.2000431(ra73).

Hiwatashi, Y., Kanno, K., Takasaki, C., Goryo, K., Sato, T., Torii, S., Sogawa, K., Yasumoto, K., 2011. PHD1 interacts with ATF4 and negatively regulates its transcriptional activity without prolyl hydroxylation. Exp. Cell Res. 317, 2789–2799, http://dx.doi.org/10.1016/j.yexcr.2011.09.005.

Hsieh, M.M., Linde, N.S., Wynter, A., Metzger, M., Wong, C., Langsetmo, I., Lin, A., Smith, R., Rodgers, G.P., Donahue, R.E., Klaus, S.J., Tisdale, J.F., 2007. HIF-prolyl hydroxylase inhibition results in endogenous erythropoietin induction, erythrocytosis, and modest fetal hemoglobin expression in rhesus macaques. Blood 110, 2140–2147, http://dx.doi.org/10.1182/blood-2007-02-073254.

Huang, J., Zhao, Q., Mooney, S.M., Lee, F.S., 2002. Sequence determinants in hypoxia-inducible factor-1α for hydroxylation by the prolyl hydroxylases PHD1, PHD2, and PHD3. J. Biol. Chem. 277, 39792–39800, http://dx.doi.org/10.1074/jbc.M206955200.

Inoki, K., Corradetti, M.N., Guan, K.-L., 2005. Dysregulation of the TSC-mTOR pathway in human disease. Nat. Genet. 37, 19–24. doi:10.1038/ng 1494.

Isaacs, J.S., Yun, J.J., Mole, D.R., Lee, S., Torres-Cabala, C., Chung, Y.L., Merino, M., Trepel, J., Zbar, B., Toro, J., Ratcliffe, P.J., Linehan, W.M., Neckers, L., 2005. HIF overexpression correlates with biallelic loss of fumarate hydratase in renal cancer: novel role of fumarate in regulation of HIF stability. Cancer Cell 8, 143–153, http://dx.doi.org/10.1016/j.ccr.2005.06.017.

Ivan, M., Haberberger, T., Gervasi, D.C., Michelson, K.S., Günzler, V., Kondo, K., Yang, H., Sorokina, I., Conaway, R.C., Conaway, J.W., Kaelin, W.G., 2002. Biochemical purification and pharmacological inhibition of a mammalian prolyl hydroxylase acting on hypoxia-inducible factor. PNAS 99, 13459–13464, http://dx.doi.org/10.1073/pnas.192342099.

Köditz, J., Nesper, J., Wottawa, M., 2007. Oxygen-dependent ATF-4 stability is mediated by the PHD3 oxygen sensor. Blood 110, 3610–3618, http://dx.doi.org/10.1182/blood-2007-06-094441.

Kaelin, W.G., Ratcliffe, P.J., 2008. Oxygen sensing by metazoans: the central role of the HIF hydroxylase pathway. Mol. Cell 30, 393–402, http://dx.doi.org/10.1016/j.molcel.2008.04.009.

Kaelin, W.G., 2005. ROS: really involved in oxygen sensing. Cell Metab. 1, 357–358, http://dx.doi.org/10.1016/j.cmet.2005.05.006.

Kapitsinou, P.P., Liu, Q., Unger, T.L., Rha, J., Davidoff, O., Keith, B., Epstein, J.A., Moores, S.L., Erickson-Miller, C.L., Haase, V.H., 2010. Hepatic HIF-2 regulates erythropoietic responses to hypoxia in renal anemia. Blood 116, 3039–3048, http://dx.doi.org/10.1182/blood-2010-02-270322.

Kasiganesan, H., Sridharan, V., Wright, G., 2007. Prolyl hydroxylase inhibitor treatment confers whole-animal hypoxia tolerance. Acta Physiol. 190, 163–169, http://dx.doi.org/10.1111/j.1748-1716.2007.01676.x.

Kato, H., Inoue, T., Asanoma, K., Nishimura, C., Matsuda, T., Wake, N., 2006. Induction of human endometrial cancer cell senescence through modulation of HIF-1α activity by EGLN1. Int. J. Cancer 118, 1144–1153, http://dx.doi.org/10.1002/ijc.21488.

Kikuchi, D., Minamishima, Y.A., Nakayama, K., 2014. Prolyl-hydroxylase PHD3 interacts with pyruvate dehydrogenase (PDH)-E1β and regulates the cellular PDH activity. Biochem. Biophys. Res. Commun. 451, 288–294, http://dx.doi.org/10.1016/j.bbrc.2014.07.114.

Kim, W.Y., Kaelin, W.G., 2004. Role of VHL gene mutation in human cancer. J. Clin. Oncol. 22, 4991–5004, http://dx.doi.org/10.1200/JCO.2004.05.061.

Kim, J.W., Tchernyshyov, I., Semenza, G.L., Dang, C.V., 2006. HIF-1-mediated expression of pyruvate dehydrogenase kinase: a metabolic switch required for cellular adaptation to hypoxia. Cell Metab. 3, 177–185, http://dx.doi.org/10.1016/j.cmet.2006.02.002.

Klotzsche-Von Ameln, A., Muschter, A., Mamlouk, S., Kalucka, J., Prade, I., Franke, K., Rezaei, M., Poitz, D.M., Breier, G., Wielockx, B., 2011. Inhibition of HIF prolyl hydroxylase-2 blocks tumor growth in mice through the antiproliferative activity of TGFβ. Cancer Res. 71, 3306–3316, http://dx.doi.org/10.1158/0008-5472 (CAN-10-3838).

Koivunen, P., Hirsilä, M., Kivirikko, K.I., Myllyharju, J., 2006. The length of peptide substrates has a marked effect on hydroxylation by the hypoxia-inducible factor prolyl 4-hydroxylases. J. Biol. Chem. 281, 28712–28720, http://dx.doi.org/10.1074/jbc.M604628200.

Koivunen, P., Hirsilä, M., Remes, A.M., Hassinen, I.E., Kivirikko, K.I., Myllyharju, J., 2007a. Inhibition of hypoxia-inducible factor (HIF) hydroxylases by citric acid cycle intermediates: possible links between cell metabolism and stabilization of HIF. J. Biol. Chem. 282, 4524–4532, http://dx.doi.org/10.1074/jbc.M610415200.

Koivunen, P., Tiainen, P., Hyvärinen, J., Williams, K.E., Sormunen, R., Klaus, S.J., Kivirikko, K.I., Myllyharju, J., 2007b. An endoplasmic reticulum transmembrane prolyl 4-hydroxylase is induced by hypoxia and acts on hypoxia-inducible factor α. J. Biol. Chem. 282, 30544–30552, http://dx.doi.org/10.1074/jbc.M704988200.

Lee, S., Nakamura, E., Yang, H., Wei, W., Linggi, M.S., Sajan, M.P., Farese, R., Freeman, V., Carter, R.S., Kaelin, B.D., Schlisio, W.G., 2005. Neuronal apoptosis linked to EglN3 prolyl hydroxylase and familial pheochromocytoma genes: developmental culling and cancer. Cancer Cell 8, 155–167, http://dx.doi.org/10.1016/j.ccr.2005.06.015.

Li, Y., Xi, M., Guo, Y., Hai, C., Yang, W., Qin, X., 2014. NADPH oxidase-mitochondria axis-derived ROS mediate arsenite-induced HIF-1α stabilization by inhibiting prolyl hydroxylases activity. Toxicol. Lett. 224, 165–174, http://dx.doi.org/10.1016/j.toxlet.2013.10.029.

Lipscomb, E.A., Sarmiere, P.D., Crowder, R.J., Freeman, R.S., 1999. Expression of the SM-20 gene promotes death in nerve growth factor-dependent sympathetic neurons. J. Neurochem. 73, 429–432, http://dx.doi.org/10.1046/j.1471-4159.1999.0730429.x.

Lok, C.N., Ponka, P., 1999. Identification of a hypoxia response element in the transferrin receptor gene. J. Biol. Chem. 274, 24147–24152, http://dx.doi.org/10.1074/jbc.274.34.24147.

Lorin, S., Tol, M.J., Bauvy, C., Strijland, A., Poüs, C., Verhoeven, A.J., Codogno, P., Meijer, A.J., 2013. Glutamate dehydrogenase contributes to leucine sensing in the regulation of autophagy. Autophagy 9, 850–860, http://dx.doi.org/10.4161/auto.24083.

Luo, W., Hu, H., Chang, R., Zhong, J., Knabel, M., O'Meally, R., Cole, R.N., Pandey, A., Semenza, G.L., 2011. Pyruvate kinase M2 is a PHD3-stimulated coactivator for hypoxia-inducible factor 1. Cell 145, 732–744, http://dx.doi.org/10.1016/j.cell.2011.03.054.

MacKenzie, E.D., Selak, M.A., Tennant, D.A., Payne, L.J., Crosby, S., Frederiksen, C.M., Watson, D.G., Gottlieb, E., 2007. Cell-permeating α-ketoglutarate derivatives alleviate pseudohypoxia in succinate dehydrogenase-deficient cells. Mol. Cell. Biol. 27, 3282–3289, http://dx.doi.org/10.1128/MCB.01927-06.

Mansfield, K.D., Guzy, R.D., Pan, Y., Young, R.M., Cash, T.P., Schumacker, P.T., Simon, M.C., 2005. Mitochondrial dysfunction resulting from loss of cytochrome c impairs cellular oxygen sensing and hypoxic HIF-α activation. Cell Metab. 1, 393–399, http://dx.doi.org/10.1016/j.cmet.2005.05.003.

Marxsen, J.H., Stengel, P., Doege, K., Heikkinen, P., Jokilehto, T., Wagner, T., Jelkmann, W., Jaakkola, P., Metzen, E., 2004. Hypoxia-inducible factor-1 (HIF-1) promotes its degradation by induction of HIF-α-prolyl-4-hydroxylases. Biochem. J. 381, 761–767, http://dx.doi.org/10.1042/BJ20040620.

Masson, N., Ratcliffe, P.J., 2014. Hypoxia signaling pathways in cancer metabolism: the importance of co-selecting interconnected physiological pathways. Cancer Metab. 2, 3, http://dx.doi.org/10.1186/2049-3002-2-3.

Maxwell, P.H., 2005. The HIF pathway in cancer. Semin. Cell Dev. Biol. 16, 523–530, http://dx.doi.org/10.1016/j.semcdb.2005.03.001.

McNeill, L.A., Hewitson, K.S., Gleadle, J.M., Horsfall, L.E., Oldham, N.J., Maxwell, P.H., Pugh, C.W., Ratcliffe, P.J., Schofield, C.J., 2002. The use of dioxygen by HIF prolyl hydroxylase (PHD1). Bioorganic Med. Chem. Lett. 12, 1547–1550, http://dx.doi.org/10.1016/S0960-894X(02)00219-6.

Metzen, E., Stiehl, D.P., Doege, K., Marxsen, J.H., Hellwig-Bürgel, T., Jelkmann, W., 2005. Regulation of the prolyl hydroxylase domain protein 2 (phd2/egln-1) gene: identification of a functional hypoxia-responsive element. Biochem. J. 387, 711–717, http://dx.doi.org/10.1042/BJ20041736.

Mikhaylova, O., Ignacak, M.L., Barankiewicz, T.J., Harbaugh, S., Yi, V., Maxwell, Y., Schneider, P.H., Van Geyte, M., Carmeliet, K., Revelo, P., Wyder, M.P., Greis, M., Meller, K.D., Czyzyk-Krzeska, J., 2008. The von Hippel-Lindau tumor suppressor protein and Egl-9-Type proline hydroxylases regulate the large subunit of RNA polymerase II in response to oxidative stress. Mol. Cell. Biol. 28, 2701–2717, http://dx.doi.org/10.1128/MCB.01231-07.

Moore, C.E.J., Mikolajek, H., Regufe da Mota, S., Wang, X., Kenney, J.W., Werner, J.M., Proud, C.G., 2015. Elongation factor 2 kinase is regulated by proline hydroxylation and protects cells during hypoxia. Mol. Cell. Biol. 35, 1788–1804, http://dx.doi.org/10.1128/MCB.01457-14.

Myllyla, R., Majamaa, K., Giinzler, V., Hanauske-abel, H.M., Kivirikko, K.I., 1984. Ascorbate is consumed stoichiometrically in the uncoupled reactions catalyzed by Prolyl 4-Hydroxylase and Lysyl Hydroxylase. J. Biol. Chem. 259, 5403–5405.

Núñez-O'Mara, A., Gerpe-Pita, A., Pozo, S., Carlevaris, O., Urzelai, B., Lopitz-Otsoa, F., Rodríguez, M.S., Berra, E., 2015. PHD3-SUMO conjugation represses HIF1 transcriptional activity independently of PHD3 catalytic activity. J. Cell Sci. 128, 40–49, http://dx.doi.org/10.1242/jcs.151514.

Nakayama, K., Frew, I.J., Hagensen, M., Skals, M., Habelhah, H., Bhoumik, A., Kadoya, T., Erdjument-Bromage, H., Tempst, P., Frappell, P.B., Bowtell, D.D., Ronai, Z., 2004. Siah2 regulates stability of prolyl-hydroxylases, controls HIF1α abundance, and modulates physiological responses to hypoxia. Cell 117, 941–952, http://dx.doi.org/10.1016/j.cell.2004.06.001.

Nandal, A., Ruiz, J.C., Subramanian, P., Ghimire-rijal, S., Ann, R., Stemmler, T.L., Bruick, R.K., Philpott, C.C., 2011. Activation of the HIF prolyl hydroxylase by the iron chaperones PCBP1 and PCBP2. Cell Metab. 14, 647–657, http://dx.doi.org/10.1016/j.cmet.2011.08.015 (Nandal).

Nangaku, M., Izuhara, Y., Takizawa, S., Yamashita, T., Fujii-Kuriyama, Y., Ohneda, O., Yamamoto, M., Van Ypersele De Strihou, C., Hirayama, N., Miyata, T., 2007. A novel class of prolyl hydroxylase inhibitors induces angiogenesis and exerts organ protection against ischemia. Arterioscler. Thromb. Vasc. Biol. 27, 2548–2554, http://dx.doi.org/10.1161/ATVBAHA.107.148551.

Oehme, F., Ellinghaus, P., Kolkhof, P., Smith, T.J., Ramakrishnan, S., Hütter, J., Schramm, M., Flamme, I., 2002. Overexpression of PH-4, a novel putative proline 4-hydroxylase, modulates activity of hypoxia-inducible transcription factors. Biochem. Biophys. Res. Commun. 296, 343–349, http://dx.doi.org/10.1016/S0006-291X(02)00862-8.

Pan, Y., Mansfield, K.D., Bertozzi, C.C., Rudenko, V., Chan, D.A., Giaccia, A.J., Simon, M.C., 2006. Multiple factors affecting cellular redox status and energy metabolism modulate hypoxia-inducible factor prolyl hydroxylase activity in vivo and In vitro. Mol. Cell. Biol. 27, 912–925, http://dx.doi.org/10.1128/MCB.01223-06.

Plas, D.R., Thompson, C.B., 2005. Akt-dependent transformation: there is more to growth than just surviving. Oncogene 24, 7435–7442, http://dx.doi.org/10.1038/sj.onc.1209097.

Pollard, P.J., Briere, J.J., Alam, N.A., Barwell, J., Barclay, E., Wortham, N.C., Hunt, T., Mitchell, M., Olpin, S., Moat, S.J., Hargreaves, I.P., Heales, S.J., Chung, Y.L., Griffiths, J.R., Dalgleish, A., McGrath, J.A., Gleeson, M.J., Hodgson, S.V., Poulsom, R., Rustin, P., Tomlinson, I.P.M., 2005. Accumulation of Krebs cycle intermediates and over-expression of HIF1α in tumours which result from germline FH and SDH mutations. Hum. Mol. Genet. 14, 2231–2239, http://dx.doi.org/10.1093/hmg/ddi227.

Quaegebeur, A., Segura, I., Schmieder, R., Verdegem, D., Decimo, I., Bifari, F., Dresselaers, T., Eelen, G., Ghosh, D., Davidson, S.M., Schoors, S., Broekaert, D., Cruys, B., Govaerts, K., De Legher, C., Bouché, A., Schoonjans, L., Ramer, M.S., Hung, G., Bossaert, G., Cleveland, D.W., Himmelreich, U., Voets, T., Lemmens, R., Bennett, C.F., Robberecht, W., De Bock, K., Dewerchin, M., Ghesquière, B., Fendt, S.M., Carmeliet, P., 2016. Deletion or inhibition of the oxygen sensor PHD1 protects against ischemic stroke via reprogramming of neuronal metabolism. Cell Metab. 23, 280–291, http://dx.doi.org/10.1016/j.cmet.2015.12.007.

Rahtu-Korpela, L., Karsikas, S., Hörkkö, S., Sequeiros, R.B., Lammentausta, E., Mäkelä, K.A., Herzig, K.H., Walkinshaw, G., Kivirikko, K.I., Myllyharju, J., Serpi, R., Koivunen, P., 2014. HIF prolyl 4-hydroxylase-2 inhibition improves glucose and lipid metabolism and protects against obesity and metabolic dysfunction. Diabetes 63, 3324–3333, http://dx.doi.org/10.2337/db14-0472.

Ratan, R.R., Siddiq, A., Smirnova, N., Karpisheva, K., Haskew-Layton, R., McConoughey, S., Langley, B., Estevez, A., Huerta, P.T., Volpe, B., Roy, S., Sen, C.K., Gazaryan, I., Cho, S., Fink, M., LaManna, J., 2007. Harnessing hypoxic adaptation to prevent, treat, and repair stroke. J. Mol. Med. 85, 1331–1338, http://dx.doi.org/10.1007/s00109-007-0283-1.

Rolfs, A., Kvietikova, I., Gassmann, M., Wenger, R.H., 1997. Oxygen-regulated transferrin expression is mediated by hypoxia inducible factor-1. J. Biol. Chem. 272, 20055–20062, http://dx.doi.org/10.1074/jbc.272.32.20055.

Salnikow, K., Donald, S.P., Bruick, R.K., Zhitkovich, A., Phang, J.M., Kasprzak, K.S., 2004. Depletion of intracellular ascorbate by the carcinogenic metals nickel and cobalt results in the induction of hypoxic stress. J. Biol. Chem. 279, 40337–40344, http://dx.doi.org/10.1074/jbc.M403057200.

Schlisio, S., Kenchappa, R.S., Vredeveld, L.C.W., George, R.E., Stewart, R., Greulich, H., Shahriari, K., Nguyen, N.V., Pigny, P., Dahia, P.L., Pomeroy, S.L., Maris, J.M., Look, A.T., Meyerson, M., Peeper, D.S., Carter, B.D., Kaelin, W.G., 2008. The kinesin KIF1B(acts downstream from EglN3 to induce apoptosis and is a potential 1p36 tumor suppressor. Genes Dev. 22, 884–893, http://dx.doi.org/10.1101/gad.1648608.

Schofield, C.J., Ratcliffe, P.J., 2004. Oxygen sensing by HIF hydroxylases. Mol. Cell Biol. 5, 343–354, http://dx.doi.org/10.1038/nrm1366.

Selak, M.A., Armour, S.M., MacKenzie, E.D., Boulahbel, H., Watson, D.G., Mansfield, K.D., Pan, Y., Simon, M.C., Thompson, C.B., Gottlieb, E., 2005. Succinate links TCA cycle dysfunction to oncogenesis by inhibiting HIF-α prolyl hydroxylase. Cancer Cell 7, 77–85, http://dx.doi.org/10.1016/j.ccr.2004.11.022.

Semenza, G.L., 2012. Hypoxia-inducible factors: mediators of cancer progression and targets for cancer therapy. Trends Pharmacol. Sci. 33, 207–214, http://dx.doi.org/10.1016/j.tips.2012.01.005.

Semenza, G.L., 2013. HIF-1 mediates metabolic responses to intratumoral hypoxia and oncogenic mutations. J. Clin. Invest. 123, 3664–3671, http://dx.doi.org/10.1172/JCI67230.

Shohet, R.V., Garcia, J.A., 2007. Keeping the engine primed: HIF factors as key regulators of cardiac metabolism and angiogenesis during ischemia. J. Mol. Med. 85, 1309–1315, http://dx.doi.org/10.1007/s00109-007-0279-x.

Siegert, I., Schodel, J., Nairz, M., Schatz, V., Dettmer, K., Dick, C., Kalucka, J., Franke, K., Ehrenschwender, M., Schley, G., Beneke, A., Sutter, J., Moll, M., Hellerbrand, C., Wielockx, B., Katschinski, D.M., Lang, R., Galy, B., Hentze, M.W., Koivunen, P., Oefner, P.J., Bogdan, C., Weiss, G., Willam, C., Jantsch, J., 2015. Ferritin-mediated iron sequestration stabilizes hypoxia-inducible factor-1α upon LPS activation in the presence of ample oxygen. Cell Rep. 13, 2048–2055, http://dx.doi.org/10.1016/j.celrep.2015.11.005.

Soulard, A., Cohen, A., Hall, M.N., 2009. TOR signaling in invertebrates. Curr. Opin. Cell Biol. 21, 825–836, http://dx.doi.org/10.1016/j.ceb.2009.08.007.

Sridharan, V., Guichard, J., Bailey, R.M., Kasiganesan, H., Beeson, C., Wright, G.L., 2007. The prolyl hydroxylase oxygen-sensing pathway is cytoprotective and allows maintenance of mitochondrial membrane potential during metabolic inhibition. Am. J. Physiol. Cell Physiol. 292, C719–28, http://dx.doi.org/10.1152/ajpcell.00100.2006.

Sridharan, V., Guichard, J., Li, C.-Y., Muise-Helmericks, R., Beeson, C.C., Wright, G.L., 2008. O(2)-sensing signal cascade: clamping of O(2) respiration, reduced ATP utilization, and inducible fumarate respiration. Am. J. Physiol. Cell Physiol. 295, C29–37, http://dx.doi.org/10.1152/ajpcell.00466.2007.

Tacchini, L., Bianchi, L., Bernelli-Zazzera, A., Cairo, G., 1999. Transferrin receptor induction by hypoxia. J. Biol. Chem. 274, 24142–24146, http://dx.doi.org/10.1074/jbc.274.34.24142.

Takai, H., Wang, R.C., Takai, K.K., Yang, H., de Lange, T., 2007. Tel2 regulates the stability of PI3K-related protein kinases. Cell 131, 1248–1259, http://dx.doi.org/10.1016/j.cell.2007.10.052.

Takeda, Y., Costa, S., Delamarre, E., Roncal, C., Leite de Oliveira, R., Squadrito, M.L., Finisguerra, V., Deschoemaeker, S., Bruyère, F., Wenes, M., Hamm, A., Serneels, J., Magat, J., Bhattacharyya, T., Anisimov, A., Jordan, B.F., Alitalo, K., Maxwell, P., Gallez, B., Zhuang, Z.W., Saito, Y., Simons, M., De Palma, M., Mazzone, M., 2011. Macrophage skewing by Phd2 haplodeficiency prevents ischaemia by inducing arteriogenesis. Nature 479, 122–128, http://dx.doi.org/10.1038/nature10507.

Tennant, D.A., Gottlieb, E., 2010. HIF prolyl hydroxylase-3 mediates alpha-ketoglutarate-induced apoptosis and tumor suppression. J. Mol. Med. 88, 839–849, http://dx.doi.org/10.1007/s00109-010-0627-0.

Tian, Y.M., Mole, D.R., Ratcliffe, P.J., Gleadle, J.M., 2006. Characterization of different isoforms of the HIF prolyl hydroxylase PHD1 generated by alternative initiation. Biochem. J. 397, 178–186, http://dx.doi.org/10.1111/j.1440-1789.2006.00679.x.

Villar, V.H., Merhi, F., Djavaheri-Mergny, M., Durán, R.V., 2015. Glutaminolysis and autophagy in cancer. Autophagy 11, 1198–1208, http://dx.doi.org/10.1080/15548627.2015.1053680.

Wullschleger, S., Loewith, R., Hall, M.N., 2006. TOR signaling in growth and metabolism. Cell 124, 471–484, http://dx.doi.org/10.1016/j.cell.2006.01.016.

Xie, L., Xiao, K., Whalen, E.J., Forrester, M.T., Freeman, R.S., Fong, G., Gygi, S.P., Lefkowitz, R.J., Stamler, J.S., 2009. Oxygen-regulated β2—adrenergic receptor hydroxylation by EGLN3 and ubiquitylation by pVHL. Sci. Signal. 2, 1–21, http://dx.doi.org/10.1126/scisignal.2000444.

Xie, L., Pi, X., Mishra, A., Fong, G., Peng, J., Patterson, C., 2012. PHD3-dependent hydroxylation of HCLK2 promotes the DNA damage response. J. Clin. Invest. 122, 2827–2836, http://dx.doi.org/10.1172/JCI62374.

Xue, J., Li, X., Jiao, S., Wei, Y., Wu, G., Fang, J., 2010. Prolyl hydroxylase-3 is down-regulated in colorectal cancer cells and inhibits IKKβ independent of hydroxylase activity. Gastroenterology 138, 606–615, http://dx.doi.org/10.1053/j.gastro.2009.09.049.

Yuan, Y., Beitner-Johnson, D., Millhorn, D.E., 2001. Hypoxia-inducible factor 2α binds to cobalt in vitro. Biochem. Biophys. Res. Commun. 288, 849–854, http://dx.doi.org/10.1006/bbrc.2001.5835.

Yuan, Y., Hilliard, G., Ferguson, T., Millhorn, D.E., 2003. Cobalt inhibits the interaction between hypoxia-inducible factor-α and von Hippel-Lindau protein by direct binding to hypoxia-inducible factor-α. J. Biol. Chem. 278, 15911–15916, http://dx.doi.org/10.1074/jbc.M300463200.

Zhang, Z., Ren, J., Harlos, K., McKinnon, C.H., Clifton, I.J., Schofield, C.J., 2002. Crystal structure of a clavaminate synthase-Fe(II)-2-oxoglutarate-substrate-NO complex: evidence for metal centred rearrangements. FEBS Lett. 517, 7–12, http://dx.doi.org/10.1016/S0014-5793(02)02520-6.

Zhdanov, A.V., Okkelman, I.A., Collins, F.W.J., Melgar, S., Papkovsky, D.B., 2015. A novel effect of DMOG on cell metabolism: direct inhibition of mitochondrial function precedes HIF target gene expression. Biochim. Biophys. Acta 1847, 1254–1266, http://dx.doi.org/10.1016/j.bbabio.2015.06.016.